# From Support to Carbocatalyst: The Aerobic and Solvent Free Epoxidation of Dec-1-ene Using Graphitic Oxide as a Catalyst

Thesis submitted in accordance with the requirement of Cardiff University for the degree of Doctor of Philosophy

**Samuel David Pattisson**

**February 2015**

**Student ID Number:** **0717503**

**Summary of Thesis:** The aerobic and solvent free epoxidation of dec-1-ene has been studied in the absence of radical initiators. This has been achieved under mild conditions and using atmospheric oxygen as the sole oxidant. The catalyst used is a form of graphitic oxide and can be prepared using modified Hofmann and Hummers methods. It was found that activity of the graphitic oxide for dec-1-ene epoxidation relied on critical amounts of oxygen coverage on the surface. It was also found that low amounts of sulphur inhibit the reactivity of low oxidised catalyst below 20 wt% oxygen. Removal of this sulphur by additional washing can activate catalysts with as low as 15 wt% surface oxygen. Extensive characterisation of each of the materials has suggested that many of the low oxidised catalysts retain a high level of graphitic character. Highly oxidised Hummers species show extensive de-graphitisation of the surface. These highly oxidised catalysts were shown to be difficult to purify, separate and dry and ultimately gave low activity for dec-1-ene epoxidation. We suggest that the use of preparation methods which do not involve sulphur such as the pyrolysis of sugars may result in highly active sulphur free epoxidation catalysts. This is to the best of our knowledge the first example of the aerobic epoxidation of terminal linear alkenes in the absence of radical initiators or stoichiometric oxidants.

# Abstract

The solvent-free selective epoxidation of dec-1-ene has been achieved under mild conditions and using atmospheric oxygen as the sole oxidant. Furthermore this has been conducted in the absence of radical initiators which is a first for such an oxidation to the best of our knowledge.

The selective epoxidation of alkenes typically requires the use of supported active metals such as gold or silver. These have been studied for the epoxidation of dec-1-ene however they were found to be inactive in the absence of radical initiators.

Alternatively, this transformation has been achieved using a graphitic oxide catalyst which harbours no active metal species. This is yet another remarkable example of the potential of carbocatalysis for green chemistry. The commonly raised issues when using carbocatalysts such as identification of active species and presence of impurities are addressed. A range of graphitic oxides have been produced using modified Hofmann and Hummers methods with attention given to the effect of amount of oxidant used compared to commonly employed literature standards.

We conclude that the popular highly oxidised Hummers materials used in the bulk production of graphene may not be the optimum material for all applications and that specification of graphitic oxides may be required to suit each application. An investigation of activity in the epoxidation of dec-1-ene partnered with a full characterisation of the surface suggests that an optimum level of oxidation is required along with the need for a surface free of potential poisons such as sulphur. We also evaluate the current methods used in the preparation and separation of these materials and suggest that for applications such as epoxidation alternative techniques may be required in order to realise its potential as a carbocatalyst.

This work provides the basis for the development of an efficient catalyst for the selective epoxidation of α-alkenes, eradicating the need for expensive stoichiometric reagents or toxic radical initiators.

# Acknowledgments

I would like to express my sincere gratitude to Professor Graham Hutchings for providing me with the opportunity to study for this PhD at the Cardiff catalysis institute. I thank him for his regular guidance, unwavering interest in my "*magnum opus*" when that of others would certainly have failed and his constant demand for only the best and ambitious science. I would like to extend these regards to all that have worked closely on the project; Dr Upendra Gupta who worked tirelessly to lay the foundations for this project during his own PhD and who also provided support as my postdoctoral assistant; Dr Ewa Nowicka who joined late on in the project but whose meticulous attitude towards chemistry played an integral role in its completion; and last but by no means least I would like to sincerely thank Dr Robert Jenkins who along with Professor Hutchings has endured this rollercoaster from start to finish. His words of encouragement when all seemed hopeless, which can be summarised by saying "nothing gained is something learned", were just as important as his enthusiasm and advice when the chemistry behaved.

I would also like to thank those that, although not directly involved in the project, have ensured the smooth running of the CCI laboratories and equipment. These are Steve Morris whose power to fix and maintain just about anything is second to none. And Christopher Morgan whose enthusiasm for batch runs is bordering on obsessive, but in the most helpful way possible. The laboratories are a much safer and efficient environment because of these gentlemen and their importance cannot be overstated.

My friends and colleagues also deserve a great deal of credit as they are the ones who on a day to day basis helped me keep my sanity, even though sadly in some cases that cannot be said of them (Of note: Adeeba, Baker, James, Mark, Ben and Paul) . They have all provided a fantastic working environment in which I have thoroughly enjoyed studying and I wish them all the very best.

I end these acknowledgements by thanking my family, to whom I owe everything. They have provided me with love and support whenever needed and a sense of humour which has often been employed to take the best from a bad situation. This thesis is for you.

# Table of Contents

# 1

# Introduction

### 1.0 Project aims

The focus of this project is to achieve the solvent free selective oxidation of an $\alpha$-alkene to epoxide using graphite supported metal catalysts. The reaction should proceed under mild conditions using atmospheric oxygen as the sole oxidant. The replacement of expensive oxidants with atmospheric oxygen will be facilitated by radical initiators, the use of which will in turn be eradicated by activation of oxygen by the catalyst. Dec-1-ene will be used as the principle reactant with a view to developing a system which can be applied to shorter chain alkenes such as propene.

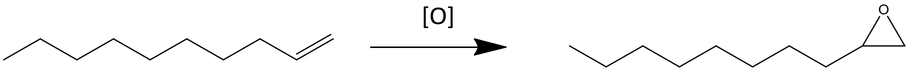

**Figure 1.0.1 Epoxidation of dec-1-ene to 1,2-epoxydecane**

### 1.1 Project overview

**Chapter 3** serves as a continuation of previous work by Gupta *et al*. considering the use of supported nano gold catalysts for the aerobic epoxidation of dec-1-ene. Bimetallic catalysts are explored along with the replacement of gold with other coinage metals. Derivation of the support is also considered in order to achieve a more active catalyst with the specific aim of removing the need for radical initiators.

**Chapter 4** provides a full investigation into the use of graphitic oxide as a catalyst for the epoxidation of dec-1-ene in the absence of radical initiators or supported metal. The effects of numerous variables on activity are considered including preparation method and amount of oxidant used.

**Chapter 5** provides characterisation of the full range of modified graphitic oxides used in this study and compares them to the literature standard catalysts.

**Chapter 6** describes the problems associated with current preparation methods and how these can be overcome. The future potential of graphitic oxide as catalyst is also discussed.

## 1.2 Green chemistry

The development of environmentally friendly chemical processes has become increasingly important over the past 25 years. The idea of green chemistry was introduced in the 1990's with companies developing new attitudes towards the use of and production of hazardous chemicals. In 1998 Anastas and Warner brought these ideas together to form the 12 principles of green chemistry given below[1,2].

1. Waste prevention is preferable to the treatment and/or disposal of waste after it has been created.
2. Atom efficiency should be considered to incorporate all atoms of the reagents into the product, thus minimising waste.
3. Methods which involve and/or produce chemicals which are low in toxicity to humans and the environments should be strived for.
4. Design of a product which is fit for purpose while maintaining low toxicity
5. The use of solvents and auxiliaries should be minimised or eradicated where possible and non-toxic or hazardous when unavoidable.
6. The entire efficiency of a process should be considered and designed to lessen the impact on environment. Ambient reaction conditions are preferred for minimising energy consumption.
7. The use of renewable raw materials is preferred over those which are already being depleted or are at a risk of being so is preferred.
8. Derivatization of intermediates should be reduced or avoided totally if possible to avoid the production of waste.
9. The process should utilise catalysis rather than the stoichiometric use of reagents.
10. Product design should aim to minimise the longevity of a product after it has fulfilled its purpose in order to minimise impact on environment.
11. Online analysis and monitoring of a system should be conducted to control unwanted hazardous waste and its release to the environment.

12. Processes should be designed so that risk is minimised with respect to hazardous waste leakage, explosions, fires and spillages.

Green chemistry is now more important than ever with global competition for food, energy and raw materials continually forcing industry to seek renewable or plentiful feedstocks and the utilisation of cleaner technologies. Each of these principles has had a major impact on formulating this project and directing the research.

## 1.3 Catalysis

The term catalysis was first introduced by Swedish scientist J.J Berzelius in 1836 in order to explain how small amounts of certain materials were required for reaction to proceed and yet did not include them in the final product. He defined this quality as "catalytic power" and said "catalytic power means that substances are able to awake affinities that are asleep at this temperature by their mere presence." [3]

The word catalysis is derived from Greek words 'kata' and 'lyein' and literally translated means 'to break down'. In the context of chemistry, it relates to the lowering or "breaking down" of energy barriers to a reaction however it is commonly used throughout language to describe the general breaking down of barriers or the initiation and acceleration of actions.

The action of catalysis is integral to all forms of life, allowing reactions to occur within our bodies at mild temperatures. Of course these biological catalysts take the form of enzymes, made from highly diverse proteins sometimes with a coordinated metal ion. These set the bar for the industrial catalysts in terms of reaction specificity, reaction rate and endurance, finely tuned through millions of years of evolution. Indeed examples can be found in biology for the majority of industrial chemical processes. Industrial catalysts normally incorporate one of, or a combination of, metals, oxides, sulphides and solid acids. Catalysts which operate in a different phase to the reactants are termed heterogeneous i.e. solid catalyst acting upon gaseous and/or liquid reactants. Catalysts that are found to be active in the same phase as the reactants are termed homogeneous. Homogeneous catalysts, for the large part, are found in the liquid phase in the form of salts or inorganic complexes, for example the formation of acetic acid by methanol carbonylation, catalysed by a Rhodium complex[4] (scheme 1.3.1).

$$CH_3OH + CO \xrightarrow{[Rh(CO)_2I_2]^-} CH_3COOH$$

**Scheme 1.3.1 Catalytic carbonylation of methanol**

However there are examples of gas phase homogeneous catalysts. An example of this can be found in the atmospheric depletion of ozone (scheme 1.3.2). This reaction is accelerated by the presence of chlorine which reacts with ozone (1) and, due to its reformation (3) and exclusion from the overall reaction equation (4), chlorine is considered a homogeneous catalyst.

$$1.\ Cl + O_3 \longrightarrow ClO_3$$
$$2.\ ClO_3 \longrightarrow ClO + O_2$$
$$3.\ ClO + O \longrightarrow Cl + O_2$$

$$4.\ O_3 + O \longrightarrow 2O_2$$

**Scheme 1.3.2 Catalytic depletion of ozone by chlorine**

The idea and understanding of catalysis has developed since it was introduced by Berzelius. F.W Ostwald refined the definition of a catalyst as “a substance which increases the rate at which a chemical system approaches equilibrium, without being consumed in the process.” This definition still stands and indeed forms one of the most important principles of catalysis research: the position of equilibrium is unchanged by the presence of a catalyst. This holds true due to the equilibrium constant K being defined by the Gibbs free energy of the system which itself is defined by changes in enthalpy and entropy as the reaction proceeds. Therefore a catalysed and uncatalysed reaction must have the same equilibrium as otherwise the thermodynamics would also have to be different.

1. $\Delta G = \Delta H - T\Delta S$
2. $K = \exp(-\Delta G/RT)$

**Scheme 1.3.3 Reliance of equilibrium constant K on the Gibbs free energy of a system**

The way in which a catalyst accelerates a reaction is by providing an alternative reaction route in which less energy is needed to achieve one or more transition states (figure 1.3.1). This is known as the activation energy. If this is lowered then there will be a higher proportion of molecules with this new energy compared to the uncatalysed activation energy and therefore reaction will proceed faster.

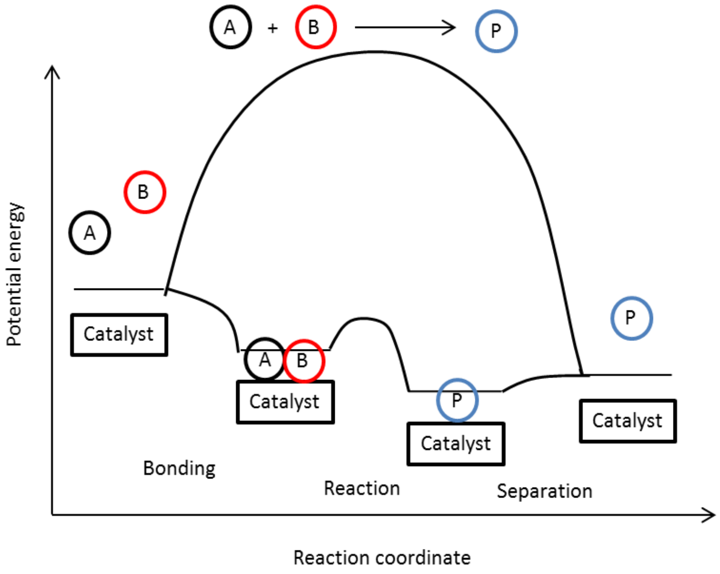

**Figure 1.3.1 A potential energy diagram of uncatalysed and heterogeneously catalysed reaction.**

## 1.4 Catalysis by gold

The inactivity of gold in the bulk phase is well known and has leant this precious metal to many applications, mainly in currency and advertisement of personal wealth throughout history. Bulk gold will not tarnish or react with air or water to rust. It can be buried in earth for centuries, to be later found unchanged. It is these characteristics that labelled gold as completely inactive and seemingly useless for chemical transitions and catalysis.

However, when finely divided into nanoparticles gold behaves extremely differently and becomes an incredibly useful catalytic material. Bond *et al*[5] first demonstrated this by using chloroauric acid precursor and a method of impregnation to support gold nanoparticles and showed that these catalysts were active for the hydrogenation of alkenes. Further research by Haruta *et al* showed gold to be highly active for CO oxidation under mild conditions[6]. Gold was also proven to be the best metal for hydrochlorination of acetylene by Hutchings *et al* who predicted the metals' activity by its standard electrode potential[7]. Gold has since been shown to be highly active in a number of reactions such as methanol synthesis[8], water gas shift[9],[10] reduction of nitric oxide[11] and a number of oxidations including that of propene to propene oxide[12].

The activity of gold is highly dependent on the formation of particles small enough, and with a low coordination number in order to efficiently dissociate reactant molecules. This would otherwise not occur in large particles with high metallic character. Other factors such as the type of support play a large role in the activity of the gold. This is the case for CO oxidation whereby, along with a low particle size of gold <5nm, these particles must be supported on oxides of the first transition series[13]. Choice of preparation method introduces more variation in activity. In the case of CO oxidation, methods such as deposition precipitation and co-precipitation ensure an optimal particle size and interaction with the oxide surface compared to catalysts prepared by impregnation methods. An even more successful catalyst is obtained when careful modifications to factors such as aging time, precursor concentration, pH of solution, temperature of solution, drying and filtration methods and calcination temperatures are made.

### 1.5 Carbocatalysis

Carbon allotropes have long been used as supports for metal induced catalysis. Their high surface area, low cost and variety of renewable sources have meant their use is continually seen in research and is easily and inexpensively scaled up to industrial scale for many important reactions. However, as relatively recent research has increasingly shown, these carbonaceous material can be used as catalysts in the absence of supported metals. Most recently, much attention has been on the use of well-known carbon catalysts such as graphene, carbon nanotubes and fullerenes. However through careful and specific functionalization of a number of carbon surfaces, a wide range of chemical reactions can be catalysed.

Carbocatalysis differs from that of organocatalysis in that the principle element in reactive species is carbon rather than organic molecules as in organocatalysis[14]. This means that carbocatalysts are commonly nanostructured carbon exhibiting high surface area and various degrees of functionality on their aromatic basal planes. Commonly no metal is present however there are some instances where metal is present as a support or contaminant which does not add to the active species.

Carbocatalysis can be dated back to around 1930 when activated charcoals were shown, in two separate cases by Kutzelnigg[15] and Kolthoff[16], to be active for the aerobic oxidation of ferrocyanide (scheme 1.5.1).

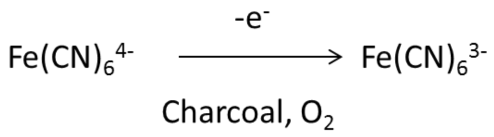

$$\mathrm{Fe(CN)_6^{4-}} \xrightarrow[\text{Charcoal, } \mathrm{O_2}]{-e^-} \mathrm{Fe(CN)_6^{3-}}$$

**Scheme 1.5.1 Oxidation of ferrocyanide using charcoal as a catalyst[17]**

This process was said to be facilitated by the presence of acidic moieties on the surface, introduced by heat treatment, which enabled the adsorption of oxygen. Charcoal was also shown by Rideal and Wright[18,19,20] to be active for the oxidation of oxalic acid to carbon dioxide and water. Another well-known use of charcoal as a carbocatalyst, discovered in 1979, is the formation of styrene by oxidative dehydrogenation of ethylbenzene[21]. In 1985 the use of graphite was found to enable the catalytic reduction of various nitrobenzenes to the corresponding anilines using hydrazine[22].

The recent emergence of carbon nanotubes (CNT's)[23], fullerenes[24] and graphene[25] has accelerated interest in carbocatalysis, providing a wide variety of available materials for various applications.

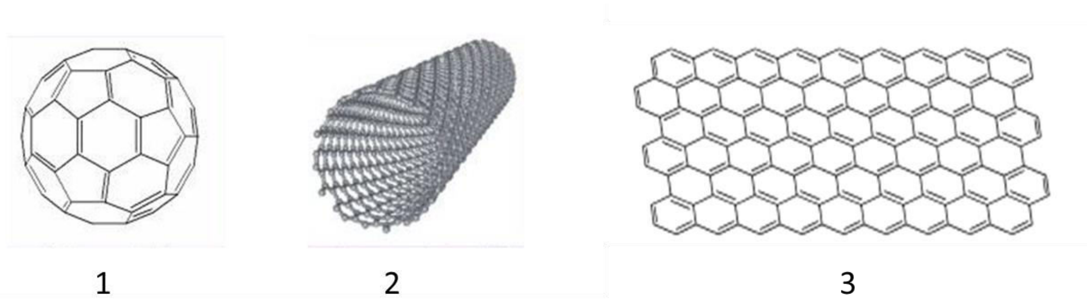

**Figure 1.5.1 Fullerene (1), Carbon nanotube (2) and Graphene (3)[26]**

CNTs have been studied for the oxidative dehydrogenation (ODH) of hydrocarbons to the relating alkenes, most notably for n-butane and propane[27,28] and also for the further ODH to dienes[29]. The CNTs activity is suggested to arise from the defects in the carbon structure, occupied by various functional groups, introduced by acid treatment. However as is common in carbocatalysis, full knowledge of the active site and active species is still coveted. The tedious synthesis of CNTs, which itself requires a catalyst[30], limits their application to large scale catalysis. There has also been little evidence to suggest the use of CNTs in place of graphene and it has been suggested that the use graphene will eclipse that of CNTs except perhaps for encapsulation of nanoparticles[31]. Graphene has been studied as a catalyst in many reactions and as expected facilitates similar reactions as the previously discussed CNTs, as in the ODH of alkanes[32]. Another example of graphene catalysis is the reduction of nitrobenzene in excess $NaBH_4$[33]. It is also particularly of interest because of its adaptability and possible functionalization.

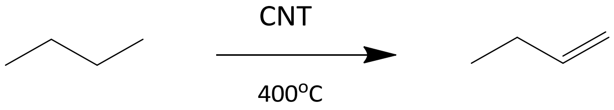

**Scheme 1.5.2 Oxidative dehydrogenation of n-butane to 1-butene**

### 1.6 Graphene, graphene oxide, graphitic oxide and graphite

Graphene has become popularised due to its inclusion in Nobel prize winning research in 2010 by Geim and Novoselov. It is often referred to as a “supermaterial” due to its remarkable mechanical[34], optical[35], thermal[36] and electronic[37] properties. It also has a high theoretical surface area[38] of 2620 $m^2g^{-1}$ although in practice this is hard to achieve[39]. These properties have propagated research into its use for transistors[40], electrodes[41], biodevices[42] and many more applications. Graphene can be considered as monolayer graphite and can be obtained from graphite using a number of methods. Geim was able to isolate graphene via the “scotch tape” method whereby layers of graphite were continually separated until a monolayer was achieved and the unique properties of the obtained graphene were able to be studied. However this method is unsuitable for the manufacturing of graphene on a bulk scale. Graphene can be synthesised via the oxidation and subsequent reduction of graphite. The oxidation of graphite yields graphite (or graphitic) oxide, which in turn can be treated chemically to produce graphene oxide.

Graphene and graphene oxide are both monolayer forms of pristine hexagonally arranged carbon, however they differ in the hybridisation of the carbon. Graphene is formed of solely $sp^2$ hybridised atoms whereas the oxygen functionality of graphene oxide introduces a degree of $sp^3$ character to the material. The further reduction of graphene oxide yields monolayer graphene or reduced graphene oxide.

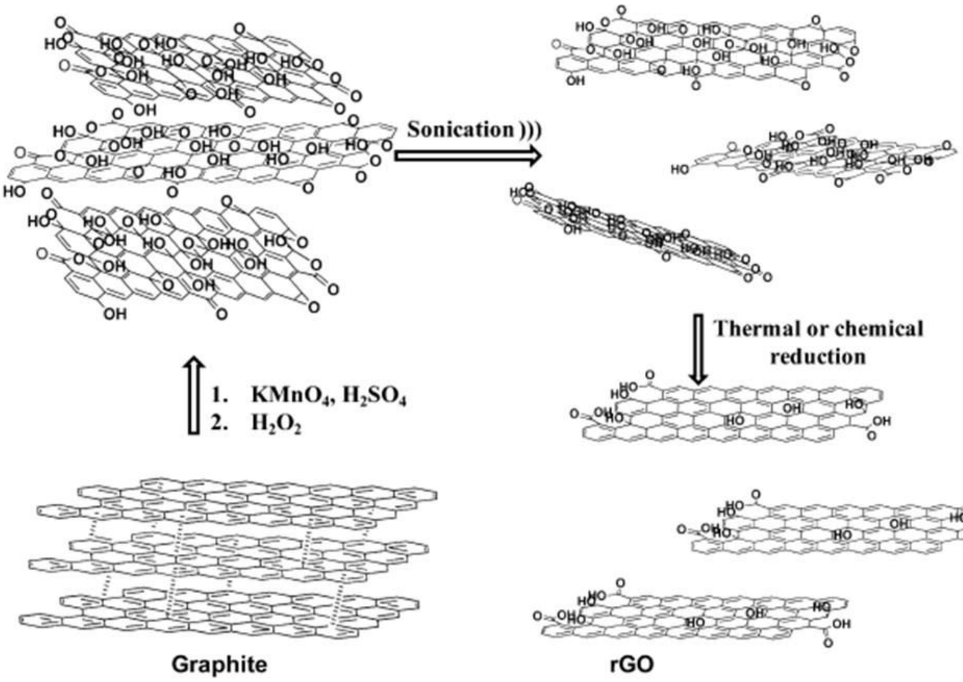

**Figure 1.6.1 Oxidation of graphite to form graphitic oxide, followed by sonication to form graphene oxide and reduced graphene oxide via chemical or thermal reduction[14].**

Although graphene has only recently been physically prepared and characterised, its oxidised relatives have been known for some time. Brodie was one of the first to prepare graphitic oxide in 1859, as a result of his experiments into the structure graphite[43]. He noted that upon the addition of potassium chlorate to a mixture of graphite and fumic nitric acid, the mass of the graphite increased. By repeating this oxidation, the mass again increased and continued until a maximum oxidation was reached after 4 steps. Brodie concluded that this new material was made up of carbon, hydrogen and oxygen. Observing its solubility with water and basic solution and insolubility with acid he determined that the oxidation of graphite must result in acidification of the surface. He therefore referred to this new material as graphic acid.

Brodie's method of oxidation was modified some years later in 1898 by Staudenmaier[44]. Here, the stepwise addition of potassium chlorate partnered with the inclusion of sulphuric acid to the reaction slurry yielded a highly oxidised material. This was found to be comparable in oxygen content to that obtained by Staudenmaier and therefore eliminated the need for multiple oxidation steps. Hofmann also used a similar method with concentrated nitric acid in place of fuming[45].

In 1958 the method for obtaining graphitic oxide was further adapted by Hummers and Offeman[46] who used potassium permanganate as the oxidant in a mixture with concentrated sulphuric acid and graphite. Sodium nitrate was also used to form the nitric acid *in situ*. This method also produced a highly oxidised graphitic oxide as before and due to the noted improvements in safety was then accepted as the method of choice in the years that followed. Other methods and modifications have been made, most notably the Tour method which replaces nitric with phosphoric acid[47]. The Hummers, Tour and Hofmann methods are now the most widely used due to their safety and production of highly oxidised materials for use as graphitic oxide and also for the manufacture of chemically modified graphenes. Potassium chlorate, when used as an oxidant in the Brodie, Staudenmaier and Hofmann methods, provides an *in situ* source of dioxygen which acts as the active species. However, the formation of explosive chlorine dioxide as a side product renders these methods dangerous with many reports of explosions during attempts to form graphitic oxide. The use of potassium permanganate yields dimanganese heptoxide as the active species after reaction of manganite with sulphuric acid. This compound is also known to be explosive, however when the reaction is kept at low temperatures, the procedure is considered much safer than those involving chlorate.

$$1.\ KMnO_4 + 3H_2SO_4 \longrightarrow K^+ + MnO_3^+ + H_3O^+ + 3HSO_4^-$$

$$2.\ MnO_3^+ + MnO_4^- \longrightarrow Mn_2O_7$$

**Scheme 1.6.1 Reaction of potassium permanganate with sulphuric acid and formation of dimanganese heptoxide.**

A summary of the most common methods, old and new, for the production of graphitic oxide is given below (table 1.6.1).

**Table 1.6.1 Summary of the methods for the preparation of graphitic oxide including type of oxidant and the acid matrix.**

| Method | Oxidant | Acid matrix |
|---|---|---|
| **Brodie** | $KClO_3$ | Fuming $HNO_3$ |
| **Staudenmaier** | $KClO_3$ | $HNO_3$+H2$SO_4$ |
| **Hofmann** | $KClO_3$ | Conc $HNO_3$ + $H_2SO_4$ |
| **Hummers** | $KMnO_4$ +$NaNO_3$ | Conc. H2SO4 |
| **Tour** | $KMnO_4$ | $H_2SO_4$ +$H_3PO_4$ |

It should be noted that other methods are available for the production of graphene and graphitic oxide which do not require the intensive oxidation of graphite. These include mechanical exfoliation (scotch tape method), epitaxial growth[48,49], chemical vapour deposition (CVD)[50,51,52] and pyrolysis of biomass such as chitosan[53] or alginate[54,55]. These methods succeed in producing higher quality graphene due to the lower number of defects, however they fail in the production of large quantities. Direct exfoliation of graphite in solvents such as ionic liquids has also been observed however again this is on an unusable and often un-isolatable scale[56,57]. Thermal exfoliation of graphite results in weakening the interlayer Van der Waals forces and the production of highly expanded graphite which in turn can be easier manipulated into few layer graphenes[58].

**Table 1.6.2 Properties of graphite, graphitic oxide, graphene oxide and graphene.**

| | Surface area ($m^2g^{-1}$) | D-spacing (nm) | Hybridisation |
|---|---|---|---|
| **Graphite** | 8 | ~0.35nm | $sp^2$ |
| **Graphitic oxide** | 10-100 | ~0.7nm | $sp^2/sp^3$ |
| **Graphene oxide** | 1600-1800 | >1.1nm | $sp^2/sp^3$ |
| **Graphene** | 2620 | - | $sp^2$ |

Graphene oxide can be prepared from highly oxidised graphitic oxide simply by stirring and/or sonication in polar solvents. Dispersion of graphene oxide is facilitated by polar solvents and is often quoted in the range of 1-4 $mgmL^{-1}$ when water is used as a solvent.[59] However, these methods can result in damage to the graphene sheets[60] and ultimately reduction in the particle size and increase in overall particle size distribution[61,62]. The preparation of graphene from graphene or graphitic oxide can be achieved through chemical reduction utilising a number of reducing agents, the most popular of which is hydrazine monohydrate due to its low reactivity with water[63]. Reducing agents such as lithium aluminium hydride react with water and are therefore deemed unsuitable due to this being the most common and greenest solvent for the dispersion of graphene oxide. Hydrazine, although effective in reduction, can introduce heteroatom functionality into the framework which has a negative impact on the produced graphene's electronic properties[64]. Sodium borohydride can be used as an efficient reductant despite having partial reactivity with water. Using a high excess of borohydride results high quality reduced graphene oxide into which heteroatoms are not introduced[65]. The thermal reduction of graphitic oxide can be achieved through exposing the material to high temperatures of over 1000 °C. [66] However this method is uncommon in practice due to the damage of graphene sheets incurred from the release of carbon oxides on heating[67]. Electrochemical reduction[68] and use of strong base[69] have also been reported to be efficient methods for the reduction of graphene oxide.

### 1.7 Structure of graphitic oxide

Despite the structure of graphene being well understood, the structure of graphitic oxide is still much debated with many models having been proposed. Problems with accurate description of the material arise from the abundance of preparation methods, sources and types of graphite, and reproducibility. The most widely accepted and referred to model is the Lerf-Klinowski model[70] which describes a material which is partly formed of $sp^2$ hybridised carbon, as seen in graphene, and oxygen rich areas of $sp^3$ hybridised carbon. Initial oxidation of the graphite is said to form hydroxyl and epoxide groups on the basal plane of the lattice with further oxidation leading to breaking up of the sheets leaving carboxylic groups on the edges. Other less referred to models, such as Dekany[71], Nakajima-Matsuo[72], Hofmann[73], Reuss[74] and the Scholz-Boehm[75] models are depicted below (figure 1.7.1). These models differ in the amount of defects introduced into the lattice but with the major difference being in variation, position and abundance of functional groups. It is clear that the variety of preparation methods described in the previous section for the production of graphene, graphene oxide and graphitic oxide lead to inherently different surfaces. Furthermore the different approaches within methods such as chemical oxidation and reduction leads to increased variety of materials and therefore it is no wonder that multiple models have been theorised. This is where the strength of the Lerf-Kilinowski model lies as it describes general areas of varying oxidation and $sp^2/sp^3$ character on the basal planes and edges of the lattice. The model also takes into account features such as carboxylic groups and presence of hydrogen which others also fail to do.

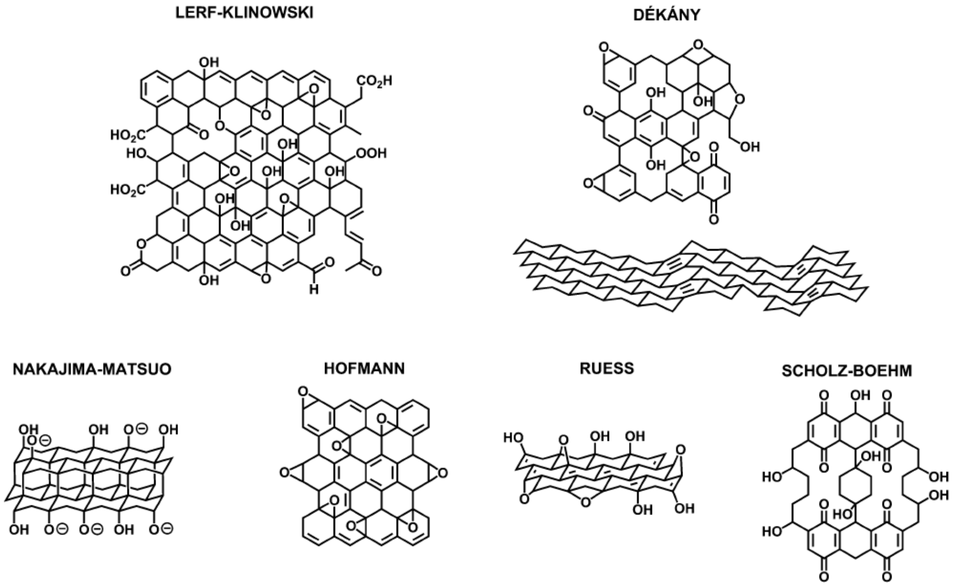

**Figure 1.7.1 Models of graphitic oxide**[76]

The variation between materials produced by different methods means that it is unlikely that a definitive model of graphitic oxide will be achieved. This is also impractical due to low reproducibility of extended structures from batch to batch of identical procedures. It is therefore far more useful to treat graphenes and graphitic oxides as a family of materials, using in-depth characterisation of prepared surfaces to understand the composition and functionality of each individual one. This can also be used to explain the adaptability of graphene-based materials to catalysis (section 1.8). Pumera *et al*[77] have pioneered the production and characterisation of graphitic oxides to study the effect of the identity of the oxidant and concentration of acid. The authors prepared graphitic oxide by Staudenmaier, Hofmann, Hummers and Tour methods. Characterisation by X-ray photoelectron spectroscopy (XPS) Electrical impedance spectroscopy (EIS) nuclear magnetic resonance (NMR) Fourier transform infrared spectroscopy (FTIR), Raman spectroscopy and electrochemical cyclic voltammetry (ECV) was conducted. Using these techniques, it was concluded that the properties of the received oxides were highly reliant on the identity of the oxidant. Methods which used potassium chlorate as oxidant (ST and HO) resulted in unique materials to those which used potassium permanganate (HU and TO) with respect to abundance and location of oxygen moieties. HU and TO methods produced highly oxidised materials which were abundant in carboxyl and carbonyl groups on the edges of the sheets. It was also noted through the electrochemical methods (EIS and CV) showed a distinct difference in heterogeneous electron transfer implicating the need for a distinct choice in preparation method for the future investigation for the use of graphitic oxide in electronics, electrocatalysis, optics and sensing. Thermal reduction of GOs produced by ST, HO and HU resulted in similar graphenes except for that produced by HU which was observed to contain nitrogen covalently incorporated into the lattice[78]. This material also exhibited superior electrochemical properties, reiterating the consequence of utilising chlorate or permanganate as oxidant.

The identity of the oxidant is not the only factor for producing uniquely functionalised GOs. Paul *et al.*[79] studied the importance of the carbon precursor and additives. Focusing on the particle size of graphite it was found that larger crystallites direct higher levels of oxidation onto the basal plane. Increased oxidation resulted in lattice strain and eventual breakup of the graphite sheets resulting in smaller crystallites. Also studied was the addition of sodium nitrate, which when partnered with larger graphites, resulted in highly oxidised and the smallest overall GO sheets. Sodium nitrate was thought to increase the interlayer distance facilitating oxidation of the basal plane rather than sheet edges. In a separate study, the choice of graphite source and the inherent defects of the graphite was shown to influence the chemical oxidative reactivity with respect to oxygen and hole transport[80].

### 1.8 Functionalisation of graphene and graphene oxide

The abundance of oxygen on GO in various functionalities lends this material to further functionalization and tethering. Production of chemically modified graphenes (CMGs) is most commonly achieved by utilising the carboxylic or epoxy groups on the GO surface. Treatment of the carboxylic groups with reagents such as thionyl chloride[81,82], 1-ethyl-3-(3-dimethylaminopropyl)-carbodiimide[83] and N,N'-dicyclohexylcarbodiimide[84] can enable the covalent tethering of amines or alcohols forming amide or ester linkages respectively. Simple ring opening of the epoxy group by the addition of amines can enable the tailoring of CMG properties such as dispersability[85,86] and stability[87] according to the amine used.

## 1.9 Carbocatalysis by graphitic oxide

Graphitic oxide has long been recognised for its oxidising properties[88], however, despite graphitic oxide being frequently prepared as an intermediate step *en route* to the production of graphene, it is only recently that its potential as a carbocatalyst has been realised. Bielawski and co-workers were some of the first to investigate GO's ability to catalyse oxidation and hydration reactions[89]. Their initial work focussed on the oxidation of benzyl alcohol to Benzaldehyde (Scheme 1.9.1).

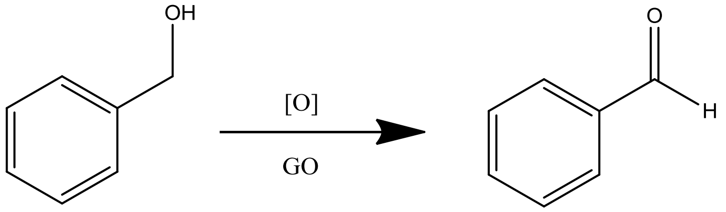

**Scheme 1.9.1 Oxidation of benzyl alcohol using graphitic oxide as catalyst**

The authors were able to conclude that the activity seen (24% conversion with 100 % selectivity to benzaldehyde after 24 hours at 100 °C, 20 wt% GO.) was indeed due to the GO rather than adhered metal contaminants on GO surface. This was studied by atomic adsorption and inductively coupled plasma mass spectrometry. Analysis by FTIR before and after reaction suggested a reduction in surface oxygen. However, activity after multiple reuses, partnered with no conversion being observed in the absence of atmospheric oxygen, confirmed that this process was catalytic rather than a stoichiometric titration of the surface oxygen. The further study of this reaction demonstrated GO's activity over a range of temperatures and loadings (25-100 °C, 5-200 wt%) although at low temperatures much higher loadings were required. The authors then extended this research to the oxidation of a variety of other cyclic alcohols and also alkenes, such as *cis*-stilbene to the corresponding dione (scheme 1.9.2) in which a 56 % conversion was achieved (24 hours at 100 °C with 200 wt% catalyst).

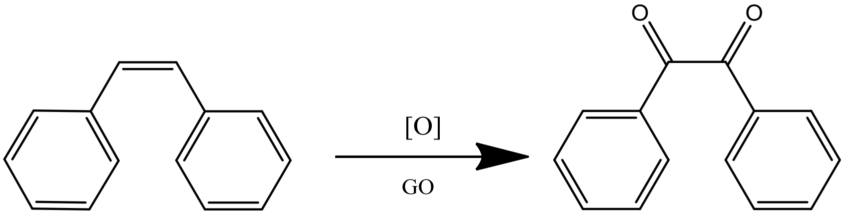

**Scheme 1.9.2 Oxidation of *cis*-stilbene using graphitic oxide as catalyst**

Many alkyne hydrations were also studied under the same conditions (24 h, 100 °C, GO 200 wt%) with high conversions being observed to the corresponding ketones particularly in phenylacetylene oxidation in which 98 % conversion was achieved. The acidic nature of the GO was said to be the key factor in alkyne hydration, which is otherwise known to be conducted in acidic media at 200 °C,[90],[91] however the authors noted that the presence of GO eradicated the need for acid and enabled the use of significantly milder conditions.

Since this work, a large number of reactions and transformations have been shown to be catalysed to some extent by the GO surface, either utilising its high surface acidity ($pK_a$ 3-4 in water) or oxygen functionality. The acidity of GO is said to arise as a result of the introduction of sulphate groups to the surface during the extensive Hummers oxidation. Garcia *et al* studied the epoxide ring opening using GO as an acid catalyst[92]. Styrene oxide was studied as an initial substrate for ring opening with methanol (scheme 1.9.3). The GO successfully catalysed this reaction with high conversions and selectivities which were unchanged over multiple uses. Filtering of the catalyst and continuation of the reaction resulted in no further conversions, confirming that reaction was due to GO catalysis and not leached species. The authors related their material to sulphated reduced graphene oxides which were previously shown to be useful for the esterification of acetic acid and hydration of propylene oxide[93] noting the more facile preparation of their material compared to hydrothermal synthesis in sulphuric acid.

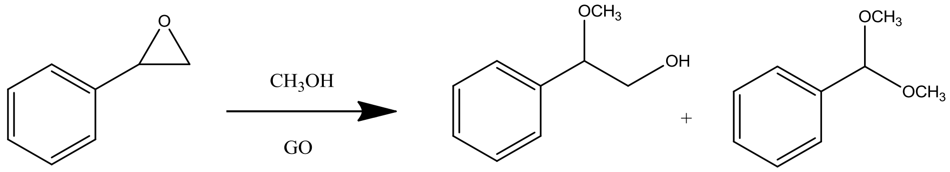

**Scheme 1.9.3 Ring opening of styrene oxide using graphitic oxide as acid catalyst**

The acidity of GO has also enabled its application to other reactions such as Friedel-Crafts additions[94], acetalization of aldehydes[95] and transformation of glucose and fructose to levulinic acid[96].

The presence of oxygen functional groups has also been shown to be crucial for a number of transformations including aqueous suphide oxidations[97], Michael additions[98], Aza-Michael additions[99], oxidation of amines to imines[100] and the previously described alcohol oxidations. In all cases the GO can be recovered and reused multiple times with little or no effect on conversion despite a slight reduction in the surface oxygen. Density functional theory (DFT) studies on the aerobic oxidation of benzyl alcohol oxidation have suggested that atmospheric oxygen can replenish active sites in a Mars van Krevelen type cycle[101]. Other DFT studies have shown that this GO may also be used for the dehydrogenation of propane to propene[102]. Although the activity of GO has been attributed to surface oxygen, it is still unclear in nearly all cases which functional group is the active species. Problems often arise when attempting to correlate activity with amount of surface oxygen or the presence of a particular group as it is difficult to obtain a species whereby a single functionality is present. Future work should attempt to address this issue for the development of highly active carbocatalysts. Research has also been conducted into the use of reduced graphene oxide for a number of oxidation[103,104] and reduction[105,106] reactions.

## 1.10 Epoxidation of alkenes

The epoxidation of alkenes is an extremely important chemical process due to the versatility of epoxides as intermediates in synthesis[107], the production of epoxy resins and adhesives and also for their use as additives in cosmetics in pharmaceuticals[108].

Historically, the production of epoxides followed multistep syntheses which involved the stoichiometric use of hazardous reagents and the production of unwanted by-products. Ethylene oxide is a classic example of this: Ethylene oxide is a huge commodity chemical due to its use in ethylene glycol formation and production of polyethers and polyurethanes. The large scale production of ethylene oxide through the epichlorohydrin process (scheme 1.10.1) resulted in large quantities of waste which had to be treated at a cost to the manufacturer. The use of chlorine and sodium hydroxide as stoichiometric reagents is also extremely unfavourable.

$$1.\ Cl_2 + NaOH \longrightarrow HOCl + NaCl$$

$$2.\ C_2H_4 + HOCl \longrightarrow CH_2Cl\text{-}CH_2OH$$

$$3.\ CH_2Cl\text{-}CH_2OH + 0.5Ca(OH)_2 \longrightarrow 0.5CaCl_2 + C_2H_4O + H_2O$$

$$4.\ Cl_2 + NaOH + 0.5Ca(OH)_2 + C_2H_4 \longrightarrow C_2H_4O + 0.5CaCl_2 + NaCl + H_2O$$

**Scheme 1.10.1 Epichlorohydrin process for production of ethylene oxide[109]**

The modern production of ethylene oxide utilises catalysis and oxygen for the direct synthesis from ethene and is an extremely atom efficient process compared to its predecessor. The epoxidation of ethene to ethylene oxide uses an α-alumina supported silver catalyst[110,111] and when promoted using small amounts of chlorine can achieve epoxide selectivites of up to 90%[112]. The ease of this epoxidation is largely due to the absence of an allylic hydrogen in ethene. Therefore, the epoxidation of higher olefins becomes much more difficult. Propene epoxidation is a much coveted process due to the high value of propylene oxide. Propylene oxide is needed for the production of polyurethane plastics, polyether polyols, propylene glycol polypropylene and propylene carbonate. The production of propylene oxide was until recently conducted in large amounts by the chlorohydrin process which forms hypochlorous acid *in situ* from chlorine and water. This results in large amounts of salt waste and the use of toxic chlorine.

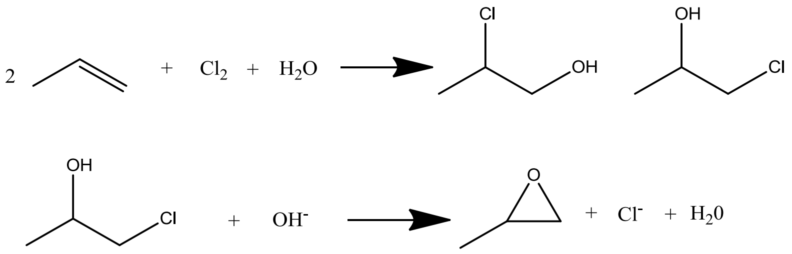

**Scheme 1.10.2 Chlorohydrin process for production of propylene oxide**

Other technologies for the production of propylene oxide involved the use of hydroperoxides ( tert-butyl, ethylbenzene and cumene hydroperoxide)[113,114,115,116,117,118]. However, these processes produce large amounts of by-products and if there is no commercial use, they need to be destroyed or recycled.

The most recent process developed for the production of propylene oxide is based on the use of TS-1 catalyst and stoichiometric amounts of hydrogen peroxide[119,120,121]. Despite this process being much cleaner than the chlorohydrin process, with the only by-product being water; it still requires large amounts of hydrogen peroxide which itself is a high value chemical. Therefore it is advantageous to obtain a process which, like in ethylene epoxidation, involves the direct oxidation using $O_2$ as the terminal oxidant or which produces the hydrogen peroxide *in situ*. This was first shown to be possible *via* the use of $H_2$ and $O_2$ gases and a supported palladium catalyst[122]. Various other research groups have extended this study utilising supported precious metal catalysts and mixtures of $H_2$ and $O_2$ for the *in situ* formation of hydrogen peroxide and subsequently epoxidation of propene. These include titania supported gold catalysts, studied by Haruta[123,124,125], bimetallic palladium-platinum catalysts supported on TS-1 developed by Holderich[126,127,128,129], and TS-1 supported gold catalysts studied by Delgass *et al.*[130] Further modifications and tuning of the supports have led to further increases in selectivity to the epoxide[131,132,133,134,135,136,137,138,139]. Hutchings *et al* also recently studied graphite supported gold-palladium catalysts for the epoxidation of propene using $O_2$ as the terminal oxidant[140]. However, radical initiators were required and upon their consumption, conversion stopped increasing.

The epoxidation of terminal alkenes other than propene has been attempted, however, to achieve high yields, stoichiometric reagents are often required such as in dec-1-ene epoxidation[141,142,143,144,145,146]. As with propene epoxidation, hydrogen peroxide can often be employed as an oxidant achieving moderate yields, and producing only water as a by-product. Dec-1-ene epoxidation under mild conditions has been studied by various groups utilising hydrogen peroxide as an oxidant[147,148,149,]. Other oxidants such as cumylhydroperoxide [150]and peracetic acid[151] have also been employed using $CuO/Al_2O_3$ and $Mn(ClO_4)_2$ catalysts respectively.

The direct use of oxygen as terminal oxidant is a much more attractive prospect for the epoxidation of alkenes due to the high atom efficiency and lack of unwanted by-products if high selectivities are achieved. It also provides a much cheaper and greener alternative to hydrogen peroxide and other expensive or toxic oxidants.

Hutchings *et al* have studied the epoxidation of cyclooctene and found that by employing catalytic amounts of radical initiators, atmospheric oxygen can be used as the terminal oxidant[152]. It was found that the use of tertiary–butyl hydroperoxide (TBHP) or hydrogen peroxide could initiate atmospheric oxygen and also achieve higher selectivities than is found in their absence. Similar epoxidation of other cyclic alkenes such as styrene was reported by Caps *et al.* who reinforced the theory that selectivity is dependent on the use of initiators[153,154,155,156]. It has also been shown that in the absence of radical initiators it is possible to epoxidise styrene using nanoparticulate gold, albeit with low selectivity[157,158].

Hutchings *et al.* continued the investigation of cycloalkenes and identified that there was a dependence on the ring size as to whether allylic oxidation or epoxidation pathways would proceed, concluding that cycloalkenes of $C_7$ or below would preferentially follow allylic oxidation[159]. Following this, hex-2-ene was also shown to be epoxidised using these gold catalysts in the presence of radical initiators[160]. A major finding was that on the removal of stabilisers found in cyclic alkenes, epoxidation can occur in the absence of radical initiators, however it was found that this is not the case for linear alkenes[161].

Hutchings *et al*. revisited cyclooctene epoxidation in order to assess the reusability of the supported gold catalyst[162]. The authors also proposed a mechanism for which the presence of TBHP assists epoxidation (figure 1.10.1). Here, the decomposition of TBHP to either a t-BuOO* or t-BuO* radical facilitates hydrogen abstraction from cyclooctene producing the allylic radical (1). Addition of atmospheric dioxygen leads to the peroxy radical (2) and on further reaction with another cyclooctene molecule results in the formation of the cylcooctene hydroperoxy species[163] (3) and another allylic radical (1) creating a cycle in which (3) and (1) are sustained. The hydroperoxy species was then suggested to dissociate on gold in a similar way to that of hydrogen peroxide[164] forming a hydroxyl radical and a cyclooctenyloxy radical (4). The formation of (4) on the gold is crucial for the epoxidation of cyclooctene as this can only be formed by the combination of (4) with a cyclooctene molecule to form (5) and the subsequent cleavage to form the epoxide and another molecule of (1). Abstraction of hydrogen from cyclooctene by the cyclooctenyloxy radical instead of combination with the double bond leads to the formation of an allylic alcohol. However the authors noted that the major product in the presence of TBHP was the epoxide.

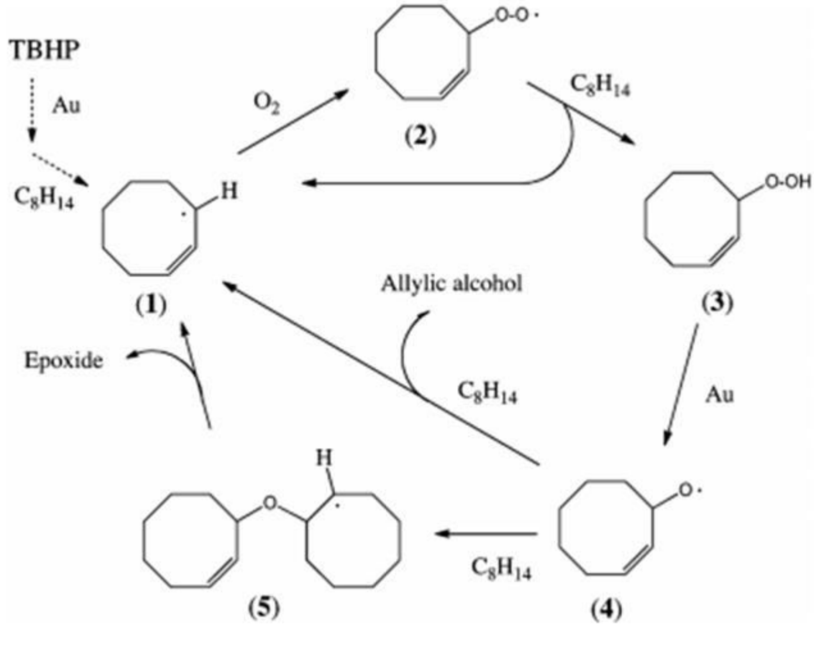

**Figure 1.10.1 Proposed reaction mechanism of cyclooctene epoxidation in the presence of gold and TBHP[162].**

The importance of radical initiators for the epoxidation of cyclohexene was noted by Corma *et al*. The epoxidation using oxygen and a ceria supported gold catalyst was totally dependent on the use of azobisisobutylnitrile (AIBN)[165].

The study of linear terminal alkenes was extended to dec-1-ene by Hutchings *et al*. where it was shown that aerobic oxidation can occur at mild temperatures using various radical initiators and a graphite supported gold catalyst[166]. The preferred initiator in this case was AIBN due to the inability of this species to act directly as an oxygenate, as with TBHP and benzoyl peroxide (BPO) initiators.

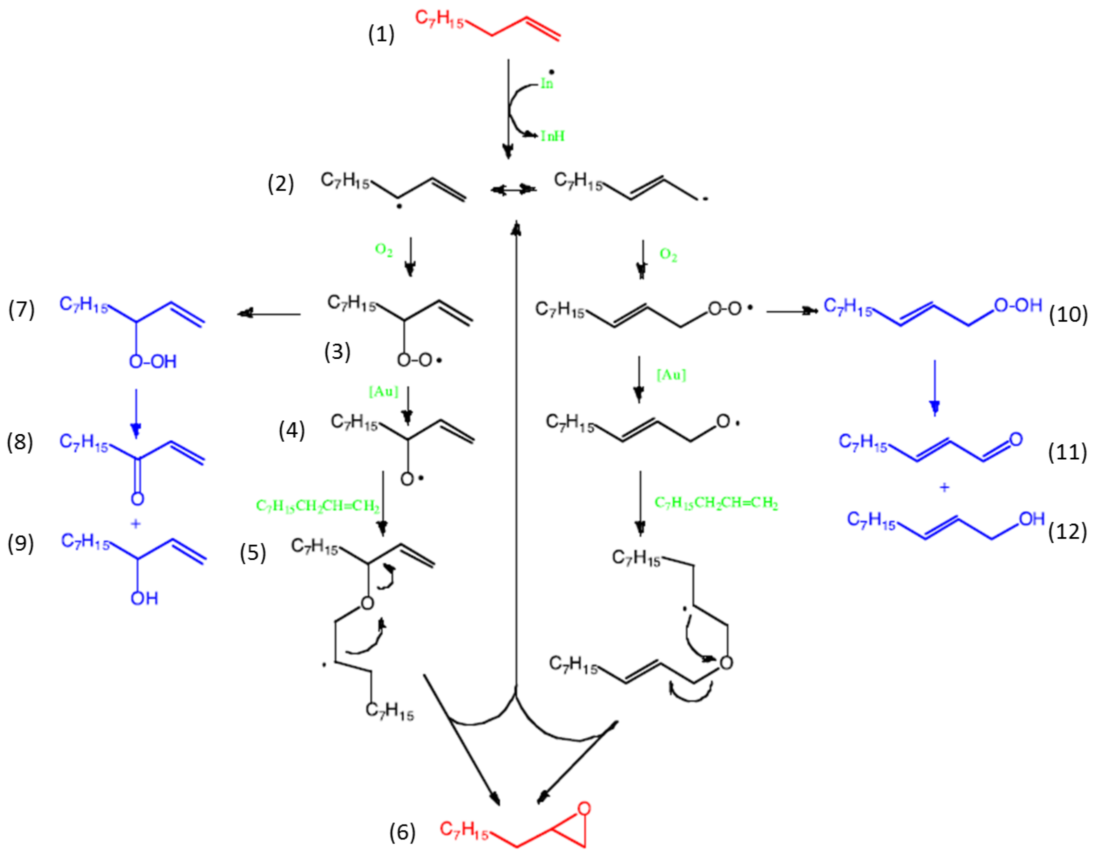

**Figure 1.10.2 Proposed reaction mechanism for the epoxidation of dec-1-ene in the presence of dec-1-ene and AIBN[168].**

The mechanism was found to be similar as that proposed for cyclooctene epoxidation (figure 1.10.1). In this case (figure 1.10.2) AIBN abstracts an allylic hydrogen from a molecule of dec-1-ene (1) forming an allylic decenyl radical (2). The addition of atmospheric oxygen forms a peroxy species (3) which in the presence of gold, fragments to form a 3-dec-1-enyloxy radical (4). Reaction with another molecule of dec-1-ene and subsequent fragmentation leads to the formation of the epoxide (6) and another allylic dec-1-enyl radical. The presence of gold was suggested to be crucial for this reaction pathway, providing a surface for the fragmentation of the peroxyspecies. In the absence of gold the build-up of this peroxy species leads to allylic abstraction from dec-1-ene molecules. The subsequent formation of hydroperoxide (7) leads to the production of unwanted allylic products dec-1-ene-2-one (8) and dec-1-ene-2-ol (9) through a Russell termination[167]. This explains the higher selectivities and conversions seen in the presence of gold. It was also suggested that a parallel mechanism which involved the canonical dec-2-enyloxy radical led to similar formation of the epoxide, however in this case the absence of gold leads to the formation of dec-2-ene-1-one (11) and dec-2-ene-1-ol (12) allylic products. The absence of the 2,3-epoxydecane was confirmed by GC-MS which the authors described as a surprise result due to the expected allylic hydrogen abstraction occurring at the 3-position leading to possible 2,3-epoxide formation. However, the absence of this epoxide led to the suggestion that oxygen attack at the 1 position could lead to the generation of a primary allylic hydroperoxide and subsequent formation of the aldehyde and furthermore the peracid, a process previously described by Mukaiyama *et al* using nickel catalysts for epoxide formation[168]. Here the presence of peracid would lead to formation of equimolar amounts of 1,2-epoxides and dec-2-enoic acid.

Hutchings *et al*. continued this study into the effect of *in situ* generated oxidants for dec-1-ene epoxidation[169]. This was investigated by the addition of aldehydes to the reaction for the *in situ* formation of the peracid for subsequent epoxide formation. The authors suggested a mechasim for the effect of addition of various aldehydes (figure 1.10.3) in the presence of radical initiators. Here, hydrogen abstraction by the initiator leads to the formation of an acyl radical (R-CO*) and upon oxygenation forms the peroxy acyl radical (R-CO-O*). The *in situ* formation of this peroxy radical can lead to reaction with a molecule of dec-1-ene and upon fragmentation leads to equimolar amounts of 1,2-epoxide and a carboxyl radical (R-CO-O*). The authors noted that depending on the identity of the aldehyde, multiple mechanistic pathways were available in which varying molar ratios of the epoxide were produced with respect to the initial amount of added aldehyde. For $R=R'CH_2$ it was suggested that decarboxylation is likely to be the fastest process and therefore produces carbon dioxide and an alkyl radical. After reaction of this alkyl radical ($R\text{-}CH_2*$) with oxygen ($RCH_2\text{—}O\text{-}O*$), allylic abstraction to form the hydroperoxy species ($RCH_2\text{-}O\text{-}OH$) and fragmentation can reproduce the initial aldehyde RCHO. Thus forming a cycle in which aldehyde is continually regenerated and further epoxidation reactions can occur. This was used to explain how the aldehyde is not just used as a sacrificial oxidant, as suggested by previous studies, and acquired concentrations of the epoxide exceed that of the added aldehyde. For aromatic or alkenyl R groups, a different pathway was suggested in which allylic hydrogen abstraction is favoured over the loss of $CO_2$ resulting in the formation of equimolar amounts of the carboxylic acid and epoxide. The conclusions offered by the researchers proposed that although addition of aldehyde was shown to be non-stoichiometric and in part catalytic, this was not seen to be continuous due to the presence of various reaction pathways and termination steps.

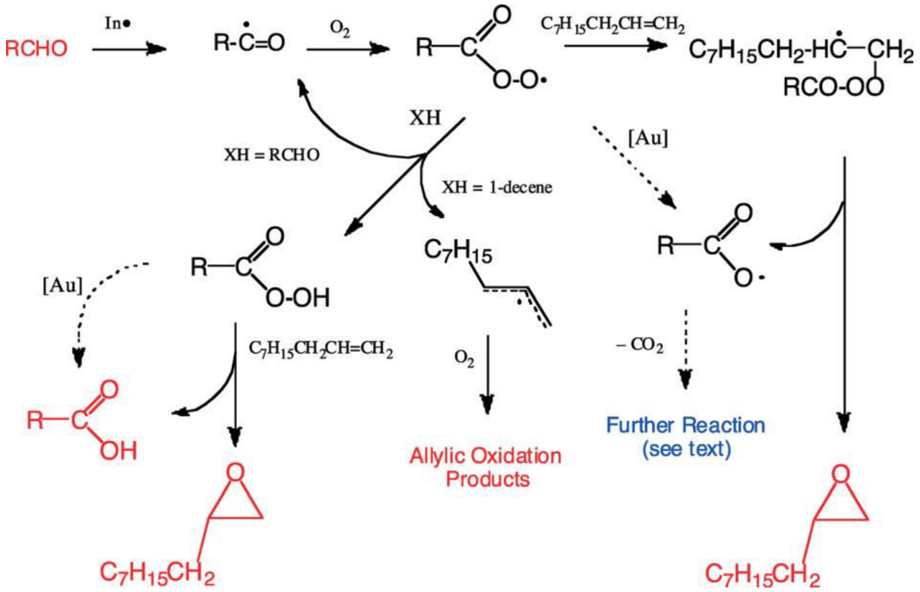

**Figure 1.10.3 Suggested mechanism of dec-1-ene epoxidation with addition of aldehydes**[169]

In summary, the epoxidation of α-alkenes, an industrially and synthetically important process, has been studied by many research groups. Various catalytic systems have been employed in order to provide cleaner technologies than the deleterious historical methods. The most popular method involves the stoichiometric use of hydrogen peroxide as an oxidant and indeed this has been scaled up for the industrial production of propylene oxide over a TS-1 catalyst. However the use of hydrogen peroxide is not entirely favourable due to the peroxide also being a valuable chemical. The *in situ* formation of hydrogen peroxide offers an alternative method, however current catalysts operate at uneconomically low conversions. The use of other peroxides and sacrificial oxidants has also been studied, however similar low yields and the equimolar production of by-products limits this method. The use of atmospheric oxygen as an oxidant is of course most advantageous due to its low cost and high abundance. However, for this to occur at mild temperatures, atmospheric oxygen must be activated using radical initiators which are themselves hazardous in large amounts and must be considered if this is to be scaled up. These methods also produce low conversions for linear alkenes. Despite some additives achieving higher than stoichiometric yields of the epoxide in the presence of catalyst and oxygen and initiators, there is no current system which enables the use of atmospheric oxygen as the sole oxidant and in the absence of radical initiators. The following study addresses the latter of these points attempting to, at first increase conversions and selectivities in the presence of initiators, and ultimately develop a catalyst which is active in their absence.

### 1.11 References

---

1 G. Rothenberg, *Catalysis*, Wiley-VCH, *Weinheim*, 2008, 2-3.

2 RA. Sheldon, I. Arends, U.Hanefeld, *Green Chemistry and Catalysis*, Wiley-VCH, Weinheim, 2007, 1-2.

3 J.J Berzerlius, *Edinburgh New Philosophical Journal*, 1836, XXI, 223.

4 I. Chorkendorff, J.W.Niemantsverdriet, *Concepts of modern catalysis and kinetics*, Wiley VCH, Weinheim, 2003, 4.

5 F.Moreau, G.C Bond, A.O. Taylor, *Journal of Catalysis,* 2005, **231**, 105.

6 M. Haruta, T. Kobayashi, H. Sano, N. Yamada, *Chemistry Letters* 1987, **405.**

7 G.J. Hutchings, *Journal of Catalysis* 1985, **96**, 292.

8 H.Sakurai, S.Tsubota, M.Haruta, *Appl Catal*. A, 1993, **102**, 125.

9 R.Si, M.Flytzani-Stephanopoloulos, *Angew.Chem.Int.Ed*., 2008, **47**, 2884.

10 Q.Fu, H.Saltsburg, M. Flytzani-Stephanopoloulos, *Science*, 2003, **301**, 935 .

11 A.Ueda, M.Haruta, *Gold Bulletin*, 1999, **32**, 3-11.

12 S,Tsubota, M.Haruta, T.Kobayashi, A.Ueda, Y.Nakahara, *Studies in surface science and catalysis*, 1991, **63**, 695.

13 G.C. Bond, D.T, Thompson, *Catalysis Reviews-Science and Engineering*, 1999, **41**, 319-388.

14 S. Navalon, A. Dhakshinamoorthy, M. Alvaro, H. Garcia, *Chemical reviews*, 2014, **114**, 6179-6212.

15 A.Kutzelnigg, *Ber. Dtsch. Chem. Ges. B*, 1930, **63**, 1753-1758.

16 I.M. Kolthoff, *J. Am. Chem. Soc*, 1932, **54**, 4473-4480.

17 D.R.Dreyer, C.W.Bielawski, *Chem.Sci*., 2001, **2**, 1233.

18 E.K. Rideal, W.M.Wright, *J.Chem.Soc.Trans*, 1925, **127**, 1347-1357.

19 E.K.Rideal, W.M. Wright, *J.Chem.Soc*, 1926, **129**, 1813-1821.

20 E.K.Rideal, W.M Wright, *J.Chem.Soc*, 1926, **129**, 3182-3190.

21 T.G. Alkhazov, A.E. Lisovskil, T.Kh.Gulakhmedova, *React.Kinet.Catal.Lett*., 1979, **12**, 189-193.

22 H.H. Byung, H.S.Dae, Y.C.Sung, *Tetrahedron Lett*, 1985, **26**, 6233-6234.

23 S.Lijima, *Nature*, 1991, **354**, 56-58.

24 H.W.Kroto, J.R.Heath, S.C.O'Brien, R.F.Curl, R.E.Smalley, *Nature*, 1985, **318**, 162-163.

25 K.S. Novoselov, A.K.Geim, , S.V. Morozov, D.Jiang, Y.Zhang, S.V.Dubonos, I.V.Grigorieva, A.A.Firsov, *Science*, 2004, **306**, 666-669.

26 L.Feng, Z.Liu, *Nanomedicine*, 2011**, 6**, 317-324.

27 X.Liu,B.Frank,W.Zhang, T.P.Cotter, R.Schlogl, D.S.Su*, Angewandte Chemie*, 2011,**50**, 3318-3322.

28 J.Zhang, X.Liu, R.Blume, A.Zhang, R.Schlogl, S.SDang, *Science*, 2008, **322**, 73-77.

29 X.Liu, D.S.Su, R.Schlogl, *Carbon*, 2008, **46**, 547-549.

30 E.Flahaut, A.Govindaraj, A.Peigney,C.Laurent, A.Rousset,C.N.R.Rao, *Chemical physics*, letters, 1999, **300**, 236-242.

31 H.Garcia, *Advances in Chemistry*, 2014**, 2014**, ID.906781.

32 V.Schwartz, W.Fu, Y.T.Tsai, *ChemSusChem*, 2013, **6**, 840-846.

33 Y.Gao, D.Ma, C.Wang, J.Guan, X.Bao, *Chemical Communications*, 2011, **47**, 2432-2434.

34 C.Lee, X.Wei, J.W.Kysar, J.Hone, *Science*, 2008, **321**, 358-388.

35 S.Pisana, M.Lizzeri, C.Casiraghi, K.S.Novoselov, A.K.Geim, A.C.Ferrari, F.Mauri, *Nat.Mater*, 2007**, 6**, 198-201.

36 A.A.Balandin, S.Ghosh, W.Bao, I.Calizo, D.Teweldebrhan, F.Miao, C.N.Lau, *Nano Lett*, 2008, **8**, 902-907.

37 S.V.Morozov, K.S. Novoselov, M.I.Katsnelson, F.Schedin, D.C.Elias, J.A.Jaszczak, A.K.Geim, *Phys. Rev. Lett*, 2008, **100**, 016602.

38 S.Park, R.S.Ruoff, *Nat.Nanotechnol*., 2009, **4**, 217-224.

39 H.K.Chae, D.Y.Siberio-Perez, J.Kim, Y.Go, M.Eddaoudi, A.J.Matzger, M.O'Keeffe, O.M.Yaghi, *Nature*, 2004, **427**, 523-527.

40 F.Schwierz, *Nat.Nanotechnology*, 2010, **5**, 487-496.

41 G.Jo, M.Choe, S. Lee, W.Park, Y.H.Kahng, T.Lee*, Nanotechnology*, 2012, **23**, 112001

42 N.Mohanty, V.Berry, *Nano Letters*, 2008, **8**, 4469-4476.

43 B.C. Brodie, *Philos. Trans. R. Soc. London*, 1859, **149**, 249-259

44 L.Staudenmaier*, Ber. Dtsch. Chem. Ges*. 1898, **31**, 1481-1487.

45 U.Hofmann, E.Konig, *Z.Anorg, Alg, Chem*, 1937, **234**, 311-336.

46 W.S. Hummers Jr, R.E. Offeman, *J. Am. Chem. Soc*, 1958, **80**, 1339.

47 D.C. Marcano, D.V. Kosynkin, J.M Berlin, A. Sinitskii, Z. Sun, A. Slesarev, L.B. Alemany, W. Lu, J.M Tour, *ACS Nano*, 2010, **4**, 4806-4814.

48 C.Berger, Z.M.Song, X.B.Li, X.S.Wu, A.Y.Ogbazghi, R.Feng, Z.T.Dai, A.N.Machenkov, E.H.Conrad, P.N.First, W.A.De Heer*, J.Phys.Chem B*, 2004, **108**, 19912-19916.

49 C.Berger, Z.M.Song, X.B.Li, X.S.Wu, N.Brown, C.Naud, D.Mayou, T.B.Li, J.Hass, A.N.Marchnkov, E.H.Conrad, P.N.First, W.A.De Heer, *Science*, 2006, **312**, 1191-1196.

50 L.G.De Arco, Y.Zhang, A.Kumar, C.Zhou, *IEEE Trans.Nanotechnol*.2009**, 8**,135-138.

51 A.Reina, X.Jia, J.Ho, D.Nezich, H.Son, V.Bulovic, M.S.Dresselhaus, j.Kong*, Nano Lett*. 2009, **9**, 30-35.

52 C.Mattevi, H.Kim, M.Chhowalla, *J.Mater.Chem*. 2011, **21**, 3324-3334.

53 A.Primo, P. Atienzar, E.Sanchez, J.MDelgado, H.Garcia, *Chemical communications*, 2012, **48**, 9254-9256.

54 P.Atienzar, A.Primo, C.Lavorato, R.Molinari, H.Garcia*, Langmuir*, 2013, **29**, 6141-6146.

55 A.Primo, A.Forneli, A.Corma, H.Garcia, *ChemSusChem*, 2012, **5**, 2207-2214.

56 S.Zhang, M.S.Miran, A.Ikoma, K.Dokko, M.Watanabe*, J.Am.Chem.Soc*.2014, **136**, 1690.

57 P.Bhunia, E.Hwang, Y.Yoon, E.Lee, S.Seo, H.Lee, *Chem.Eur.J*.2012, **18**, 12207.

58 W.Qian, S.Cottingham, J.Jiao, Appl.Surf.Sci, 2013, **275**, 342.

59 Y.Si, E.T.Samuski, *Nano Lett*., 2008**, 8**, 1679-1682.

60 J.I.Paredes, S.Villar-Rodil, A.Martinez-Alonso, J.M.D.Tascon*, Langmuir*, 2008, **24**, 10560-10564.

61 H.A.Becerril, J.Mao, Z.Liu, R.M.Stoltenberg, Z.Bao, Y.Chen*, ACS Nano*, 2008, **2**, 463-470.

62 C.Gomez-Navarro, R.T.Weitz, A.M.Bittner, M. Scolari, A.Mews, M.Burghard, K.Kem, *Nano Lett.*, 2007, **7**, 3499-3503.

63 S.Stankovich, D.A.Dikin, R.D.Piner, K.A.Kohlhaas,A.Kleinhammes, Y.Jia,Y.Wu, S.T.Nguyen, R.S.Ruoff, *Carbon*, 2007, **45**, 1558-1565.

64 S.J.Kanh, C. Kocabas, T.Ozel, M.Shim, N.Pimparkar, M.A.Alam, S.V.Rotkin, J.A.Rogers*, Nat. Nanotechnol.*, 2007, **2**, 230-236.

65 H.-J.Shin, K.K.Sim, A.Benayad, S.-M.Yoon, H.K.Park, I.-S. Jung, M.H. Jin, H.-K.Jeong, J.M.Kim, J.-Y. Choi, Y.H. Lee, *Adv, Funct. Mater*., 2009, **19**, 1987-1992.

66 H.P. Boehm, A.Clauss, G.O. Fischer, U.Hofmann, *Z.Anorg.Allg.Chem*., 1962, **316**, 119-127.

67 K.N. Kudin, B.Ozbas, H.C. Schiepp, R.K. Prud'homme, I.A.Aksay, R.Car, *Nano Lett.,* 2008, **8**, 36-41.

68 M.Zhou, Y.Wang, Y.Zhai, J.Zhai, W.Ren, F.Wang, S.Dong, *Chem-Eur.J.*, 2009, **15**, 6116-6120.

69 X.Fan, W.Peng, Y.Li, X.Li, S.Wang, G.Zhang, F.Zhang, *Adv.Mater.*,2008, **20**, 4490-4493.

70 A.Lerf,H.He, M.Forster, J.Kilnowski*, J.Phy.Chem.B*, 1998, **102**, 4477-4482.

71 T.Szabo, O.Berkesi, P.Forgo, K.Josepovetis, Y.Sanakis, D.Petridis, I.Dekany, *Chem. Mater*. 2006, **18**, 2740-2749.

72 T.Nakajima, A.Mabuchi, R.Hagiwara, *Carbon*, 1988,**26**,357-361.

73 U.Hofmann, R.Holst, *Ber.Dtsch.Chem.Ges*.1939,**72**,754-771.

74 G.Reuss, *Monatsh.Chem*.1947,**76**,381-417.

75 W.Scholz,H.P.Boehm*, Z.Anorg.Allg.Chem*.1969, **369**,327-340.

76 D.R. Dreyer, A.D.Todd, C.W.Bielawski*, Chem.Soc.Rev*, 2014, **43**, 5288-5301.

77 C.K.Chua, Z.Sofer.M.Pumera, *Chem.Eur.J*.2012, **18**, 13453-13459.

78 H.L.Poh, F.Sanek,A.Ambrosi, G.Zhao,Z.Sofer, M.Pumera, *Nanoscale*, 2012**, 4**, 3515-3522.

79 D.R.Chowdhury, C.Singh, A.Paul*, RSC Adv*,2014,**4**,15138.

80 Z.L.Chen, F.Y.Kam, R.G.S.Goh, J.Song, G.K.Lim, L.L.Chua, *Chem. Mater*.2013, 2944-2949.

81 S.Niyogi, E.Bekyarova, M.E. Itkis, J.L.McWilliams, M.A.Hamon, R.C.Haddon, *J.Am.Chem.Soc.*, 2006, **128**, 7720.

82 Y.Xu, Z.Liu, X.Zhang, Y.Wang, J.Tian, Y.Huang, Y.Ma, X.Zhang, Y.Chen, *Avd.Mater.*, 2009, **21**, 1-5.

83 Z.Liu, J.T.Robinson, X.Sun, H.Dai, *J.Am.Chem.Soc.*, 2008**, 130**, 10876-10877.

84 L.M.Veca, F.Lu, M.J.Meziani, L.Cao, P.Zhang, G.Qi, L.Qu, M.Shrestha, Y.-P.Sun, *Chem. Commun.*, 2009, 2565-2567.

85 S.Wang, P.-J.Chia, L.-L.Chua, L.-H. Zhao, R.-Q.Png, S.Sivaramakirshnan, M.Zhou, R.G-s.Goh, R.H.Friend, A.T.S. Wee, P.K.-H. Ho, *Adv. Mater.*, 2008, **20**, 3440-3446.

86 H.Yang, C.Shan, F.Li, D.Han, Q.Zhang, L.Niu, *Chem.Commun.*, 2009, 3880-3882.

87 H.Yang, F.Li, C.Shan, D.Han, Q.Zhang, L.Niu, A.Ivaska, *J.Mater.Chem.*,2009, **19**, 4632-4638.

88 H.P. Boehm, A.Clauss, G.Fisher, U.Hofmann, *Fifth Conference on Carbon*, University park, Pennsyvania, 1962.

89 D.R.Dreyer, H.-P. Jia, C.W.Bielawski, *Angew.Chem., Int. Ed.*,2012, **49**, 6813-6816.

90 N.Manshe, D.Reshef, Y.Shvo*, J.Org.Chem*. 1991, **56**, 2912-2914.

91 J.An, L.Bagnell, T.Cableweski, C.R.Strauss, R.W.Trainor, *J.Org, Chem*, 1997**, 62**, 2505-2511.

92 A.Dhakshinamoorthy, M.Alvaro, P.Concepcion, V.Fornes, H.Garcia, *Chem.Commun*., 2012, **48**, 5443-5445.

93 F.Liu, J.Sun, L.Zhu, X.Meng, X.Mu, *J.Mater.Chem*., 2012, **22**, 1283.

94 A.V.Kumar, K.R.Rao, *Tetrahedron Lett*., 2011, **52**, 5188-5191.

95 A.Dhakshinamoorthy, M.Alvaro, M.Puche, V.Formes, H.Garcia, *ChemCatChem*, 2012, **4**, 2026.

96 P.P.Upare, J.-W.Yoon, M.-Y.Kim, H.-Y.Kang,D.Hwang, Y.K.Hwang, H.H.Kung, J.-S.Chang, *GreenChem*, 2013, **15**, 2935.,

97 B.R.S.Lemos, I.F.Teixeira, B.FMachado, M.R.A.Alves, J.P.De Mesquita, R.R.Ribeiro, R.R.Basca, P.Serp, R.M.J.Lago, *Mater.Chem*.2013, **1**,9491.

98 Y.Kim, S.Some, H.Lee, *Chem.Commun*, 2013, **49**, 5702. .

99 S.Verma, H.P.Mungse, N.Kumar, S.Choudhary, S.L.Jain, B.Sain, O.P.Khatri, *Chem.Commun*, 2011, **47**, 12673.

100 C.Su, M.Acik, K.Takai, J.Lu, S.J.Hao, Y.Zheng, P.Wu, Q.Bao, T.Enoki, Y.-J.Chabal, K.P.Loh. *Nat.commun*.,2012**, 3**, 2315.

101 D.W.Boukhvalov, D.R.Dreyer, C.W.Bielawski, Y.-W.Son, *ChemCatChem*. 2012, **4**, 1844.

102 S.Tang, Z.Cao,*Phys.Chem.Chem.Phys.* 2012, **14**, 16558.

103 J.-H.Yang, G.Sun, Y.Gao, H.Zhao, P.Tang, J.Tan, A.-H.Lu, D.Ma, *Energy Environ.Sci*., 2013,**6**,793.

104 H.Sun, S.Liu, G.Zhou, H.M.Ang,M.O.Tade, S.Wang, *ACS Appl.Mater.Interfaces*, 2012, **4**, 5466.

105 Y.Gao, D.Ma, C.Wang, J.Guan, X.Bao, *Chem.Commun*.2011,**47**,2432.

106 T.L.Perhun, I.B.Bychko, A.I.Trypolsky, P.E.Strizhak, *Theor.Exp.Chem*. 2013, **48**, 367.

107 Kirk-Othmer, *Encyclopedia of chemical technology*, J.Wiley and sons, New York, 1994, **9**, 915.

108 A.Ansmann, R, Kawa, M.Neuss, US Patent 7083780 B2 Aug 1 2006 assigned to Cognis Deutschland.

109 I. Chorkendorff, J.W.Niemantsverdriet, *Concepts of modern catalysis and kinetics*, Wiley VCH, Weinheim, 2003, 8-9.

110 P. Christopher, S.Linic*, J.Am.Chem.Soc*, **130**, 11254-11265.

111 H.Pines, D.D.Eley, P.B. Weisz, *Advances in Catalysis*, Academic Press, New York, 1987, 265-321.

112 M.O.Ozbek, R.A.Van Santen, *Catal.Lett*, 2013, **143**, 131-141

113 J.P.Schmidt, R.L.Bobeck, FR Patent 1 539 885, 1968.

114 J.P. Schmidt, US Patent 3 988353, 1976, to Oxirane Co.

115 F.Wattimena, H.P.Wulff, GB Patent 1 249079, 1971, to Shell oil Co.

116 J.Tsuji, J.Yamamoto, M.Ishino, N.Oku, Development of new propylene manufacturing processes, Sumitomo Kagaku, Osaka, Japan, 2006, **1**, 4-10.

117 J.Tsuji, J.Yamamoto, A.Corma, F.Rey, US Patent 6 211 388, 1988 to Sumitomo Chemical Company, Ltd.

118 M.T, Navarro, A.Corma, J.L.Jorda F.Rey, WO 2000007710 A2, 2000.

119 M.G.Clerici, G.Bellusi, U.Romano, *J.Catal*, 1991, **129**, 159-167.

120 M.G.Clerici, P.Ingallina, *J.Catal*, 1993, **140**, 71.

121 B.Notari, *Catal.Today*, 1993, **18**, 163.

122 S.Sato, T.Miyake, JP Patent 04 352 771, 1992 to Tosoh Corp.

123 T.Hayashi, M.Haruta, Shokubai, 1995, **37**, 72.

124 T.Hayashi, K.Tanaka, M.Haruta, *J.Catal*.1998, **178**, 566.

125 M.haruta, S.Tsubota, T.Hayashi, JP Patent 2 615 432, 1996 to AIST.

126 R.Meiers, U.Dingerdissen, W.F.Holderich, *J.Catal*., 1988, **176**, 376.

127 W.F.Holderich, F.Kollmer*, Pure Appl.Chem*., 200, **72**, 1273.

128 W.F. Holderich, *Appl.Catal.A.Gen*.,2001, **213**, 163.

129 W.Laufer, W.F.Holderich, *Appl.Catal.A.Gen*, 2001, **213**, 163.

130 B.Taylor, J.Lauterbach, W.N.Delgass, *Appl.Catal.A:Gen*, 2005, **291**, 188.

131 T.A.Nijhuis, T.Visser, B.M.Weckhuysen, *J.Phys.Chem.B*, 2005, **109**, 19309.

132 T.A.Nijhuis, B.J.Huizinga, M.A.Makkee, J.A.Moulijn*, Ind.Eng.Chem.Res*., 1999, **38**, 884.

133 B.S.Uphade, S.Tsubota, T.Hayashi, M.Haruta, *Chem.Lett*.,1998, 1277.

134 T.A.Nijhuis, T.Visser, B.M.Weckhuysen, *Angew.Chem., Int.Ed*.,2005, **44**, 1115.

135 A.Zwijnenburg, M.Makkee, J.A.Moulijn, *Appl.Catal., A*. 2004, **270**, 49.

136 C.Qi, T.Akita, M.Okumura, K.Kuraoka, M.Haruta, *Appl.Catal.A*. 2003, **253**, 75.

137 A.K.Sinha, S.Seelan, M.Okumura, A.Akita, S.Tsubota, M.Haruta, *J.Phys.Chem.B*,2005,**109**,3956.

138 B.Chowdury, J.J.Bravo-Suarez,K.K.Bando, T.Fujitani, S.T.Oyama, *J.Catal*., 2007, **250**,235.

139 E.Sacaliuc, A.M.Beale, B.M.Weckhuysen, T.A.Nijhuis, *J.Catal*.,2007,**248**,235.

140 U.N.Gupta, R.L.Jenkins, N.F.Dummer, D.Bethell, G.J.Hutchings, *Catal Lett*., DOI 10.1007/s10562-014-1439-6.

141 P.Bassler, M.Weidenbach, H.Goebbel, *Chem.Eng.Trans*. « 010, **21**, 571-576

142 E.L.Lines, R.J.Fairbrother, J.A.Herbst, US 4157346, 1979, assigned to Olin Corporation.

143 M.Rameswaran, R.N Cochran, US 5081267, 1992. Assigned to Arco Chemical technology.

144 T.A. Nijhuis, M. Makkee, J.A.Mouljin, B.M. Weckhuysen, *Ind. Eng.Chem.Res*, 2006, **45**, 3447-3459.

145 K. Weissermel, H.J.Arpe, Industrial Organic Chemical, VCH Publisher Inc. ,New York, 3rd, 1993, 141-264.

146 J.G.Zajaceck, D.Pa, G.LCrocco, US 5214168, 1993, assigned to Arco Chemical technology.

147 P.P.Pescarmona, P.A.Jacobs, *Catal.Today*, 2008 , **137**, 52-60.

148 D.Mandelli, M.C.A. Van van Vilet, R.A. Sheldon, U.Schuchardt, *Appl.Catal.A:Gen*, 2001, **219**, 209-213.

149 B.S.Lane, K.Burgess, *J.Am.Chem Soc*., 2001, **123**, 2933-2934.

150 N.Scotti, N. Ravasio, N.F. Zaccheria, R.Psaro, C.Evangelisti, *Chem.Commun*, 2013, **49**,1957.

151 K.P.Ho, W.L.Wong, K.M.Lam, .C.P.lai, T.H.Chan, K.Y.Wong, *Chem Eur J*.,2008, **14**, 7988-7996.

152 M.D.Hughes, Y.-J.Xu,P.Jenkins, P.McMorn,P.Landon,D.I.Enache,A.F.Carley, G.A.Attard, G.J.Hutchings, F.King, E.H.Stitt,P.Johnson,K.Griffin, C.J.Kiely,Nature, 2005, **437** ,1132.

153 P.Lignier, F.Morfin, S.Mangematin, L.Massin, J.-L.Rousset, V.Caps, *Chem.Coimmun*., 2007, 186.

154 P.Lignier, S.Mangematin, F.Morfin, J.-L.Rousset, V.Caps, *Catal.Today*, 2008, **138**, 50.

155 P.Lignier, F.Morfin,L.Piccolo,J.-L.Rousset,V.Caps,*Catal.Today*, 2007, **22**, 284.

156 D.Gajan,K.Guillois,P.Delichere,J.-M.Basset, J.-P.Candy, V.Caps, C.Coperet, A.lesage, L.Emsley, *J.Am.Chem.Soc*.,2009, **131**, 14667.

157 X.Deng, C.M.Friend,*J.Am.Chem.Soc*., 2005, **127**, 17178.

158 M.Turner, V.B.Golovko, O.P.H.vaughan, P.Abdulkin, A.Berenguer-Marcia,M.S.Tikhov, B.F.G.Jonson, R.M.Lambert*, Nature*, 2008, **454**, 981.

159 H.Alshammari, P.J.Medziak, D.W.Knight, D.J.Willock, G.J. Hutchings, *Catal, Sci. Technol*, 2013, **3**, 1531-1539.

160 H.Alshammri, P.J. Medziak, S.Bawaked, D.W.Knight, G.J. Hutchings, *Chem.Cat.Chem*, 2012, **4**, 1565-1517.

161 H.Alshammari, P.J.Medziak, D.J.Morgan, D.W.Knight, G.J.Hutchings, *Green Chem*, 2013, **15**, 1244-1254.

---

162 S.Bawaked, N.F.Dummer, D.Bethell,D.W.Knight, G.J.Hutchings, *Green Chem*., 2011, **13**, 127.

163 S.Bawaked, N.F.Dummer, N.Dimitratos, D.Bethell, Q.He,C.J.Kiely, G.J.Hutchings, *Green Chem.*, 2009, **11**, 1037.

164 A.Theford, G.J.Hutchings, S.H.Taylor, D.J.Willock, *Proc,R.Soc.A*, 2011, **467**, 1885-1899.

165 M.Alvaro, C.Aprile, A.Corma, B.Ferrer, H.Garcia, *J.Catal*, 2007, **245**, 249-252.

166 U.N.Gupta, N.F. Dummer, S.Pattisson, R.L.Jenkins, D.W.Knight, D.Bethell, G.J.Hutchings, *Catal Lett*, 2014, DOI 10.1007/s10562-014-1425-z.

167 RA Sheldon, JK Kochi, Metal-catalysed oxidation of organic compounds, Academic Press, New York, 1981.

168 T.Yamada, K.Takahashi, T.Kato, T.Takai, S.Inoki, T.Mukaiyama, *Chem. Lett*. 1991, **20**, 641-644.

169 U.N.Gupta, H.Ashammari, N.F.Dummer, R.L.Jenkins, D.Bethell, G.J.Hutchings. *Cat.Sci.Technol*. 2014, DOI 10.1039/c4cy01355g.

# 2

# Experimental

### 2.0 Introduction

This section aims to give an overview of the main experimental techniques used throughout this PhD, with respect to catalyst preparation, characterisation and testing. Also, the methods used for product analysis are identified and explained.

### 2.0.1 Chemicals

Below is a list of the most commonly used chemicals and materials used throughout this work accompanied by their purity and the company from which they were acquired:

Dec-1-ene, $C_{10}H_{20,}$ 96% + isomers, Alfa Aesar

Graphite, powder < 20µm, Sigma Aldrich

Chloroauric acid, $HAuCl_4.3H_2O$, 99.9%, Sigma Aldrich

Sulphuric acid, $H_2SO_4$, 95%, Fisher

Nitric acid, $HNO_3$, 70%, Fisher

Potassium chlorate, $KClO_3$, 99%, Sigma Aldrich

Potassium permanganate, $KMnO_4$, 97%, Sigma Aldrich

Hydrogen peroxide, $H_2O_2$, 30%, Fluka

Sodium nitrate, $NaNO_3$, 99%, Sigma Aldrich

α,α-Azoisobutyronitrile (AIBN), $C_8H_{12}N_4$, 98%, Sigma Aldrich

Butylated hydroxytoluene (BHT), $C_{15}H_{24}O$, 99%, Sigma Aldrich

## 2.1. Catalyst preparation

### 2.1.1 Preparation of supported gold catalysts *via* incipient wetness impregnation (IWI)

1% Au/Graphite was prepared according to the previously reported method for epoxidation of dec-1-ene[1]. Graphite (1.98 g) was added to an evaporating basin. Aqueous chloroauric acid solution (1 ml) (20 mg/ml) was further diluted with deionised water (1 ml). This was then added drop wise in separate portions to the carbon support followed by air drying. After each addition and subsequent drying in static air, the catalyst was ground before the addition of the next portion to ensure even coverage of the support. After the total addition of the acid, the catalyst was dried for 16 hours at 110 °C.

### 2.1.2 Preparation of supported gold catalysts *via* wet impregnation (Impreg)

Graphite (1.98 g) was added to a beaker (50 ml). Aqueous chloroauric acid solution (1 ml) (20 mg/ml) was further diluted to 3 ml and added to the beaker. The mixture was heated at 80 °C with stirring until a paste was formed. This was then dried overnight at 110 °C to finally yield 1% Au/Graphite.

### 2.1.3 Preparation of supported gold catalysts *via* sol immobilisation (SI)

Pre-prepared chloroauric solution (1ml) (Au 20mg/ml) was added to deionised water (800ml) and stirred vigorously for 15 minutes in a beaker (1 L). Polyvinyl alcohol (PVA) (0.1 M) solution was prepared by dissolving PVA (0.1 g) in deionised water (10 ml). Sonication was employed to achieve complete dissolution of the PVA. PVA solution (0.1 M) (1.3 ml) was then added to the beaker. Stirring was continued for a further 15 minutes. $NaBH_4$ (0.2 M) was prepared by dissolving $NaBH_4$ (0.0756 g) in deionised water (10 ml). $NaBH_4$ (0.2 M) (2.538 ml) was added to the beaker causing the solution to turn red. After 30 minutes of sol generation, the colloid was immobilised by the addition of graphite (1.98g). After 1 hour of stirring, the pH of the solution was adjusted to 1 by the addition of concentrated sulphuric acid (2-3drops). After a final 1 hour stirring, the solid was filtered and washed with deionised water (2 L) to remove all dissolved ions. Finally, the filter cake was dried at 110 °C for 16 hours to achieve 1% Au/Graphite.

### 2.1.4 Preparation of graphitic oxide (GO) *via* Hofmann (HO) and modified Hofmann methods

Graphitic oxide was produced according to the reported method[2] and other similar methods subject to our own modifications. Graphite (5 g) was immersed in 3:1 concentrated sulphuric acid to concentrated nitric acid (100 ml). The mixture was stirred vigorously and cooled in an ice bath for 10 minutes to ensure the temperature remained low (0-10 C°). Potassium chlorate (15 g) was then added in a stepwise manner over a period of 30 minutes taking care of this exothermic reaction and ensuring no sudden increment in temperature to avoid formation of chlorine dioxide and a potential explosion. After complete addition of the chlorate, the mixture was allowed to reach room temperature over a period of 1 hour. This was followed by removal of the ice bath. The mixture was then stirred vigorously overnight before the stirring was stopped and the mixture was left for a further 4 days. On return, the liquid was decanted and the solid was dispersed in 400 ml deionised water. The mixture was then repeatedly centrifuged (14000 rpm, 30 minutes, 20 °C) and re-dispersed in deionised water until a neutral pH was achieved. The obtained solid was then dried at 110 °C in an oven for 16 hours. The obtained dry solid was ground to obtain graphitic oxide powder. NOTE: This method differs from the reported procedure by the amount of chlorate used, the rate and extent of stirring and the methods used to wash and dry the formed material. Initial experiments used 15g of potassium chlorate as a precaution to avoid formation of the explosive chlorine dioxide gas. Due to the lowly oxidised nature of the material, it was possible to dry the material at 110 °C. This method was repeated using various amounts of potassium chlorate from 1-55g, the latter of which obtained a highly oxidised material more familiar to that reported in the literature. These highly oxidised samples often required extended washings and more delicate drying conditions to those previously mentioned. Graphitic oxide prepared using amounts equal to or greater than 30 g of potassium chlorate were dried for 48 hours in a vacuum oven. The decision to wash the catalysts using deionised water instead of 5 % HCl solutions was made in order to reduce the amount of residual chlorine on the final catalyst.

### 2.1.5 Preparation of graphitic oxide *via* Hummers (HU) and modified Hummers methods

Graphitic oxide was prepared according to the conventional Hummers method[3] whereby graphite (5 g) and sodium nitrate (2.5 g) was added to sulphuric acid (95%)

(115 ml). The mixture was then cooled in an ice bath for 10 minutes allowing the temperature to reach 0 °C. Potassium permanganate (15 g) was then added stepwise over a period of 2 hours. On complete addition, the temperature of the mixture was allowed to rise to room temperature over a period of 4 hours. The mixture was then heated to 35 °C and maintained for 30 minutes. Deionised water (250ml) was then poured in to the mixture causing the temperature of the mixture to rise rapidly to 70 °C. This temperature was then maintained for a further 15 minutes before the whole mixture was poured into a beaker containing deionised water (1 L). Hydrogen peroxide solution (3 %) (100 ml) was used to quench any unreacted potassium permanganate causing foaming of the solution and a colour change to light brown. The material was allowed to settle overnight and the liquid was decanted prior to further purification. The graphitic oxide was repeatedly centrifuged (14000 rpm, 30 minutes, 20 °C) and re-dispersed in deionised water until a neutral pH was obtained. The wet solid was dried at 30 °C for 4 days using a vacuum oven. For modified Hummers methods, nitric acid was used in place of sodium nitrate to eliminate sodium from the reaction. Sulphuric acid (87ml) and nitric acid (27 ml) were mixed in a beaker prior to addition of the graphite. This yielded graphitic oxide analogous to the conventional method. Various reported drying conditions proved to be too harsh for this material yielding a mixture of graphene oxide film and high density and unworkable graphitic oxide lumps.

### 2.1.6 Graphitic oxide prepared by modified Staudenmaier (ST) method

Graphitic oxide was prepared according to the reported Staudenmaier method[4]. Graphite (5 g) was added to a beaker containing concentrated sulphuric acid and fuming nitric acid (3:1) (100 ml). The mixture was cooled in an ice bath until the temperature reached 0 °C. Potassium chlorate (15 g) was added in a stepwise manner over a period of 30 minutes avoiding any sudden increment in temperature and the formation of the explosive chlorine dioxide. On the complete addition of the chlorate, the mixture was vigorously stirred overnight and subsequently left in air for a further 4 days allowing oxidation of the graphite and also for the material to settle. The liquid was then decanted and the graphitic oxide was re-dispersed in deionised water (400 ml). This was then repeatedly centrifuged (14000 rpm, 30 minutes, 20 °C) and re-dispersed in deionised water until a neutral pH was obtained. The solid was then dried at 110 °C for 16 hours. This was then ground to yield graphitic oxide powder. Reported methods use 55 g of potassium chlorate, however, due to safety precautions and comparison with the modified Hofmann methods only 15 g was used here.

### 2.1.7 Centrifugation

Centrifugation of graphitic oxide samples was conducted using the previously mentioned conditions (14000 rpm, 30 minutes, 20 °C) using a Beckman coulter centrifuge, JLA.16.250 rotor and appropriate capsules. Samples were dispersed in deionised water (200 ml) before centrifugation. This was repeated until a neutral pH was obtained after which the final supernatant was decanted and the retained solid was dried either by vacuum (20 °C) or regular oven (110 °C).

## 2.2 Catalytic testing

### 2.2.1 Epoxidation of dec-1-ene

The oxidation of dec-1-ene was carried out under mild conditions using atmospheric oxygen as the oxidant. For a typical reaction, dec-1-ene (10 ml) was charged to a round bottomed flask (50 ml) with addition of catalyst (0.1 g). For initiated reactions, AIBN (0.006 g) was added. The flask was then fitted with a reflux condenser and heated to 90 °C using an oil bath. The reaction was stirred using a magnetic stirrer. Reactions using 1% Au catalysts were typically run for 24 hours compared to those catalysed by graphitic oxide which were run for 48 hours. This was due to uninitiated reactions producing lower conversions; therefore longer reactions provided elucidation of the reaction products. After completion of the reaction time, the products were separated from the catalyst using filtration under gravity ready for analysis by gas chromatography (section 2.3.1).

### 2.2.2 Epoxidation of propene

Oxidation of propene was conducted by Dr Upendra Gupta, within an autoclave using the following conditions: The Autoclave was thoroughly washed using acetonitrile. Acetonitrile (30 ml) was placed into the autoclave along with the catalyst (typically 40 mg). This was then connected and purged using nitrogen. Propene (3 bar) was charged to the autoclave followed by nitrogen (12 bar), oxygen (3 bar) and further addition of nitrogen (12 bar). The temperature was increased to 80 °C and maintained for the duration of the reaction with continuous and vigorous stirring. Following the reaction, stirring and heating were halted and the autoclave was cooled to 0 °C using an ice bath. The gaseous products were collected using a gas bag and analysed using gas chromatography. An aliquot of the liquid (5 ml) was collected to which *o*-xylene (100µL) was added as an external standard (section 2.3.2)

### 2.2.3 Oxidation of benzyl alcohol

Benzyl alcohol oxidation was carried out using Radleys reactors (50 ml). Benzyl alcohol (2 g) was added to the glass reactor along with graphitic oxide (0.2 g). The reaction vessel was sealed and charged with oxygen (1 bar). This was then heated to 100 °C and left for 24 hours, after which samples were centrifuged and prepared for analysis by gas chromatography (section 2.3.3).

## 2.3 Analysis of reaction products by gas chromatography

### Theory

Gas chromatography (GC) is an essential analysis technique in catalysis for the separation, identification and quantification of reaction products[5]. The basic components of a GC (figure 2.3.1) consist of an injector, a column contained within an oven and a detector. On injection, a sample is heated into the gas phase and mixed with an inert carrier gas (commonly Ar, He or $N_2$) followed by transportation through the column. A capillary column is generally made of fused silica with a polymer coating called the stationary phase. Separation of products is facilitated by the length of columns which for capillary columns can be up to 100 m. A wide range of stationary phases are also available for the separation of many complex mixtures. These columns can range in polarity, length and also analysis temperature.

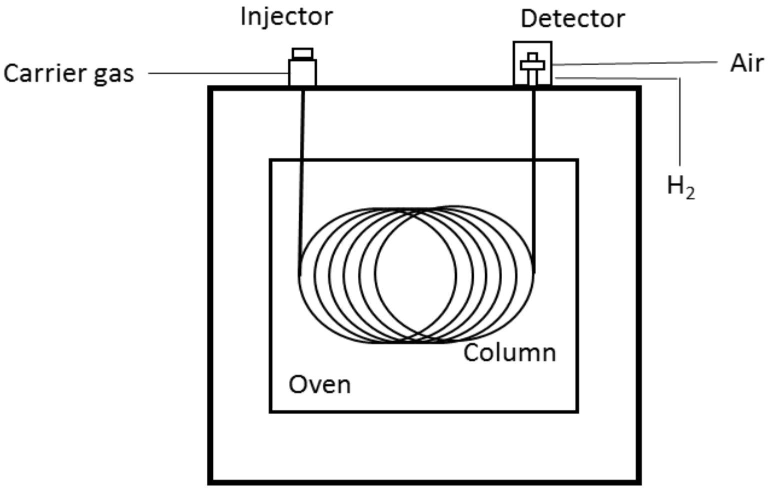

**Figure 2.3.1 Basic schematic of a gas chromatograph**

Capillary columns are widely used for the analysis of complex mixtures; however they are insufficient for large volumes. Here, a small volume should be injected compared to when using a packed column, or the use of a split injector. The basic set up of a split/splitless injector (figure 2.3.2) comprises of a rubber septum through which the syringe is inserted. The sample is injected into a heated glass liner where it is vaporised and mixed with a carrier gas. In a splitless injector set up using small volumes, the sample is carried through the liner and passes on to the column. For use of a split injector, the sample is split via variation of the ratio between the flow rates of the carrier gas and that which exits the split vent. Therefore only a portion of the injected sample passes through the column.

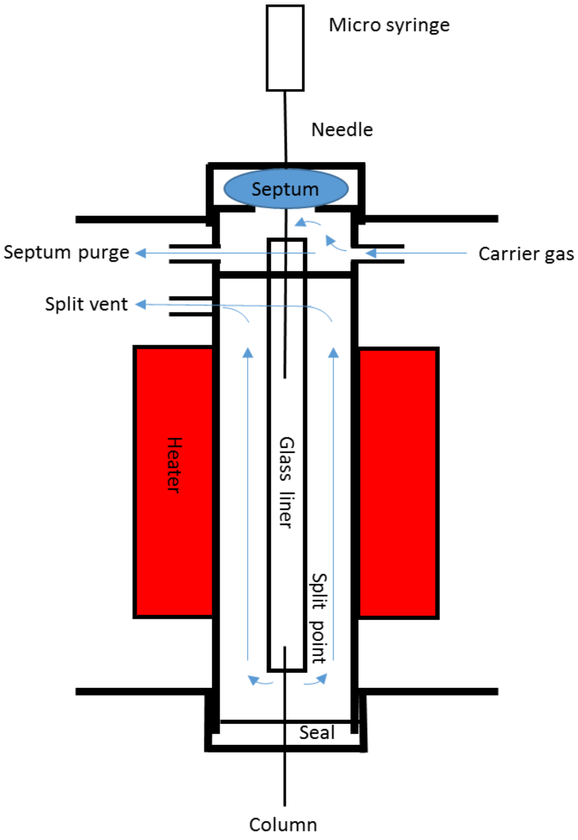

**Figure 2.3.2 Schematic of a split/splitless injector onto a capillary column in gas chromatography**

Various detectors are available for use in gas chromatography, each with different benefits and detection limits. Typical detectors include flame ionisation (FID), thermal conductivity (TCD) and mass spectrometry (MS). An FID was used for the purpose of this project due to its ability to detect organic compounds. The basic setup of an FID (figure 2.3.3) comprises a hydrogen flame in excess oxygen, a cathode, and an anode detector placed just above the flame. The use of hydrogen results in a flame that produces low amounts of ions and therefore low background noise. When organic and ionisable material is separated via the column and subsequently combusted within the flame, a change in current can be detected[6]. When amplified, a signal is achieved of remarkable sensitivity. This allows for the detection of very low amounts of material which is a major advantage of FID over other detectors. A disadvantage of this type of detector is the fact that it is destructive in terms of analytes. A TCD uses the thermal conductivity of the analytes and their effects on the mobile phase to identify compounds. Although this is useful for all types of analytes, the detection limits do not reach that of an FID. However, *via* the use of a post-detector cold trap, analytes can be recovered.

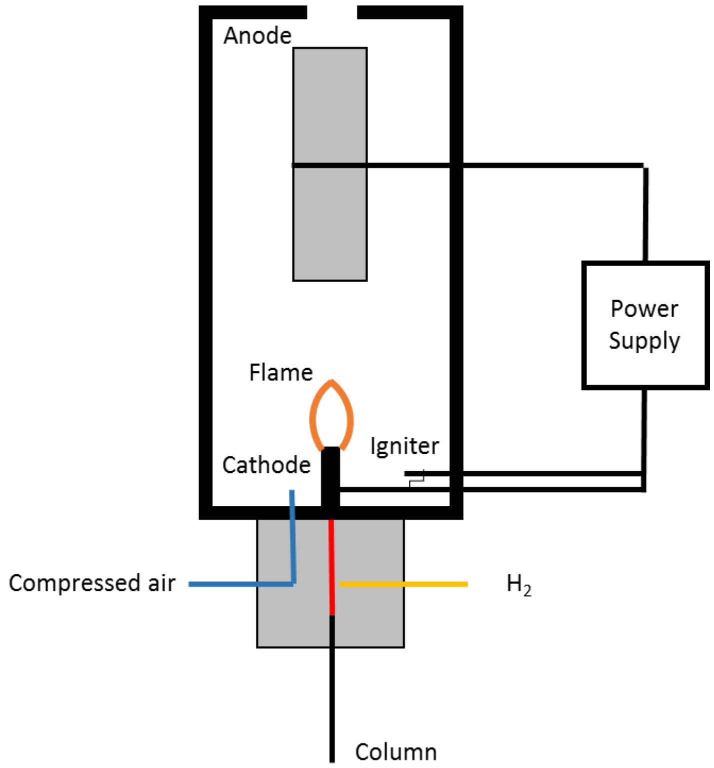

**Figure 2.3.3 Components of a flame ionisation detector**

### 2.3.1 Analysis of dec-1-ene oxidation reaction products by gas chromatography

Products of dec-1-ene oxidation were analysed after filtration from the catalyst. Products were analysed using a Varian 3300 gas chromatograph using a Zebron ZB-wax column for the separation and a flame ionisation detector (FID) for detection of products. Typically, 0.02 µL of sample was injected using a 0.5 µL syringe. The standard GC conditions used included a constant injector and detector temperature of 250 °C, an initial column temperature of 60 °C with a ramp of 10 °C/min. Once the final column temperature of 200 °C was reached, the temperature was held for a further 16 minutes after which all products had eluted and the GC run was complete.

Analysis of products by gas chromatography was conducted using the method previously developed by Dr. Upendra Gupta: Response factors of known products were calculated using bought standards or literature values. For calibration, three solutions were made containing 10 g of dec-1-ene and 20, 30 or 50 mg of each known product. The response factor used was an average of the 3 values obtained according to the formula:

$$Response\ factor = \frac{GC\ count\ of product \div Wt\ \%\ of\ product}{GC\ count\ of\ dec-1-ene\ \ \div Wt\ \%\ of\ dec-1-ene}$$

The response factors calculated for each of the 22 known products are as follows.

**Table 2.3.1.1 Response factors calculated for each of the 22 known products of dec-1-ene epoxidation.**

| Product | Response factor |
|---|---|
| Dec-1-ene | 1.00 |
| Octanal | 0.87 |
| Cyclododecane | 1.00 |
| 3-Nonanone | 0.89 |
| Nonanal | 0.89 |
| 1-Heptanol | 0.77 |
| Epoxide | 0.76 |
| 2-Decanone | 0.90 |
| 1-Decen-3-one | 0.90 |
| 1-Octanol | 0.80 |
| 2-Decanal | 0.90 |

| | |
|---|---|
| 1-decen-3-ol | 0.83 |
| 3-Nonen-1-ol | 0.82 |
| Cycolodecanol | 0.84 |
| 2-Decen-1-ol | 0.83 |
| Heptanoic acid | 0.75 |
| Nonalactone | 0.81 |
| Octanoic acid | 0.78 |
| Epoxy-hexadecane | 0.93 |
| Nonanoic acid | 0.80 |
| 1,2-Decanediol | 0.71 |
| 2-Decanoic acid | 0.81 |

The acquired response factors were used to determine conversion of dec-1-ene and selectivity of products according to the following equations using total GC counts.

$$Conversion\ (\%) = 100 \times \frac{\Sigma\ Corrected\ products}{\Sigma\ Corrected\ products + \ \Sigma\ Dec - 1 - ene}$$

$$Selectivity\ (\%) = 100 \times \frac{Corrected\ product}{\Sigma\ Corrected\ products}$$

### 2.3.2 Analysis of propene epoxidation products by gas chromatography

Analysis of propene epoxidation products was conducted by Dr Upendra Gupta. The analysis was done using a Varian 3800 GC fitted with a CP-wax 52 CB capillary column and an FID detector. The injector and detector temperatures were 150 and 200 °C respectively. The initial column temperature was 40 °C. This was maintained for 5 minutes before heating to 200 °C at a rate of 10 °C/min. *o*-xylene was used as an external standard.

### 2.3.3 Analysis of benzyl alcohol oxidation products by gas chromatography

Analysis of benzyl alcohol oxidation products was carried out using a Varian CP-3800 gas chromatograph. Samples were centrifuged after reaction followed by a sample (0.5 ml) being taken and mixed with equal volume of mesitylene (0.5 ml) as an external standard.

### 2.3.4 Gas chromatography mass spectrometry (GC-MS)

**Theory**

The combination of gas chromatography and mass spectrometry allows for the separation, detection and identification of analytes from a mixture of compounds. As previously described (section 2.3), gas chromatography separates the compounds via the use of a column. Once separated, the compounds are passed into a mass spectrometer. Here the molecules are ionised, in this case by an accelerated electron beam (electron ionisation) however chemical ionisation is also possible. Bombardment with electrons results in either the loss of an electron, causing positive ions or less commonly the gain of an electron resulting in negative ions. The loss of one electron from the parent molecule results in a peak termed the molecular ion. This is representative of the molecular weight of the original molecule. Other peaks of lower molecular weights are obtained through the fragmentation of the molecular ion, as a product of the energy imparted in the initial ionisation. The high amount of fragmentation seen is characteristic of each analyte and therefore can give vital information regarding each molecule eluting from the GC. The mass of each of these ions can be analysed in several ways including ion traps, quadrupole analysers, time of flight, magnetic sectors and cyclotron resonance. In the case of this study, time of flight analysis was utilised. This uses an electron field of known and constant strength to create ions that, assuming they have the same charge, will also have the same kinetic energy[7]. The velocity, and therefore the time for which an ion takes to travel over a known distance to a detector will be directly related to its "mass to charge ratio". Ions of high mass with travel slower through to the detector than those of lower mass. Therefore accurate descriptions of the mass of fragments can be obtained and a fingerprint of the initial molecule is observed leading to identification. The detection and quantification of ions can be conducted by the use of a Faraday cup or an electron multiplier. In the case of a Faraday cup, positively or negatively charged ions impact onto an electric plate which cause a current and therefore enable the recording of a signal.

Chemical ionisation can be used in place of electron ionisation. This first involves the ionisation of methane and subsequently the chemical ionisation of a molecule. The lower energy involved in this ionisation results in lower amounts of fragmentation. This gives a less complete fingerprint of the studied molecule but does result in the molecular ion peak, which is not always the case in electron ionisation[8].

**Experimental**

All GC-MS was conducted by the Cardiff university GC-MS service and analysed by Dr. Robert Jenkins. Analysis was conducted using a Waters GCT premier equipped with a BPX-5 column. The mass spectrometry technique used was electron ionisation.

## 2.4 Catalyst characterisation and analysis

The following section gives a brief overview of the techniques which were used to probe the nature of the catalysts used in this study. An introduction to the underlying principles and the method used particular to this research is given.

### 2.4.1 Microwave plasma atomic emission spectroscopy (MP-AES)

**Theory**

MP-AES is an elemental analysis technique based on the principles of atomic emission. The technique relies on a microwave and magnetically excited nitrogen plasma heated to around 5000 K and is formed within a quartz torch. All samples are in liquid form or digested into solution and therefore energy from the torch is used for atomisation and excitation of the sample. However this limits samples to soluble or digestible catalysts whereas inductively coupled plasma optical emission spectrometers can analyse solid samples via a laser ablation system.

Atomisation of the sample is facilitated by the high temperatures from this plasma source which also leads to a high population of excited states. This gives MP-AES a higher sensitivity over lower temperature techniques such as flame atomic absorption spectrometers. The diagram below (2.4.1.1) shows the basic principles behind MP-AES from the introduction of a liquid sample to the nitrogen plasma. After excitation, electrons relax into lower quantised energy levels releasing photons of defined energies and wavelengths which are characteristic for each element. One of the main benefits of this type of technique is the ability to analyse each wavelength individually and sequentially using a monochromator detector and mirror grating. This, along with the high intensities observed, leads to a high sensitivity and low interference for each element.

It is also possible to use multiple emission wavelengths for each element. This is useful when analysing solutions comprising many different elements, as interference from nearby wavelengths can occur, leading to false positives and concentrations.

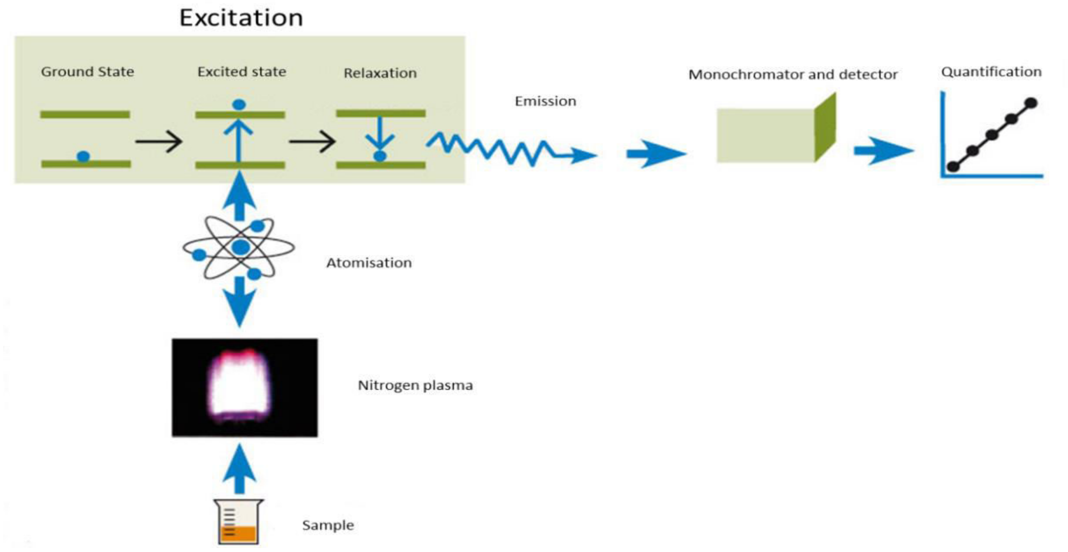

**Figure 2.4.1.1 Flowchart showing basic principles of microwave plasma atomic emission spectroscopy**

**Experimental**

Multiple samples were prepared for MP-AES analysis according to the following procedure. GO (50 mg) was placed into a volumetric flask (50 ml) and submerged in freshly prepared *aqua regia* (4 ml) These samples were left for 24 hours to allow any metal ions to leach into solution. Samples were then diluted using deionised water (50 ml) and filtered using PTFE syringe filters (0.45 µm). Samples were then analysed using an Agilent MP-AES 4100. Samples were tested for Cu, Ca, Mn, Mg, Fe, K, Na and Ni using multiple wavelength calibrations for each element.

### 2.4.2 Ion chromatography (IC)

**Theory**

Ion chromatography is a useful tool for detecting ions in solution that may be beyond the scope of other elemental analysis techniques such as the previously described MP-AES. Ion chromatography can be used for the detection of phosphate ($PO_4^{3-}$), chloride ($Cl^-$), nitrate ($NO_3^-$) sulphate ($SO_4^{2-}$). The process relies on the basic principles of chromatography and the extent of the interaction between the analytes and the stationary phase. Displacement of a resin bound anion by an analyte will result in retention. Constant flow will gradually move analytes through the column leading to their eventual elution at a characteristic retention time. This can be used for the separation and quantification of ions.

### Experimental

Samples were analysed using a Thermo scientific dionex ion chromatography system fitted with a dionex ionpac AS22-fast column. Each sample was prepared by washing graphitic oxide with HPLC grade water to leach any ions into solution. Samples were then filtered using 0.45 µm PTFE syringe filters. These were then quantified for nitrate, chloride and sulphate content with respect to calibration standards.

## 2.4.3 Powder x-ray diffraction (XRD)

### Theory

XRD is a technique commonly used for characterisation of crystalline catalysts. By bombarding an x-ray source with electrons to create a core hole, x-rays are generated due to x-ray fluorescence from a number of transitions. The Cu Kα line used in this technique is formed due to the transition of an electron from the L-shell to the K-shell[9]. By directing these emitted x-rays at a sample it is possible to probe the lattice parameters within. When x-rays are scattered by a crystalline material, constructive interference will occur when scattered x-rays are in-phase with one another (figure 2.4.3.1) and a reflection will appear in the diffraction pattern.

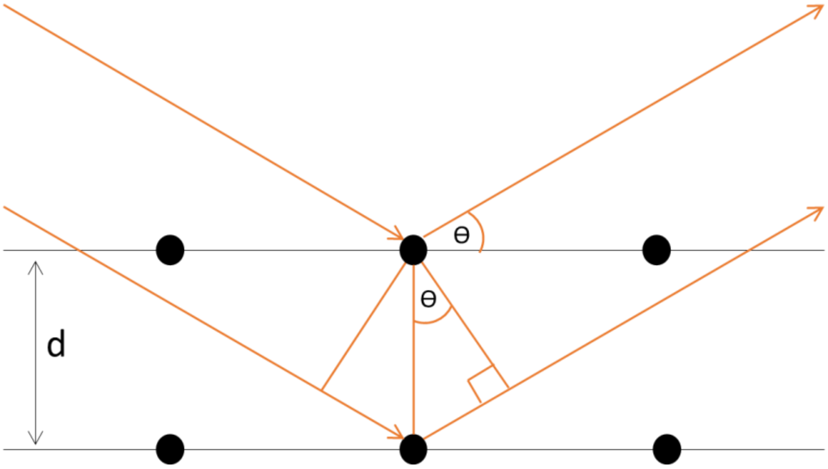

**Figure 2.4.3.1 Interaction of x-rays within a crystalline surface**

It is possible to analyse a sample using a range of angles to find where these peaks are most intense and use the Bragg relationship, given below, to obtain d-spacings and information on the overall crystal structure.

$$n\lambda = 2d \sin\theta$$

Where:

$\lambda$= wavelength of X-rays

d= interplanar distance

$\theta$= angle of incident x-rays to the reflecting lattice plane

n= an integer (1, 2,…)

The diagram below shows the general set up of an x-ray diffractometer whereby the x-ray can move to analyse angles as a function of 2θ. The setup also includes a rotating sample stage to increase the contribution from atoms in the samples to the diffraction pattern. Each material has its own characteristic diffraction pattern, therefore by creating a database of known materials, we can identify known phases and also any contributions from impurities.

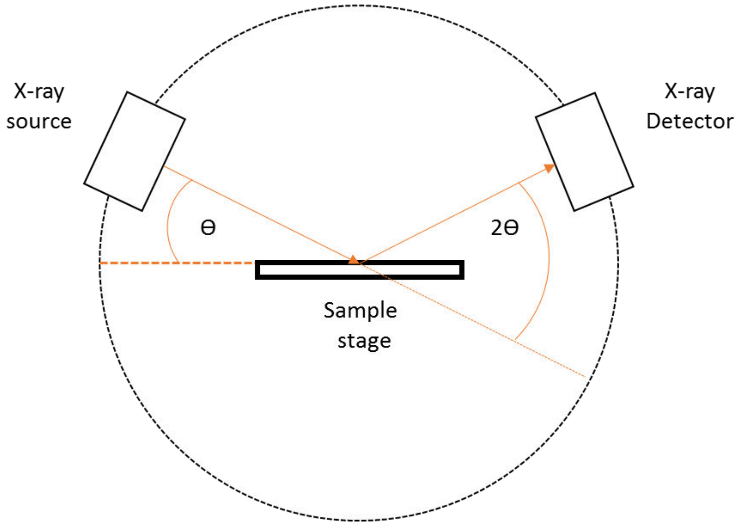

**Figure 2.4.3.2 Basic set up of an x-ray diffractometer**

X-ray diffraction can also be measured *in situ* using a cell permeable to x-rays. This allows the experimenter to monitor phase changes as a function of time and/or temperature under exposure to gases. This can give information on how catalysts may activate or deactivate under various conditions and also the rates at which this may occur.

**Experimental**

XRD analysis was conducted using a PANalytical X'pert pro diffractometer using a Cu Kα x-ray source. Typical scans were from 2θ of 10 to 80 ° at 40 kV and 40 mA although some wide scans were conducted for higher oxidised samples below 10° due to the appearance of a reflection at approximately this angle.

### 2.4.4 X-ray photoelectron spectroscopy (XPS)

**Theory**

XPS is one of the most important techniques in the field of catalysis. It is commonly used for the determination of elemental composition of a surface and furthermore the oxidation state of the elements found. Due to the short mean free path of electrons with kinetic energies between 15 and 1000 eV, XPS can only be used to probe a short distance into the surface (<2 nm) however depth selective information can be obtained by altering the angle of the flat sample to the electron energy analyser[10]. Therefore in some cases XPS can also be used to identify where one phase may be covered by another.

The technique is based on the principles of the photo-electric effect whereby atoms that are irradiated with light will absorb a photon of energy and emit electrons. These photoelectrons will possess a kinetic energy which is characteristic of the wavelength of irradiating light and the binding energy of the electron.

$$E_k = h\nu - E_b$$

Where:

$E_k$ = kinetic energy of the photoelectron

h = planck's constant

$\nu$= frequency of radiation

$E_b$= binding energy of the photoelectron or ionisation energy

The basic set up for XPS (2.4.4.1) includes an x-ray source, a variable angle sample stage for depth dependant analysis and an electron energy analyser.

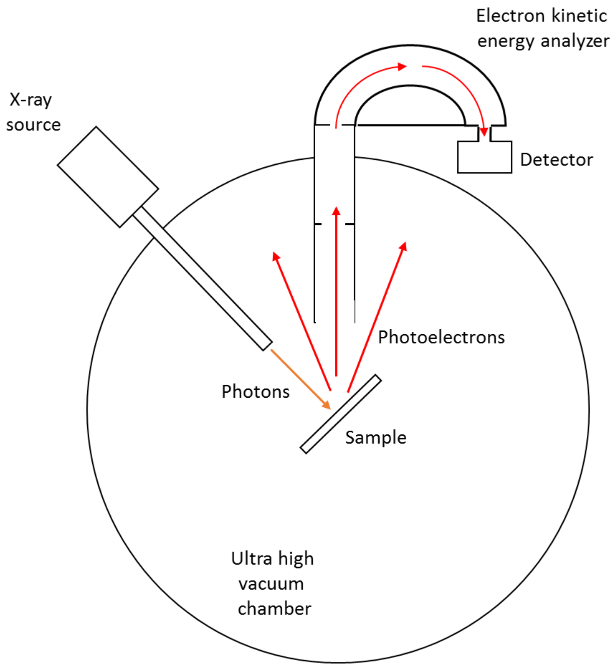

**Figure 2.4.4.1 Schematic of an x-ray photoelectron spectrometer**

## Experimental

All XPS was carried out by Dr David Morgan using a Kratos Axis Ultra DLD system and according to the following method. A monochromatic Al $K\alpha$ X-ray source operating at 120 W. Data was collected with pass energies of 160 eV for survey spectra, and 40 eV for the high resolution scans. The system was operated in the Hybrid mode, using a combination of magnetic immersion and electrostatic lenses and acquired over an area approximately 300 × 700 $\mu m^2$. A magnetically confined charge compensation system was used to minimize charging of the sample surface, and all spectra were taken with a 90 ° take off angle. A base pressure of ~ $1\times10^{-9}$ Torr was maintained during collection of the spectra. Binding energies were calibrated using the C1s binding energy of carbon taken as 284.7 eV.

### 2.4.5 Raman spectroscopy

#### Theory

Raman spectroscopy uses the inelastic scattering of photons. This occurs when a sample is irradiated with photons which experience either a gain or loss in energy after excitation of a vibration within the molecule[11]. This differs to infrared-spectroscopy whereby a vibration will occur with the elastic scattering of light. Here, electrons will absorb energy from the irradiating photons and move to a higher energy level, after which relaxation to the ground state occurs releasing energy similar to that which was absorbed. This is known as Rayleigh scattering (figure 2.4.5.1). Scattering of light which either loses or gains energy is termed stokes and anti-stokes scattering, respectively.

There is also criteria for a sample to be Raman active. Whereas infrared spectroscopy requires a change in dipole during vibration, for Raman the species must have a changeable polarizability. Therefore, with respect to organic samples as studied in this project, Raman can be used to give information on the carbon-carbon nature of the material as opposed to functional groups on the surface which can be observed by infrared spectroscopy.

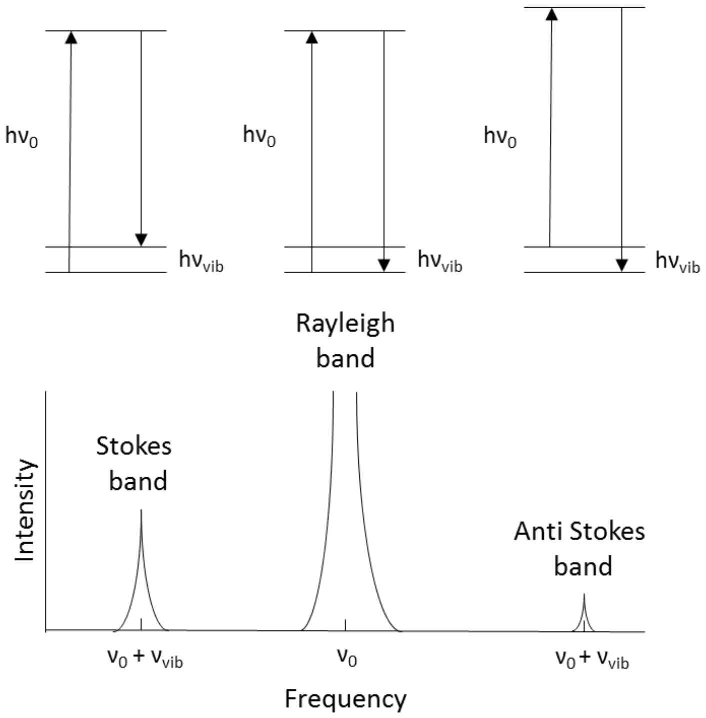

**Figure 2.4.5.1 Energy level transitions resulting in Stokes, Rayleigh, and anti-Stokes bands**

Raman spectroscopy can also be studied *in situ*. This is due to the low interaction between the inelastically scattered light and gas-phase molecules. Therefore, catalyst samples can be exposed to reaction conditions and the effects monitored.

As the Stokes and anti-Stokes transitions are of a lower magnitude compared to the Rayleigh band. A laser must be employed to enhance all intensities for ease of analysis. However this can lead to heating of the surface and the subsequent desorbing of molecules of interest.

A problem commonly encountered with Raman spectroscopy is the fluorescence of a sample. This produces an intense spectral background which can eclipse any weak Raman signals being analysed. This can in some cases be overcome using a lower intensity ultraviolet laser. This shifts any signals out of the visible range where fluorescence is prominent. This is a commonly used technique during analysis of carbon-based samples, as they commonly produce high amounts of fluorescence.

**Experimental**

Raman spectroscopy of graphitic oxide was conducted using a Renishaw ramascope using a spectrophysics 514 nm HeNe laser at a power of 20 mW. Spectra were generally obtained in the region of 800-2000 cm$^{-1}$ to incorporate the D (sp$^3$) and G (sp$^2$) bands of sp$^2$ hybridised carbons.

### 2.4.6 Thermal gravimetric analysis (TGA)

**Theory**

Thermal gravimetric analysis is an adaptable method for the characterisation of materials by weight. This can be done isothermally as a function of time, or over a temperature range to study its effects on the physical and chemical composition of the material. By introducing various atmospheres it is possible to study oxidation or reduction of catalysts as a function of temperature, and in inert atmospheres it is possible to study the overall thermal stability of the material. Desorption of adsorbed species can also be studied. The general set-up of a TGA (figure 2.4.6.1) involves a high precision balance encased in a heated chamber and a thermocouple for accurate temperature measurements. TGA can also be modified by the use of fourier transform infrared spectroscopy (FTIR) and GC-MS as an end-on analysis of desorbed gases. This allows for the separation and identification of species which are either a product of thermal decomposition or desorption from catalyst surface.

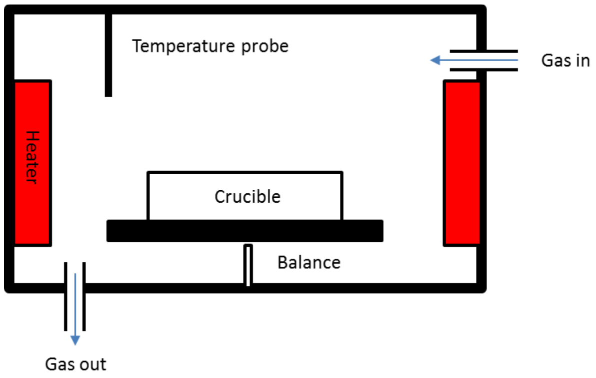

**Figure 2.4.6.1 General set up for thermal gravimetric analysis**

**Experimental**

Thermal gravimetric analysis was carried out using a Perkin Elmer TGA 4000. Standard conditions were consistent with those recommended in the literature. Graphitic oxide samples were typically heated from 30-500 °C with a ramp rate of 5 °C/min using a $N_2$ flow of 20 ml/min. Approximately 10 mg of catalyst was used. This was more important for highly oxidised samples whereby amounts above 25 mg were seen to rapidly expand at 180 °C in an explosive manner. Lowly oxidised samples did not demonstrate the same explosive nature and therefore more catalyst could be used (50 mg).

### 2.4.7 Brunauer, Emmett and Teller analysis of surface area (BET)

**Theory**

The use of BET is commonplace in catalysis for the determination of surface area of a given catalyst. The BET equation can be explained as an adaption of the Langmuir isotherm which states that:

$$\theta = \frac{K_p}{1 + K_p} \; where \; K = \frac{k_a}{k_d}$$

The Langmuir isotherm only considers monolayer formation ie, $\theta$<1 whereas the BET equation expands on this to consider multilayer formation ie, $\theta$>1. It is also not a requirement for a full monolayer to be formed before multilayer formation can proceed. Therefore the BET equation, as an expansion of the Langmuir can be given as:

$$v = \frac{\left(\frac{v_m c}{p_0} p\right)}{\left(1 + \frac{c}{p_0} p\right)}$$

When rearranged we can obtain the following form which we can use to form a plot of y=mx+c:

$$\frac{p}{v(v_0 - p)} = \frac{1}{v_m c} + \left(\frac{c-1}{v_m c}\right)\left(\frac{p}{p_0}\right) \; and \; c = exp\left(\frac{E_{1-}E_L}{RT}\right)$$

Where:

$p$ = pressure of adsorbate gas in pascals, $v$ =volume of adsorbed gas at standard temperature and pressure, $p_0$=saturation pressure in pascals,, $v_m$= molar volume of gas to form monolayer, $E_1$=heat of adsorption for monolayer formation, $E_2$=heat of adsorption for multilayer formation, $R$=gas constant, $T$=Temperature(K).

Therefore plotting $\frac{p}{v(v_0-p)}$ against $\left(\frac{p}{p_0}\right)$ will yield a straight line graph with intercept $\frac{1}{v_m c}$ and a gradient of $\left(\frac{c-1}{v_m c}\right)$. By obtaining $v_m$ we can calculate specific surface area using the following equation:

$$S = (N_a)(v_m)(A)$$

Where $S$ =specific surface area, $N_a$=Avogadro's number, $v_m$= molar volume of gas to form a complete monolayer, $A$=cross sectional area of adsorbent gas. For nitrogen this is 16 Å$^2$.

**Experimental**

BET surface area analysis of samples was conducted using a Micromeritics Gemini 2360 analyser. Samples were pre-treated at 120 °C under a flow of nitrogen for 1 hour with an accurate mass taken prior to analysis.

### 2.4.8 Fourier transform infrared spectroscopy (FTIR)

#### Theory

FTIR is a technique based on the principles of infrared spectroscopy[12]. This evaluates the vibrational modes of molecules within a gas, liquid or solid after irradiation with a polychromatic light source. A Fourier transfom is the mathematical method which allows multiple wavelengths to be studied at once. By shining a light source of multiple frequencies and repeatedly modifying these frequencies over numerous scans it is possible to build up an adsorption spectrum of the sample over a large range.

The infrared region of light is in the range of 12800 - 10 cm$^{-1}$. This is commonly divided into three regions referred to as the near infrared (12800 - 4000 cm$^{-1}$), mid-infrared (4000 - 200cm$^{-1}$) and far infrared (50 - 1000 cm$^{-1}$) regions. For catalysis, the mid-infrared region is most commonly studied as the majority of organic compounds and functional groups adsorb radiation in this range. Vibrational spectroscopy requires a change in dipole occurring with vibration and therefore homonuclear diatomic molecules are not infrared active ($H_2$, $N_2$, $O_2$). As described, this change in dipole only has to occur during vibration; however molecules with a permanent dipole (CO, NO) will absorb much stronger than those in which only exhibit a dipole during certain vibrations.

Advantages of FTIR arise from the use of multiple scans over a wide range. This lowers the susceptibility of the technique to interference from stray light and also provides a high signal to noise ratio.

FTIR spectrometry can be used in various ways to analyse various gaseous, liquid and solid samples. This allows for multiple end on analyses such as gas chromatography-infrared spectroscopy and thermogravimetry-infrared spectroscopy.

#### Experimental

All samples were analysed using a Shimadzu IRAffinity-1S fourier transform infrared spectrophotometer. All scans were conducted between 400 and 4000 cm$^{-1}$.

## 2.5 References

---

1 U.N.Gupta, N.F. Dummer, S.Pattisson, R.L.Jenkins, D.W.Knight, D.Bethell, G.J.Hutchings, *Catal Lett*, 2014, DOI 10.1007/s10562-014-1425-z.

2 U.Hofmann, E.Konig, *Z.Anorg, Alg, Chem*, 1937, **234**, 311-336.

3 W.S. Hummers Jr, R.E. Offeman, *J. Am. Chem. Soc*, 1958, **80**, 1339.

4 L.Staudenmaier*, Ber. Dtsch. Chem. Ges*. 1898, **31**, 1481-1487.

5 F.F.Kitson, B.S.Larsen,C.N.McEwen, *Gas chromatography and mass spectrometry*, Academic press, London, 1996,4-5.

6 D.C.Harris, *Quantitative chemical analysis*, W.H.Freeman and company, 1999, **5**, 675-712.

7 W.E. Stephens, *Phys. Rev*., 1946, **69**, 691.

8 F.F.Kitson, B.S.Larsen,C.N.McEwen, *Gas chromatography and mass spectrometry*, Academic press, London, 1996, 16-17.

9 J.W. Niemantsverdriet, *Spectroscopy in catalysis*, Wiley-VCH, Weinheim, 2007, 3, 148-149.

10 J.W. Niemantsverdriet, *Spectroscopy in catalysis*, Wiley-VCH, Weinheim, 2007, 3, 39-42.

11 J.W. Niemantsverdriet, *Spectroscopy in catalysis*, Wiley-VCH, Weinheim, 2007, 3, 238.

12 J.W. Niemantsverdriet, *Spectroscopy in catalysis*, Wiley-VCH, Weinheim, 2007, 3, 217-233.

# 3

# Oxidation of alkene to epoxide over carbon supported gold catalysts.

## 3.0 Introduction

The epoxidation of dec-1-ene using carbon supported gold catalysts has previously been reported by Hutchings *et al*. The following chapter serves as a continuation of the previously reported work and also as an introduction into the catalysis by graphitic oxide, described in later chapters.

## 3.1 Epoxidation of alkenes

Epoxides are of great commercial and synthetic importance due to their use as intermediates in organic synthesis, leading to a plethora of valuable chemicals such as diols, polyols, polyethers and amino alcohols. Epoxides are also important additives in pharmaceuticals and cosmetics facilitating the mixing of lipid soluble acids in creams and lotions[1]. Epoxides also find use in the development of epoxy resins for the manufacture of adhesives. Therefore, the selective epoxidation of α-alkenes is a much coveted process both in industry and academia. The epoxidation of ethene to ethylene oxide is well documented and is catalysed using an α-alumina supported silver catalyst[2,3], with the addition of promoters this catalyst can achieve selectivity to the epoxide of up to 90 %[4]. The ease of this epoxidation is due to the absence of an allylic hydrogen. The epoxidation of olefins above ethene, with respect to carbon chain length, becomes much less facile due to the presence of this allylic hydrogen. Abstraction of the hydrogen, followed by autoxidation is favoured over direct oxidation of the double bond. For this reason, the production of propylene oxide through the direct oxidation of propene is still one of the major challenges in chemistry. Despite this, propene is still in huge demand and is produced on a large scale. Traditionally this was done through the chlorohydrin process, however, this involved the use of chlorinated reagents and the formation of unwanted by products such as calcium chloride which had to be disposed of at great expense. More recent developments involve the oxidation of propene over a TS-1 catalyst, however this involves the use of stoichiometric amounts of hydrogen peroxide[5,6,7].

Previous attempts at oxidising terminal alkenes such as dec-1-ene have also required stoichiometric amounts of expensive or toxic oxidants[8,9,10,11,12,13,]. As with propene epoxidation, hydrogen peroxide is commonly employed as oxidant, this was used for the epoxidation of dec-1-ene by Pescarmona *et al.*[14]. Mandelli also achieved moderate yields of epoxydecane *via* the use of hydrogen peroxide, however, large amounts of alumina were used[15]. Alternatively, Scotti *et al.*[16] used cumyl hydroperoxide as an oxidant for the epoxidation of dec-1-ene over a $CuO/Al_2O_3$ catalyst.

### 3.2 Previous work by Hutchings *et al.* for aerobic epoxidation

The use of atmospheric oxygen represents a much cheaper and greener alternative to these sacrificial oxidants. The Hutchings group studied this concept, initially using cycloalkenes as substrates[17]. It was shown that cyclo-octene could be oxidised over nano-gold catalysts using catalytic amounts of a peroxide as an initiator. Further studies showed a dependence on ring size as to whether allylic oxidation or epoxidation pathways would dominate, with $C_7$ and below cycloalkenes preferring allylic oxidation[18]. This discovery was also extended to internal linear alkenes such as hex-2-ene[19]. It was shown that on removal of stabilisers from cycloalkenes, epoxidation could be carried out in the absence of radical initiators[20]. However linear alkenes still required peroxide initiators such as t-butyl hydroperoxide. Solvent free dec-1-ene epoxidation has been studied extensively using carbon supported gold catalysts[21]. It was shown that competing mechanisms between allylic oxidation and epoxidation were present at high temperatures. However, at lower temperatures, no oxidation occurred in the absence of radical initiators. When initiated, the presence of graphite promoted allylic oxidation and the formation of alcohols and ketones through a Russell termination (figure 3.2.1) yet the addition of 1% gold nanoparticles to the graphite promoted selectivity to the epoxide. The reaction profile of the initiated reaction (figure 3.2.2), when in the presence of gold, was suggested to follow a similar pathway to that reported for cyclooctene epoxidation.

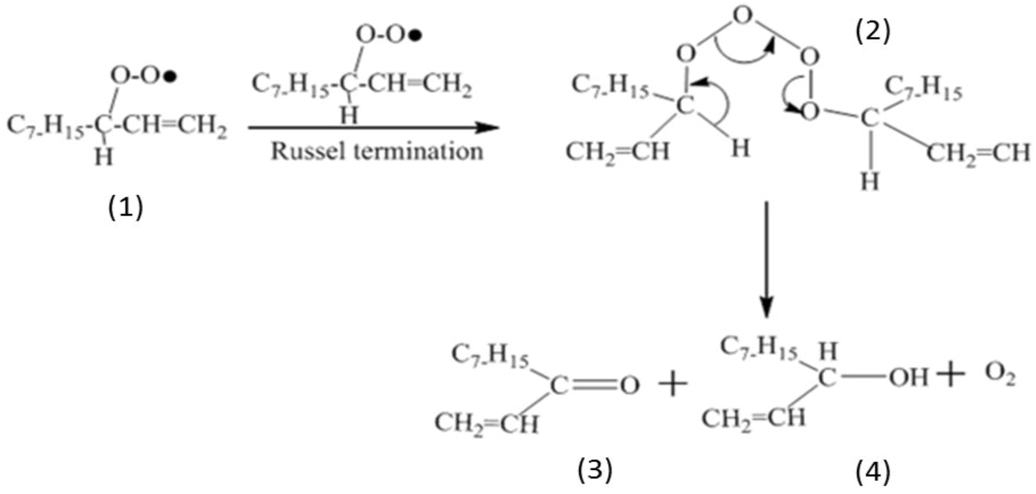

**Figure 3.2.1 Russell termination of peroxy radicals (1) and subsequent formation of allylic products dec-1-ene-3-one (3) and dec-1-ene-3-ol[21].**

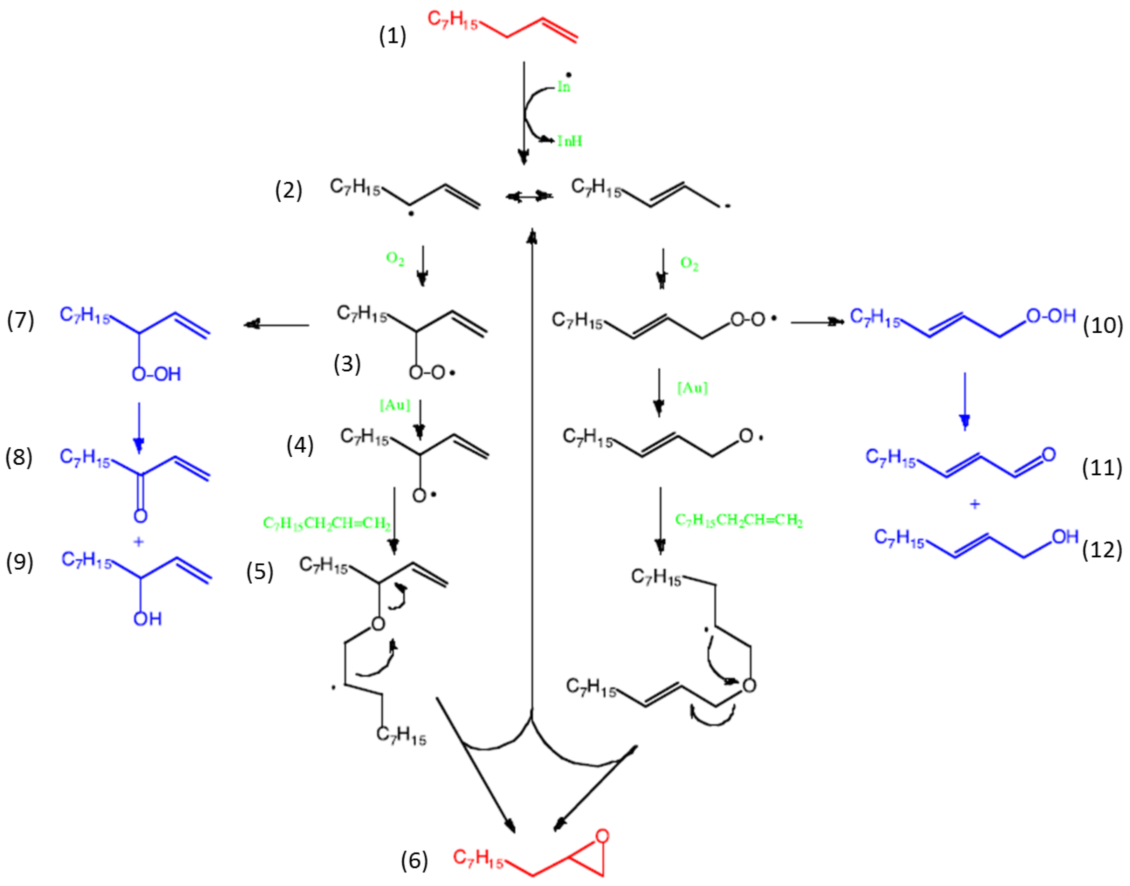

**Figure 3.2.2 Suggested mechanism for the radical initiated epoxidation of dec-1-ene in the presence of gold catalysts.** [21]

The presence of azobisisobutylnitrile (AIBN) leads to the abstraction of an allylic hydrogen. The so formed dec-1-enyl radical (2) reacts with dioxygen to form a peroxy radical species (3). Fragmentation on the surface of gold leads to the formation of a 3-dec-1-enyloxy radical (4) which after reaction with dec-1-ene and subsequent fragmentation results in the formation of the epoxide (6) and a dec-1-enyl radical, thus ensuring the continuation of the radical process. The presence of gold was said to be crucial in directing conversion towards the epoxide rather than allowing build-up of hydroperoxy species and formation of allylic products.

The conditions for dec-1-ene epoxidation were optimised according to the amount of catalyst used, the reaction temperature and the concentration and type of radical initiator. It was observed that no reaction took place at reaction temperatures below 100 °C in the absence of catalyst and radical initiators, thus, reaction temperatures below 100 °C could be investigated for catalysis. It was found that the optimum amount of catalyst to be used in the reaction was 0.1 g per 10 ml of dec-1-ene. Amounts below this saw a dramatic decrease in conversion and selectivity and only minor gains in epoxide yield were observed when doubling or tripling this amount. AIBN, tertiarybutyl hydroperoxide (TBHP) and benzoyl peroxide (BPO) were screened as possible initiators with AIBN chosen as the initiator for further use because AIBN cannot act as a source of oxygen (as with TBHP and BPO) thus any oxidation of dec-1-ene was presumed to be due to activation of atmospheric oxygen and not reaction with the initiator itself..

The main focus of this work was to investigate the effect of the catalyst preparation method and the activation of oxygen in the absence of radical initiators.

### 3.3 Reproduction and continuation of previous work

Initially, attempts were made to reproduce the reported 1% Au/graphite catalyst by incipient wetness impregnation method (IWI)[22]. It was observed that newly prepared catalysts consistently displayed slightly higher selectivity to the epoxide albeit with a small decrease in activity compared to previous work[21] (table 3.3.1).

The catalyst was shown to be reproducible for epoxidation of dec-1-ene. The addition of AIBN to the reaction was again found to be crucial with no conversion seen in its absence at temperatures below 100 °C. Above these temperatures, addition of the gold catalyst has a negligible effect on activity due to the main process being that of autoxidation. The presence of the 1,2-epoxydecane was confirmed by gas chromatography mass spectrometry (GC-MS) by comparing retention times and mass spectra with a commercial 1,2-epoxydecane standard. GC-MS was also compared to a 2,3-Epoxydecane simulated spectrum from the NIST database . The lack of agreement further confirmed the presence of the 1,2-epoxide (figure 3.3.1).

**Table 3.3.1 Comparison of prepared 1%Au/Graphite with literature standard. (24 h, 90 °C, catalyst 0.1 g, AIBN 0.006 g, dec-1-ene 10 ml)**

| | 1%Au/G (Literature[21]) | 1% Au/G | 1% Au/G |
|---|---|---|---|
| **Conversion (%)** | 12.3 | 11.4 | 11.5 |
| **Epoxide** | 30.9 | 40.7 | 41.1 |
| **Dec-1-en-3-one** | 5.4 | 4.8 | 4.5 |
| **Dec-1-en-3-ol** | 5.1 | 4.3 | 5.0 |
| **Dec-2-enal** | 7.2 | 6.1 | 7.6 |
| **Dec-2-en-1-ol** | 7.3 | 6.8 | 7.0 |
| **1,2-Decanediol** | 1.8 | 1.7 | 1.6 |
| **Dec-2-enoic acid** | 3.8 | 2.4 | 3.5 |
| **Dec-2-anone** | 0.4 | 0.5 | 0.4 |
| **C8 + C9 aldehyde** | 1.1 | 0.8 | 1.4 |
| **C7 + C8 alcohols** | 1.6 | 0.7 | 1.6 |
| **C7 + C8 + C9 acids** | 10.3 | 8.2 | 7.8 |
| **Non-3-en-1-ol** | 1.0 | 0.6 | 1.1 |
| **Nonan-3-one** | 3.3 | 5.3 | 4.5 |
| **Cyclododecane** | 1.2 | 2.0 | 1.6 |
| **Cyclodecanol** | 0.4 | 0.4 | 0.8 |
| **Nonalactone** | 0.5 | 0.2 | 0.1 |
| **C16 Epoxide** | 1.7 | 0.4 | 0.5 |
| **∑unknowns liquid products** | 8.0 | 13.9 | 9.8 |

.

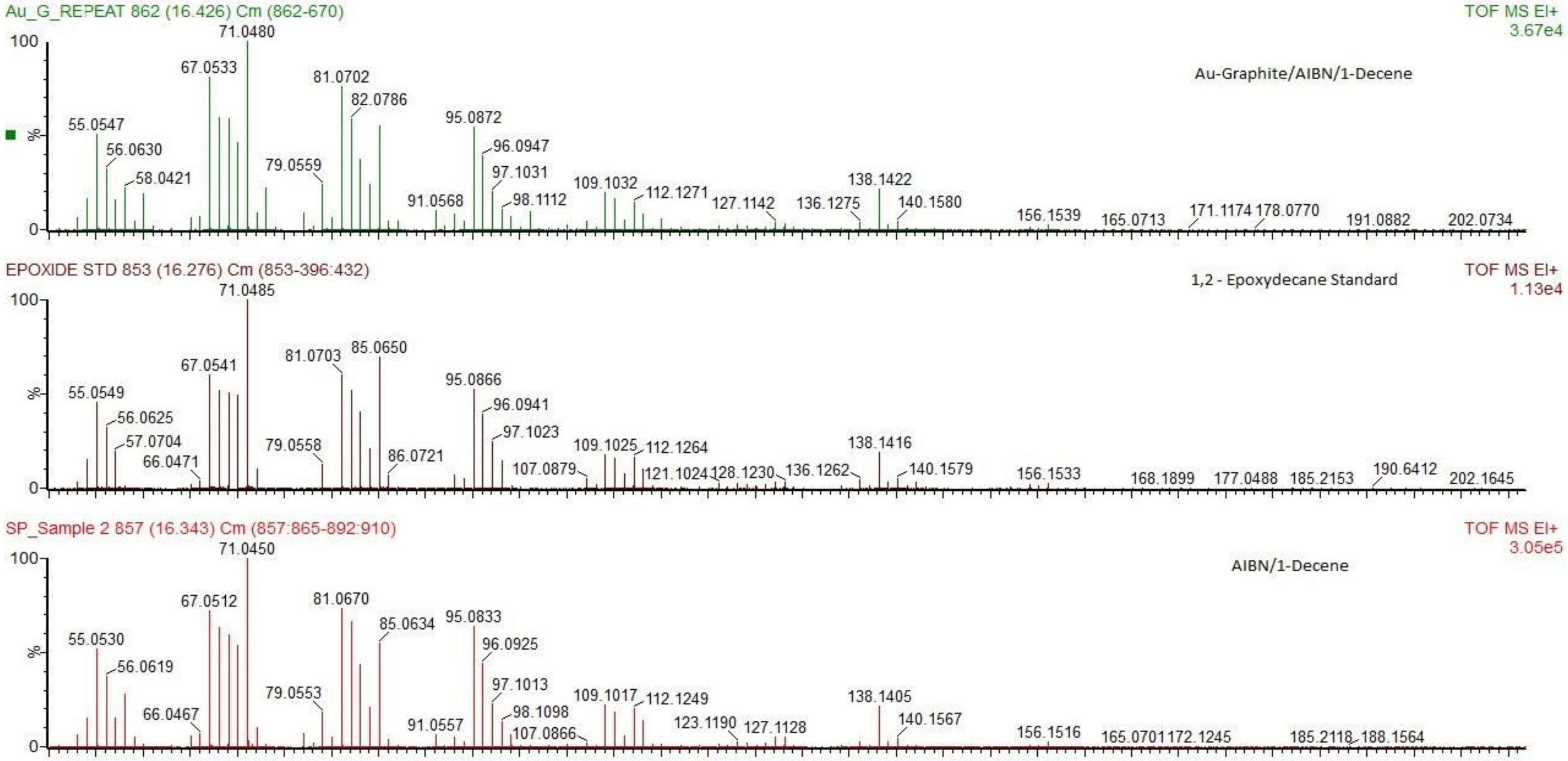

**Figure 3.3.1 GC-MS data of reaction products resulting from gold catalysed epoxidation of dec-1-ene.**

The GC-MS data for the gold catalysed epoxidation product shows an excellent agreement with that of the bought 1,2-epoxydecane standard. Even in the absence of catalyst, only the 1,2 epoxide derivative is observed. As a 2,3 epoxydecane standard was unavailable, a comparison was made with a simulated spectrum available on the NIST database. This was used to confirm the absence of the 2,3 epoxide.

### 3.4 Investigation into the effect of catalyst preparation method on dec-1-ene epoxidation

The 1% Au catalyst has been previously shown by Hutchings *et al.*[21] to be stable for epoxidation of dec-1-ene and reusable after washing with either acetone or deionised water. Even though the catalyst is uncalcined there appears to be a very low amount of leaching of gold under reaction conditions. This suggests that gold adheres to the graphite surface after regular drying at 110 °C, proving difficult to remove under these reaction conditions. The IWI method of catalyst preparation is a crude method and can be subjective with respect to addition of the metal precursor or drying intervals. The method usually yields nanoparticles in the range of 2-40 nm depending on gold loading[22] and therefore offers limited control over the gold nanoparticle size. Sol immobilisation (SI) has been extensively studied and implemented in catalysis and exhibits excellent control over the particle size to a few nanometres in both monometallic and bimetallic systems[23,24]. The method is also highly reproducible, for these reasons, 1% Au on graphite was prepared multiple times by SI in an attempt to improve on the current catalysts prepared by incipient wetness impregnation. The procedure was followed according to the literature with chloroauric acid again as the gold precursor[23,24].

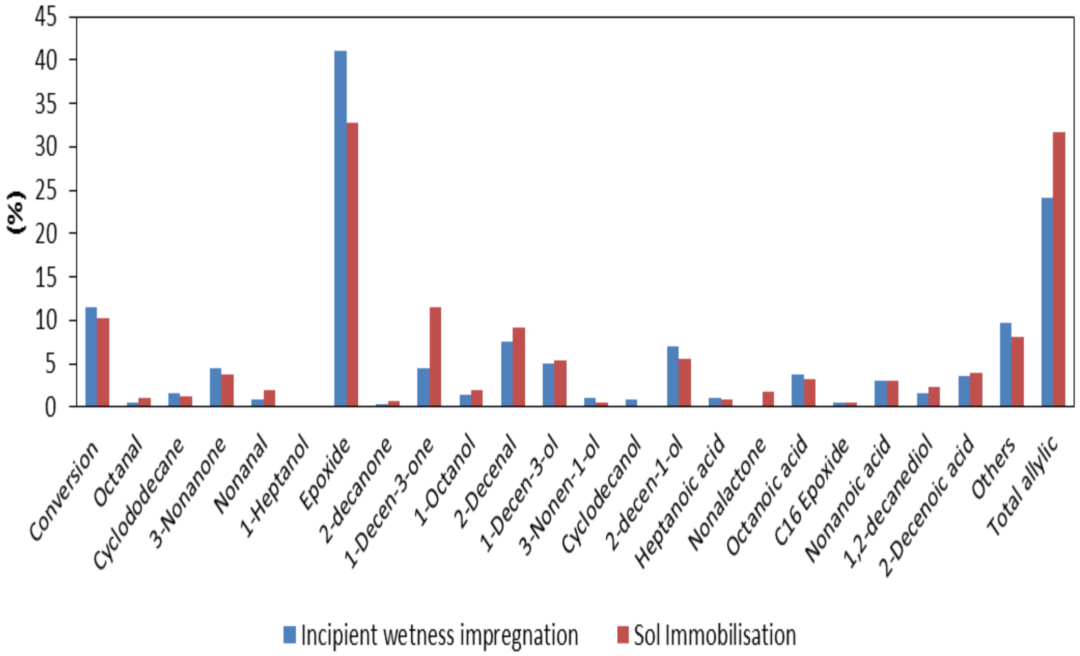

**Figure 3.4.1 Comparison of activity and selectivity of IWI and SI prepared catalysts. (24 h, 90 °C, catalyst 0.1 g, AIBN 0.006 g, dec-1-ene 10 ml)**

It can be seen (figure 3.4.1) that catalysts prepared by SI performed at a lower standard than those prepared by incipient wetness. Although conversion was only marginally lower by approximately 1.2%, the selectivity to the epoxide was dramatically lower at around 32.7 % for the SI catalyst. However, the observed selectivity is similar to that of the 1 % Au/graphite prepared by IWI reported by Hutchings[21]. The SI catalyst is still beneficial for dec-1-ene epoxidation with a much higher selectivity to the epoxide than the uncatalysed reaction.

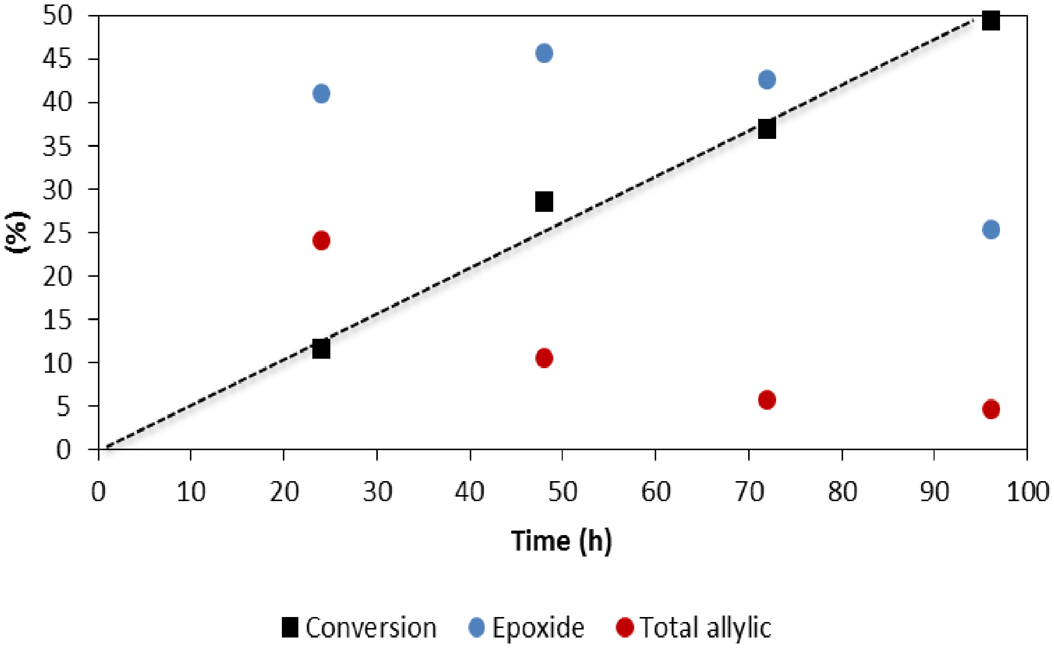

**Figure 3.4.2 Time online study of IWI prepared catalyst for epoxidation of dec-1-ene. ( 90 °C, catalyst 0.1 g, AIBN 0.006 g, dec-1-ene 10 ml)**

A time online study of the IWI and SI catalysts was conducted in order to assess their overall activity and stability over an extended reaction period. As previously reported, the initial high abundance of allylic products is quickly diminished as the process of epoxidation overtakes that of the allylic oxidation. Epoxide selectivity peaks at around 45 % after 48 hours at a conversion of 29 % for the IWI catalyst (figure 3.4.2), after which further oxidation occurs yielding a higher proportion of acids and diol.

When the same time online study is conducted for the SI catalyst a similar trend is observed (figure 3.4.3). The initial lower epoxide selectivity is seen to increase to the same level as the IWI catalyst, but over a longer time frame of 72 hours. The selectivity to the epoxide peaks at around 42 % and unlike with the IWI catalyst, the selectivity does not decrease within the time frame studied. This may be assumed to be due to a higher stability of the catalyst, however when comparing reaction conversion with the IWI catalyst, it is seen that the SI reaction is approximately 24 hours behind and it is likely that in longer reactions, the selectivity would indeed begin to fall as with the IWI catalyst. Further studies are needed to confirm this.

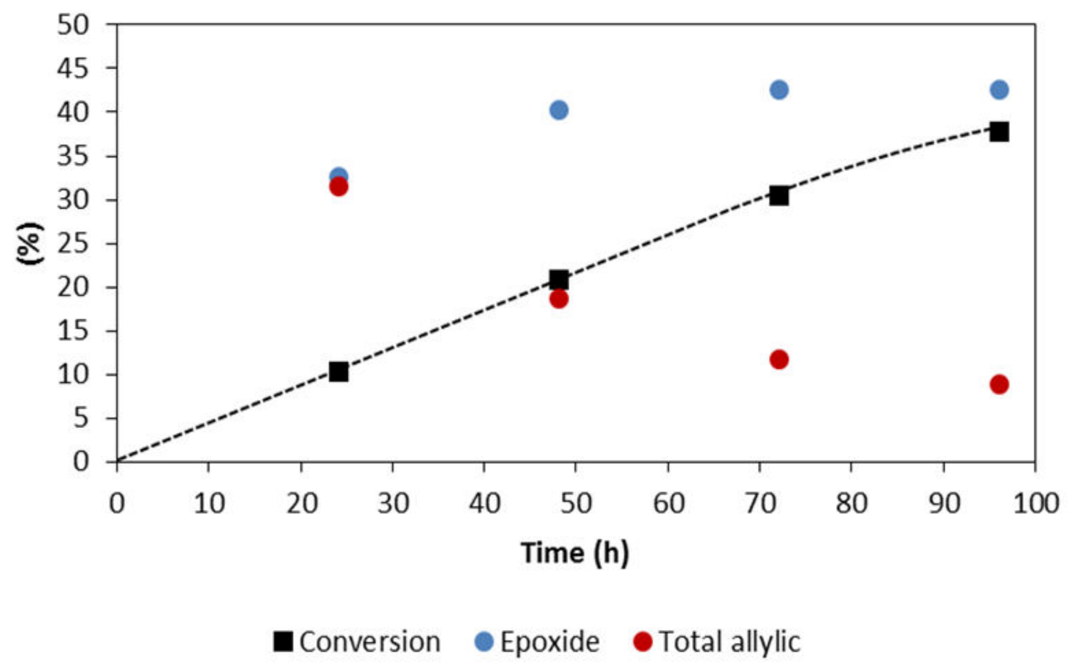

**Figure 3.4.3 Time online study of SI prepared catalyst for epoxidation of dec-1-ene. ( 90 °C, catalyst 0.1 g, AIBN 0.006 g, dec-1-ene 10 ml)**

The longer induction period seen in the SI catalyst could be caused by a coating of the nanoparticles with residual polyvinyl alcohol (PVA) stabiliser from the preparation method. Previous reports have shown that residual ligand can be removed by a simple reflux in water leading to higher exposure of the active metal and therefore a more active catalyst[25]. For this reason, a portion of the SI 1 % Au/graphite was refluxed in water at 90 °C to remove any PVA coating. This was shown to have no effect on activity or selectivity when the catalyst was refluxed for 30 minutes or 2 hours (table 3.4.1) However, Raman spectroscopy would need to be employed in order to confirm the removal of PVA.

**Table 3.4.1 Effect of removal of PVA from the catalyst *via* a 2 hour reflux at 90°C. (24h, 90°C, catalyst 0.1g, AIBN 0.006g, dec-1-ene 10ml)**

| | SI Unrefluxed | SI Refluxed for 2 hours at 90°C |
|---|---|---|
| **Conversion (%)** | 10.3 | 10.4 |
| **Epoxide (selectivity %)** | 32.7 | 32.3 |

To further investigate the effect of the PVA, tetrakis(hydroxymethyl)phosphonium chloride (THPC) was used to replace this stabiliser for the sol immobilisation of the gold catalyst. THPC has previously been shown to be successful in forming metal gold nanoparticles and useful in cases where PVA does not result in gold fully adhering to the support[26]. The use of THPC in place of PVA had no great effect on the overall activity of the catalyst (3.4.4). The conversion was seen to be identical to the PVA sol catalyst however the selectivity to the epoxide was slightly reduced while the selectivity to the allylic compounds increased. It is therefore unlikely that the observed differences between the SI and IWI catalysts is due to presence of the stabiliser. The difference is more likely to be attributed to the difference in particle size achieved with the two methods. Additional studies need to be conducted in order to clarify this. A range of SI catalysts could be prepared using differing amounts of stabiliser to probe the effect of particle size, this would need to be partnered with TEM analysis to determine the gold particle size.

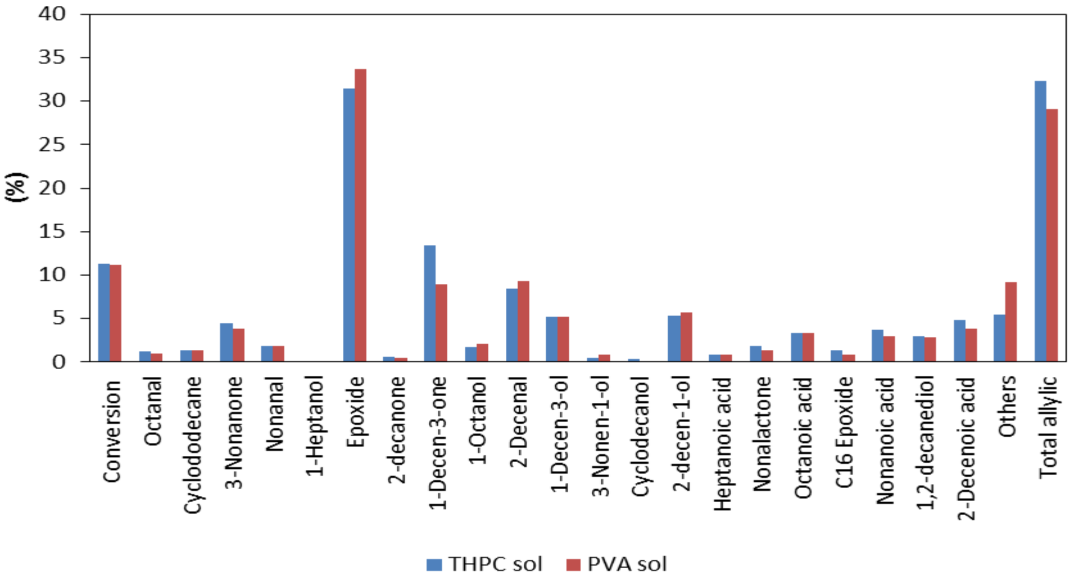

**Figure 3.4.4 Comparison of activity and selectivity of 1 % Au/Graphite prepared using PVA and THPC stabilisers. (24 h, 90 °C, catalyst 0.1 g, AIBN 0.006 g, dec-1-ene 10 ml)**

The effect of the amount of gold on the surface was briefly explored using a 0.5 % Au/Graphite prepared by SI (figure 3.4.5). It was shown to have the expected result of lower selectivity however overall conversion was similar. The catalysts with the lowest gold loading yielded the highest amount of allylic products, seemingly due to inefficiencies in preventing the build-up of hydroperoxide followed by Russell termination. Once again it is again unclear as to whether this effect was the result of the low gold catalyst loading, or because of a smaller gold particle size. To investigate this, a 0.5 % Au sol with half the amount of usual PVA could be prepared. Transmission electron microscopy (TEM) investigations would also give a better insight into the particle size distribution on the graphite surface.

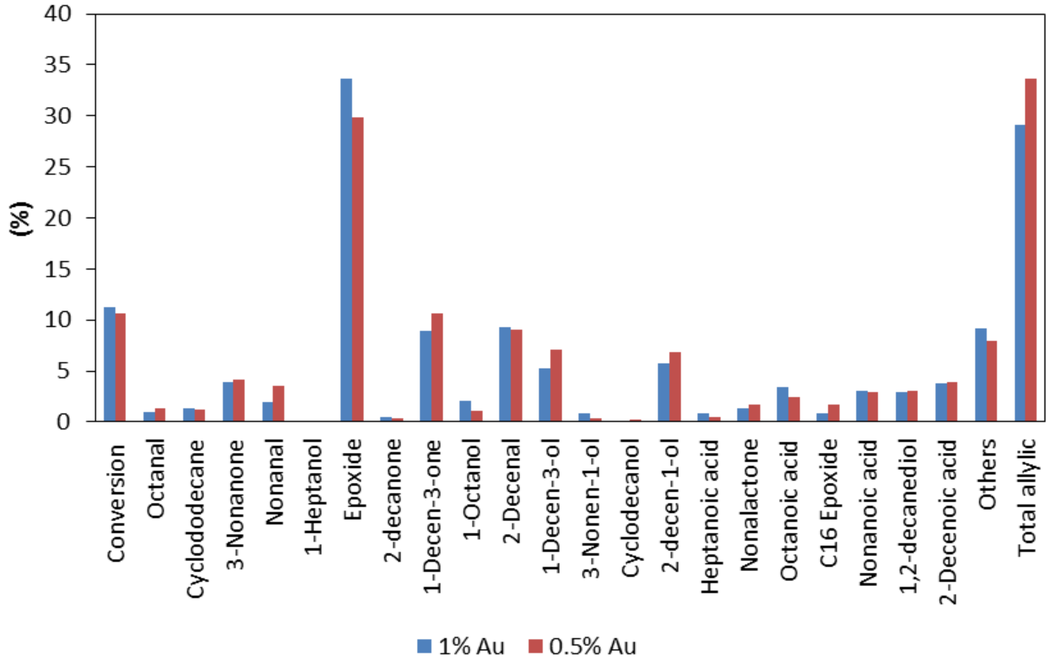

**Figure 3.4.5 Comparison of 0.5 % and 1 % gold loadings for epoxidation of dec-1-ene (24 h, 90 °C, catalyst 0.1 g, AIBN 0.006 g, dec-1-ene 10 ml).**

### 3.5 Replacement of gold with suitable transition metal elements

A brief study was conducted into the possible replacement of gold with other transition metals (figure 3.5.1). A range of 1 % metal on graphite catalysts were prepared by IWI and screened for activity in the epoxidation of dec-1-ene. The study was unsuccessful in finding a metal which approaches the activity of gold and its ability to direct the reaction towards the epoxide. The activity of the palladium and silver catalysts were just over half of that of gold, however the selectivity was dramatically lower.

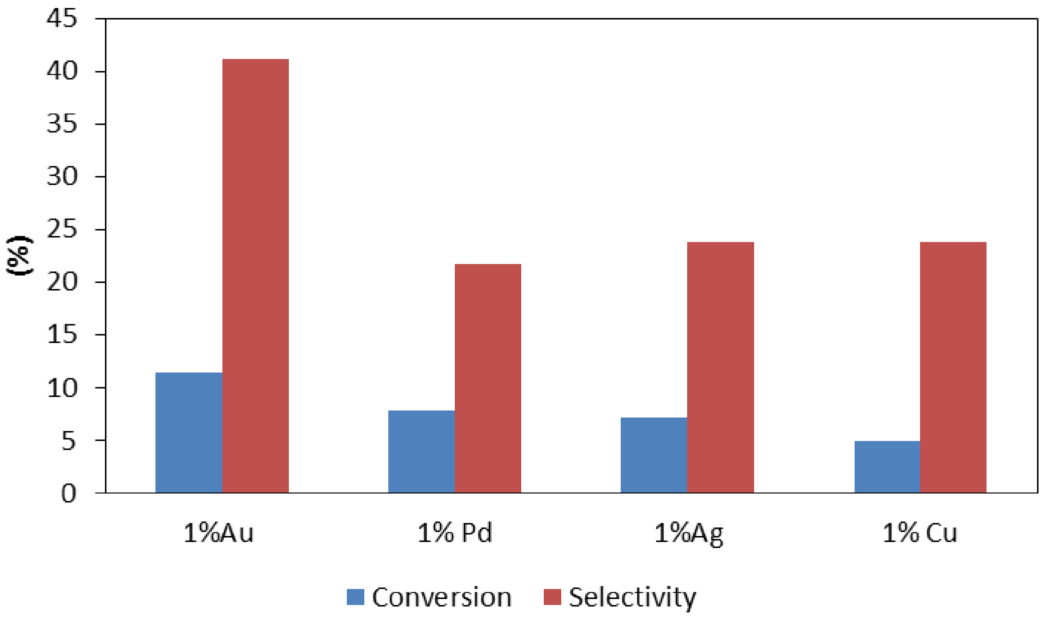

**Figure 3.5.1 Comparison of activities and selectivites of monometallic catalysts. (24 h, 90 °C, catalyst 0.1 g, AIBN 0.006 g, dec-1-ene 10 ml).**

Clearly, these metals do not have potential for the use as a monometallic alternative to gold when supported on graphite for the epoxidation of dec-1-ene. However, further studies were conducted to assess if any of these metals could be used as a bimetallic or promoter to further enhance the superior activity of gold.

## 3.6 Bimetallic studies

### 3.6.1 Gold and silver bimetallic catalysts prepared by IWI

Silver was explored for the possibility of forming a bimetallic catalyst with gold. A range of catalysts with different ratios of gold and silver were made *via* IWI. The catalysts were all designed to have a final total metal loading of 1 wt %. In all cases, replacement of some of the gold with silver resulted in a dramatic decrease in selectivity and/or conversion (figure 3.6.1). The use of a 0.9:0.1 Au:Ag ratio catalyst resulted in a similarly active catalyst, however the selectivity to the epoxide is reduced by over 10 %. This is unsurprising given silver's low activity as a monometallic, however it does rule out the benefit when adding it to the gold.

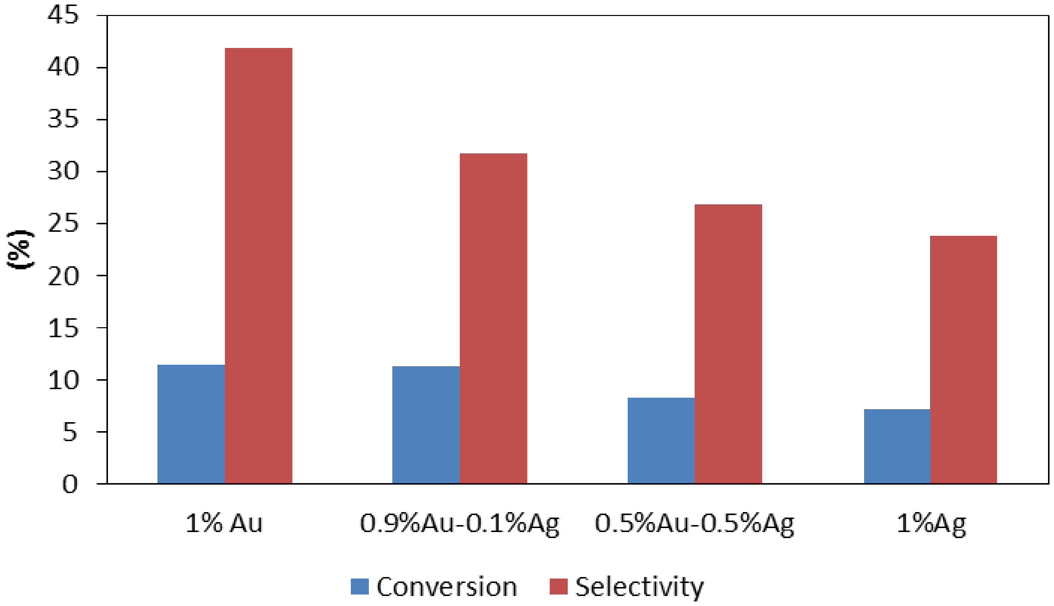

**Figure 3.6.1 Comparison of gold and silver bimetallic catalysts. (24 h, 90 °C, catalyst 0.1 g, AIBN 0.006 g, dec-1-ene 10 ml).**

### 3.6.2 Gold and Palladium Bimetallic catalysts prepared by IWI

Palladium was also explored as a potential additive to the gold system (figure 3.6.2). However a similar effect was observed to that of Au-Ag bimetallic catalysts. Monometallic palladium was seen to be less active than gold, and any addition of palladium to the gold catalyst resulted in a decrease in efficiency of the catalyst. This is a similar trend to that observed by Hutchings *et al*. when studying the epoxidation of cis-cyclooctene[27]. However, in cis-cyclooctene epoxidation, selectivity was shown to be unaffected by the Au:Pd metal ratio, albeit with massive effects on conversion. Here we clearly see a dramatic decrease from the selectivity observed with monotmetallic gold when Pd is added to the catalytic system.

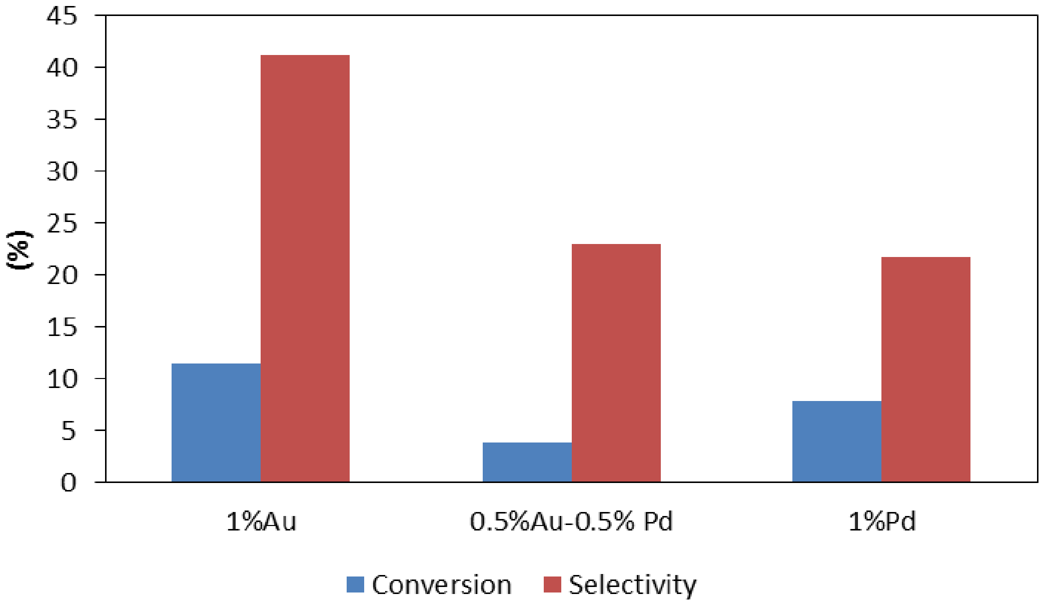

**Figure 3.6.2 Comparison of gold and palladium bimetallic catalysts. (24 h, 90 °C, catalyst 0.1 g, AIBN 0.006 g, dec-1-ene 10 ml).**

### 3.6.3 Gold and Copper bimetallic catalysts prepared by IWI

Copper is a slightly more interesting option for increasing the efficiency of the catalyst. As shown below, a 1%Au-1%Cu-Graphite catalyst was shown to be slightly more active than the monometallic 1% gold Catalyst however this was accompanied with a slightly lower selectivity to the epoxide. When the same catalyst was produced by SI, the activity and selectivity significantly reduced and were both lower than that of the 1% Au/Graphite IWI standard catalyst.

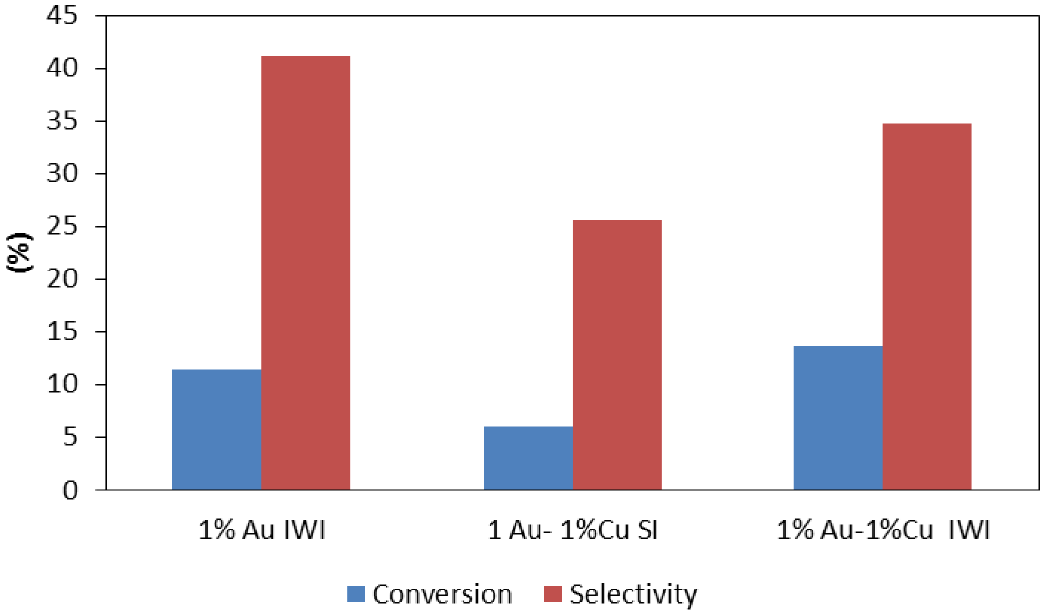

**Figure 3.6.3.1 Comparison of gold and copper bimetallic catalysts prepared by SI and IWI. (24 h, 90 °C, catalyst 0.1 g, AIBN 0.006 g, dec-1-ene 10 ml).**

Initial concerns were that the copper was leaching off of the graphite when prepared by IWI. An alternative explanation for the lower activity seen by the SI catalyst could be that a lower amount of copper has been adhered to the surface than in the IWI where all of the added copper would remain on the surface due to the details of the method.

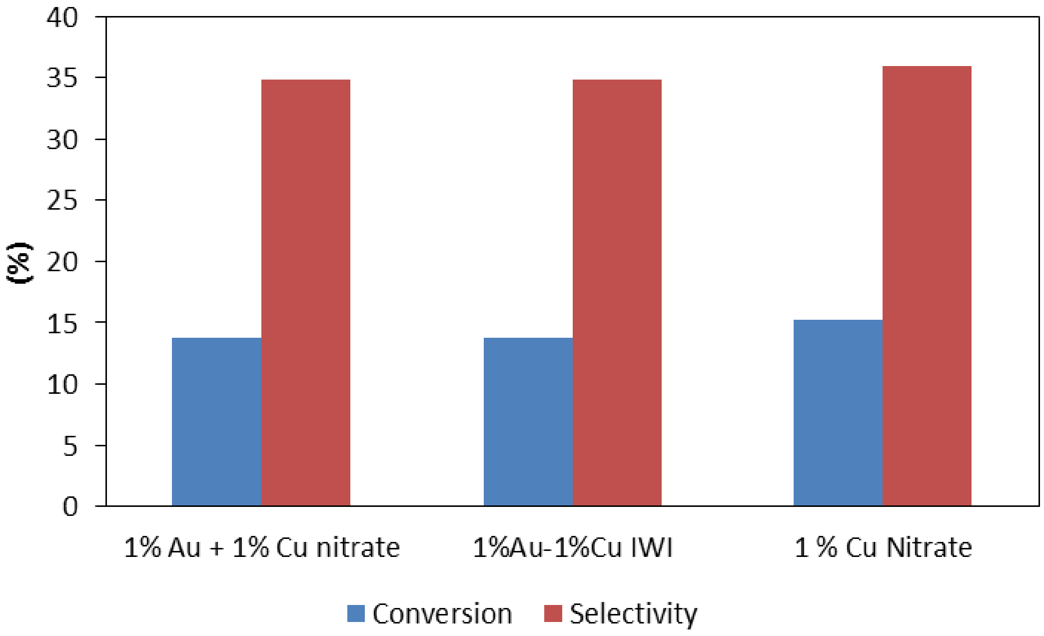

**Figure 3.6.3.2 Comparison of activity and selectivity of gold and copper bimetallic with a homogenous copper nitrate system.**
**(24 h, 90 °C, catalyst 0.1 g, AIBN 0.006 g, dec-1-ene 10 ml).**

A study was conducted to compare the activity of this IWI prepared Au-Cu bimetallic with that of copper nitrate salt and also when the salt is added to the reaction in the presence of an SI 1% Au catalyst. It can be seen that copper nitrate is active for epoxidation of dec-1-ene in the presence of AIBN. This suggests that if any copper leached from the catalyst in the form of nitrate then this would likely have a beneficial effect on activity. Certainly, when the nitrate is added into reaction in the presence of a 1 %Au catalyst then the overall activity reaches the level of that observed for the 1 %Au-1 %Cu IWI catalyst. Although this does not confirm that copper is leaching, it definitely demonstrates the need to be aware of the activity of the nitrate precursor. Analysis of post reaction solution by MP-AES would give an insight to the level of leaching.

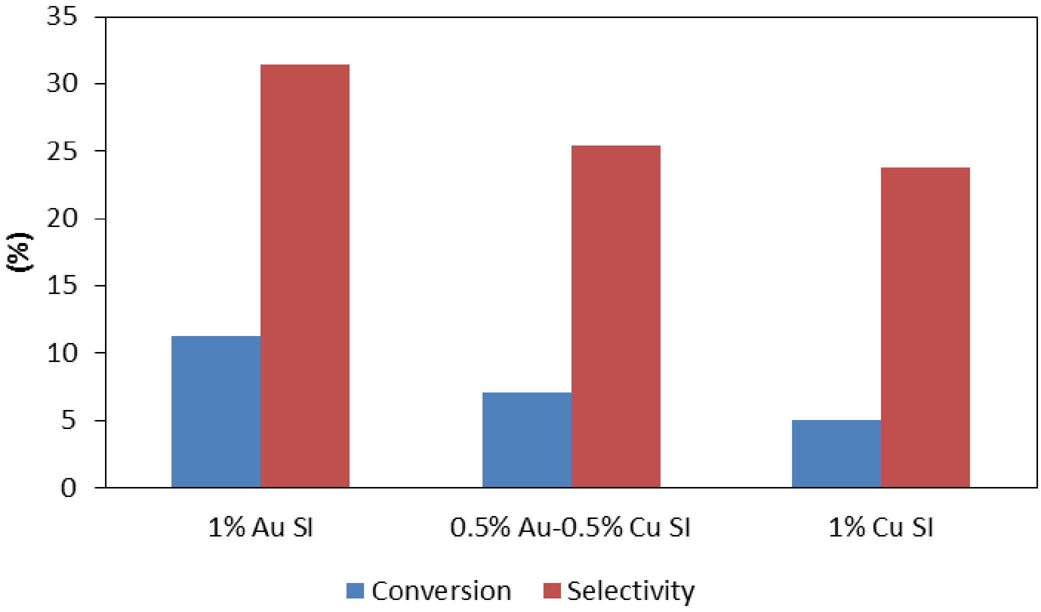

**Figure 3.6.3.2 Comparison of conversion and selectivity of gold and copper bimetallic catalysts prepared by SI.**
**(24 h, 90 °C, catalyst 0.1 g, AIBN 0.006 g, dec-1-ene 10 ml).**

Due to the presumed instability of IWI prepared catalyst, a 0.5% Au- 0.5% Cu catalyst was prepared by SI to further explore the possibility of forming a successful bimetallic nanoparticle system. However the results above confirm that this is unlikely due to the diminished actvity and selectivity of the catalyst when compared to the 1 % standard gold catalyst. However, the activity of copper in the IWI catalyst, whether it is confirmed to be homogeneous or heterogeneous in reaction, gives promise to the development of a cheaper alternative to gold.

Overall the activity of nanoparticle gold supported on graphite seems to be most effective when operating strictly as a monometallic. The addition of metals to form alloys which have demonstrated synergistic effects for other oxidation reactions, have proven to be inferior to the gold itself for the epoxidation of dec-1-ene.

## 3.7 Catalyst supports

### 3.7.1 Effect of graphite

The graphite support used in this study proved to have a much greater role on catalysis than previously thought. Subsequent batches of graphite <20μm, although sourced from the same supplier, demonstrated vastly different capabilities for producing a highly active catalyst. This was shown by comparing identically prerpared IWI 1 % Au-graphite catalysts using various graphite batches all purchased using the same batch code.

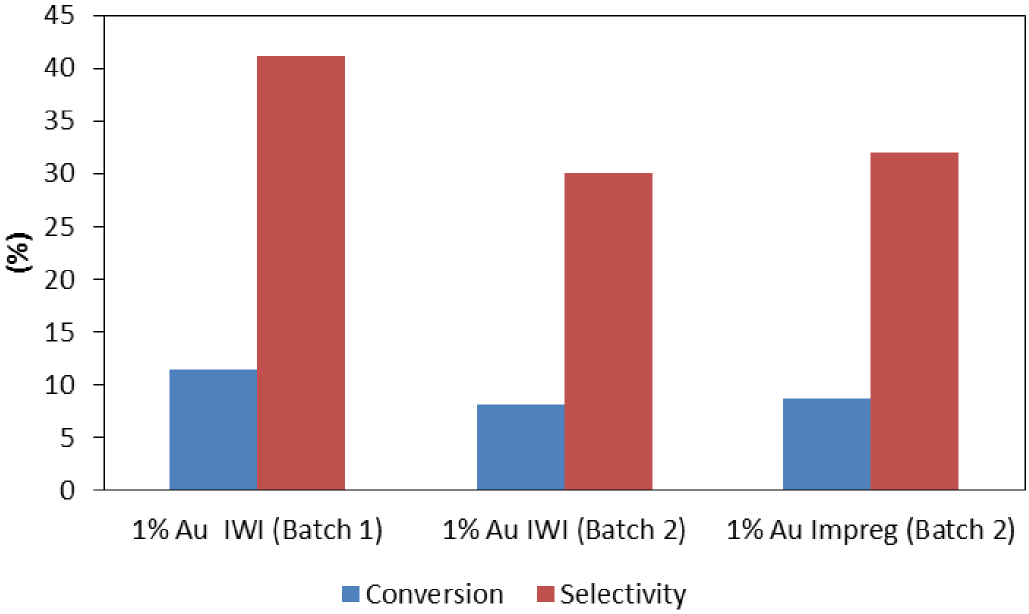

**Figure 3.7.1 Comparison of activity and selectivity of 1 % Au catalysts prepared by IWI using various graphite batches.**
**(24 h, 90 °C, catalyst 0.1 g, AIBN 0.006 g, dec-1-ene 10 ml).**

It can be seen that catalysts produced using graphite from batch 2 showed distinctly lower activities compared to batch 1. Conversions and selectivities were lower by approximately 3 and 10 % respectively. This was also the case when the catalyst was prepared by the IWI and wet impregnation (Impreg) techniques, thus showing similarities between the two methods. The unreliable nature of graphite supports is well known, with carbon source and processing giving rise to differing levels of impurities and surface defects. Many groups have expressed the need for a treatment of the carbon supports prior to impregnation of the metal. This was demonstrated by Hutchings *et al.* when researching the hydrochlorination of acetylene[28,29]. An acid pre treatment followed by a further treatment after the reaction was shown to be integral for the activity and regeneration of the catalyst. For use as a support for gold catalysts, graphite has been extensively studied by Davies *et al.*[30,31] Davies has shown that acid treatment of highly ordered pyrolitic graphite (HOPG) leads to the formation of functional groups and surface defects which facilitate the dispersion of gold upon the surface. It was also found that the extent and functionality of the groups relied on the identity of the acid. Further investigation into the observed irregularity between graphite batches for dec-1-ene epoxidation is needed. A full characterisation of the surface *via* XPS and TEM could give clues as to the inherent difference of the support and also the dispersion of gold when loaded onto the graphite.

### 3.7.2 Derivitisation of the graphite support

The epoxidation of terminal alkenes has been studied extensively due to their aforementioned importance in industry and academia. Through catalysis, oxidation can either occur *via* the use of stoichiometric amounts of valuable oxidant such as hydrogen peroxide. As described earlier, atmospheric oxygen may be employed as a green alternative. However for the use of atmospheric oxygen, temperatures must be employed whereby autooxidation does not occur and overwhelm epoxidation. At these temperatures it becomes essential to use a radical initiator in order to propagate reaction of oxygen, after which the catalyst promotes the selective formation of the epoxide. Currently, the majority of the research directed at terminal alkene epoxidation incorporates one of the above, however in a few cases, reactions are catalysed above the autoxidation temperature to eradicate the use of an initiator. However, for low temperature epoxidation, catalysts must be developed that can simultaneously activate oxygen through oxygen reduction and catalyse the selective epoxidation without the need for additional oxidations or initiators. Even though initiators like those used in this study are only employed in catalytic amounts, they are potentially carcinogenic and therefore should be eradicated from the procedure if possible. It is therefore the aim of the remainder of this work to study alternatives to the current gold-graphite catalyst which can fulfil this criteria.

Initially, derivitisation of the graphite support was studied in order to explore new methods for the activation of oxygen and to also serve as a solution to the leaching of metals from graphite supports.

Graphitic oxide (GO) was explored as a support due to its high oxygen coverage, tunable surface functionality and its use in many oxidation reactions. It has also been suggested that GO could provide the ideal support for gold for certain oxidation reactions[32]. This was partnered with a study into the use of iron catalysts for the activation of oxygen due to the well known oxidation capabilities of iron. Gold was also incorporated into the study due to its previously shown superiority in the field of olefin epoxidation.

Therefore a range of graphitic oxide, gold and iron catalysts were prepared by incipient wetness impregnation and tested for activity for epoxidation of dec-1-ene. The graphitic oxide was prepared by a modified Hofmann method[33] whereby for safety, only 15g potassium chlorate was used (GO-HO15). This resulted in lower formation of the explosive gas chlorine dioxide, but also resulted in a lower oxygen catalyst content than that reported in the literature when 55g potassium chlorate was used in the catalyst preparation.

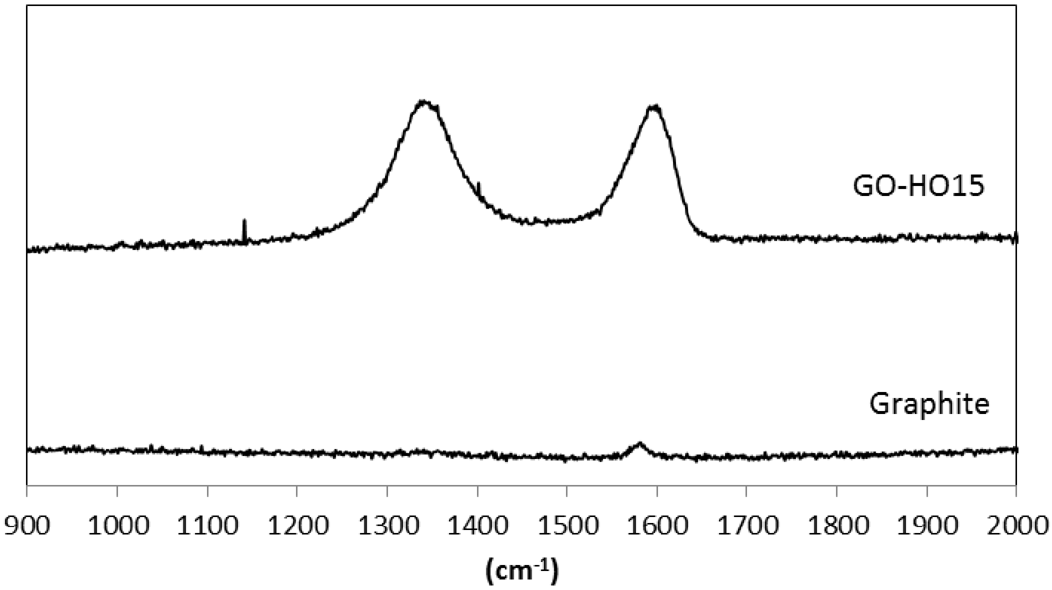

**Figure 3.7.2.1 Raman spectroscopy of graphite and graphitic oxide prepared by modified Hofmann method.**

Raman spectra (taken using a 514nm He Ne laser) were used to confirm the oxidation of the graphite precursor (figure 3.7.2.1). The presence of a disorder induced D band at 1330cm$^{-1}$and the broadened and blue shifted G band at 1590cm$^{-1}$ is indicative of oxidation and interruption of the sp$^2$ lattice of graphite[34].

Once graphitic oxide had been synthesised, catalysts were prepared in identical fashion to that of the supported graphite catalysts through the stepwise addition of metal precursors.

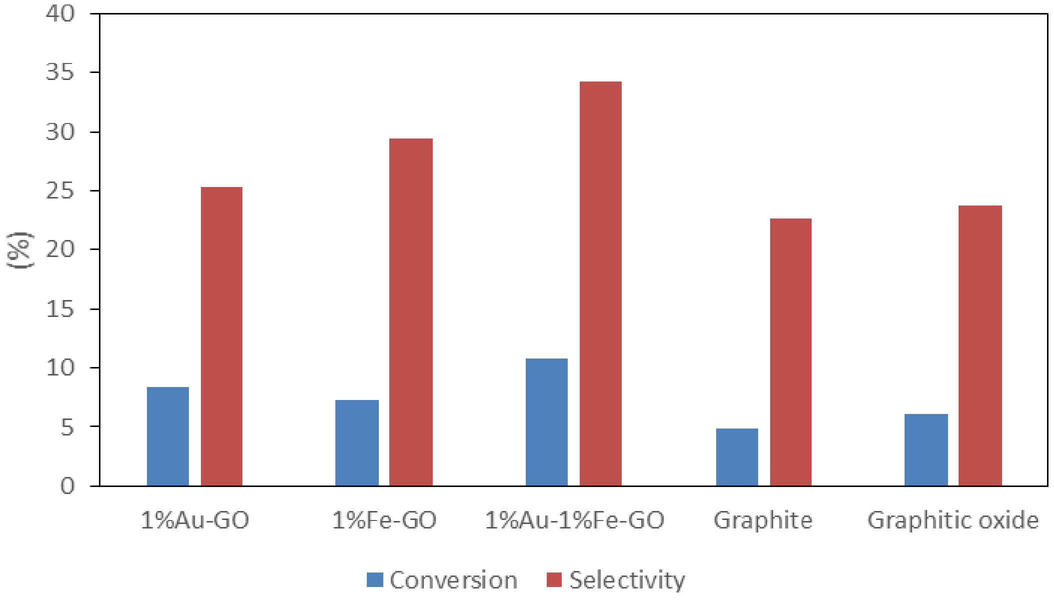

**Figure 3.7.2.2 Comparison of activities and selectivities of gold and iron catalysts supported on graphitic oxide.**
**(24 h, 90 °C, catalyst 0.1 g, AIBN 0.006 g, dec-1-ene 10 ml).**

All catalysts were tested for dec-1-ene epoxidation in the presence of AIBN, all catalysts displayed lower activity than the graphite supported gold analogue. Both iron and supported GO catalysts exhibit low activities of around 7 % conversion. However, a 1 %Au-1 %Fe-GO catalyst shows a conversion of 10.8 % illustrating a potential synergy between the two metals for dec-1-ene epoxidation. This activity is similar to that observed for the gold-graphite standard catalyst however accompanied by a reduction in selectivity. The graphitic oxide shows a small increase in activity and selectivity when compared to the graphite precursor. Although the results are seemingly lower than the previously reported for gold catalysts, there are encouraging signs that both GO and iron modified GO are potential catalysts for dec-1-ene epoxidation.

The most significant results were obtained when the catalysts were screened for blank reactions in the absence of AIBN, shown below. Here, all catalysts that incorporated graphitic oxide were shown to be active in the absence of radical initiators. The reaction times were extended to allow increase in conversion for ease of comparison between the catalysts. It can be seen that even the graphitic oxide was active for epoxidation in the absence of initiator compared to the completely blank graphite support. It should be reiterated here that dec-1-ene at 90 °C shows absolutely no conversion in the absence of initiators.

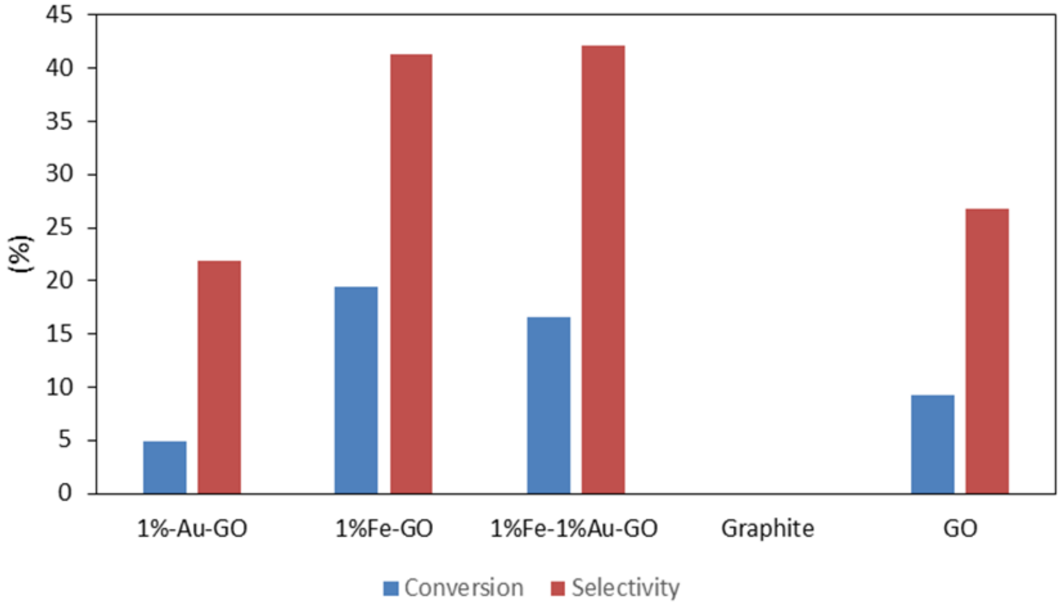

**Figure 3.7.2.3 Comparison of activities and selectivities of gold and iron catalysts supported on graphitic oxide in the absence of radical initiators. (48 h, 90 °C, catalyst 0.1 g, dec-1-ene 10 ml).**

An intriguing observation related to the data (figure 3.7.2.3) is the lower activity of the Au-GO catalyst compared to the blank GO support. It can also be seen that the 1 %Au-1 %Fe GO is also lower in activity that observed for the 1 % Fe-GO catalyst. This is a surprising result given the higher activity of 1%Au-1%Fe GO in the presence of AIBN shown earlier. It may be that the addition of the gold to the GO either poisons the surface by chlorine contamination from chloroauric acid. Another possibility is that the gold itself acts as a radical inhibitor and offers a competing mechanism to that occurring on the GO surface. Addition of iron to the GO surface clearly has a positive effect on both conversion and selectivity compared to the unmodified GO catalyst.

A time online study of the 1 %Au-1 %Fe GO catalyst was conducted to explore the long term stability of the catalyst for dec-1-ene epoxidation. It can be seen that the uninitiated reaction suffers from a lengthy induction period, resulting in low conversion and poor selectivity after 24 hours of reaction. After 72 hours the reaction has reached a comparable level of conversion to that of the free radical initiated 1% Au-/Graphite catalyst reaction previously described. The 1 %Au-1 %Fe GO catalyst gave a conversion of 31.2% and a high selectivity to the epoxide of 44.6 % compared to the IWI 1 %Au/Graphite catalyst which yielded 36.9% and 42.7% respectively.

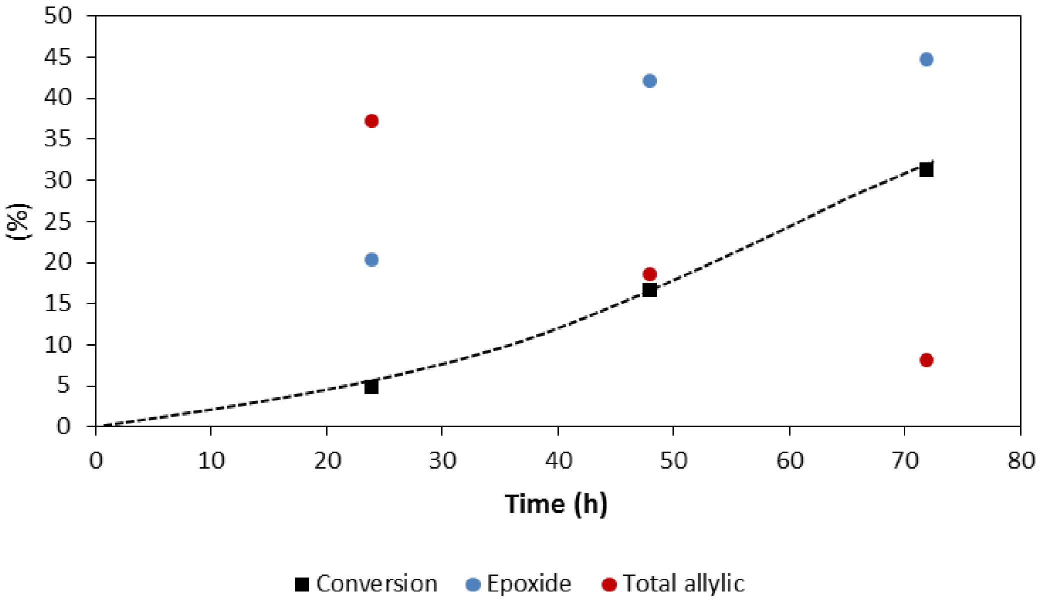

**Figure 3.7.2.4 Time online study of 1%Au-1%Fe/GO catalyst in the absence of radical initiators.**
**(90 °C, catalyst 0.1 g, dec-1-ene 10 ml).**

Promotion by iron on the GO surface was further explored by adding the precursor iron nitrate nonahydrate into a reaction with dec-1-ene in the absence of AIBN to see if iron could propagate reaction homogeneously. An equivalent amount of iron was used as to what would be present in 0.1 g of 1 %Fe-GO catalyst. This required adding approximately 0.0072 g of the iron precursor to 10 ml of dec-1-ene. It was found that iron in this form could initiate the epoxidation of dec-1-ene in the absence of any other catalyst or radical initiator. Trace amounts of iron nitrate were shown to have a higher activity than the GO support and 1 %Au-GO catalyst over the same time frame. This data suggests that it is possible that any leaching of iron into the reaction solution from the catalyst could homogeneously catalyse the reaction. Analysis of post reaction solutions *via* ICP-OES or MP-AES could provide quantification and identification of any leached species. Similarly, these techniques could be employed to analyse digested samples of pre and post reaction catalysts to quantify total metal loading. However, digestion of carbon supports is notoriously difficult employing harsh oxidising conditions.

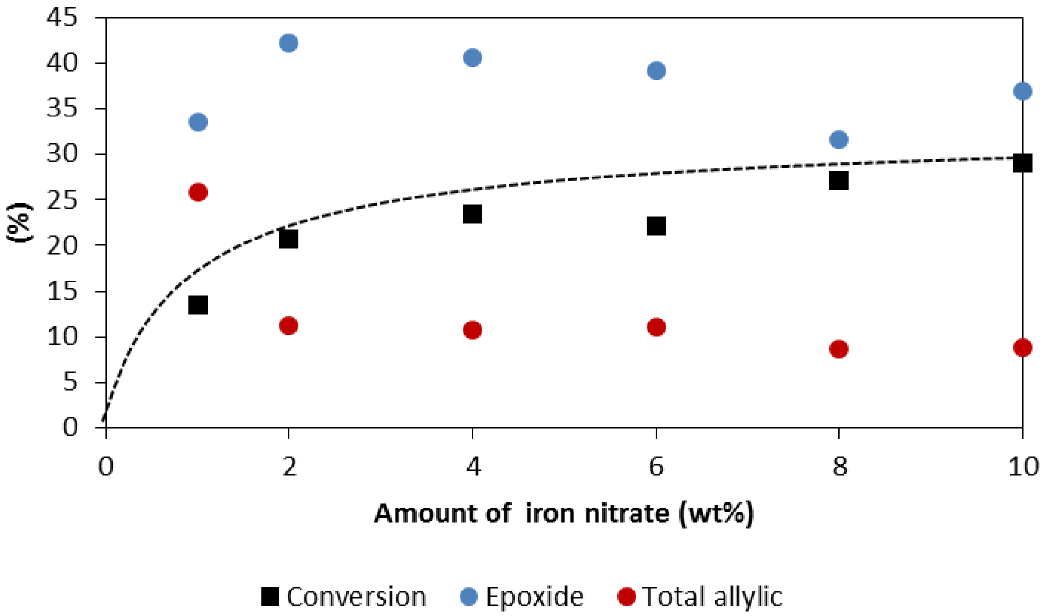

**Figure 3.7.2.5 Investigation into the activity of iron nitrate nonahydrate and the effect of weight loading on conversion and selectivity.**
**(48 h, 90 °C, dec-1-ene 10 ml).**

The interesting behaviour of homogeneous iron was further explored by investigating the effect of the amount of iron used in the reaction. Again, the amounts used were analogous to what would be present for different weight loadings on a 0.1 g catalyst sample. As before 1% corresponds to 0.0072 g of iron nitrate nonahydrate, whereas 10 % corresponds to 0.072 g of the precursor. Iron nitrate was shown to be extremely active at 90 °C for the epoxidation of dec-1-ene achieving conversions of up to 30 % in 48 h when using 0.072 g of the precursor. Over this time frame it appears to be more beneficial to use a lower amount of iron to sacrifice a small amount of conversion for a high selectivity to the epoxide. As previously mentioned, it is unclear as to whether this lower selectivity at higher conversions is due to a less selective catalyst or if in fact it is due to a maximum being reached in the reaction, followed by further oxidation to carboxylic acids and diols. A higher proportion of unknown liquid products is also observed at these higher conversions indicating further cracked products and higher oxidised species.

The use of iron is a promising option for the activation of oxygen in the absence of radical initiators. Even though these studies are homogeneous, the activity seen when added to the GO catalyst is encouraging for developing a highly active epoxidation catalyst at low temperatures. Therefore further studies were conducted to probe the temperature range over which this iron species could catalyse the reaction. A 10 % iron nitrate nonahydrate (0.072 g) solution was used and reacted for 48 h in the absence of initiators. It was found that reaction activity was observed at temperatures as low as 75 °C. This is a promising result as it is over 25 °C below the autoxidation temperatures of dec-1-ene. This provides the basis for low temperature catalysts to be designed for epoxidation of terminal alkenes at low cost.

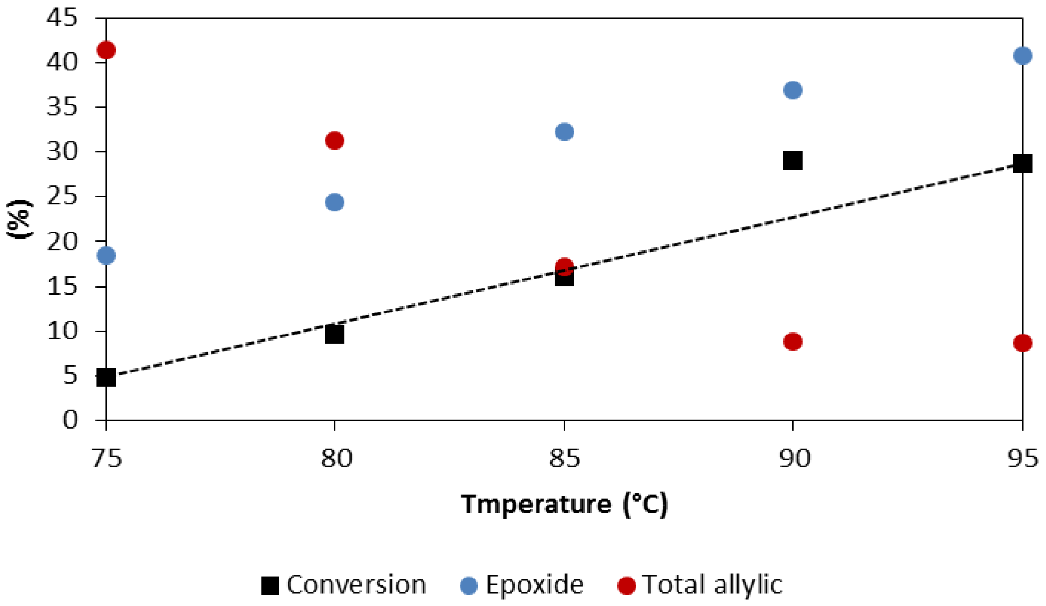

**Figure 3.7.2.5 Effect of temperature on the activity of iron nitrate nonahydrate for the epoxidation of dec-1-ene.**
**(48 h, Iron nitrate nonahydrate 0.072 g, dec-1-ene 10 ml).**

The 1 %-Au-1 % Fe catalyst was prepared on graphite and graphitic oxide using a sol immobilisation technique. However as expected, both catalysts showed no activity for the epoxidation of dec-1-ene in the absence of radical initiators. It is likely that use of sodium borohydride reduced the oxygen from the graphitic oxide surface forming an inactive reduced graphene oxide type material. It is also possible that iron did not adhere to the surface under these conditions. As previously mentioned, full analysis of the surface composition would be needed to confirm the absence of iron.

## 3.8 Conclusions

It has been previously shown that gold is an excellent candidate for catalysing the selective oxidation of dec-1-ene to the epoxide. The presence of AIBN initiator allows for the use of atmospheric oxygen as an oxidant in place of expensive and environmentally hazardous alternatives. Here, the benefit of using nanoparticle gold has been further supported as it has shown to be a far more active metal than its monometallic counterparts. Unsuccessful attempts were conducted to find at least one metal which could promote the significant activity and selectivity of gold. All attempts not only failed to increase activity but were also shown to hinder the gold system. Various methods of preparation of the gold catalyst were also attempted with incipient wetness impregnation remaining as the optimum procedure for preparation of the active catalyst. This catalyst has previously been shown to be stable over multiple uses and therefore drops in selectivity seen in time online studies are perhaps more like to be due to either coating of the active site or switching of the mechanism due to changes in the reaction medium over time. Full qualification of unknown liquid products which become more and more prominent with time will give a better insight into how the epoxide is undergoing further oxidation and potentially causing the observed drop in activity. This analysis would perhaps be tedious due to the already great number of known products and over 30 unknown liquid products; however this could lead to better development of a reaction system for high selectivities.

The derivatisation of the graphite support to graphitic oxide has provided some great opportunities for the development of a catalyst which does not require radical initiators for the activation of oxygen. This combined with the use of iron could lead to a terminal alkene epoxidation catalyst which is more environmentally friendly. The lower activity observed for the Au-GO catalyst compared to just the support suggests that incorporation of these highly selective nanoparticles would be problematic in future work.

Future work would aim to identify the amount of leaching seen by all of these catalysts and attempt to produce a truly heterogeneous catalyst for epoxidation. MP-AES or ICP-OES needs be employed to test post reaction mixtures for leached metals. It is important to test the unique catalysts observed here for epoxidation of a wider range of substrates such as linear, cyclic, terminal and internal alkenes to explore if the benefits seen with dec-1-ene can be further utilised.

Due to the unexpected activity of graphitic oxide in the absence of any metal or radical initator, it was decided to explore the origin of this trait for the development of a carbocatalyst, the findings of which are outlined in chapter 4.

### 3.9 References

---

1 A.Ansmann, R, Kawa, M.Neuss, US Patent 7083780 B2 Aug 1 2006 assigned to Cognis Deutschland

2 P. Christopher, S.Linic, *J.Am.Chem.Soc*, **130**, 11254-11265

3 H.Pines, D.D.Eley, P.B. Weisz, Advances in Catalysis, Academic Press, New York, 1987, 265-321

4 M.O.Ozbek, R.A.Van Santen, *Catal.Lett*, 2013, **143**, 131-141

5 M.G.Clerici, G.Bellusi, U.Romano*, J.Catal*, 1991, **129**, 159-167

6 M.G.Clerici, P.Ingallina, *J.Catal*, 1993, **140**, 71

7 B.Notari, Catal.Today, 1993, **18**, 163

8 P.Bassler, M.Weidenbach, H.Goebbel, *Chem.Eng.Trans*. 2010, **21**, 571-576

9 E.L.Lines, R.J.Fairbrother, J.A.Herbst, US 4157346,1979, assigned to Olin Corporation

10 M.Rameswaran, R.N Cochran, US 5081267, 1992. Assigned to Arco Chemical technology

11 T.A. Nijhuis, M. Makkee, J.A.Mouljin, B>M. Weckhuusen, *Ind. Eng.Chem.Res*, 2006, **45**, 3447-3459

12 K. Weissermel, H.J.Arpe, Industrial Organic Chemical, VCH Publisher Inc. ,New York, 3rd, 1993, 141-264

13 J.G.Zajaceck, D.Pa, G.LCrocco, US 5214168, 1993, assigned to Arco Chemical technology

14 P.P.Pescarmona, P.A.Jacobs, *Catal.Today*, 2008, , **137**, 52-60

15 D.Mandelli, M.C.A. Van van Vilet, R.A. Sheldon, U.Schuchardt, *Appl.Catal.A:Gen*, 2001, **219**, 209-213

16 N.Scotti, N. Ravasio, N.F. Zaccheria, R.Psaro, C.Evangelisti, *Chem.Commun*, 2013, **49**,1957

17 M.D. Hughes, Y.X.Xu, P.Jenkins, P.Macmorn, P.London, D.I.Enache, A.F.Carley, G.A.Attard, G.J.Hutchings, F.King, F.E.H.Stitt, P. Johnston, K.Griffin, C.J. Kiely, *Nature*, 2005, **437**, 1132-1135

18 H.Alshammari, P.J.Medziak, D.W.Knight, D.J.Willock, G.J. Hutchings, *Catal, Sci. Technol*,2013, **3**, 1531-1539

19 H.Alshammri, P.J. Medziak, S.Bawaked, D.W.Knight, G.J. Hutchings, *Chem.Cat.Chem*, 2012, **4**, 1565-1517

20 H.Alshammari, P.J.Medziak, D.J.Morgan, D.W.Knight, G.J.Hutchings, *Green Chem*, 2013, **15**, 1244-1254

21 U.N.Gupta, N.F. Dummer, S.Pattisson, R.L.Jenkins, D.W.Knight, D.Bethell, G.J.Hutchings, *Catal Lett*, 2014, DOI 10.1007/s10562-014-1425-z

22 C.Baatz, U.Prube, *J.Catal*, 2007, **249**, 34-40

23 N.Dimitratos, J.A.Lopez-Sanchez, D.Morgan, A.Carley, L.Prati, G.J.Hutchings, *Catal.Today*, 2007, **122**, 317

24 J.A.Lopez-Sanchez, N.Dimitratos, P.Miedziak, E.Ntainjua, J.K.Edwards, D.Morgan, A.F.Carley, R.Tiruvalam, C.J.Kiely, G.J.Hutchings, *Phys.Chem.Chem.Phys*., 2008, **10**, 1921-1930

25 J.A. Lopez-Sanchez, N.Dimitratos, C.Hammon, G.L.Brett, L.Kesavan, S.White, P.Medziak, R.Tiruvalam, R.L.Jenkins, A.F.Carley, D.W.Knight, C.J.Kiely, G.J.Hutchings, *Nature Chemistry*, 2011, **3**, 551-556

26 G.L.Brett, P.J.Medziak, N.Dimitratos, J.A.Lopez-Sanchez, N.F.Dummer, R.Tiruvalam, C.J.Kiely, D.W.Knight, S.H.Taylor, D.J.Morgan, A.F.Carley, G.J.Hutchings, *Catal.Sci.Technol*, 2012, **2**, 97-104

27 S.Bawaked, Q.He, N.F.Dummer, A.F.Carley, D.W.Knight, D.Bethell, C.J.Kiely, G.J.Hutchings, Cat.Sci.Technol, 2011, **1**, 747-759.

28 M.Conte, C.J.Davies, D.J.Morgan, T.E.Davies, D.J.Elias, A.F.Carley, P.Johnston, G.J.Hutchings, *Journal of Catalysis*, 2013, **297**, 128-136

29 M.Conte, A.Carley, G.J Hutchings, Catal Lett, 2008, **124**, 165-167

30 E.Bouleghlimat, P.R.Davies, R.J.Davies, R.Howarth, J.Kulhavy, D.J. Morgan, *Carbon*, 2013, **61**, 124-133

31 C.Buono, P.R.Davies, R.J.Davies, T.Jones, J.Kulhavy, R.Lewis, D.J.Morgan, N.Robertson, D.J.Willock, *Farady Discuss*, 2014, **173**, 257-272

32 M.Yang, M.Zhou, A.Zhang, C.Zhang, *J.Phys.Chem C*., 2012, **116**, 22336-22340

33 U.Hofmann, E.Konig, *Z.Anorg, Alg, Chem*, 1937, **234**, 311-336.

34 N.R.Wilson, P.A.Pandey, R.Beanland, R.Y.Young, I.A.Kinloch, L.Gong, Z.Liu, K.Suenaga, J.P.Rourke, S.J.York, J.Sloan, *ACS Nano*, 2009, **3**, 2547-2556

# 4

# From support to carbocatalyst: Epoxidation of dec-1-ene using graphitic oxide as a catalyst. An investigation into the origin of activity.

## 4.0 Introduction

This chapter acts as a continuation of the investigation of the remarkable activity displayed by graphitic oxide (GO) for the epoxidation of dec-1-ene, first noted in chapter 3 when used as a support for gold- iron catalysts, most importantly in the absence of radical initiators. Due to the fluctuating behaviour of the graphitic oxide and low reproducibility of the active surface, it was deemed necessary to conduct a full investigation into the origin of activity and indeed the causes of inactivity. The need for this becomes clear when comparing the activity of the modified Hofmann samples with that of literature standard Hofmann methods[1] and also graphitic oxide produced by other methods such as Hummers[2] and Staudenmaier[3]. This chapter initially focuses on the early work conducted on the modified Hofmann sample where even though low reproducibility was observed, an active catalyst was consistently obtained. There then came a point where a number of factors out of our control coincided with the sudden production of an inactive graphitic oxide catalyst. These included changing of graphite batches, purity of deionised water, change in potassium chlorate batch. This resulted in a thorough study into which, if any of these variables were the cause of this inactivity. All attempts to use this material as a support were therefore halted until a reproducibly active catalyst was obtained.

Graphene and its analogues have received much attention since Geim and Novoselov's seminal work[4]. Its thermal[5], mechanical[6], optical[7] and electronic[8] properties have lent its use to many applications within science and engineering. Recent research has focussed on graphitic oxide (GO) which can be obtained via a simple treatment of graphite with acid and a strong oxidising agent. Early methods which utilised potassium chlorate as oxidant by Staudenmaier and Hofmann have been succeeded by Hummers and Tour[9] who use potassium permanganate instead. This ensures a harsher environment for the oxidation of the graphite surface while avoiding the formation of explosive chlorine dioxide gas. The resulting surface, in all methods, is abundant with a range of oxygen containing functional groups such as epoxides, alcohols and carboxylic acids, all of which lend this material to further modification and covalent functionalisation[10]. It is of no surprise that there has been a flurry of research into the anchoring of nanoparticles[11,12,13,14,15]on the surface of GO as well as the formation of metal oxide composites[16]. Although GO has been used extensively in these areas, mainly for the production of highly efficient electrocatalysts, it is only recently that it has been found to be useful in organic transformations. Indeed, its surface bound oxygen functional groups are active in a variety of reactions including primary and secondary alcohol oxidations[17]. It has been suggested that although these surface bound oxygen species are included into the oxidised products, regeneration of the surface sites can occur due to incorporation of atmospheric oxygen and therefore the entire process can be thought of as catalytic rather than stoichiometric by using and replenishing the surface oxygen in a Mars-van Krevelen type mechanism . The data presented in this study indicates that catalytic use of the surface oxygen is crucial for the activation of atmospheric dioxygen for the epoxidation of dec-1-ene. Hummers (HU) and Tour (TO) oxidations of graphite are known to be useful for obtaining a high oxygen coverage, however, they also yield a high ratio of carbonyl and carboxyl functionalities when compared to that obtained via Staudenmaier (ST) and Hoffman (HO) methods. Pumera and co-workers[18] studied the extent to which these conditions affect the ratios of surface groups and discussed their impact on the previously mentioned applications. Also mentioned was the higher heterogeneous electron transfer observed by chlorate synthesised GO, which could prove to be a factor when selecting a method for use in electronic applications. Despite this research into the physical differences obtained from individual preparation methods, there seems to be little research concerning catalytic behaviour of the various samples. Bielawski and co-workers noted little difference in the activities of Staudenmaier and Hummers prepared GO for benzyl alcohol oxidation. However, the high amounts of catalyst used (20 wt. %) exhibited limited activity in the given time frame. Attempts to identify the determining factor for the catalytic activity of GO have proven ineffective to date. Whilst it seems clear that activity is not directly proportional to total oxygen content, other theories have been left unresolved. Liang et al[19] proposed that for oxidative dehydrogenation of isobutane, activity may be dictated by a high $sp^3$ character of materials, in which the number of potential active sites is related to the fraction of exposed edges at which oxygen moieties can form.

### 4.1 Experimental

The GO used in this study was initially obtained via a modified Hofmann method (and denoted GO-HO15 ). For safety reasons a smaller amount of potassium chlorate (15g) was used than is common in the literature (55g). This was shown to be active for dec-1-ene epoxidation under mild conditions in the absence of radical initiators.  Interestingly, no or little activity for epoxidation was observed when GO was prepared by the standard Hummers (GO-HU15) or modified Staudenmaier (GO-ST15) methods. This suggests that specific surface oxygen species could be pivotal in the activity of the surface.

GO-HO15 was obtained *via* the stepwise addition of potassium chlorate to a slurry of graphite and 3:1 concentrated sulphuric acid: concentrated nitric acid. Following a 96 h oxidation period, GO-HO15 was repeatedly washed and re-dispersed in deionised water *via* a centrifuge. The GO-HO15 was then dried overnight in static air at 110 °C.

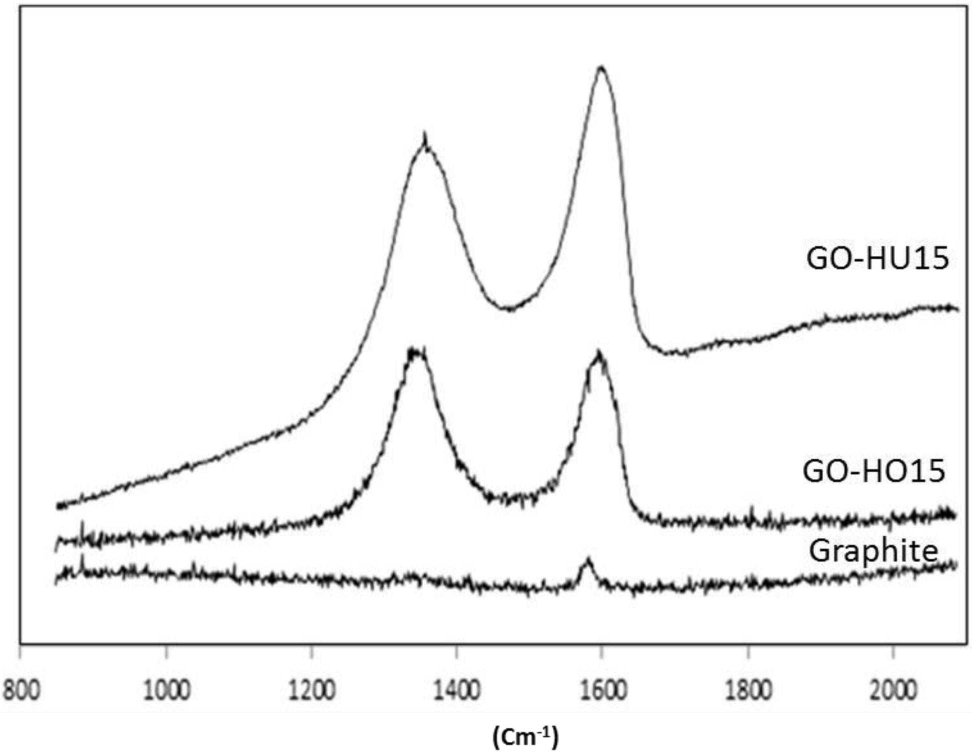

**Figure 4.1.1 Raman spectra of Graphite, active GO-HO15 and inactive GO-HU15**

The material obtained was initially characterised *via* Raman spectroscopy, x-ray photoelectron spectroscopy (XPS) and fourier transform infrared spectroscopy (FTIR). It can be assumed, unless otherwise stated that the GO used in this study was GO-HO15 prepared using the Hofmann method.

The Raman spectra obtained (figure 4.1.1) confirm the oxidation of graphite through the presence of the disorder induced D band at 1330 $cm^{-1}$ and the broadened and blue shifted G Band at $1590cm^{-1}$. These spectral traits become even more pronounced in the Hummers sample because of increased level of oxidation and disorder introduced into the lattice[20].

For use in reaction, GO (0.1 g) was added to dec-1-ene (10ml) in a round bottomed flask and reacted for 48 h at 90 °C in the presence of atmospheric oxygen.

Reaction products were also analysed by gas chromatography mass spectrometry (GC-MS) (figure 4.1.2) and used to confirm the presence of 1,2-epoxydecane. This was compared to a commercial 1,2-epoxydecane standard. Traces were also compared to a NIST database simulated standard[21] for 2,3-epoxydecane to confirm the identity of the epoxide.

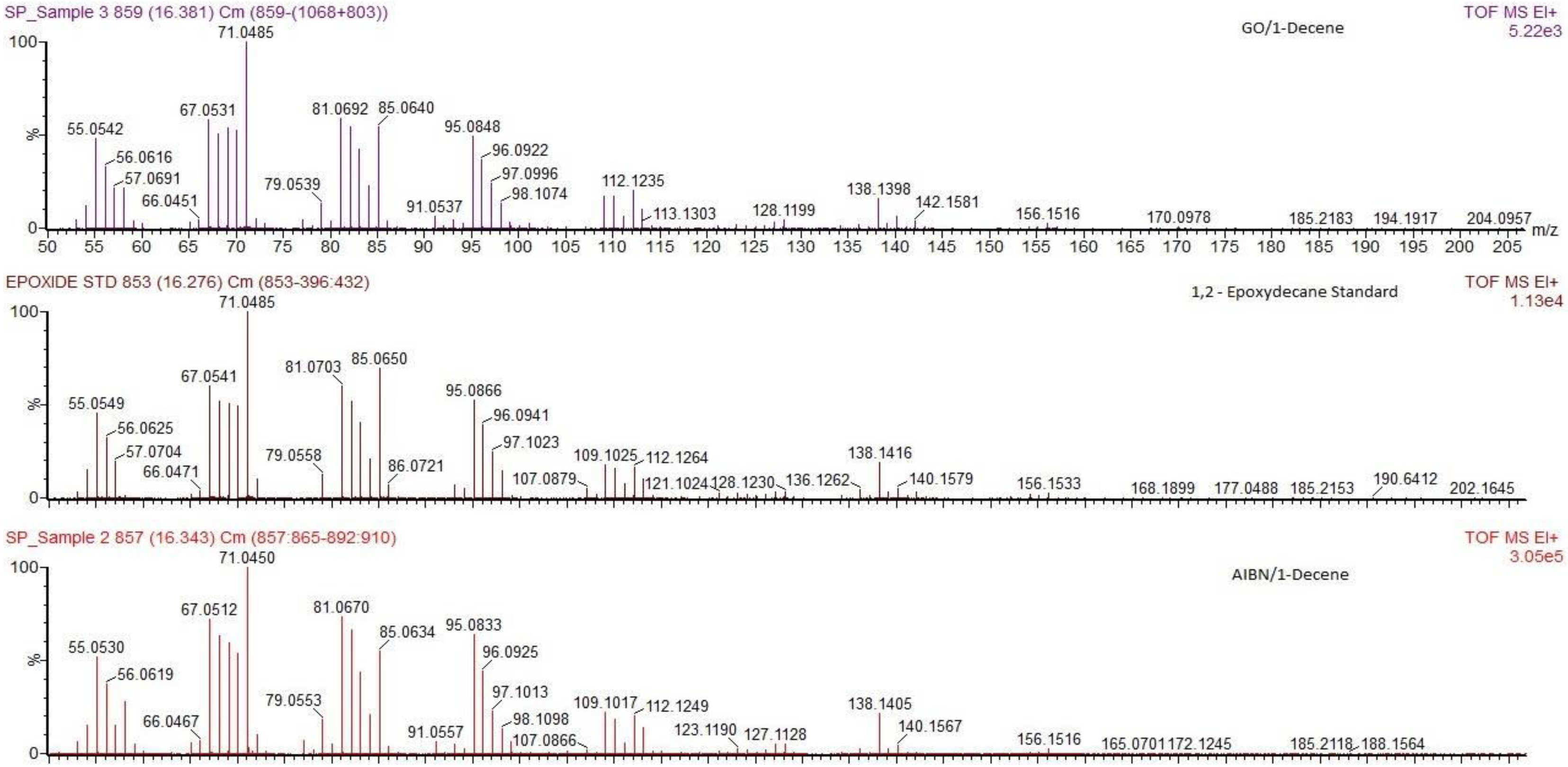

**Figure 4.1.2 GC-MS data of post reaction solutions resulting from GO catalysed epoxidation of dec-1-ene.**

The above GC-MS data of the graphitic oxide catalysed dec-1-ene epoxidation products provides great agreement with that of the 1,2 epoxydecane standard. This provides evidence that this reaction leads to the formation of the 1,2 epoxide and that no 2,3 epoxide is observed. This is also the case for the catalyst free reaction initiated by AIBN confirming that in all cases, reaction with atmospheric oxygen of this terminal alkene leads to formation of the terminal epoxide. This is in agreement with results previously seen for the Au-Graphite catalysed reactions.

## 4.2 Epoxidation of dec-1-ene in the absence of radical initiators using graphitic oxide as a catalyst

As detailed above, no reaction is observed when using neat 1-decene or unmodified graphite. Although the conversion when using GO-HO15 as a catalyst over such a time period is modest, the results are encouraging for an epoxidation of a terminal linear alkene. Epoxidation of alkenes using atmospheric oxygen under mild conditions usually requires supported metal catalysts. It has previously been shown by the Hutchings group, studying the oxidation of cyclooctene[22], that even with such catalysts, no reaction will occur unless in the presence of catalytic amounts of the radical initiator tertiarybutyl hydroperoxide (TBHP). After the removal of stabilisers, cyclic alkene oxidation became possible[23]. However for the epoxidation of linear alkenes, radical initiators were still required. Epoxidation of dec-1-ene was also studied and AIBN was found to be crucial for reaction when using supported gold catalysts[24] at 90°C.

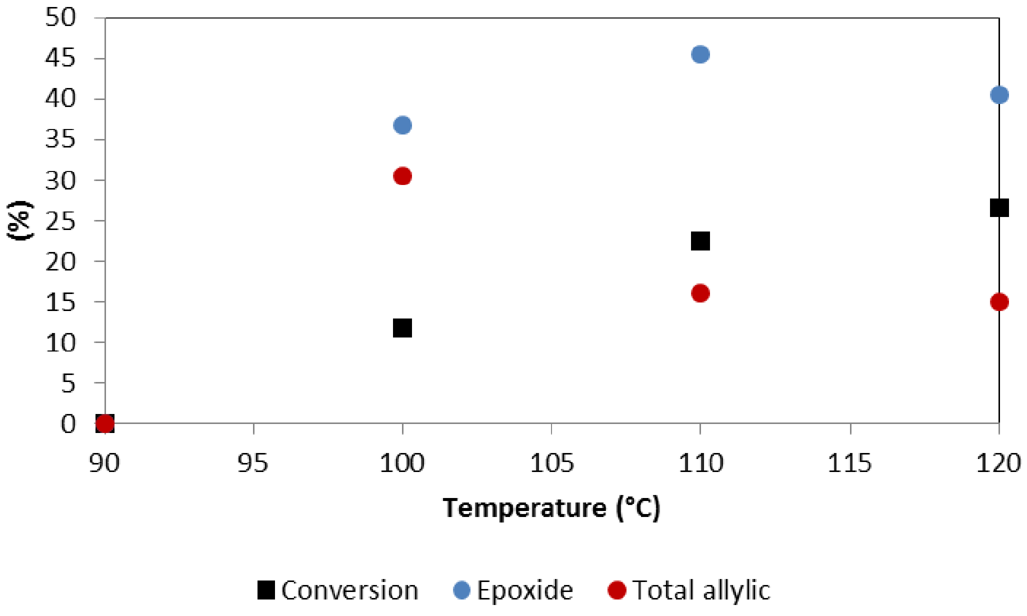

**Figure 4.2.1 Effect of temperature on the oxidation of dec-1-ene in the absence of radical initiators.**
**(48 h, dec-1-ene 10 ml)**

As before when studying supported gold catalysts, reactions in the presence and absence of graphite were conducted to assess at what temperature autoxidation would occur, however in this case reactions were extended to 48 h to mimic those for GO. Here it was found that autoxidation proceeds at a lower temperature when graphite is not present (figure 4.2.1) suggesting some inhibition of autoxidation by the support.

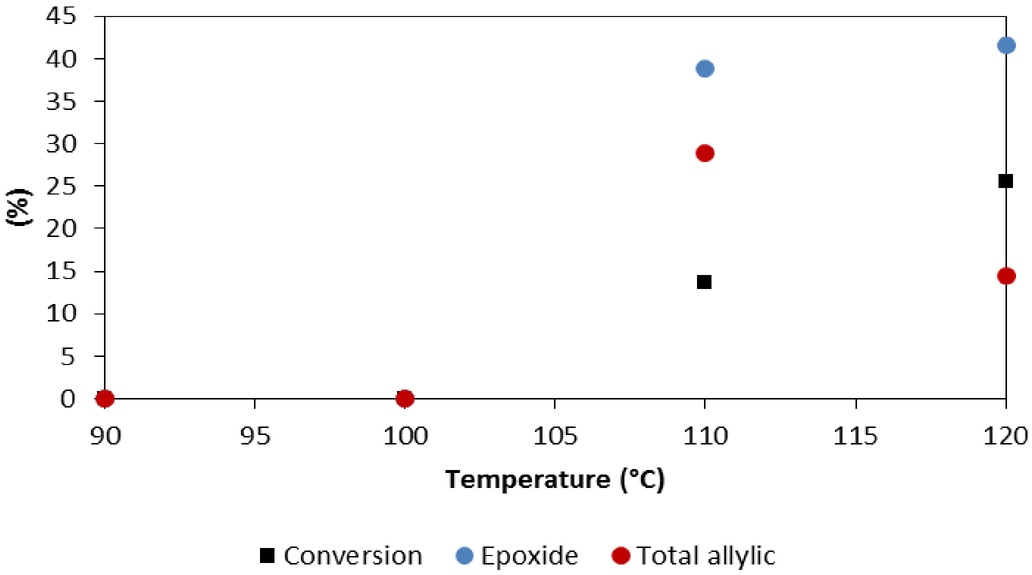

**Figure 4.2.2 Effect of temperature and presence of graphite on the oxidation of dec-1-ene in the absence of radical initiators.**
**(48 h, graphite 0.1 g, dec-1-ene 10 ml)**

Initially, GO-HO15 was washed using 1.5L deionised water. Extended washings of separate catalysts were conducted *via* centrifuge using 3 L of deionised water. This proved to increase yields from 9.1 % to 13.1% accompanied by a rise in selectivity (table 4.2.1). This enhancement discredits any notion of the activity arising from residual species such as acids or oxidant. On the contrary it would seem that any species left over from the catalyst preparation appears to have a detrimental effect on catalysis. No further increase in activity was observed with washings over 3 L and therefore this was accepted as the new method.

**Table 4.2.1 Epoxidation of dec-1-ene in the absence of radical initiators. (90 °C, 48 h, GO-HO15 0.1 g, dec-1-ene 10 ml)**

| Catalyst | Conversion (%) | Selectivity(%) |
|---|---|---|
| **Dec-1-ene** | 0 | 0 |
| **Graphite** | 0 | 0 |
| **1 %-Au-Graphite** | 0 | 0 |
| **GO-HO15 Cent 3 L** | 13.1 | 33.9 |
| **GO-HO15 Cent 1.5 L** | 9.3 | 26.8 |
| **G-HO15 Filtered 2 L** | 10.1 | 28.5 |

To ensure this observed catalysis was not due to any leached species, the catalyst was reused over a number of steps (table 4.2.2). Oxidation is still observed, albeit with diminished activity and selectivity to the epoxide. Although it has been suggested that surface oxygen can regenerate over the course of a reaction, it is unclear as to whether the identity of the oxygen species is retained. If not, this could be used to explain the decline in activity. Alternatively, a general reduction or re-graphitisation of the surface could also lead to catalyst deactivation. Further reuse experiments need to be conducted in which the amount of GO used is the same each time.

**Table 4.2.2 Reuse of GO-HO15. (90 °C, 48 h , Following each stage, the catalyst was collected via filtration washed with acetone (50 ml) and deionised water (1 L) and dried at 110 °C for 16 h)**

| Amount of catalyst (g) | Conversion (%) | Selectivity (%) |
|---|---|---|
| **0.4** | 19.8 | 37.2 |
| **0.15** | 8.0 | 25.4 |
| **0.03** | 3.8 | 13.7 |

XPS (table 4.2.3, and figure 4.2.3), FTIR (figure 4.2.4) data were collected following each step in order to track the reduction and deactivation of the catalyst. There is a distinct change in the FTIR region between 1500 and 1700 cm$^{-1}$ representative of the carbonyl and carboxyl groups.

**Table 4.2.3 XPS analysis of GO-HO15 after reuse. (An insufficient amount of catalyst was recovered after the 3rd use in order to run XPS)**

| | O1s (Wt %) | C1s Wt %) | S2p (Wt %) |
|---|---|---|---|
| **Fresh** | 24.12 | 73.94 | 1.74 |
| **1st use** | 17.16 | 82.45 | 0.40 |
| **2nd use** | 15.71 | 84.01 | 0.28 |

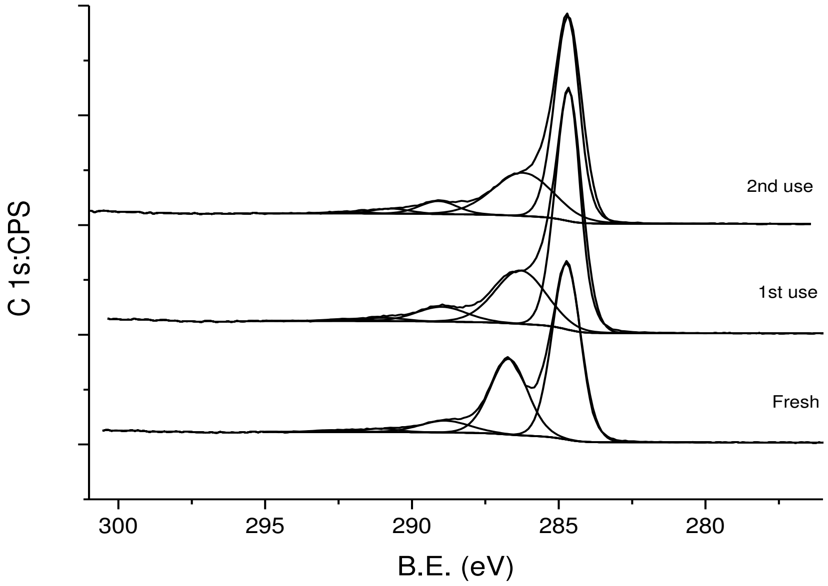

**Figure 4.2.3 XPS of GO-HO15 reuse study**

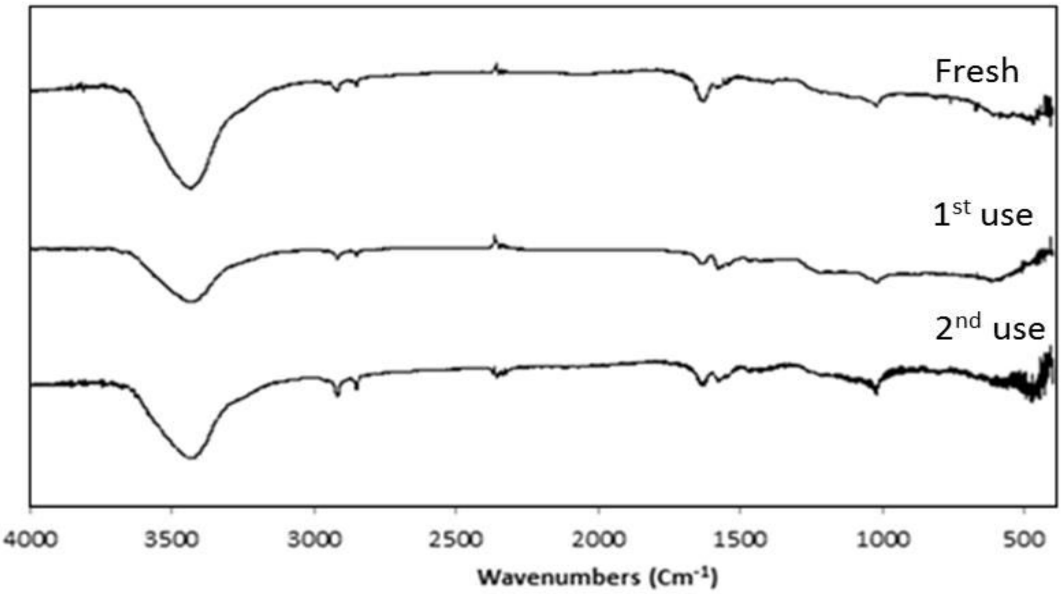

**Figure 4.2.4 FTIR comparison of fresh GO-HO15 and after two uses. (Insufficient amount of catalyst was obtained after 3rd use in order to run FTIR)**

Assuming that the observed activity is indeed due to surface oxygen species and not attributed to a leached species, a time online study was conducted to ensure this was a catalytic process as opposed to stoichiometric use of the graphitic oxygen. The sustained oxidation up to and over 192h suggests a turnover of oxygen. The dramatic drop in selectivity to the epoxide is most likely due to condensation of water within the reaction. Autoclave reactions were conducted whereby GO-HO15 (0.3 g) was stirred with dec-1-ene (30 ml) under nitrogen atmosphere in the absence of oxygen. After 48 h at 90 °C, no reaction was observed stressing the importance of atmospheric oxygen and role of the GO-HO15 being catalytic rather stoichiometric.

### 4.3 Time online study of epoxidation of dec-1-ene using graphitic oxide as a catalyst.

Two reactions were started 8 hours from each other in order to sample every 4 hours. A small portion of reaction solution was taken at each 4 hour interval, enough for GC analysis to be conducted after centrifuging of the sample. After sampling, stirring was re-started and the reaction was left to proceed (figures 4.3.1 and 4.3.2).

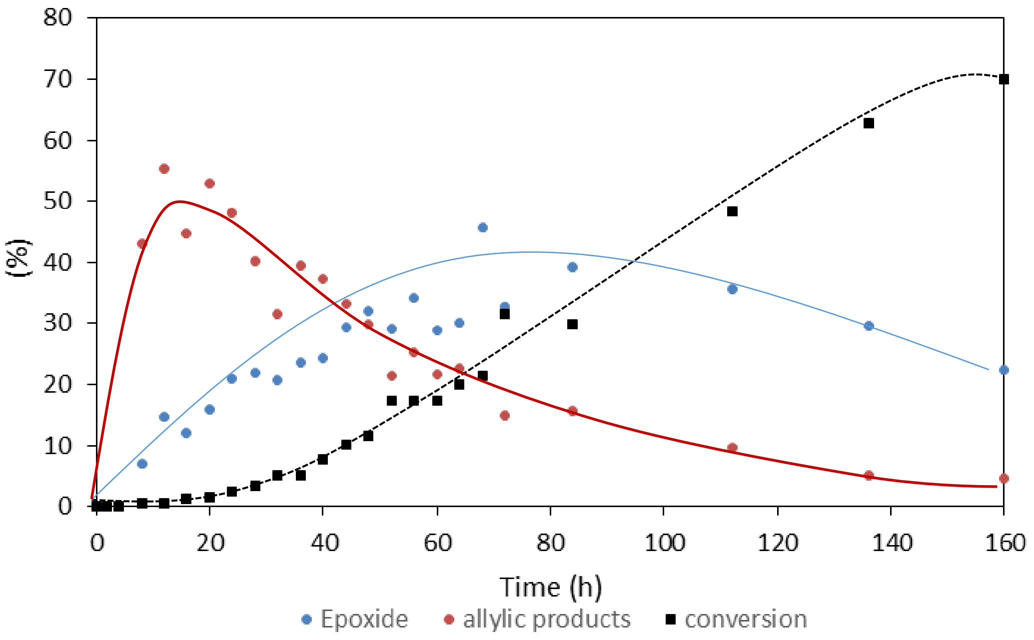

**Figure 4.3.1 Time online study of epoxidation of 1-decene using graphitic oxide as catalyst.**
**(90 °C, GO-HO15 0.1 g, dec-1-ene 10 ml)**

Reaction follows the previously reported pathway[24] via formation of allylic products with direction towards epoxide. Epoxide selectivity increases with conversion until maximum is reached after which epoxide selectivity drops with increased selectivity towards acids and diol.

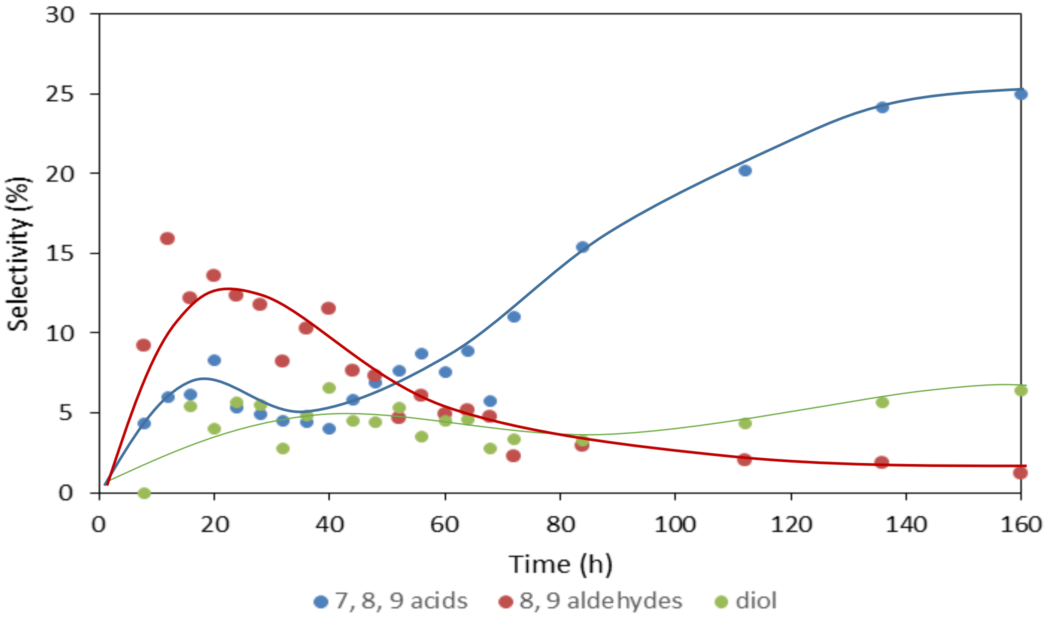

**Figure 4.3.2 Time online study of GO-HO15. Concentration of acids, aldehydes and diol as reaction proceeds.**
**(90 °C, GO-HO15 0.1 g, dec-1-ene 10 ml)**

### 4.4 Further investigation into the activity of GO-HO15 in epoxidation of dec-1-ene

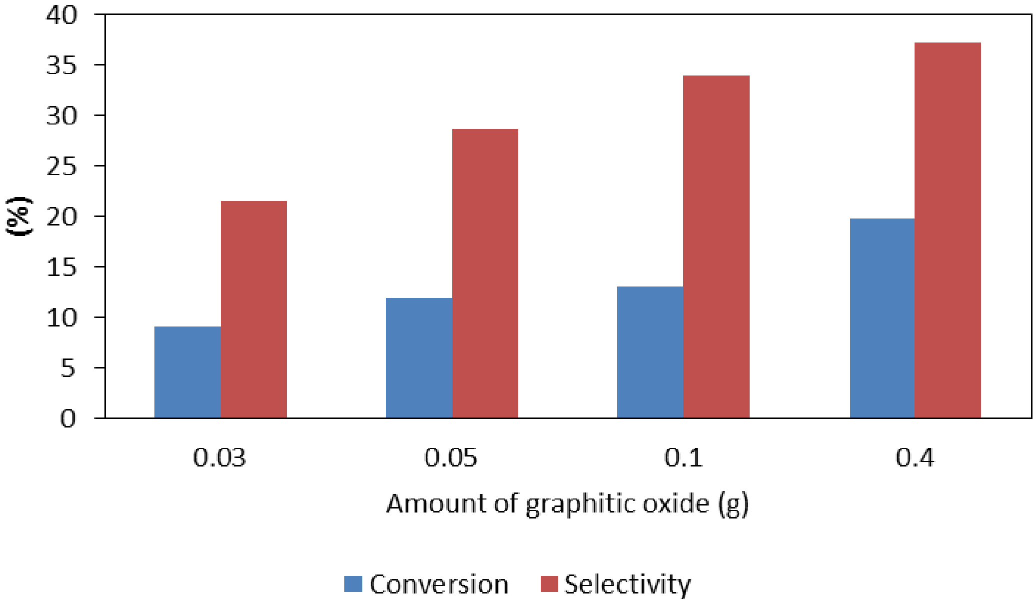

**Figure 4.4.1 Effect of amount of GO on epoxidation of dec-1-ene (90 °C, 48 h, dec-1-ene 10ml)**

An increase in the amount of GO-HO15 used in the reaction was accompanied by an increase in activity and selectivity to the epoxide (figure 4.4.1). This process remains cost effective despite the high amounts of catalyst used due to the low cost of its preparation.

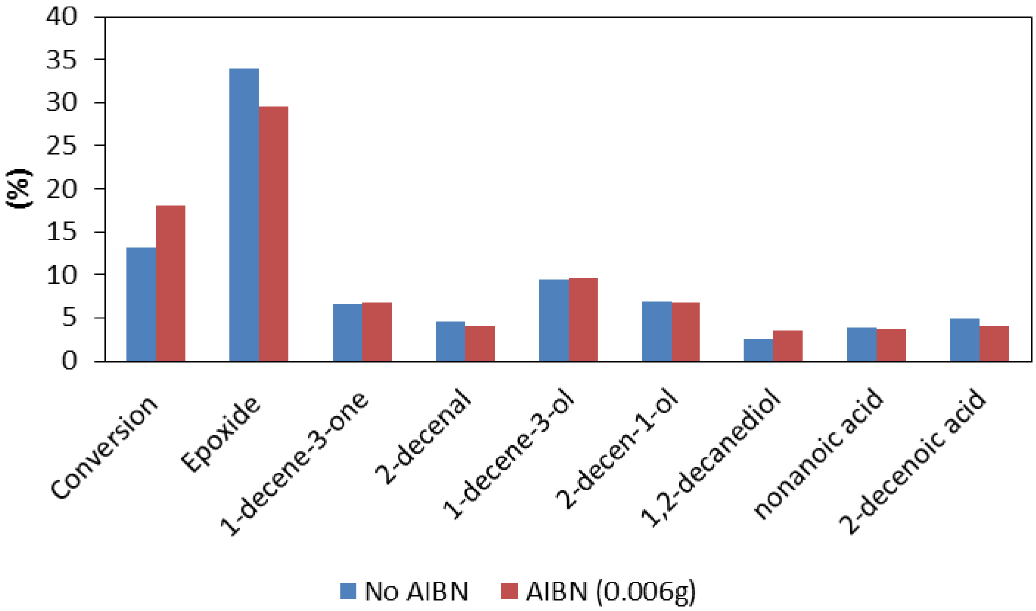

**Figure 4.4.2 Epoxidation of dec-1-ene over GO-HO15. Distribution of major products in the presence and absence of radical initiator AIBN**
**(90 °C, 48 h, GO-HO15 0.1 g, AIBN 0.006 g dec-1-ene 10 ml)**

Experiments were also carried out in the presence of the radical inhibitor butylated hydroxytoluene (BHT), where the GO-HO15 material and BHT were used in a 1:1 ratio. This was seen to completely inhibit any reaction from occurring, possibly due to the trapping of oxygen radicals required for epoxidation. To ensure that the reduced activity was not a result of surface poisoning, lower ratios of 2:1 and 4:1 were also used. As previously seen, no reaction was observed indicating that the GO-HO15 material acts through radical initiation of atmospheric oxygen as opposed to direct epoxidation of adsorbed dec-1-ene. The activity in the presence of AIBN was further studied (figures 4.4.2 and 4.4.3) and found that amounts as small as 5 mg were sufficient to boost catalysis. It is assumed that the presence of AIBN eradicates the lengthy induction period, it is also possible that the addition of AIBN only generates higher conversion from the additional initiated radical mechanism along with that catalysed by graphitic oxide.

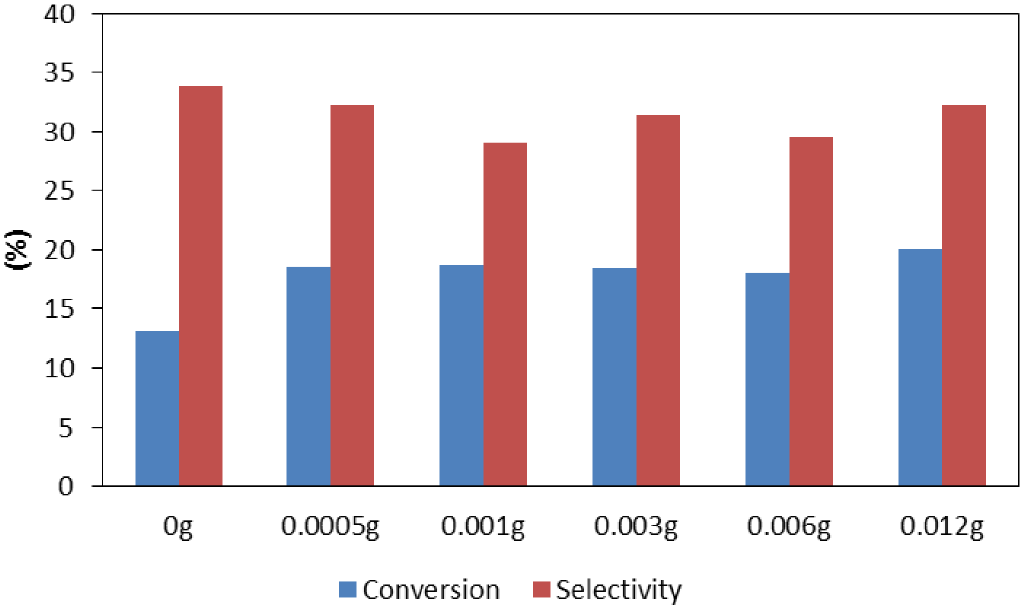

**Figure 4.4.3: Effect of amount of AIBN on the epoxidation of dec-1-ene using GO as a catalyst**
**(90 °C, 48 h, GO-HO15 0.1 g, dec-1-ene 10 ml)**

The activity observed for benzyl alcohol oxidation by GO-HO15 (figure 4.4.4) is analogous to those reported by Bielawski and co-workers for both GO-ST15 and GO-HU15 catalyst despite only having used half the amount of catalyst (10 wt %) in the reaction. In all cases, GO-HU15 was found to be the most efficient catalyst for this oxidation, which contradicts the results found for dec-1-ene epoxidation where no reaction is observed. Catalysts were also tested for propene epoxidation although no activity was observed.

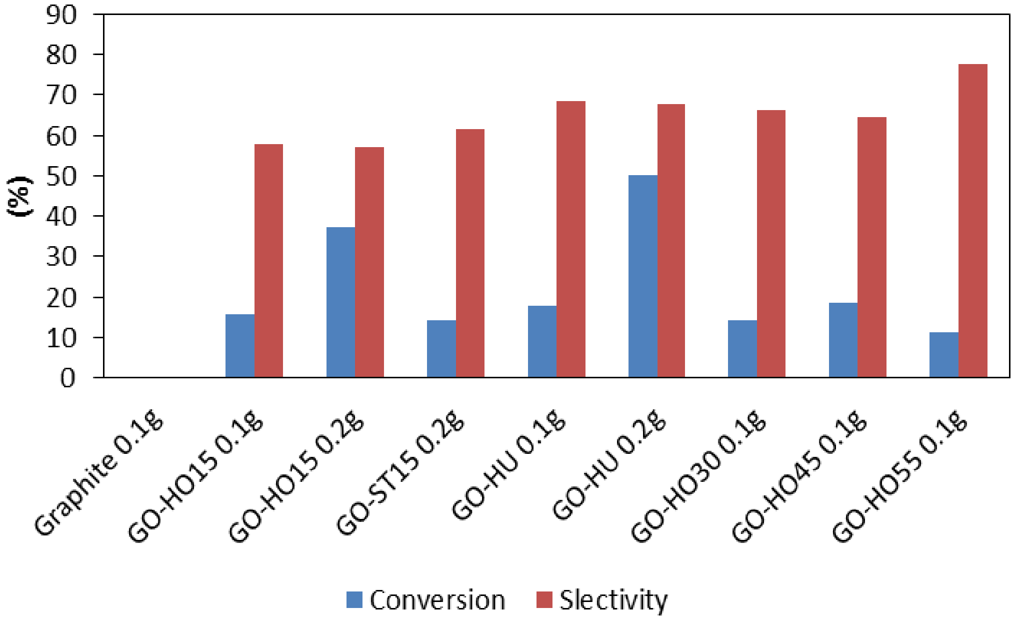

**Figure 4.4.4 Benzyl alcohol oxidation using graphitic oxide as a catalyst. (100 °C, 24 h, benzyl alcohol 2 g)**

The contradiction between optimum GO catalysts for benzyl alcohol and dec-1-ene oxidation, combined with the fact that there seems to be no correlation between oxygen composition and activity in either case, suggests that there is a need to tailor GO to the given reaction. It was thus necessary to further probe the origin of activity in the epoxidation of dec-1-ene and understand the reason why the HU method produces an inferior catalyst to HO method of preparation. XPS of the original GO-HU15 showed small amounts of various contaminants including Na, Cl and S ions. As these were either absent or, in the case of sulphur, present at lower quantities in GO-HO15, it was initially thought that one or all of these could be poisoning the catalysis. Subsequently a number of GO-HU15 catalysts were produced, first of all repeating the original method of preparation *via* the introduction of a longer washing step via centrifuge. In other cases the *in situ* formation of nitric acid *via* the addition of sodium nitrate was replaced with conc. nitric acid being added straight to the starting slurry. While all of these resulted in a higher purity of GO-HU15 catalyst being obtained, no link to activity was observed, with all samples either showing no or little activity (0-4 % conversion) compared to GO-HO15 (13.1 %). As expected, the eradication of sulphuric acid from the preparation method resulted in no oxidation of the surface and therefore failed to produce GO altogether. This was also the case when nitric acid was removed from the preparation signifying the importance of the presence of both acids. Samples of GO-HU15 and GO-ST15 were also subjected to multi staging reactions similar to that of GO-HO15 to establish further if any leached species could be poisoning catalysis. When each GO material (0.2 g) was reacted with dec-1-ene (10 ml), washed, filtered, dried and reused (0.1 g), no reaction was observed..

### 4.5 XRD analysis

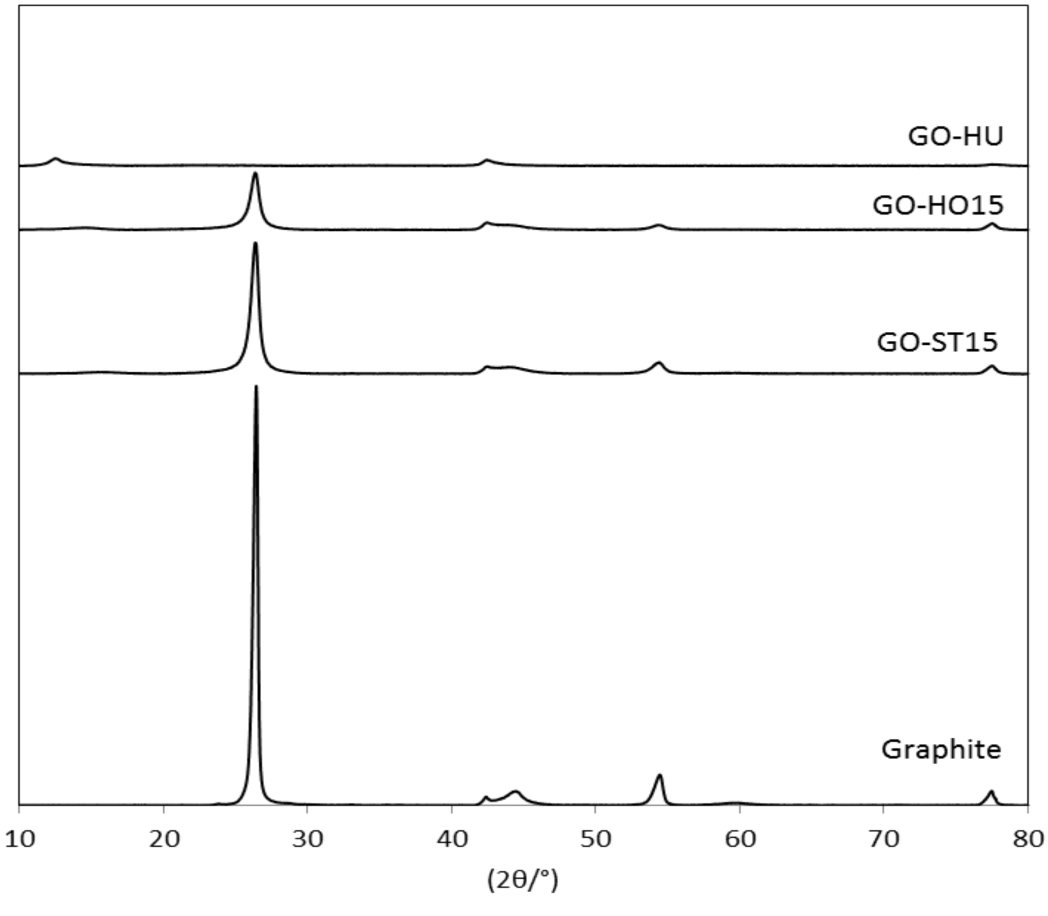

**Figure 4.5.1 XRD comparison of GO's prepared by Staudenmaier, Hofmann and Hummers preparation methods.**

XRD analysis of GO-HU15, GO-HO15 and GO-HO15 (figure 4.5.1) shows the varying extent of oxidation and de-graphitisation of the surface. The GO-HU material appears to have lost a significant amount of its graphitic character compared to the more modest levels of oxidation in both the GO-HO15 and GO-ST15 materials. Despite this, there is still a significant difference between the GO-HO15 and GO-ST15 materials with respect to the intensities of the 002 peak (26.7 °) and also the development of a peak at lower 2θ/° values (10.8 °) in GO-HO15 relating to the increased d-spacing. This is a surprise result, along with the GO-ST15 being completely inactive for epoxidation, as the only difference between the two methods is the concentration of nitric acid (conc and fuming). The activity of the GO-HO15 material has led us to believe an optimum level of oxidation is necessary even though total oxygen content is irrelevant. Unlike Liang and co-workers who used a range of heat sources and hydrogen to prepare reduced GO's (RGO), GO-HO samples were prepared according to the given method, using varying amounts of potassium chlorate, ranging from 5g up to 55g which is the amount most commonly used in the literature. XRD analysis of the resulting samples (Figure 4.5.2) demonstrates the gradual oxidation from graphite like materials through to the de-graphitised GO-HO55. Epoxidation activity was seen to decrease with the increased oxidation, resulting in highly oxidised surfaces analogous to the GO-HU15 being inactive. The same can be said for decreased oxidation with materials similar to GO-ST15 also showing no activity. This is not the case however for benzyl alcohol oxidation where the extent of oxidation of HO samples showed to have no effect on activity. Despite this, GO-HU15 samples shown to be most active, indicating inherent differences to highly oxidised HO samples the identity of which are not clear through XPS or XRD analysis.

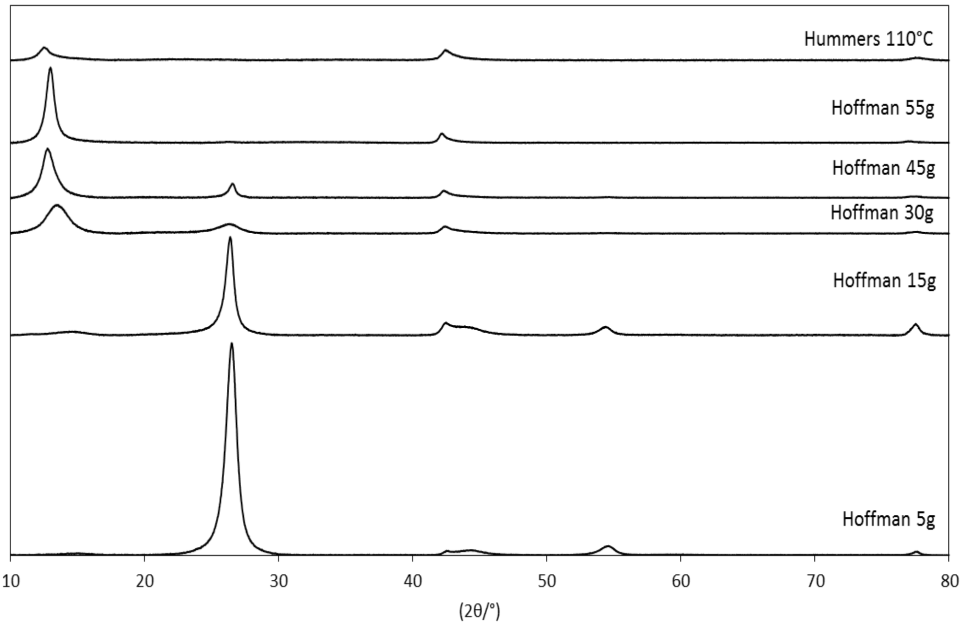

**Figure 4.5.2 XRD comparison of GO's prepared using progressive amounts of potassium chlorate with that prepared using potassium permanganate.**

## 4.6 Inactive catalyst study

The previously discussed activity of GO-HO15 for the epoxidation of dec-1-ene was shown to be variable between different batches. Although catalysts were consistently active, level of activity fluctuated from 9 to 13 % over 48 hours. The sudden production of completely inactive GO-HO15 catalysts (table 4.6.1) provoked a level of confusion as no change to preparation or washing step had been made. Although HU and ST methods of preparation were known to produce inactive catalysts, the exact reason had not been established. Little correlation between the level of oxidation or amount of contaminants with that of conversion had been observed. It was therefore necessary to explore a number of variables which could have unintentionally affected the prepared catalyst, for example graphite batch and water purity were early suspects as will be explained below.

**Table 4.6.1 Production of inactive GO-HO15 samples. (90 °C, 48 h, GO-HO15 0.1 g, dec-1-ene 10 ml)**

| Catalyst | Preparation Method | Conversion % | Selectivity % |
|---|---|---|---|
| 1. **GO** | Hoffman 15g | 0 | 0 |
| 2. **GO** | Hoffman 15g | 0 | 0 |

### 4.6.1 Effect of graphite on the production of active GO materials

The sudden production of an inactive GO-HO15 catalyst provoked the investigation into the causes of this inactivity. Graphite was identified as one variable which could have an effect on the GO. As previously discussed in chapter 3 when investigating gold catalysis, successive graphite batches behaved differently to those which were originally used as supports in the epoxidation of dec-1-ene. Although no explanation for this was found, repeated low activity of the new catalysts showed inherent differences between the supports. This changing of graphite batches also coincided with the period in which inactive GO-HO15 catalysts were being obtained. XRD analysis of the unoxidised graphites along with GOs prepared from these separate batches was conducted.

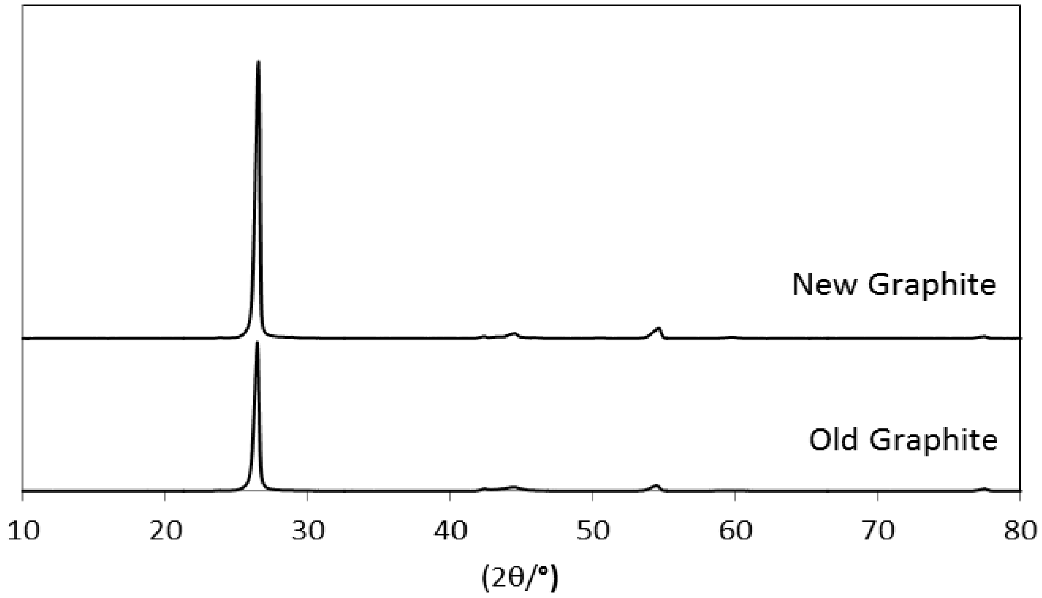

**Figure 4.6.1.1 XRD comparison of unoxidsed graphite batches**

The XRD patterns of the graphites showed a difference in the intensity of the 002 peak at ~27 ° (figure 4.6.1.1). The decrease in intensity of this peak was previously seen when increasing the oxidation of the graphite surface causing de-graphitisation and loss of crystallinity (figure 4.5.2). This difference in XRD patterns was consistently seen, however in order to infer significance, an internal standard would need to be used. Graphitic oxides produced from these graphites also showed large differences in the XRD patterns obtained (figure 4.6.1.2). The 002 peak proved to be much broader in all GO materials produced from the new batch of graphite. This gained significance after successive batches all proved to be inactive, while retaining the same broadened 002 peak. This fuelled the theory that graphite may be dictating the activity of the final product, with XRD of all active catalysts showing a sharp 002 peak, possibly indicating a higher crystallinity of the catalyst. A fresh GO sample was then prepared using a sample of old graphite for further comparison. It was again shown that GO-HO15 material prepared using old graphite gives a highly crystalline species (figure 4.6.1.4) which almost definitely means the amorphous nature and unique XRD pattern is due to the new source of graphite. However, despite this crystalline material being more characteristic of the previous catalysts, it has still returned a 0 % reaction conversion (table 4.6.1.1). Therefore, despite XRD pattern being an interesting trait of the individual graphites, it was concluded that this was not the cause of the new found inactivity.

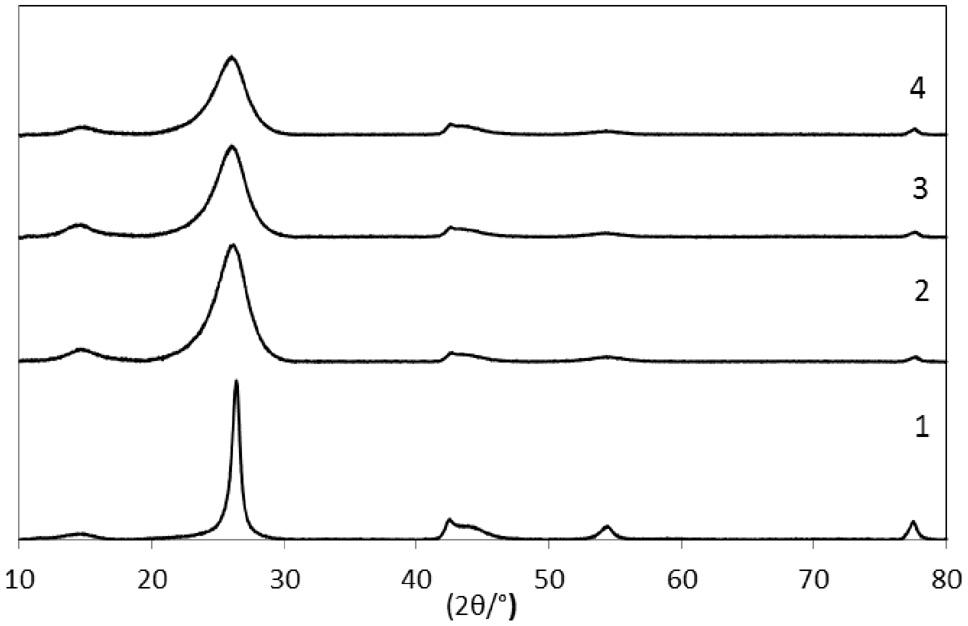

**Figure 4.6.1.2 XRD comparison of GO's prepared by old graphite (1) and new graphite (2,3,4)**

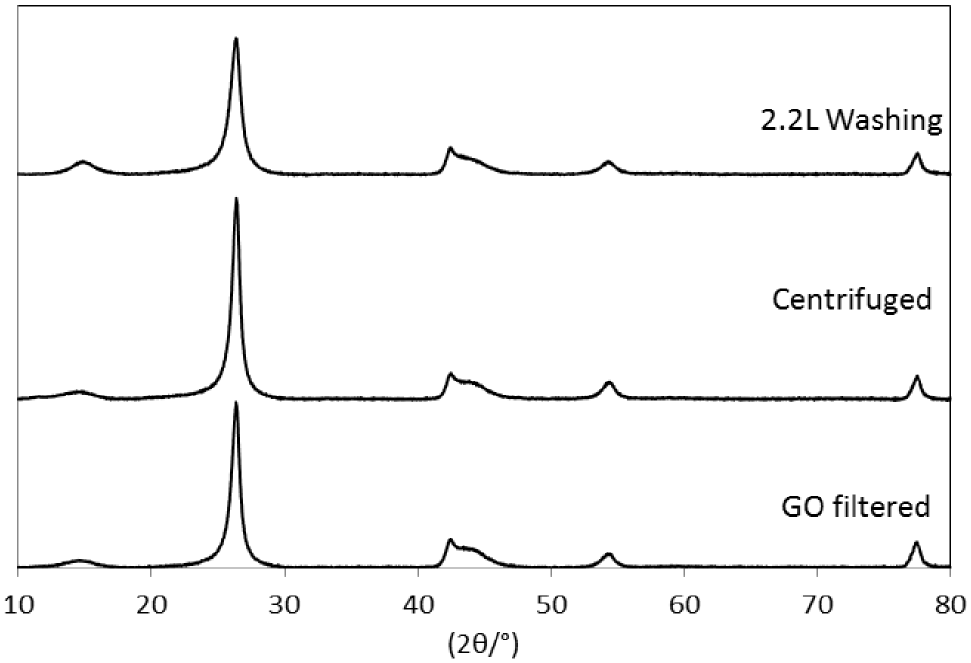

**Figure 4.6.1.3 XRD comparsion of active catalysts derived from old graphite**

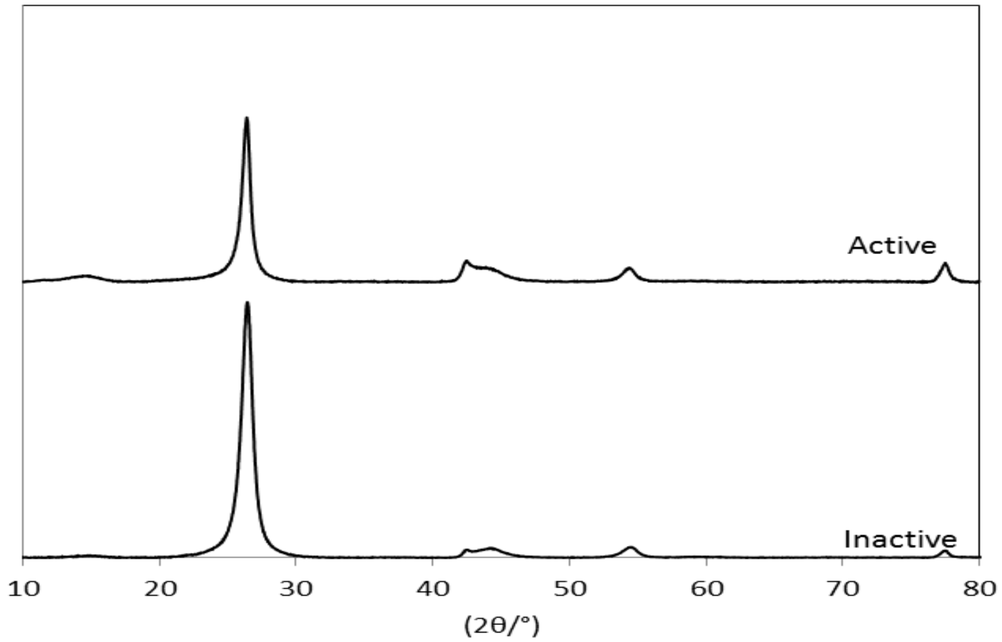

**Figure 4.6.1.4 XRD comparison of inactive and active GO-HO15 produced from old graphite batch.**

**Table 4.6.1.1- Comparison of old and new batch of GO-HO15 using old graphite. (90 °C, 48 h, AIBN 0.006 g, GO-HO15 0.1 g, dec-1-ene 10ml)**

| | AIBN (g) | Conversion (%) | Selectivity (%) |
|---|---|---|---|
| **GO-HO15** | 0 | 13.10 | 33.90 |
| **GO-HO15** | 0.006 | 18.10 | 29.60 |
| **GO-HO15 new batch** | 0 | 0 | 0 |
| **GO-HO15 new batch** | 0.006 | 12.81 | 33.23 |

### 4.6.2 Acid pre-treatment of graphite

Following the identification of physical differences between the graphite batches, acid treatment of graphites was conducted prior to oxidation in the preparation of GO. Two batches of acid treated graphite have been prepared using 10 % and 70 % Nitric acid in an attempt to remove any contaminants that may be inhibiting reaction or production of active graphitic oxide. Graphite (10 g) was stirred in the given amount of nitric acid overnight (20 hours), washed with deionised water until neutral (2 L) and dried overnight (110 °C).These samples were then tested for activity for dec-1-ene epoxidation in the presence of AIBN (table 4.6.2.1).

**Table 4.6.2.1 Epoxidation of 1 Decene (48 h, 90 °C, AIBN 0.006 g, Graphite 0.1 g, dec-1-ene 10 ml)**

| | **Conversion (%)** | **Selectivity (%)** |
|---|---|---|
| **10 % Nitric washed Graphite** | 19.4 | 44.1 |
| **70 % Nitric washed graphite** | 9.7 | 21.7 |

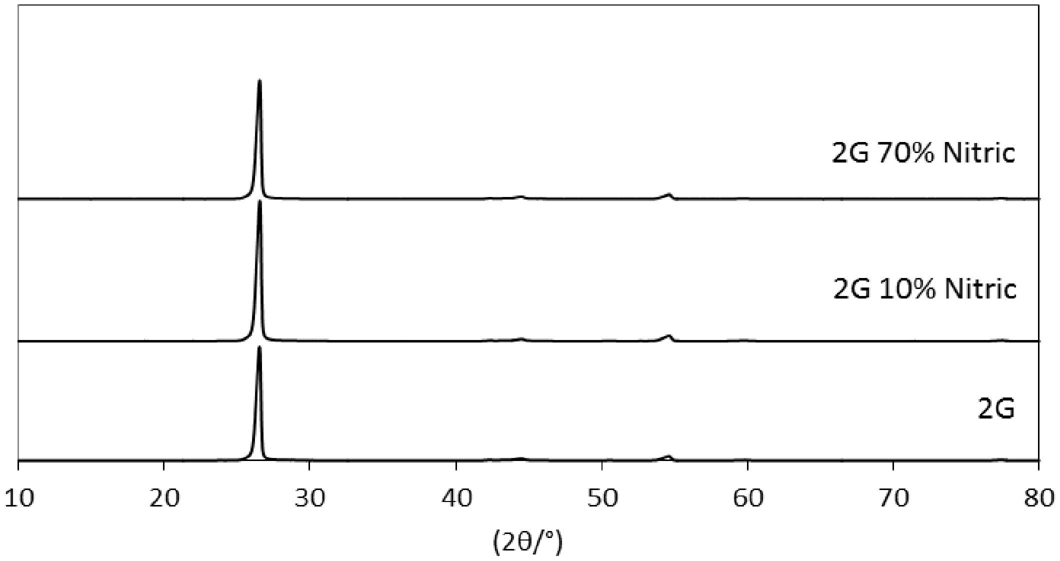

**Figure 4.6.2.1 XRD of graphite before and after acid treatment**

Initial XRD of acid treated graphite showed no difference to the parent batch (figure 4.6.2.1). GO-HO15 prepared using these acid treated graphites showed the same broadened 002 peak seen in the analogous GO's (figure 4.6.2.2). These catalysts were all shown to be inactive in the absence of radical initiators.

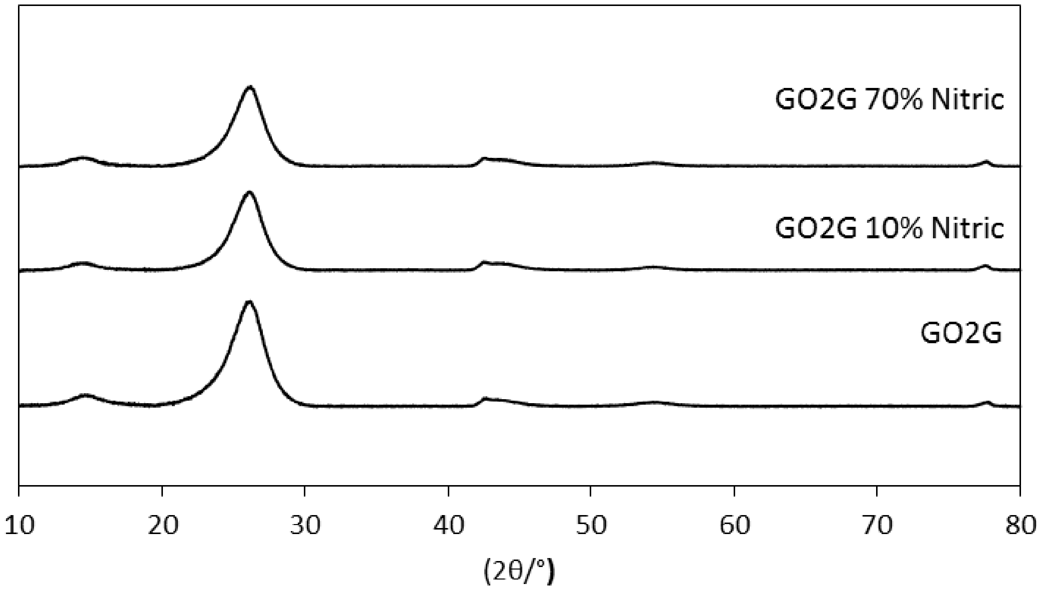

**Figure 4.6.2.2 XRD comparison of GO-HO15 materials prepared using acid pretreated carbons.**

### 4.6.3 Purity of deionised water

One important discovery was the malfunctioning of the deionised water machine. It was found that the machine had been producing DI water with a high conductivity for some time. This high conductivity meant the possibility of high levels of cations and anions and essentially unpurified water. The repair of the deioniser also coincided with the production of inactive catalysts, a study was conducted in order to conclude whether the purity of water washings affected the overall activity of the catalyst. Tap water was used as a source of unpurified water.

**Graphitic oxide preparation**:

Graphitic oxide was prepared according to a modified Hofmann GO method. In order to investigate fully the effect of potassium chlorate, three separate batches of GO-HO were prepared using 10, 15, 20 and 55 g chlorate. These batches were then split post oxidation and washed with equal amounts of either deionised or tap water via centrifuge. These samples were subsequently dried overnight in static air at 110 °C and tested for activity.

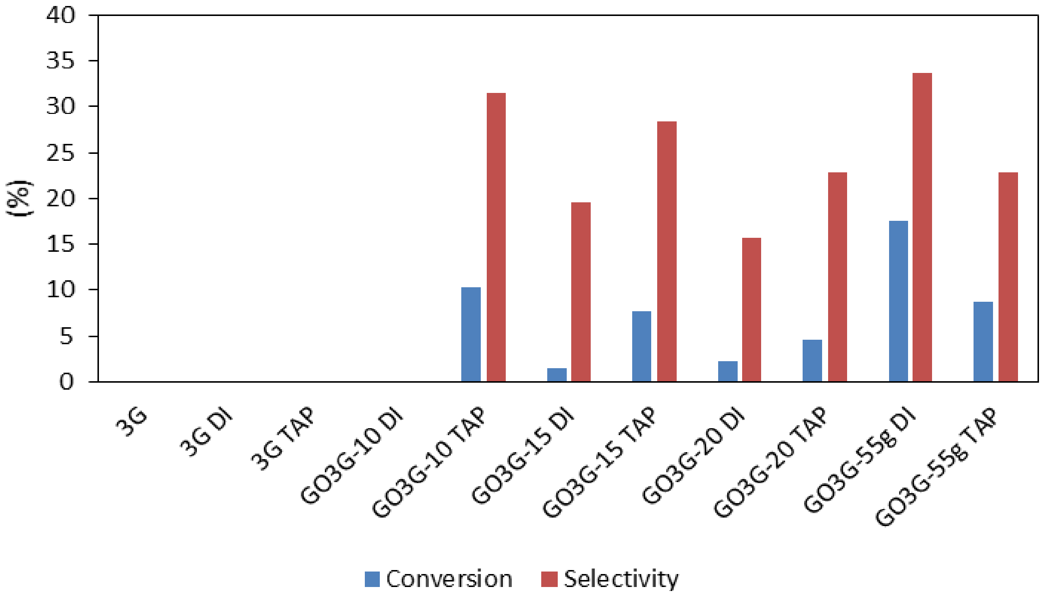

**Figure 4.6.3.1 Comparison of GO-HOs after washing with tap or deionised water. (90 °C, 48 h, AIBN 0.006 g, GO-HO 0.1 g)**

GO-HO catalysts were shown to produced differing levels of activity according to which purity of water they were washed with (figure 4.6.3.1). The catalysts were washed using equal amounts of water. In all cases, catalysts showed different levels of activity. GO-HO10 and GO-HO15 were shown to have little or no activity when washed with DI water. However upon washing with an equal amount of TAP water, activity was seen to be comparable to previously prepared catalysts. There also appeared to be a clear effect of oxidant with higher oxidised materials exhibiting a high level of conversion when washed with deionised water.

### 4.6.3.1 Welsh water report

The difference in activity between catalysts washed with either DI or TAP water suggested that there may be contaminants in the water which could be contributing to catalysis. It was therefore necessary to obtain a full analysis of TAP water quality which was provided by welsh water. On Assessment of the obtained welsh water report (Zone 1089 N15,Cardiff east, 01/03/2013-31/12/2013) a number of metal ions were discovered which could affect catalysis including Mg, Cu, Fe, Ca, Na and K. Calcium was not included in the report, however it was included in further investigations as it will commonly be present at high concentrations in tap water. Catalysts washed by TAP and DI water were analysed *via* microwave plasma atomic emission spectroscopy (MP-AES) for content of these metal ions (table 4.6.3.1).

**Table 4.6.3.1 MP-AES of digested catalysts. (50 mg Catalyst, 4 ml Aqua regia, 46 ml DI)**

| Sample | Mg(ppm) | Cu(ppm) | Fe(ppm) | Ca(ppm) | Na(ppm) | K(ppm) |
|---|---|---|---|---|---|---|
| **Cold Tap** | 5.3 | 0.12 | 0.27 | 42.75 | 15.23 | 2.26 |
| **Hot Tap** | 5.4 | 0.34 | 0.24 | 41.70 | 14.42 | 2.20 |
| **DI water** | 0.06 | 0.08 | 0.22 | 0.17 | 0.25 | 0.22 |
| **10g DI** | 0.12 | 0.15 | 0.29 | 0.33 | 1.40 | 0.93 |
| **10g Tap** | 0.12 | 0.13 | 0.39 | **1.67** | 1.54 | 0.66 |
| **15g DI** | 0.11 | 0.11 | 0.30 | 0.33 | 0.99 | 0.72 |
| **15g Tap** | 0.22 | 0.11 | 0.32 | **1.49** | 1.62 | 0.70 |
| **20g DI** | 0.12 | 0.10 | 0.32 | 0.35 | 1.21 | 0.96 |
| **20g Tap** | 0.17 | 0.16 | 0.21 | **1.53** | 2.34 | 1.89 |
| **55g DI** | 0.08 | 0.21 | 0.16 | 0.35 | 1.71 | 6.55 |
| **55g Tap** | 0.23 | 0.06 | 0.16 | **1.61** | 1.79 | 4.02 |
| **Graphite 2** | 0.12 | 0.04 | 0.14 | 0.33 | 2.50 | 0.65 |
| **Graphite 3** | 0.11 | 0.05 | 0.14 | 0.31 | 2.36 | 0.61 |

P, Mn, Ni were also tested for however 0ppm was found in all cases.

MP-AES data shows high level of calcium ion present in tap water which is not detailed in the welsh water report. Catalysts washed using tap water showed higher levels of calcium than those washed with deionised water. This is the only ion which is consistently higher in tap washed catalysts. The possibility of this ion contributing to the change in activity was further investigated.

**Table 4.6.3.2 MP-AES of carbon supports. Extent of metal adsorption in different carbons. (2.5 g Carbon source washed with 2 L TAP water)**

| Sample | Mg(ppm) | Cu(ppm) | Fe(ppm) | Ca(ppm) | Na(ppm) | K(ppm) |
|---|---|---|---|---|---|---|
| **Graphite TAP** | 0.08 | 0.08 | 0.16 | 0.33 | 0.96 | 0.38 |
| **C60 TAP** | 0.11 | 0.08 | 0.15 | 0.44 | 0.92 | 0.33 |
| **CNT TAP** | 1.00 | 0.08 | 0.25 | **1.35** | 1.30 | 0.39 |

| | | | | | | |
|---|---|---|---|---|---|---|
| **GO3G 10g TAP** | 0.12 | 0.13 | 0.39 | **1.67** | 1.54 | 0.66 |
| **GO3G 15g TAP** | 0.22 | 0.11 | 0.32 | **1.49** | 1.62 | 0.70 |
| **GO3G 20g TAP** | 0.17 | 0.16 | 0.21 | **1.53** | 2.34 | 1.89 |

Multiple carbons were washed with tap water to compare the level of adsorption of calcium and other metals compared to the GO catalysts (table 4.6.3.2). Graphite and C60 were shown to adsorb low levels of calcium. These were also shown to be inactive for epoxidation of dec-1-ene. Carbon nanotube (CNT) showed high levels of adsorption of calcium. However this was also shown to be inactive for dec-1-ene epoxidation in absence of radical initiators. Graphene is known to be an efficient adsorbent and often used in water purification[25]. Therefore the purity of water used to wash the GO could heavily affect activity as any ion present could potentially adhere to the surface groups. The water study suggests that $Ca^{2+}$ could be influencing activity.

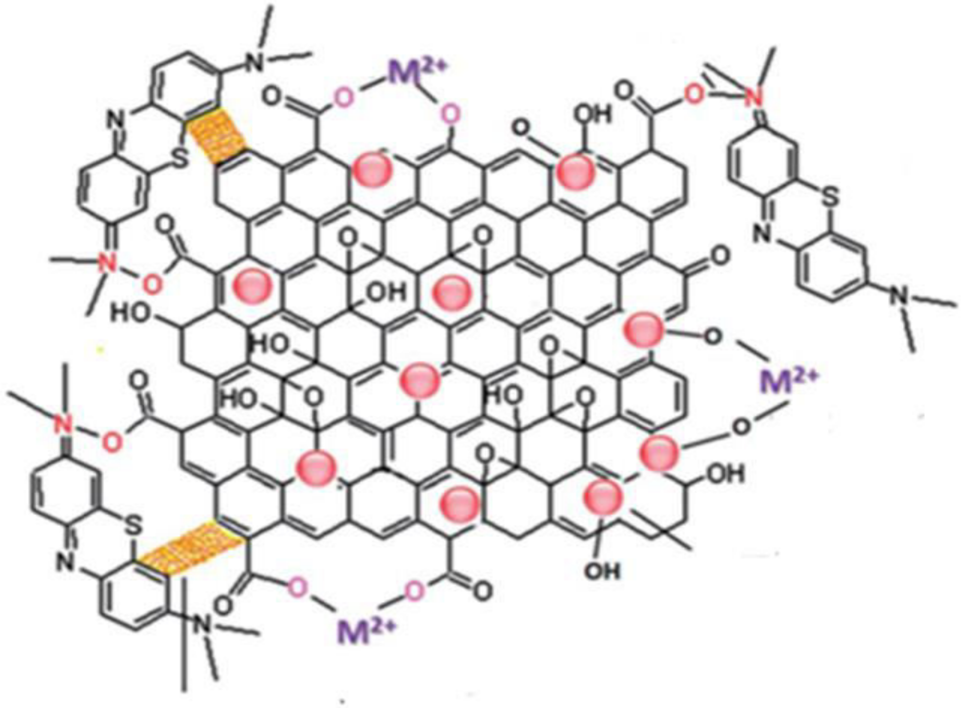

**Figure 4.6.3.2 Possible metal ion binding sites within the GO structure**[25]

### 4.6.4 $Ca^{2+}$ impregnation study

Oxidation catalysis by calcium is not often seen therefore the role of calcium was further investigated for its effects in successfully activating graphitic oxide for epoxidation of dec-1-ene. The GO-HO15 material was washed with 2 L DI water followed by 2 L of solution $CuCl_2$ (32 ppm $Ca^{2+}$). Catalysts were subsequently dried at 110 °C for 16 h in static air.

**Table 4.6.4.1 MP-AES of Hofmann catalysts washed with $CuCl_2$ solution (32ppm Ca $^{2+}$)**

| Sample | Ca (ppm) | K (ppm) |
|---|---|---|
| **GO-HO15** | 0.19 | 0.19 |
| **GO-HO15 $Ca^{2+}$** | 0.77 | 0.38 |

MP-AES of the catalysts (table 4.6.4.1) showed a small presence of calcium on the surface. Catalysts were also tested for residual potassium species which could be left over from the oxidant. This was also found to be present at small concentrations.

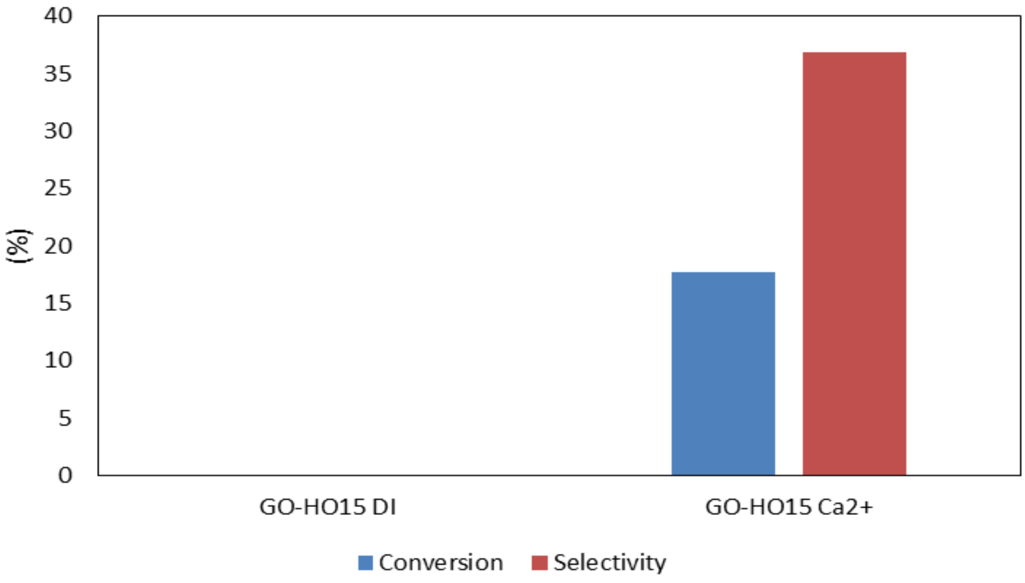

**Figure 4.6.4.2 Epoxidation of dec-1-ene using DI or $Ca^{2+}$ washed GO-HO15. (90°C, 48h, GO 0.1g, dec-1-ene 10 ml)**

The testing results (figure 4.6.4.2) show an apparently dramatic effect of calcium washing for the epoxidation of dec-1-ene when compared to washing with equal amount of deionised water which consistently yielded inactive catalysts. The use of calcium chloride in solution with dec-1-ene was also found to be inactive.

Repeating this experiment yielded some interesting results. A separate batch of GO-HO15 was made and washed with calcium solution. It was found that the catalyst was less active with approximately 6 % conversion compared to 17 % (figure4.6.4.3).

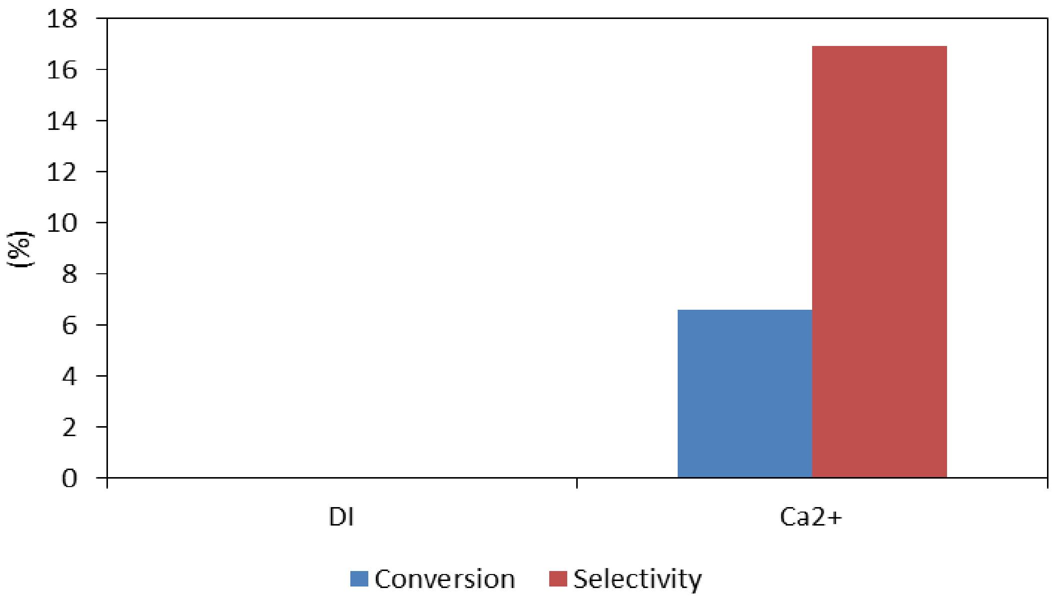

**Figure 4.6.4.3 Repeat of GO-HO15 washed with Ca solution. (90 °C, 48 h, GO 0.1 g, dec-1-ene 10 ml)**

**Table 4.6.4.2 AES data of repeated GO-HO15 catalysts.**

| | Ca (ppm) | K (ppm) |
|---|---|---|
| **GO-HO15 DI** | 0.20 | 0.72 |
| **GO-HO15 $Ca^{2+}$** | 0.77 | 0.76 |

MP-AES analysis of the catalysts (table 4.6.4.2) showed that an identical amount of calcium was present on both catalysts, despite the discrepancy in activity. The GO washed with DI water returned completely inactive. Both the DI and Ca washed catalyst were then rewashed in $Ca^{2+}$ solution to investigate the possibility of activating the inactive DI catalyst and also improving the activity of the $Ca^{2+}$ catalyst.

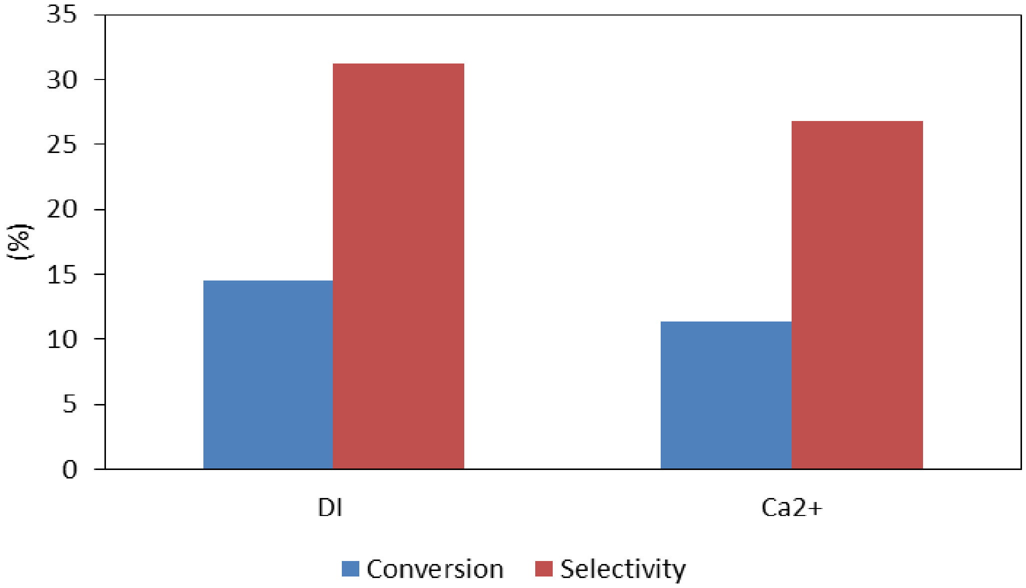

**Figure 4.6.4.4 Activity of GO-HO15 materials after rewashing of catalysts in $Ca^{2+}$ solution (90 °C, 48 h, GO 0.1 g, dec-1-ene 10 ml)**

**Table 4.6.4.2 AES Data for rewashed catalysts**

| | **Ca (ppm)** | **K (ppm)** |
|---|---|---|
| **GO-HO15 DI** | 0.44 | 0.41 |
| **GO-HO15 Ca** | 0.56 | 0.39 |

Rewashing of the catalysts resulted in activity for the epoxidation of dec-1-ene in both cases (figure 4.6.4.4). The lowly active $Ca^{2+}$ catalyst increased in activity from 6 % to 13 % and the completely inactive DI catalyst was found to be active to a comparable level as the $Ca^{2+}$. Catalyst. However, in the case of the Ca catalyst, the level of calcium actually decreased with increasing conversion (table 4.6.4.2). It was therefore concluded that the correlation between activity and calcium concentration previously seen when washing with tap or deionised water was down to coincidence, rather than resulting from previously unseen calcium catalysis or promotion. To confirm this, catalysts were produced and washed with magnesium chloride solution and found to be active to the same degree. This suggests that although there seems to be a correlation between the purity of water and activity of catalysts produced, the catalysis observed is not due to the presence of these ions on the surface. Indeed it is more likely that the activity seen is a result of the additional washing step and the removal of an as yet unknown species. This theory was further investigated by additional post centrifuge washings.

### 4.6.5 Acid washing post oxidation

GO-HO15 was again produced and washed and separated by centrifuge. The GO was washed using various mediums *via* stirring to assess the origin of activity.

As before, GO-HO15 was inactive after separation and washing in DI *via* centrifuge. It was then shown for it to be possible to activate samples following a number of different additional washing steps (table 4.6.5.1). Minor differences were also observed according to whether or not the GO was dried before the additional washing step. Graphite was also washed with 5% HCl and was shown to be inactive.

**Table 4.6.5.1 Effect of washing step on activity of GO (90 °C, 48 h, dec-1-ene 10 ml, GO 0.1 g)**

| | **Conversion (%)** | **Selectivity (%)** |
|---|---|---|
| **Graphite 5% HCl** | 0 | 0 |
| **5% HCl 2h** | 11.1 | 28.5 |
| **5% HCl 6h** | 13.8 | 32.3 |
| **5% $HNO_3$ 2h** | 16.0 | 36.3 |
| **5% $HNO_3$** | 12.1 | 30.9 |
| **Ca(NO3)2 40ppm** | 15.3 | 35.7 |
| **HPLC washed** | 13.1 | 34.7 |
| **HNO3 20ppm** | 7.0 | 29.6 |
| **Millipore washed** | 8.8 | 28.5 |
| **HPLC washed** | 9.2 | 30.1 |
| **DI washed** | 9.0 | 30.8 |

### 4.7 Use of Ion chromatography

MP-AES has allowed the study of metal ions adsorbed onto the catalyst surface. These can be present simply as residual species from the preparation method, or ions adsorbed from washing media. However the nature of MP-AES has limited this study to metal cations. The recent availability of ion chromatography has enabled the analysis of anions such as sulphate, chloride and nitrate which are all likely to be present after the preparation of graphitic oxide. Therefore GO-HO catalysts were prepared using 15,30 and 55 g potassium chlorate. The catalysts prep included a treatment of HCl prior to centrifuge, as is common in the literature to remove sulphate ions. It was found that these catalysts were all active to some degree (table 4.7.1). Even GO-HO15 was active after the additional acid treatment. However when larger amounts of catalyst were used (0.2-0.4 g) no activity was observed.

**Table 4.7.1 Effect of amount of oxidant and an extended washing step. (90C, 48h, dec-1-ene 10ml, GO 0.1 g) (400 ml HPLC water /0.6 g catalyst)**

| Catalyst | Conversion (%) | Selectivity (%) |
|---|---|---|
| **GO15 HCl** | 7.6 | 25.7 |
| **GO30 HCl** | 6.2 | 23.0 |
| **GO55 HCl** | 9.1 | 27.5 |

Additional washings of these catalysts were conducted (0.3 g catalyst, 300 ml HPLC water, 6 h stirring) after which a sample was taken from each solution and tested via ion chromatography (table 4.7.2). A high level of sulphate was found in each of the catalysts. Chloride was also present, most likely as a result of the acid washing prior to centrifuging.

**Table 4.7.2 Ion chromatography of acid washed samples.**

| Catalyst | Chloride (ppm) | Nitrate (ppm) | Sulfate (ppm) | Wt % sulphate |
|---|---|---|---|---|
| **GO15 HCl** | 7.5 | 3.0 | 17.5 | 1.1 |
| **GO30 HCl** | 6.0 | 3.0 | 35.0 | 2.3 |
| **GO55 HCl** | 7.8 | 2.4 | 33.8 | 2.2 |

The HPLC washing resulted in a higher activity for the epoxidation of dec-1-ene with the exception of GO-HO55 which remained the same

**Table 4.7.3 Epoxidation of 1-Decene using above GO's after additional HPLC washing. (90 °C, 48 h, dec-1-ene 10 ml, GO=0.1 g)**

| **Catalyst** | **Conversion (%)** | **Selectivity (%)** |
|---|---|---|
| **GO15** | 9.4 | 31.0 |
| **GO30** | 8.7 | 28.2 |
| **GO55** | 9.0 | 30.0 |

It is suggested that the presence of sulphur may be inhibiting catalysis. It is clear that washing with acid and/or centrifuging is an inadequate technique for the removal of these sulphate ions which amount to 1-2.3 wt% on the catalyst. For effective removal of these ions, vigorous stirring in high purity water was found to be optimum. It was also found that use of HCl prior to centrifuging was unnecessary if this additional washing step was employed. Centrifuging, at this stage, remains integral to the method in order to remove the majority of acid and residual oxidant. However GO-HO15 catalysts produced after extensive centrifugation remain inactive. The ability to activate these catalysts using an additional washing step was further explored. The inactive GO-HO15 material was taken and washed using various amounts of HPLC water under vigorous stirring for 6 hours. All catalysts were then retested for activity (table 4.7.4).

**Table 4.7.4 Epoxidation of dec-1-ene using inactive GO-HO15 batch washed with varying amounts of HPLC water. (90 °C, 48 h, dec-1-ene 10 ml, GO-HO15 0.1 g)**

| **Catalyst** | **Conversion (%)** | **Selectivity (%)** |
|---|---|---|
| **GO (10ml)** | 6.1 | 28.1 |
| **GO (20ml)** | 7.7 | 28.9 |
| **GO (50ml)** | 6.8 | 25.3 |
| **GO (75ml)** | 9.4 | 31.8 |
| **GO (150ml)** | 9.4 | 28.5 |
| **GO (300ml)** | **8.0** | **25.4** |

It was found that all catalysts were active after being subjected to this vigorous washing step. Amounts as little as 10 ml could be used however these resulted in lower activity. Volumes of water of 75 ml and above were found to be most successful in activating the catalyst for epoxidation. Ion chromatography (table 4.7.5) showed that in all cases a high level of sulphate was removed equating to approximately 1.2 wt%. Variations in activity were thought to be due to the fluctuations in amount of sulphur being removed, however this is not supported by the ion chromatography. Further analysis of the catalysts is needed to identify whether the sulphur that is removed is the total amount present. CHNS analysis of all the catalysts should be conducted in order to obtain an absolute value for the sulphur content. Subsequent washing could also be conducted of the less active catalysts to see if activity can be improved.

**Table 4.7.5 Ion chromatography of washings taken from the above GO materials before reaction with dec-1-ene.**

| | **Chloride (ppm)** | **Nitrate (ppm)** | **Sulphate (ppm)** | **Wt % sulphate** |
|---|---|---|---|---|
| **GO (10ml)** | 8.4 | 6.7 | 344.4 | 1.1 |
| **GO (20ml)** | 8.9 | 4.7 | 173.3 | 1.1 |
| **GO (50ml)** | 3.7 | 3.2 | 66.8 | 1.1 |
| **GO (75ml)** | 2.2 | 2.6 | 49.9 | 1.2 |
| **GO (150ml)** | 2.3 | 1.9 | 23.3 | 1.1 |
| **GO (300ml)** | 2.3 | 2.3 | 12.1 | 1.2 |

Recent work by Eigler *et al*[26] described the presence of organosulphates in highly oxidised Hummers samples which upon washing form acidic sulphur groups rather than being eradicated from the surface (figure 4.7.1). The authors also described a process by which these can removed from the surface using sodium hydroxide. These findings could be used to explain the inactivity of the highly oxidised Hummers samples and the presence of high amounts of sulphur, described in more detail in the next section.

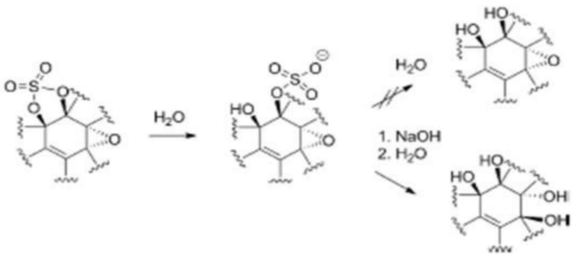

**Figure 4.7.1 Presence of organosulphates in GO and hydrolysis to acidic moieties.**

### 4.8 Investigation of amount of oxidant used and effect of additional washing

As previously discussed, the ability to acquire an active catalyst via an additional washing step encouraged a re-examination of the theory of an optimum amount of oxidant being needed for an effective catalyst.

### 4.8.1 Effect of oxidation and washing on Hofmann samples

A range of Hofmann samples were prepared using various amounts of potassium chlorate ranging from 0 to 55 g. These samples were tested for activity for dec-1-ene epoxidation after undergoing the standard centrifuge procedure.

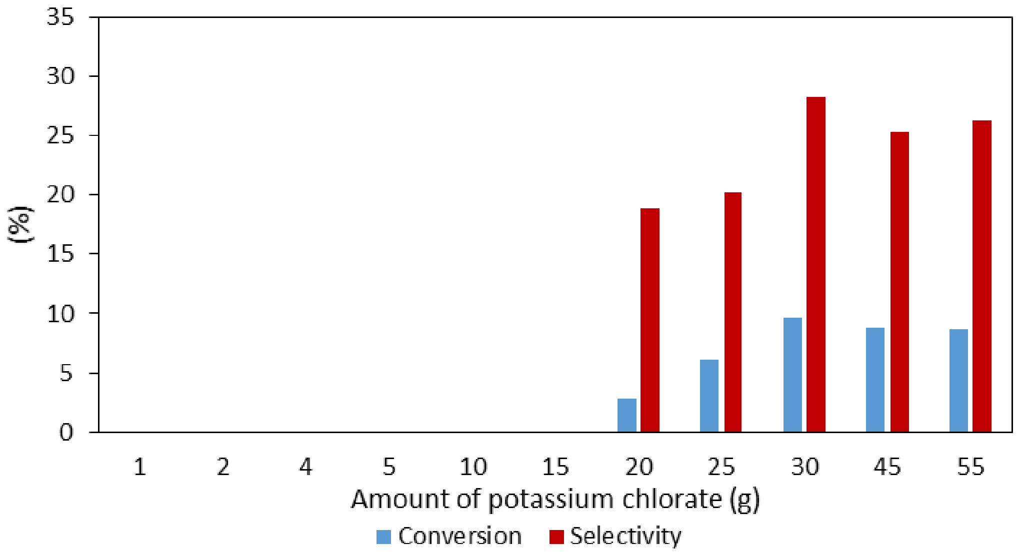

**Figure 4.8.1.1 Comparison of conversion and activity of GO-HO samples prepared using range of amounts of potassium chlorate. (90 °C, 48 h, dec-1-ene 10 ml, GO 0.1 g)**

The activity of the unwashed samples was shown to be as expected (4.8.1.1). All samples using amounts of potassium chlorate below 20g were shown to be inactive. All samples over this amount were active to some degree.

Fresh portions of these catalysts were then taken and subjected to an additional washing step (as before, 300ml HPLC water, 6h vigorous stirring). After which they were dried and re-tested for activity for epoxidation of dec-1-ene. This washing has been previously shown to activate GO-HO15 which appears to be on the barrier of amount of oxidant needed. Here, washing was shown to have a significant effect on a number of catalysts (table 4.8.1.2). Catalysts which were made using amounts of chlorate as low as 4 g, became activate after washing. Even though overall conversion was low (~6 %), this is a significant result as catalysts can be made active using dramatically lower amounts of oxidant than is common in the literature.

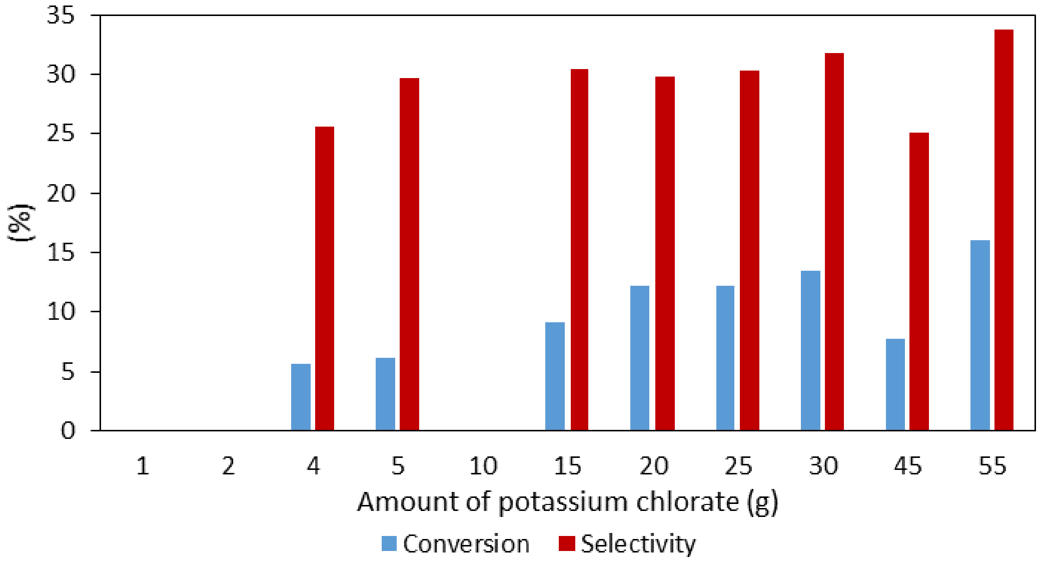

**Figure 4.8.1.2 Comparison of conversion and selectivity of GO-HO samples prepared using range of amounts of potassium chlorate. Results were obtained after the catalysts were subjected to additional washing step.**
**(0.3 g catalyst, 300 ml HPLC grade water, stirring for 6 hours followed by filtering and drying) (90 °C, 48 h, dec-1-ene 10 ml, GO 0.1 g)**

### 4.8.2 Effect of oxidation and washing on activity of Hummers samples

Hummers samples were treated the same as the above Hofmann samples whereby samples were produced using various amounts of oxidant, in this case potassium permanganate, and then tested for activity for dec-1-ene epoxidation with and without the additional washing step. The literature standard amount of potassium permanganate is 15 g. Therefore amounts of 5, 10 and 15 g of permanganate were used.

In this case, the unwashed lower oxidised samples were shown to be more active than the commonly used 15 g version (figure 4.8.2.1). Highly oxidised hummers samples are known to be difficult to wash due to the clay like consistency. Lower oxidised forms are similar to the medium Hofmann samples (20-30 g) and are therefore easier to purify. Washing the samples resulted in the lower oxidised forms increasing in activity and selectivity similar to the Hofmann samples, however the highly oxidised versions reduced completely in activity (figure 4.8.2.2).

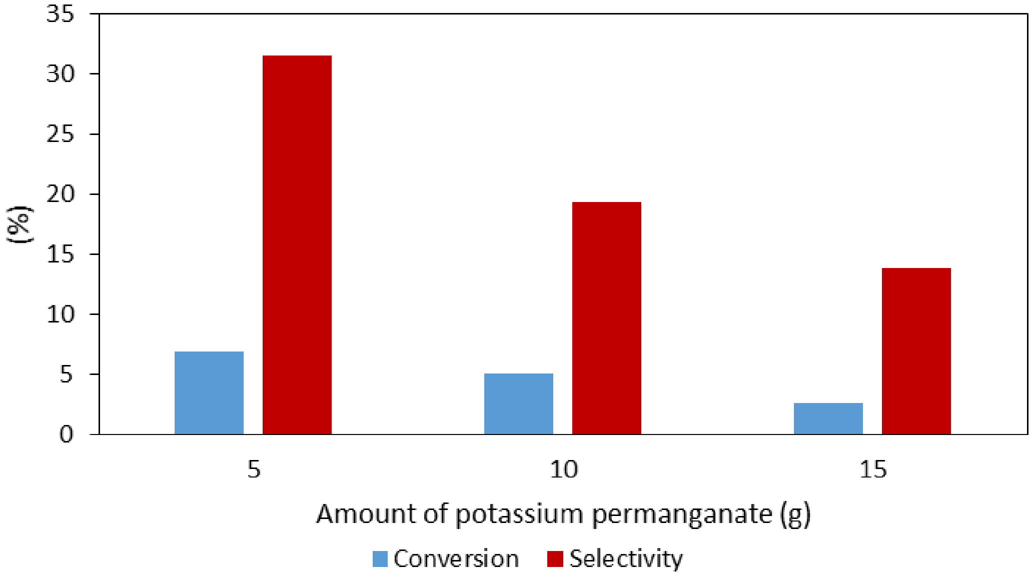

**Figure 4.8.2.1 Comparison of conversion and selectivity of GO-HU samples prepared using range of amounts of potassium permanganate.**
**(90 °C, 48 h, dec-1-ene 10 ml, GO 0.1 g)**

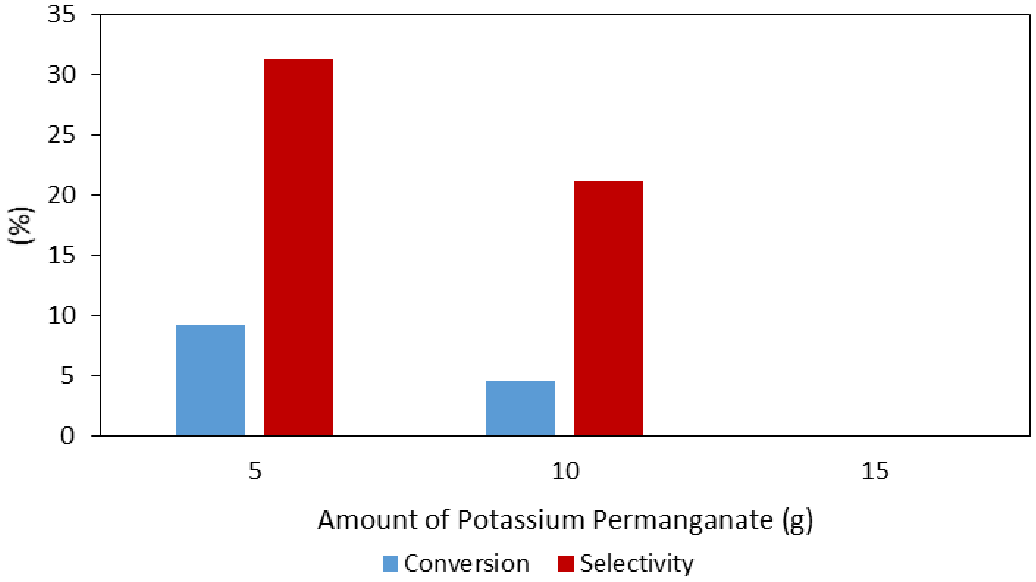

**Figure 4.8.2.2 Comparison of conversion and selectivity of GO-HU samples prepared using range of amounts of potassium permanganate. Results were obtained after samples were subjected to additional washing step.**
**(90 °C, 48 h, dec-1-ene 10 ml, GO 0.1 g)**

### 4.8.3 XPS analysis of oxygen coverage

An in depth XPS analysis was conducted on all of the above GOs before and after washing. Initial comparisons were made between the amount of oxygen present on the surface of GOs prepared by Hofmann and Hummers methods. This was due to the unusual trend seen in increasing and decreasing amounts of oxidant. Further compatsions were made on level of sulphur present in all catalysts, which will be discussed later.

An interesting observation was that in the GO-HO preparation, increasing the amount of oxidant from 1 to 30 g has a significant effect on total oxygen content (figure 4.8.3.1), however this trend is seen to decrease as a maximum level of oxygen is achieved. Increasing the amount of chlorate from 45 to 55 g seemingly has no effect on total wt % oxygen.

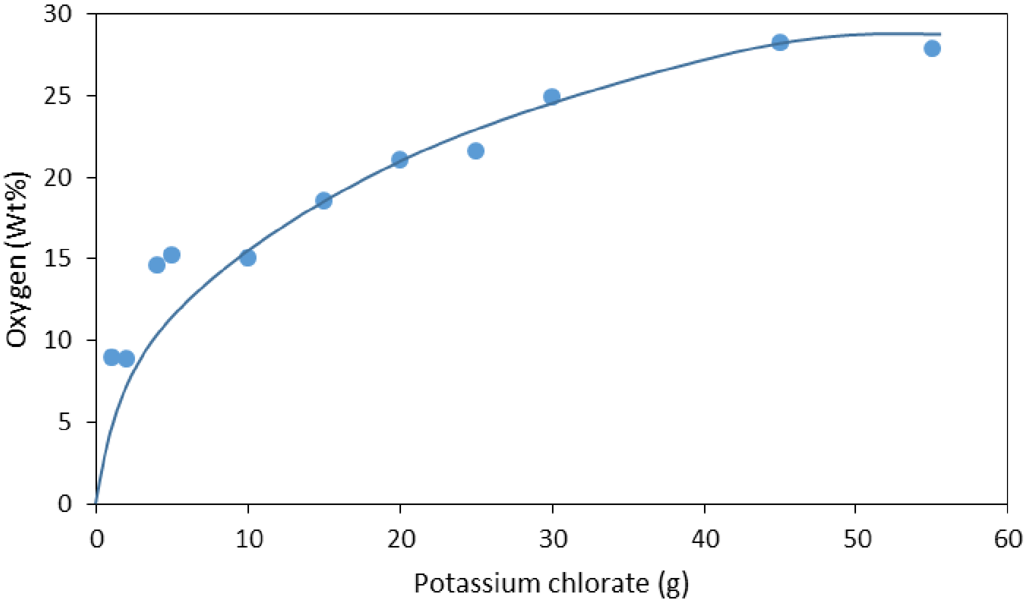

**Figure 4.8.3.1 XPS comparison of total oxygen wt % on various unwashed GO-HO samples.**

A similar trend is seen with Hummers oxidation whereby the effect of increasing the amount of permanganate quickly diminishes (figure 4.8.3.2). An increase from 10 to 15 g only results in an extra 2 wt% of oxygen. The previously seen higher activity of the GO-HU10 material compared to GO-HU15 material suggests inherent differences other than surface oxygen (figure 4.8.2.2). Further studies need to be conducted to assess the effect of higher levels of oxidant on lattice disorder. Washing of the catalysts result in no change to the level of oxygen in either Hofmann or Hummers catalysts (figure 4.8.3.3 and 4.8.3.4 respectively)

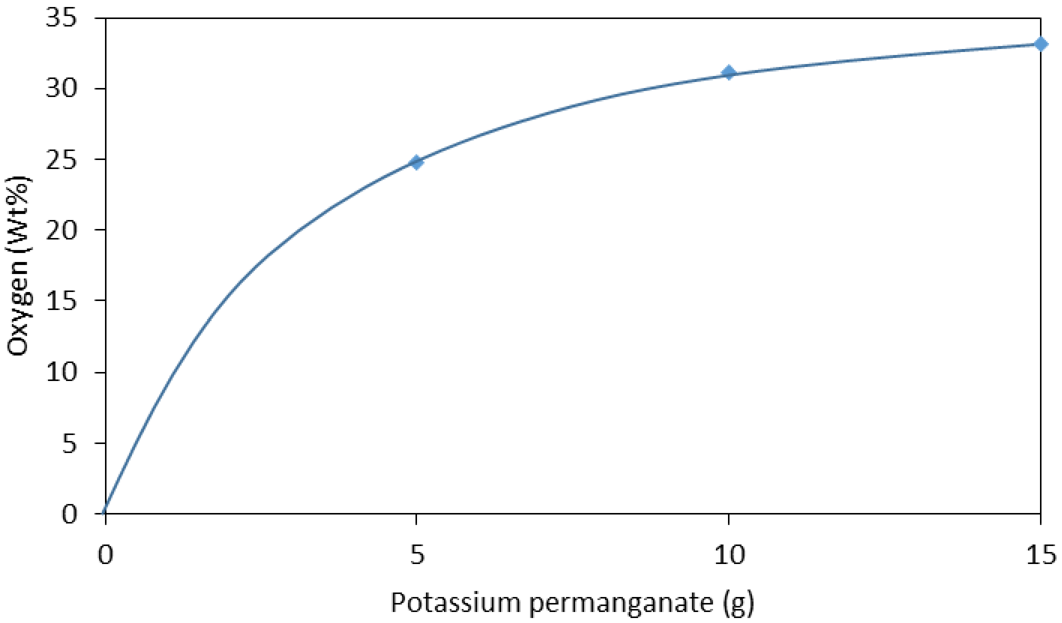

**Figure 4.8.3.2 XPS comparison of total oxygen wt% on various unwashed GO-HU samples.**

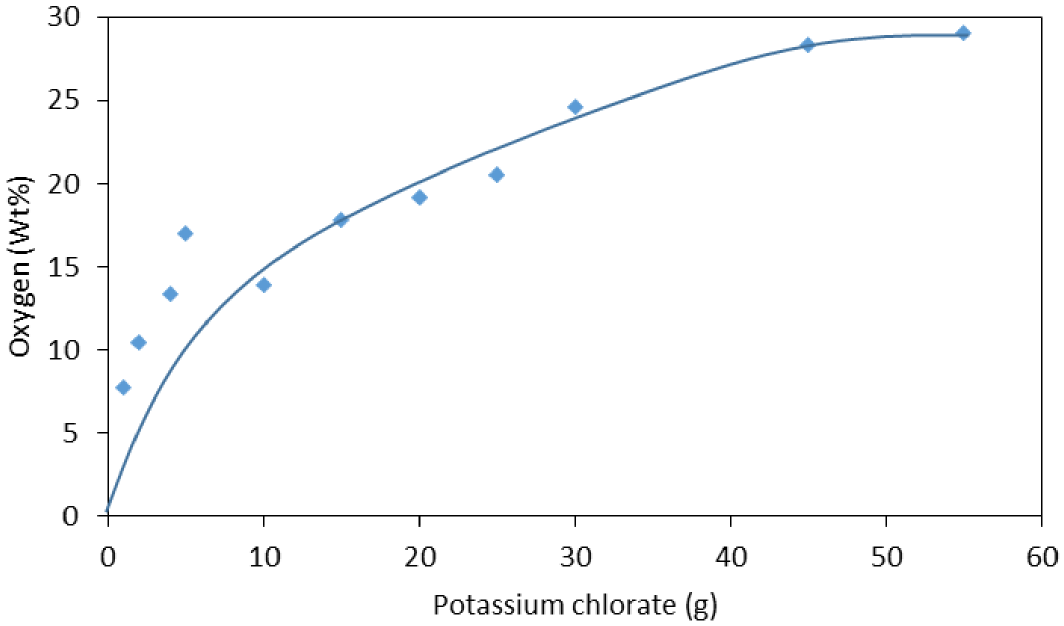

**Figure 4.8.3.3 Oxygen weight % obtained using a range of amounts of potassium chlorate in washed GO-HO samples.**

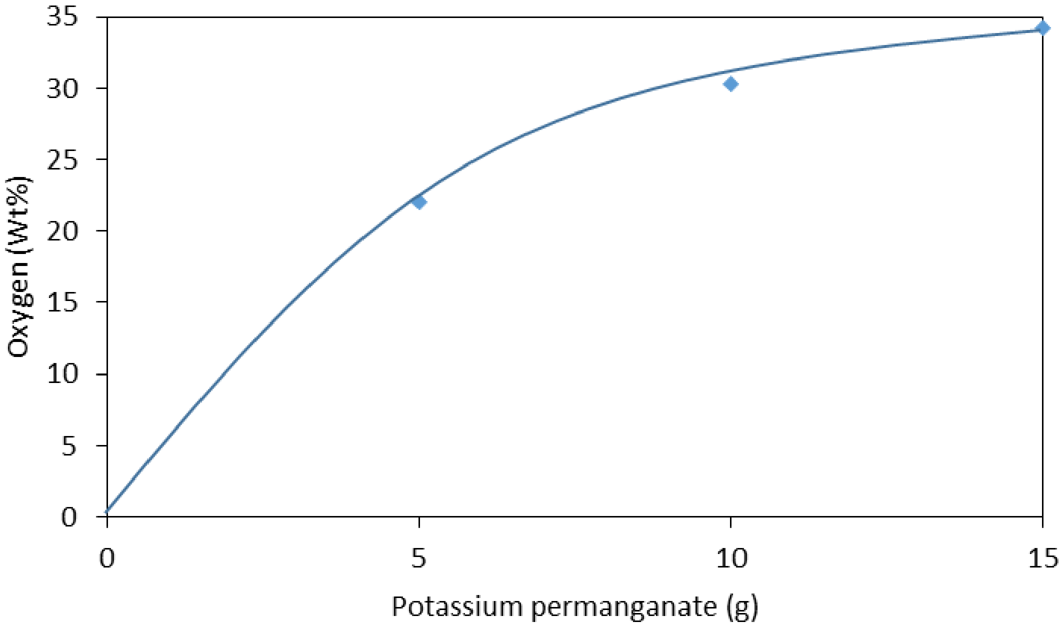

**Figure 4.8.3.4 Oxygen weight % obtained using a range of amounts of potassium permanganate in washed GO-HU samples**

While analysing the data obtained by XPS, it became apparent that there was a need to assess the conversion of dec-1-ene with respect to oxygen coverage. This was due to a non-linear progression of oxygen obtained when using varying amounts of oxidant in both HO and HU preparations. In the case of the GO-HO10 material it was found that the total wt% of oxygen was actually lower than the GO-HO5 material, which could explain the inactivity of this catalyst. Therefore all of the previous data obtained from unwashed and washed HO and HU methods was reassessed according to the total wt% of oxygen. This also allowed the combination and direct comparison of HO and HU samples which has been tedious up to this point. Analysis of the unwashed samples (figure 4.8.3.5) showed that an optimum level of oxidation was necessary, between 20 and 35 %, with activity and selectivity both peaking at 25 %. Below 20 %, no activity was observed. This explains the variation in activity of GO-HO15 samples as all recent inactive catalysts contain approximately 18.5 % oxygen. It also becomes clear why the HU samples seem to follow the opposite trend to HO samples in that increasing amount of oxidation results in less active catalysts with the GO-HU15 material often being completely inactive. The HU catalysts also peak at an optimum of 25 wt % oxygen after which activity decreases, as observed the HO samples. Vigorously washing the catalysts (4.8.3.6) showed that GOs with a low levels of oxidation can be activated, as described previously. Here, catalysts lower than the previous threshold of 20 wt % oxygen are now active.

A similar trend is obtained compared to the unwashed catalysts, however the oxygen wt % range in which activity occurs is extended down to 13.37 % prepared using 4g of potassium chlorate. However the inactivity of the GO-HO10 catalyst which contains 13.91 % oxygen seems to be an anomalous result and needs to be repeated. Again, the higher oxidised samples seem to steadily reduce in activity as higher oxygen wt % are obtained. HU samples again show low activity which almost perfectly fits this trend even after washing. The activity and selectivity of GO-HO55 at an oxygen wt of 29.04 % seems to also be an anomalous result to this trend and should be further investigated.

Analysis of the sulphur wt % of unwashed HO samples (figure 4.8.3.7) shows at least 0.8% on all catalysts with some containing nearly 2 %. The inactivity of the GO-HO10 catalyst may be explained by a combination of the lower than expected oxygen composition partnered with a high level of sulphur, both of which have been shown to contribute to inactivity of GO. However the continued inactivity post washing, leads to further confusion. Continued washing of this catalyst in an attempt to remove even more sulphur may result in an active catalyst, although its low oxygen content may suggest it simply lies just short of the point at which we see activity. All washed catalysts return with a lower level of sulphur, however some highly oxidised samples retain up to 0.8 % which could be used to explain the drop in activity at higher oxygen wt %. All catalysts need to be studied by CHNS analysis to obtain a total wt % of sulphur.

Analysis of the sulphur wt% of unwashed HU samples (figure 4.8.3.8) shows an even higher level of sulphur with GO-HU10 and GO-HU15 materials containing approximately 2.3 % and 2.8 % respectively. Washing of Hummers samples is notoriously difficult due to its swelling and formation of a clay like substance. It has also been suggested that in highly oxidised GO, sulphur becomes covalently attached to the GO surface which will not be affected by washing. The presence of this level of sulphur after centrifugation demonstrates the unsuitability for washing of GO. The additional vigorous washing step is able to remove high amounts of this sulphur, however the GO-HU10 and GO-HU15 materials still retain at least 1 % sulphur which could explain their low activities. The complete inactivity of the GO-HU15 material after washing compared to the slight activity before is at this point unexplained.

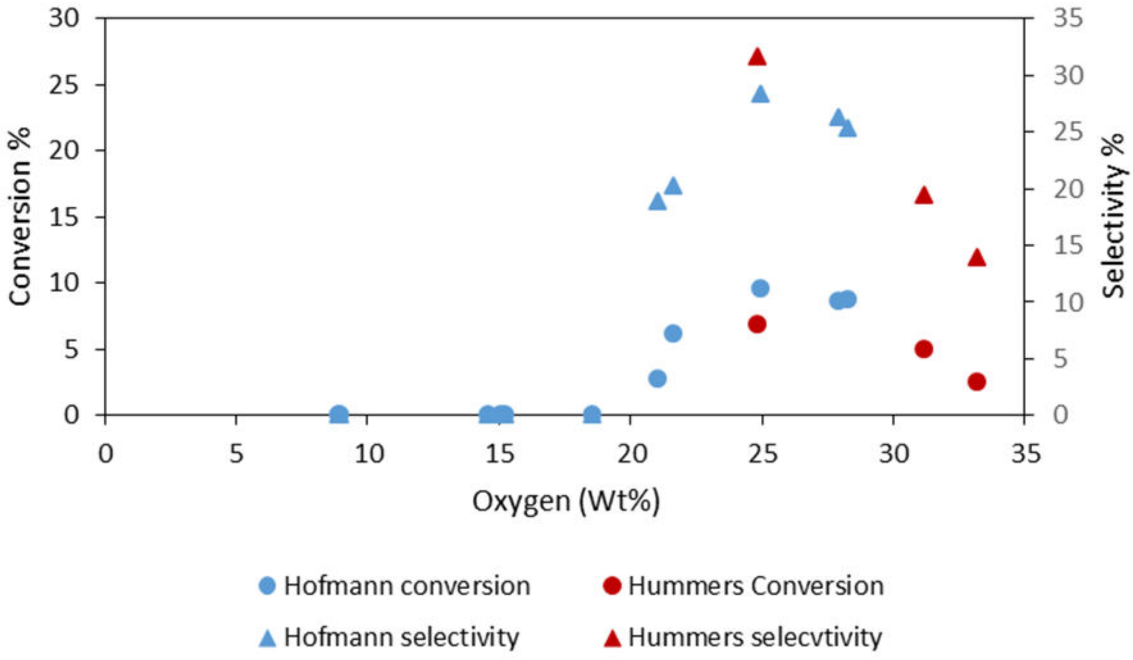

**Figure 4.8.3.5 Combined analysis of unwashed GO-HO samples and GO-HU samples. (90 °C, 48 h, dec-1-ene 10ml, GO 0.1 g)**

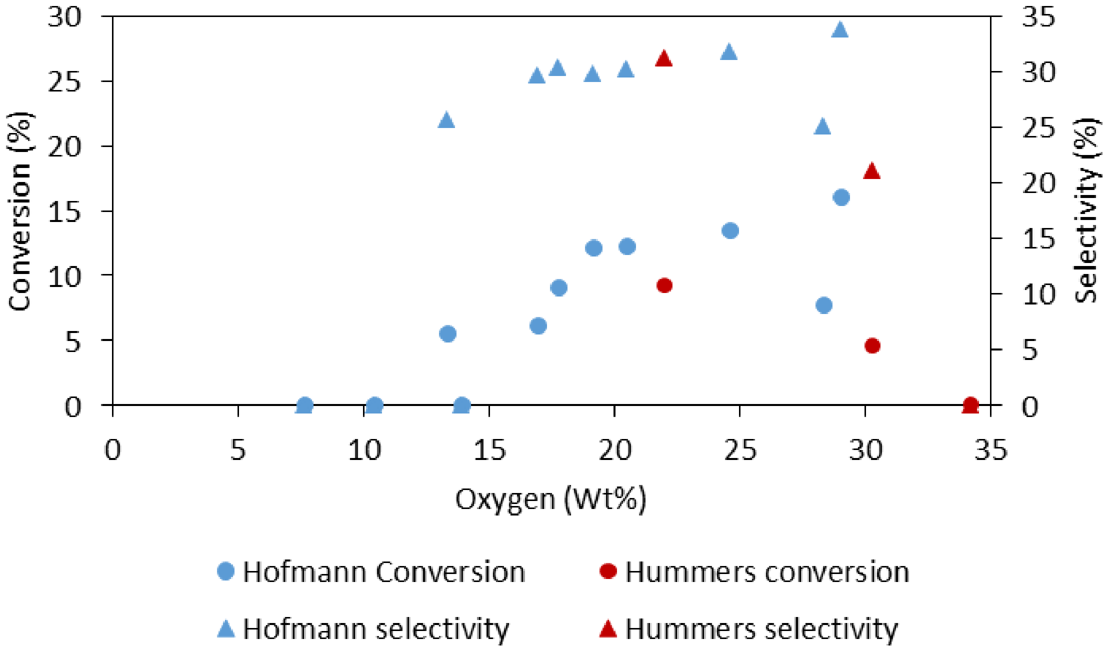

**Figure 4.8.3.6 Combined analysis of washed GO-HO and GO-HU samples (90 °C, 48 h, dec-1-ene 10 ml, GO 0.1 g)**

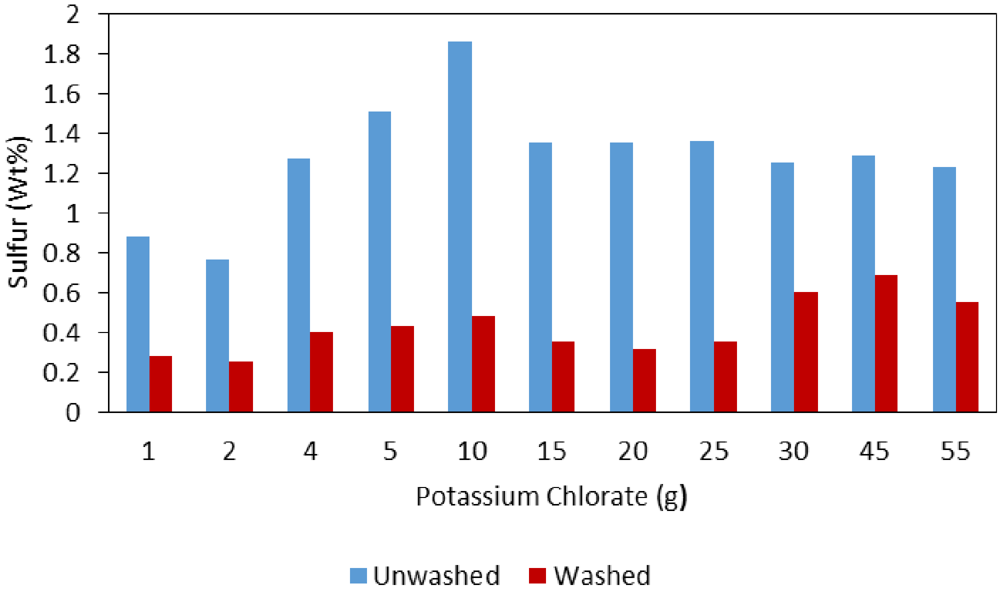

**Figure 4.8.3.7 Amount of sulphur present on GO-HO samples before and after extended washing.**

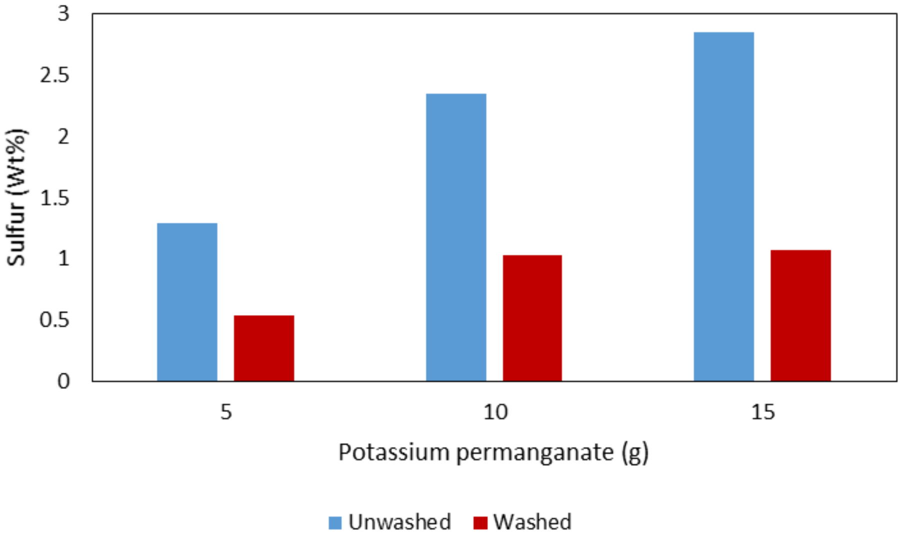

**Figure 4.8.3.8 Amount of sulphur present on GO-HU samples before and after extended washing.**

## 4.9 Conclusion

Graphitic oxide has been shown to be active for the aerobic and solvent free epoxidation of dec-1-ene in the absence of radical initiators. This is, to the best of our knowledge, the first example of a metal free catalyst being active for the epoxidation of an alkene. It also appears to be the first case in which the use of atmospheric oxygen is enabled without the use of a radical initiator or co-oxidant such as hydrogen peroxide.

An extensive range of both Hofmann and Hummers graphitic oxide catalysts have been prepared using varying amounts of oxidant. Hofmann samples using over 20 g potassium chlorate in their synthesis are active after standard centrifuge procedure. In both cases, washing of lower oxidised samples has the effect of increasing conversion and selectivity.

Remarkably, Hofmann samples using as little as 4 g of potassium chlorate are active for epoxidation of dec-1-ene. This implies that for the preparation of this carbocatalyst, much less oxidant can be used compared to the literature standard of 55 g, rendering the procedure much safer due to the decreased amount of chlorine dioxide produced. This is also the case with Hummers samples, however in this example, lower oxidised samples are more active before and after washing. This suggests that the optimised conditions for producing pristine graphene from graphene oxide are not transferable to producing an efficient catalyst. Previous groups have shown that there is no correlation between the level of oxidation of the surface/surface oxygen content and activity of the catalyst. This has previously been shown using a top down approach implementing thermal reduction. This new approach using a bottom up oxidation of graphite, uses less oxidant, safer conditions and produces a more workable catalyst compared to the clay like hummers 15 g catalyst. XPS analysis implies that there is in fact a correlation between oxygen content and activity, however the correlation is not linear and finds an optimum at 25 wt%. This has been shown to be the case for dec-1-ene epoxidation. However, activity was also shown to be extremely reliant on sulphur contamination, the removal of which led to the formation of low oxidised, active catalyst. The activity has been assigned to the surface oxygen groups as opposed to leached species, confirmed by the reuse of the catalyst, XPS analysis and inactivity in the absence of oxygen. At this point, it is unclear as to which oxygen species is providing activity, as all samples are abundant in a variety of oxygen moieties. For use in catalysis, more effort is needed into understanding the role of certain surface oxygen species and tailoring the preparation of GO for producing those pivotal in activation, as opposed to aiming for maximum oxygen coverage via conditions which could favour highly oxidised, but inactive species. Graphitic oxide has already been studied by other groups for a number of different chemical transformations. The sensitivity of the catalyst for epoxidation must be further investigated and many more substrate should be investigated. It may well be the case that tuning of the oxygen content is needed to each specific reaction. It also becomes clear that the traditional use of a centrifuge in order to separate and wash graphitic oxide is inadequate for obtaining a highly pure catalyst, even when using HCl as a washing medium. Advances in cross flow filtration and the sensitivity of conductometers should allow the progression of these catalyst washing techniques past simple centrifugation using the precipitation of barium nitrate as an end test for sulphur.

### 4.10 References

---

1 U.Hofmann, E.Konig, *Z.Anorg, Alg, Chem*, 1937, **234**, 311-336.

2 W.S. Hummers Jr, R.E. Offeman*, J. Am. Chem. Soc*, 1958, **80**, 1339.

3 L.Staudenmaier, *Ber. Dtsch. Chem. Ges*. 1898, **31**, 1481-1487.

4 K.S. Novoselov, A.K.Geim, , S.V. Morozov, D.Jiang, Y.Zhang, S.V.Dubonos, I.V.Grigorieva, A.A.Firsov, *Science*, 2004, **306**, 666-669.

5 A.A.Balandin, S.Ghosh, W.Bao, I.Calizo, D.Teweldebrhan, F.Miao, C.N.Lau, *Nano Lett*, 2008, **8**, 902-907.

6 C.Lee, X.Wei, J.W.Kysar, J.Hone, *Science*, 2008, **321**, 358-388.

7 S.Pisana, M.Lizzeri, C.Casiraghi, K.S.Novoselov, A.K.Geim, A.C.Ferrari, F.Mauri, *Nat.Mater*, 2007, **6**, 198-201.

8 S.V.Morozov, K.S. Novoselov, M.I.Katsnelson, F.Schedin, D.C.Elias, J.A.Jaszczak, A.K.Geim, *Phys.Rev.Lett*, 2008, **100**, 016602.

9 D.C. Marcano, D.V. Kosynkin, J.M Berlin, A. Sinitskii, Z. Sun, A. Slesarev, L.B. Alemany, W. Lu, J.M Tour, *ACS Nano*, 2010, **4**, 4806-4814.

10 D.R.Dreyer, S.Park, C.w.Bielawski, R.S.Ruoff, *Chem.Soc.Rev*.,2010, **39**, 228-240.

11 K.Morishige,T.Hamada, *Langmuir*, 2005, **21**, 6277-6281.

12 A.Mastalir, Z.Kiraly,A.Patzko, I.Dekany, P.L'Argentiere, *Carbon*, 2008, 1631-1637.

13 K.Gotoh, K.Kawabata, E.Fujii, K.Morishige, T.Kinumoto, Y.Miyazaki, *Carbon*, 2009, **47**, 2120-2124.

14 K.Gotoh, T.Kinumoto, E.Fujii, Aki,Yamamoto, H.Hashimoto, T. Ohkubo, A.Itadani, Y.Kuroda, H.Ishida, *Carbon*, 2011, **49**, 1118-1125 .

15 Z.L.Hu, M.Aizawa, Z.M.Wang,H.Hatori, *Carbon*, 2009, **47**, 3377-3380.

16 V.K.Singh,Mk.K.Patra,M.Manoth,G.S.Gowd.S.R.Vadera,N.Kumar, *New carbon Materials*, 2009, **24**, 147-152.

17 D.R.Dreyer, H.P.Jia, C.W.Bielawski, *Angew.Chem.Int.Ed.*,2010, **49**, 6813-6816.

18 H.L.Poh, F.Sanek, A.Ambrosi, G.Zhao, Z.Sofer, M.Pumera*, Nanoscale*, 2012, **4**, 3515-3522.

19 V.Schwartz, W.Fu, Y.T.Tsai, H.M.Meyer, A.J.Rondinone, J.Chen, Z.Wu, S.H.Overbury, C.Liang, *Chem.Sus.Chem*, 2013, **6**, 840-846.

20 N.R.Wilson, P.A.Pandey, R.Beanland, R.Y.Young, I.A.Kinloch, L.Gong, Z.Liu, K.Suenaga, J.P.Rourke, S.J.York, J.Sloan, *ACS Nano*, 2009, **3**, 2547-2556.

21 NIST database, http://webbook.nist.gov/cgi/cbook.cgi?ID=C54125392&Units=SI&Mask=3FFF 19.01.2015

22 M.D. Hughes, Y.X.Xu, P.Jenkins, P.Macmorn, P.London, D.I.Enache, A.F.Carley, G.A.Attard, G.J.Hutchings, F.King, F.E.H.Stitt, P. Johnston, K.Griffin, C.J. Kiely, *Nature*, 2005, **437**, 1132-1135.

23 H.Alshammari, P.J.Medziak, D.J.Morgan, D.W.Knight, G.J.Hutchings, *Green Chem*, 2013, **15**, 1244-1254.

24 U.N.Gupta, N.F. Dummer, S.Pattisson, R.L.Jenkins, D.W.Knight, D.Bethell, G.J.Hutchings, *Catal Lett*, 2014, DOI 10.1007/s10562-014-1425-z.

25 R.K.Upadhyay, N.Soin, S.S.Roy, *RSC Adv.*,2014, **4**, 3823-3851.

26 S.Eigler, C.Dotzer, F.Hof, W.Bauer, A.Hirsch, *Chem, Eur. J*, 2013, **19**, 9490-9496.

# 5

# Characterisation of Graphitic oxide: Progressive oxidation of graphite and development of a catalytic surface.

## 5.0 Introduction

This chapter supplements the ideas previously described in chapter 4 with respect to the ability to epoxidise dec-1-ene using a range of graphitic oxides prepared using modified Hofmann or Hummers techniques. Characterisation of each of the samples is conducted using a range of techniques focusing on the effect of increasing levels of oxidation.

### 5.0.1 Characterisation of graphene and graphitic oxide

The characterisation of graphene and graphitic oxide materials is vital for understanding their use as carbocatalysts. The wide range of preparation methods, and analogues within such techniques lead to varying of functional groups, amount of defects, heteroatom functionality, surface area and other traits. Many characterisation methods are available and often employed in order to obtain deep knowledge of the origin of catalysis occuring on these materials.

Elemental analyses such as microwave plasma atomic emission (MP-AES), inductively coupled plasma optical emission spectrosocpy (ICP-OES) (or mass spectrometry ICP-MS) and combustion analysis (CHNS) are commonly employed to obtain knowledge of metal impurities upon the surface of graphitic oxide. Metal such as manganese, potassium and sodium can remain on the catalyst after preparation due to their inclusion in oxidants such as potassium permanganate and potassium chlorate. Analysis of these elements can confirm whether these are contributing to reaction or whether GO materials are truly operating as carbocatalysts.

Microscopic techniques such as transmission electron microscopy (TEM), scanning electron microscopy (SEM) and atomic force microscopy (AFM) can study the surface morphology and single layer sheets. These are less useful in terms of liquid phase catalysis due to the rarity of forming single layer sheets. They are more commonly employed for applications in which the graphene materials are used as films.

Thermal analysis such as thermogravimmetric analysis (TGA) and temperature programmed desorption (TPD) can study the stability and reactivity of the GO surface in oxidising and reducing atmospheres. This can be studied as a function of time and/or temperature to investigate the long term and thermal stability of the materials.

Spectroscopic methods including Raman spectroscopy, fourier transform infrared (FT-IR), X-ray photoelectronic spectroscopy (XPS), Ultraviolet-visible spectroscopy (UV-Vis) and solid state nuclear magnetic resonance (NMR) are extremely important in identifying functionality upon the GO surfaces. XPS is the most important and commonly used of these in catalysis due to its ability to give information on which elements are present with their relative abundancies and importantly for carbon, the various functionalities.

Diffraction techniques such as X-ray diffraction (XRD) and neutron diffraction can be employed to study the long range order and crystallinity in the bulk. These are sometimes not relevant in liquid phase catalysis due to agglomeration of the materials when drying and reduction of interlayer spacings. However they do provide important information on the morphology and crystallite size of GO sheets. It is also useful for tracking the oxidation of the graphitic surface and reduction in crystallinity of the material as will be discussed later.

Brunauer-Emmett-Teller (BET) analysis is often employed to study the surface area of GO. However the large theoretical surface area of GO is rarely observed due to the need for dry samples in analysis. This leads to contraction of the lattice spacings and agglomeration of the GO sheets.

## 5.1 TGA

TGA analysis was conducted on the full range of Hofmann (GO-HO1 to GO-HO55)(figure 5.1.1) and Hummers catalysts (GO-HU5 to GO-HU15) (figure 5.1.2) in order to track the decomposition of the materials under an inert atmosphere over time. The thermal stability of samples was studied between 50 and 500 °C are given as a function of the weight percent of the orginal material.

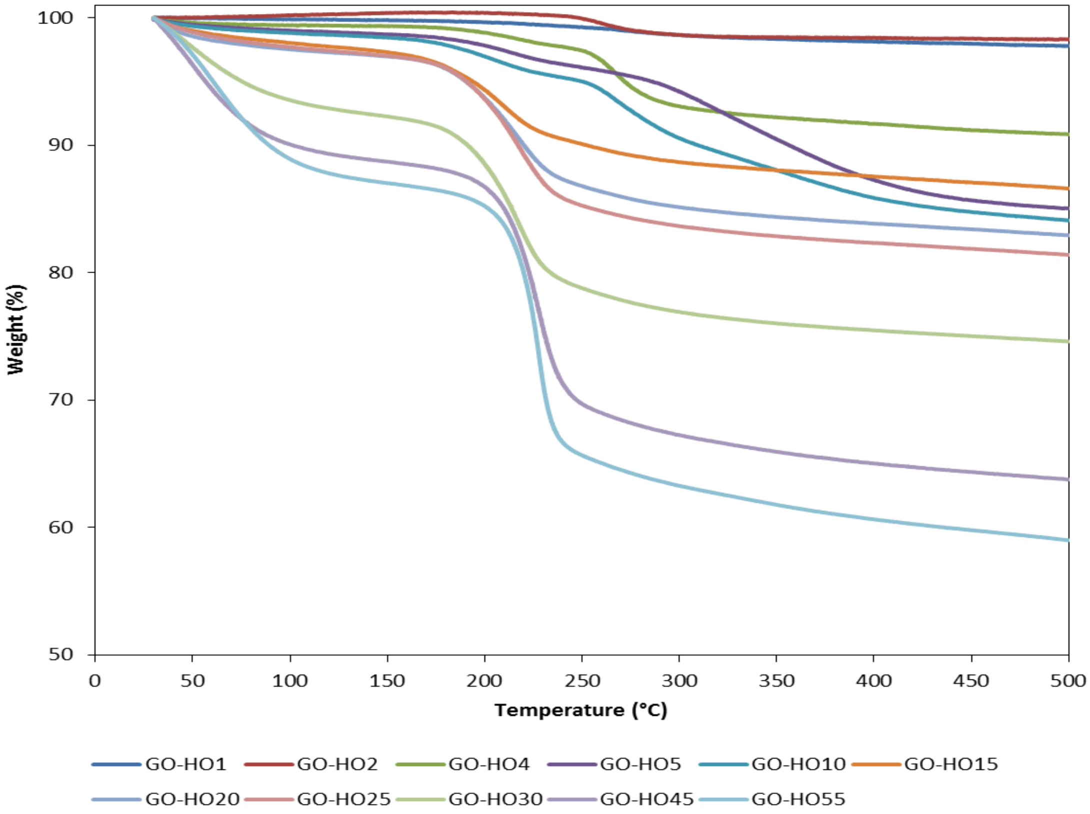

**Figure 5.1.1 TGA of Hofmann samples prepared using increasing amounts of potassium chlorate. (30-500 °C, 5 °C/min, $N_2$ 20 mL/min, GO ca 20-50 mg)**

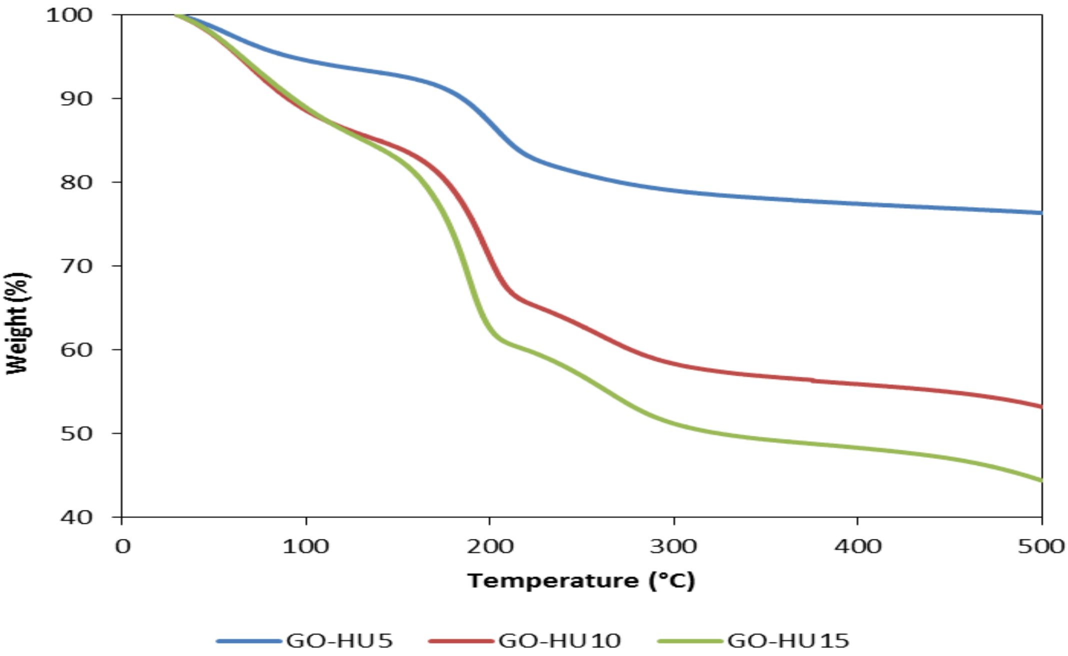

**Figure 5.1.2 TGA of Hummers samples prepared using increasing amounts of potassium permanganate. (30-500 °C, 5 °C/min, $N_2$ 20 mL/min, GO ca 10 mg)**

Partially oxidised Hofmann samples (figure 5.1.1) such as GO-HO1 and GO-HO2 show little or no weight loss over the temperature range. A slight weight loss can be observed at approximately 250 °C which may be due to water escaping from the tightly pack graphitic lattice. These samples have already been dried at 110 °C after their preparation and therefore only slight weight loss is expected at lower temperatures. In slightly higher oxidised species such as GO-HO4, GO-HO5 and GO-HO10 this weight loss at 250 °C is preceded by an initial weight loss up to 200 °C most likely due to the formation of carbon dioxide, carbon monoxide and lower temperature release of water. This lower temperature weight loss is possibly due to incomplete drying after preparation or in fact adsorbing or atmospheric water post preparation. This is more likely in higher oxidised species due to their hygroscopic nature. The weight loss of more highly oxidised Hofmann samples (GO-HO15 to GO-HO55) is more clearly understood. The initial weight loss between room temperature and 120 °C is almost certainly due to the release of adsorbed water. This loss of water is combined with the formation or CO and $CO_2$ between approximately 50 °C and 200 °C[1]. The significant weight loss between 200 °C and 250 °C in GO-HO30, GO-HO45 and GO-HO55 is not very well understood. This weight loss of about 10 to 15 % in the higher oxidised samples could be explained by some recent work by Eigler et al[2]. This group noted the lack of study into weight losses occurring between 200 and 250 °C and therefore investigated this region using TGA partnered with mass spectrometry and FT-IR for analysis of the escaping molecules. The authors attributed this loss of approximately 15 wt% to the breakdown of organosulphate species present on the surface of the GO. This was said to be combined with further desorption of water and production of CO and $CO_2$. This was confirmed by thermal decomposition of sodium dodecylsulphate as a reference and production of $SO_2$ monitored by IR. The samples studied by Eigler and co-workers are similar to our highly oxidised Hummers samples (figure 5.1.2). Certainly GO-HU10 and GO-HU15 exhibited weight losses almost identically to those reported with an initial weight loss of $H_2O$, CO and $CO_2$, followed by more dramatic release of CO and $CO_2$ up to temperatures of around 200 °C. As previously described, the approximate weight loss of 15 wt% between 200 and 300 °C may be attributed to the presence of organosulphate covalently bound to the catalyst surface. This would explain the high levels of sulphur remaining on the Hummers catalysts after extensive washings and ultimately their inactivity for the epoxidation of dec-1-ene. Further studies need to be conducted on these samples using TGA-FTIR-GC-MS to confirm the identity of the evolved species.

### 5.2 Raman

Raman spectroscopy has been shown to be useful for the characterisation of graphene, graphene oxide and graphitic oxide. The technique is useful for monitoring the amount of defects present in these structures and also the introduction of functional groups through oxidation. This main use of Raman is when studying 2D graphenic materials as the relative intensity of D to G bands found at 1350 $cm^{-1}$ and 1600 $cm^{-1}$ respectively is a good indicator of quality of the sheets. This is important when utilising these materials for the electronic capabilities. Raman is less useful for the study of stacked layers or highly functionalised materials for which accurate quantification of different groups is needed, however intensities of the D band can be an indicator of amount of dopants and therefore this is often studied when dopants are suspected to play a role in activity[3]. As previously described, Raman was used in this study to confirm differing levels of oxidation in Hofmann catalysts (figure 5.2.1) from the parent graphite. Indeed, the formation of a disorder induced D band at 1330 $cm^{-1}$ and a broadened and blue shifted G band at 1590 $cm^{-1}$ are indicative of the amount of disorder and functionality introduced into the $sp^2$ lattice[4].

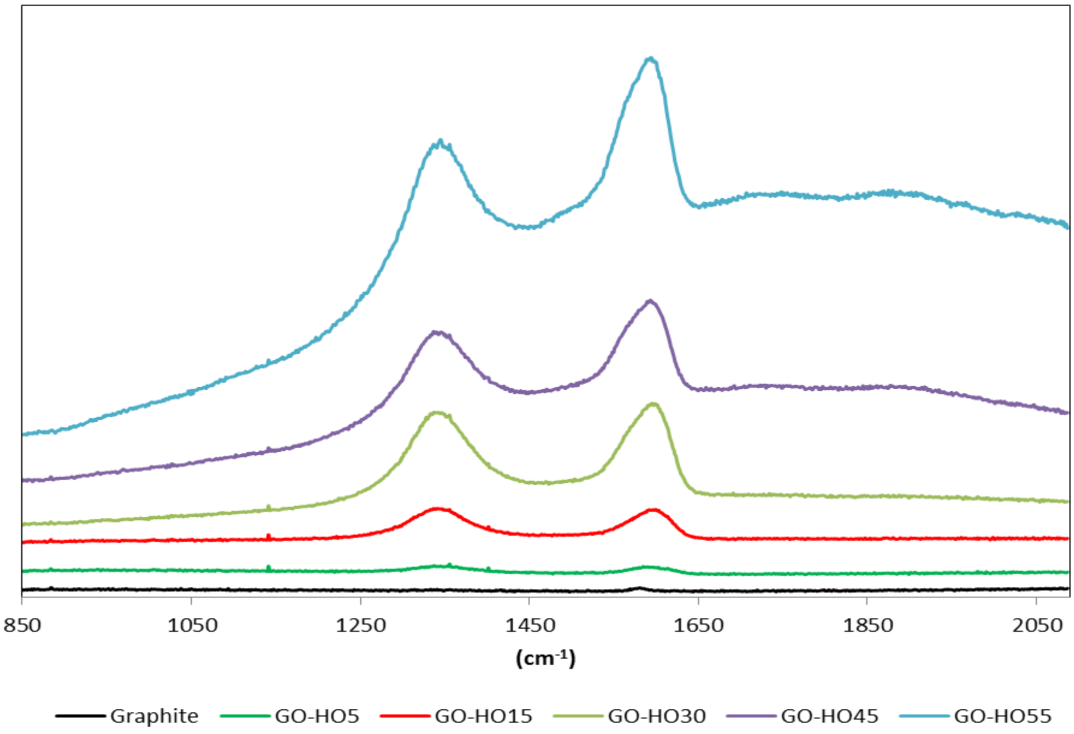

**Figure 5.2.1 Raman spectroscopy of Hofmann samples prepared using an increasing amount of oxidant.**

Hummers samples were also studied by Raman spectroscopy (figure 5.2.2) and found to exhibit similar spectra to that of highly oxidised Hofmann samples. Once more the intensified and blue shifted G band at 1590 $cm^{-1}$ and the formation of the D band at 1330 $cm^{-1}$ is a strong indicator of oxidation of the parent graphite and break-up of this structure. The use of Raman in this study seemed to be limited to confirming oxidation and could not give us the information on amount of oxygen present and which functionalities were prominent, possibly causing activity or inactivity for the epoxidation of dec-1-ene. For a more in depth investigation on types of oxygen present and their relative abundancies, characterisation techniques such as FT-IR and XPS were employed.

It has been suggested that the activity of graphitic oxide for the oxidative dehydrogenation of isobutane may rely not on the amount of oxygen present or abundance of certain functional groups, but instead on the $sp^2$ to $sp^3$ ratio within the carbon framework. Liang *et al.*[5] studied this reaction with partially reduced graphene oxides and suggested that this ratio may play crucial role. It may be that activity relies on the presence of certain functional groups at specific lattice positions which would explain the general lack of correlation between activity and level of oxidation in these catalysts.

In our study we also found a lack of linear correlation between level of oxygen and activity for epoxidation. Raman could not explain this discrepancy as active GO-HO catalysts had similar spectra to inactive GO-HU catalysts leading us to more in depth study.

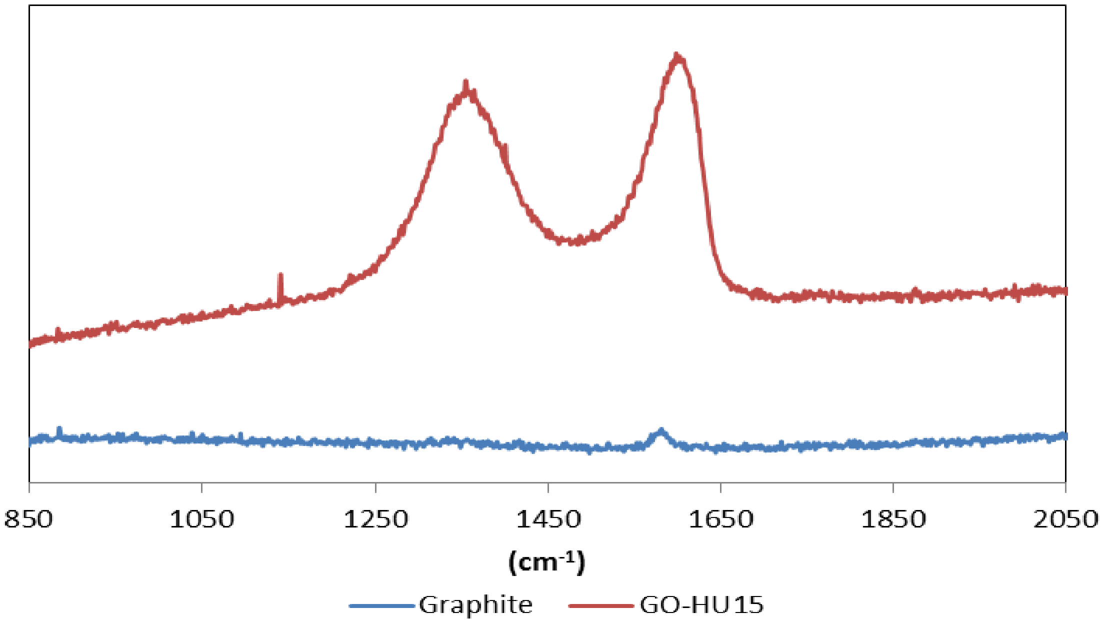

**Figure 5.2.2 Raman comparison of graphite and GO-HU15**

### 5.3 FT-IR

FT-IR was used to study the various oxygen functionalities on the GO surface in an attempt to identify a possible active species and explain the differences in activity between the various preparation methods. Various functionalities are observable in the FT-IR spectra of GO-HO15, GO-ST15 and GO-HU15 (figure 5.3.1) and can be seen at various intensities and wavenumbers. The broad peak at around 3400 cm$^{-1}$ in all materials is suggested to be O-H stretches arising from hydroxyl groups and also from adsorbed water. GO-HO15 and GO-ST15 materials exhibit very similar stretches. The stretch at approximately 1630 cm$^{-1}$ in all materials is indicative of water. The peak adjacent to this at approximately 1736 cm$^{-1}$ which is only present in GO-HU15 is representative of carbonyl groups residing at the edges of the graphitic oxide sheets. This is a result of the higher oxidation of the GO-HU15 compared to the GO-HO15 and GO-ST15. The other peaks present in all materials at 1400, 1225 and 1050 cm$^{-1}$ represent the presence of hydrogen bonding, epoxy groups and C-O vibrations respectively.

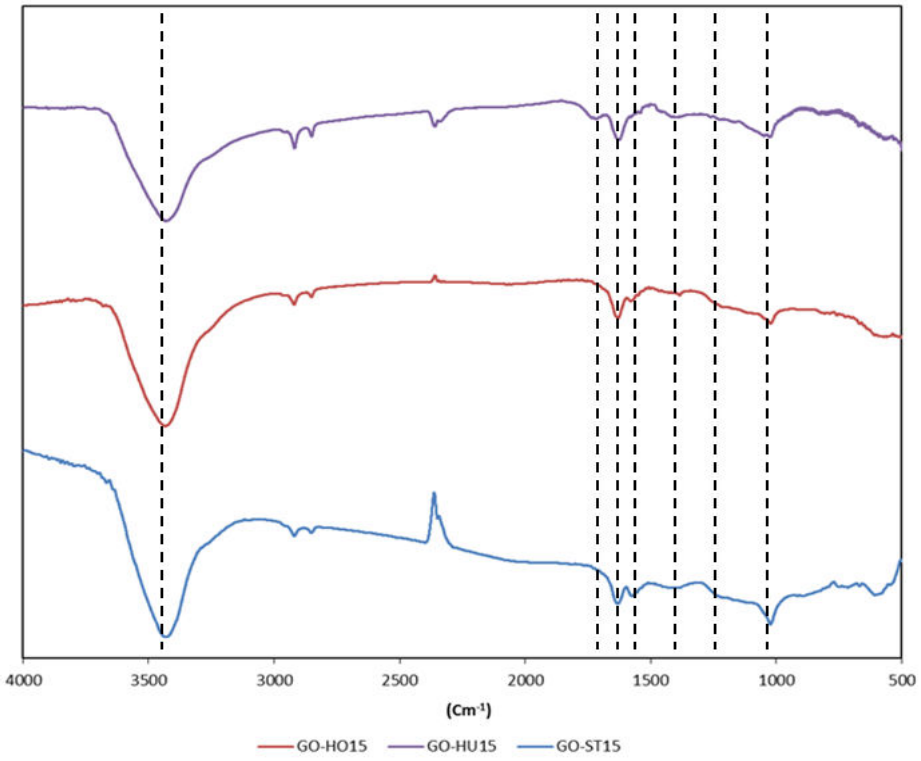

**Figure 5.3.1 Fourier transform infrared spectroscopy of GO-HO15, GO-ST15 and GO-HU15 catalysts.**

## 5.4 XRD

XRD analysis was conducted upon all of the GOs produced in this study producing an elegant description of the transformation from graphite to graphitic oxide through oxidation previously unseen in the literature. Highly oxidised GOs have often been prepared and compared to reduced graphene oxide and the parent graphite. Researchers frequently note the disappearance of the reflection at 26.5° corresponding to the 002 plane of graphite[6]. This is replaced by a lower intensity peak at approximately 10° representative of the 002 plane of graphitic oxide. This peak remains in reduced graphene oxides and graphene and indicates the increase in d-spacing from 3.5 to 7 Å.

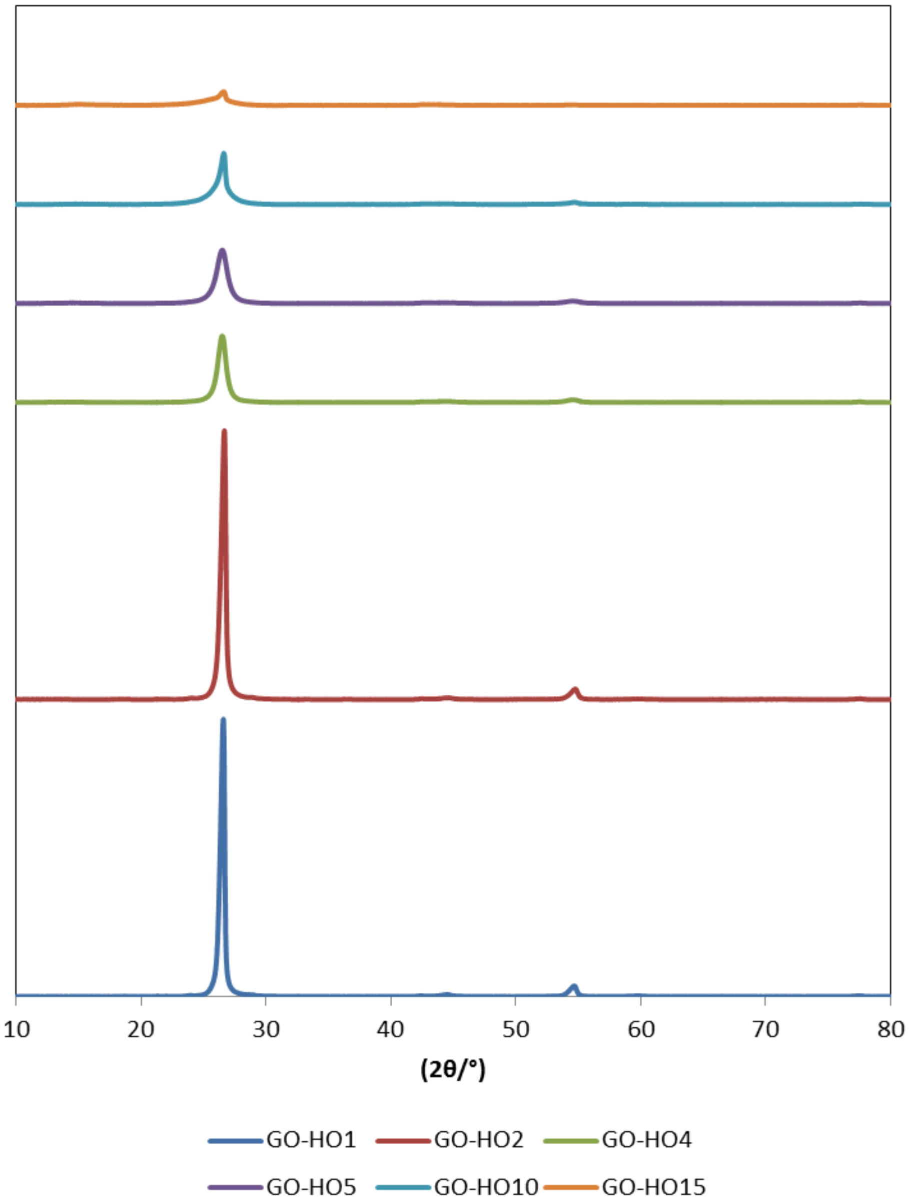

**Figure 5.4.1 XRD analysis of Hofmann samples GO-HO1 to GO-HO15**

The XRD of low oxidised Hofmann samples GO-HO1 to GO-HO15 (figure 5.4.1) shows the gradual oxidation of the graphite surface with the increase in amount of oxidation. This results in the gradual breakup of the lattice and loss of crystallinity and an overall decrease in the intensity of the 002 peak at 26.5°. The 101 and 004 peaks at 45° and 55° respectively also decrease, showing the gradual degraphitisation of the surface. Further increase in amount of oxidant used results in the eventual switching of highly crystalline graphitic like materials to amorphous graphitic oxide type materials in which the principle XRD peak is at 11° representative of the 002 plane and an increased d-spacing for 3.5 to 7 Å. The 101 peak remains even in highly oxidised species, however the 004 peak completely disappears, suggesting the loss of long range order in these fairly amorphous materials.

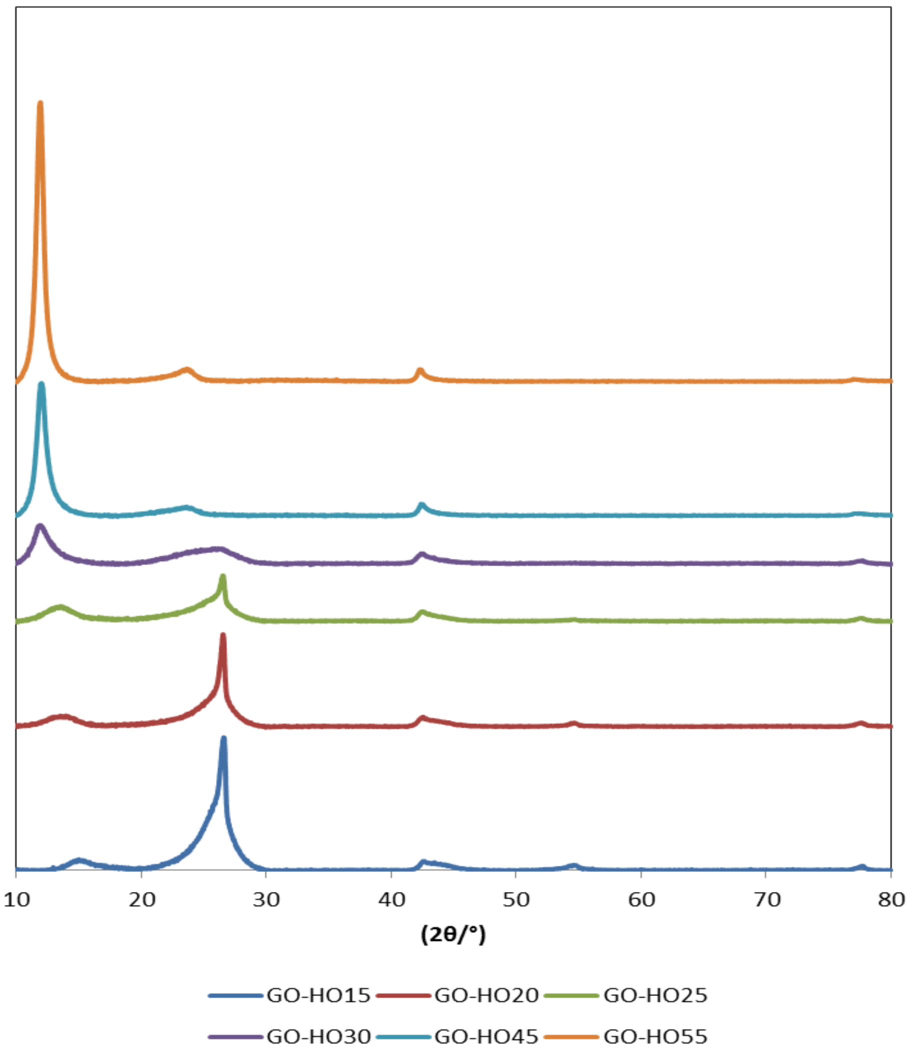

**Figure 5.4.2 XRD analysis of Hofmann samples GO-HO15 to GO-HO55**

The XRD patterns observed for Hummers samples (figure 5.4.3) GO-HU5, GO-HU10 and GO-HU15 are similar to the highly oxidised Hofmann samples. Even the low amounts of potassium permanganate used in GO-HU5 is enough to disrupt the graphitic lattice, decreasing the peak at 26.5° and cause the development of the 002 peak at 10 to 11°. These results are in agreement with literature evaluations of highly oxide graphitic oxides and reduced graphene oxides and show the degraphitisation of the surface leading to a loss of crystallinity and an increase in d-spacing from 3.5 to 7 Å. GO-HU15 shows no presence of the reflection at 26.5° with only two clear peaks occurring at 11 and 45° representative of the 002 and 101 planes of graphitic oxide.

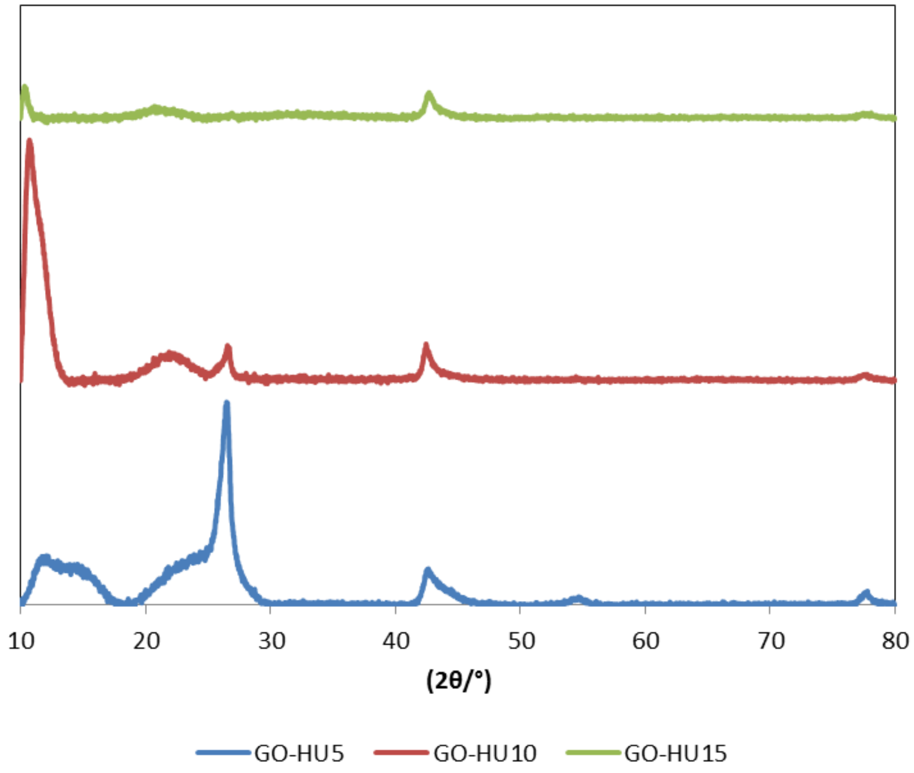

**Figure 5.4.3 XRD of Hummers samples produced with increasing amounts of potassium permanganate.**

## 5.5 XPS

XPS is often referred to as the most useful technique for the characterisation of graphitic oxides in catalysis[7]. This is due to the ability to identify and quantify certain elements present on the materials. To accompany this, it is also possible to identify the various oxidation states of metals and functionalities. This makes this techniques extremely useful in analysis of GO materials as oxygen composition and functionality can be quantified along with any other impurities which may be residing on the surface from the preparation methods.

The full range of Hoffman and Hummers samples were analysed by XPS and partnered with ion chromatography data resulted in some of the most important results obtained in this project. The XPS of Hofmann samples (figure 5.5.1) shows the progressive oxidation from graphite to graphitic oxide. The peak at 284.6 eV is normally attributed to the C-C bonding of $sp^2$ carbon atoms. The decrease in intensity of this peak from GO-HO1 to GO-HO55 can be explained by the oxidation of the lattice and breaking of these C-C bonds, along with the introduction of functional groups and $sp^3$ hybridised carbons. Increasing oxidation is also accompanied by the development of a peak at 286.7 eV which corresponds to the hydroxyl functionality. This is present to a small degree in all samples, however it becomes prominent in highly oxidised samples such as GO-HO45 and GO-HO55. Other functionalities are also present in these Hofmann samples such as carboxylic ketone and epoxy moieties above 287 eV however these are only present in small amounts.

Carboxyl functionalities are more easily observed in the highly oxidised Hummers samples (figure 5.5.2) at approximately 289 eV, explaining also the presence of the carbonyl stretch found in FT-IR for these materials. The Hummers samples GO-HU10 and GO-HU15 also show the highest hydroxyl functionality compared to the Hofmann catalysts, a result of the deep oxidation that occurs during this preparation method. These results are in agreement with previous investigations by Pumera *et al.*[8] who described the higher carboxylic acid functionality on the edges of Hummers prepared GO's compared to Hofmann catalysts which are mostly abundant with hydroxyl and epoxy moieties upon the basal planes.

Despite the usefulness of this technique, we were still unable to identify which of these functional groups was responsible for activity in the epoxidation of dec-1-ene.

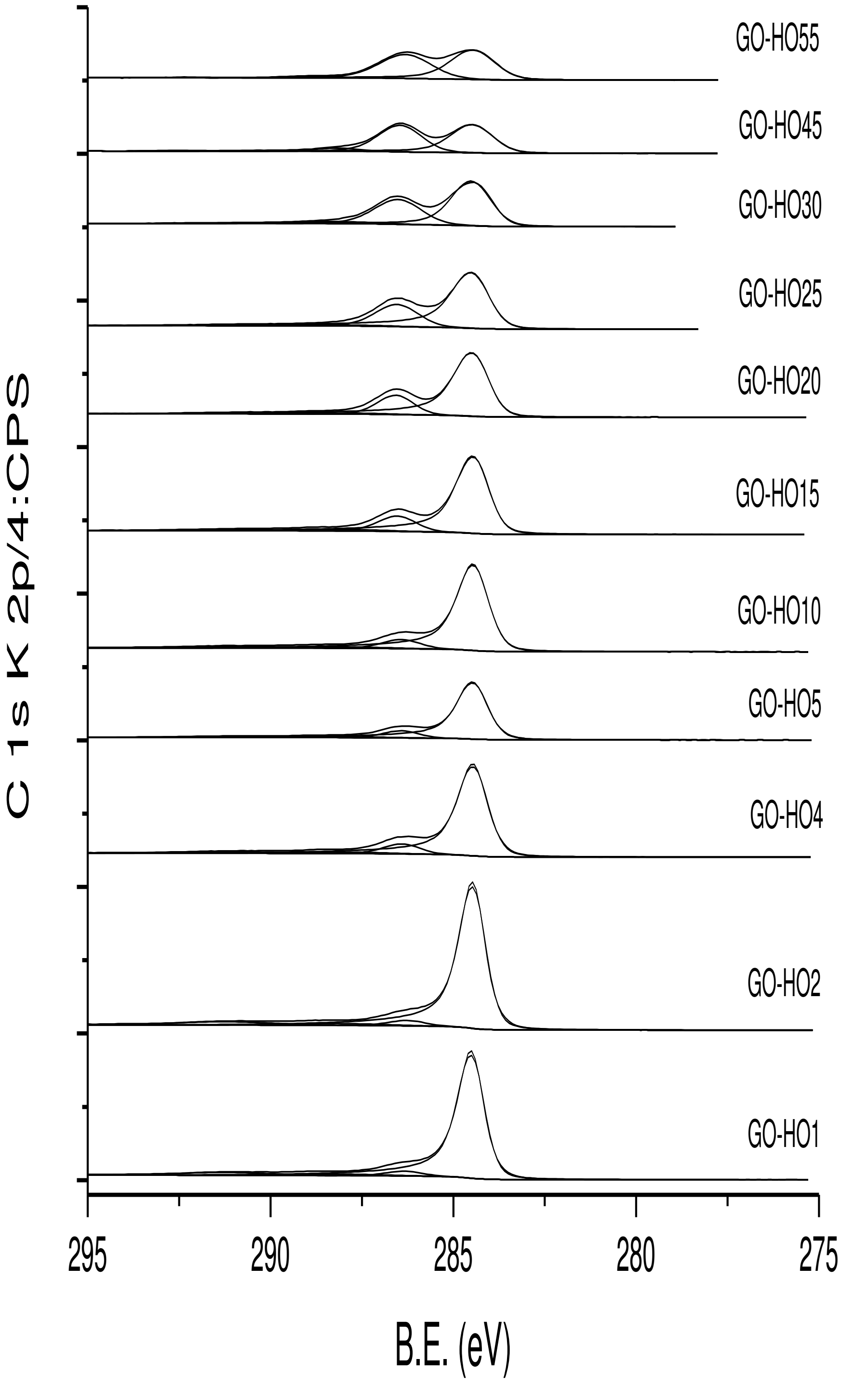

Figure 5.5.1 XPS C1s region of Hofmann graphitic oxide samples GO-HO1 to GO-HO55

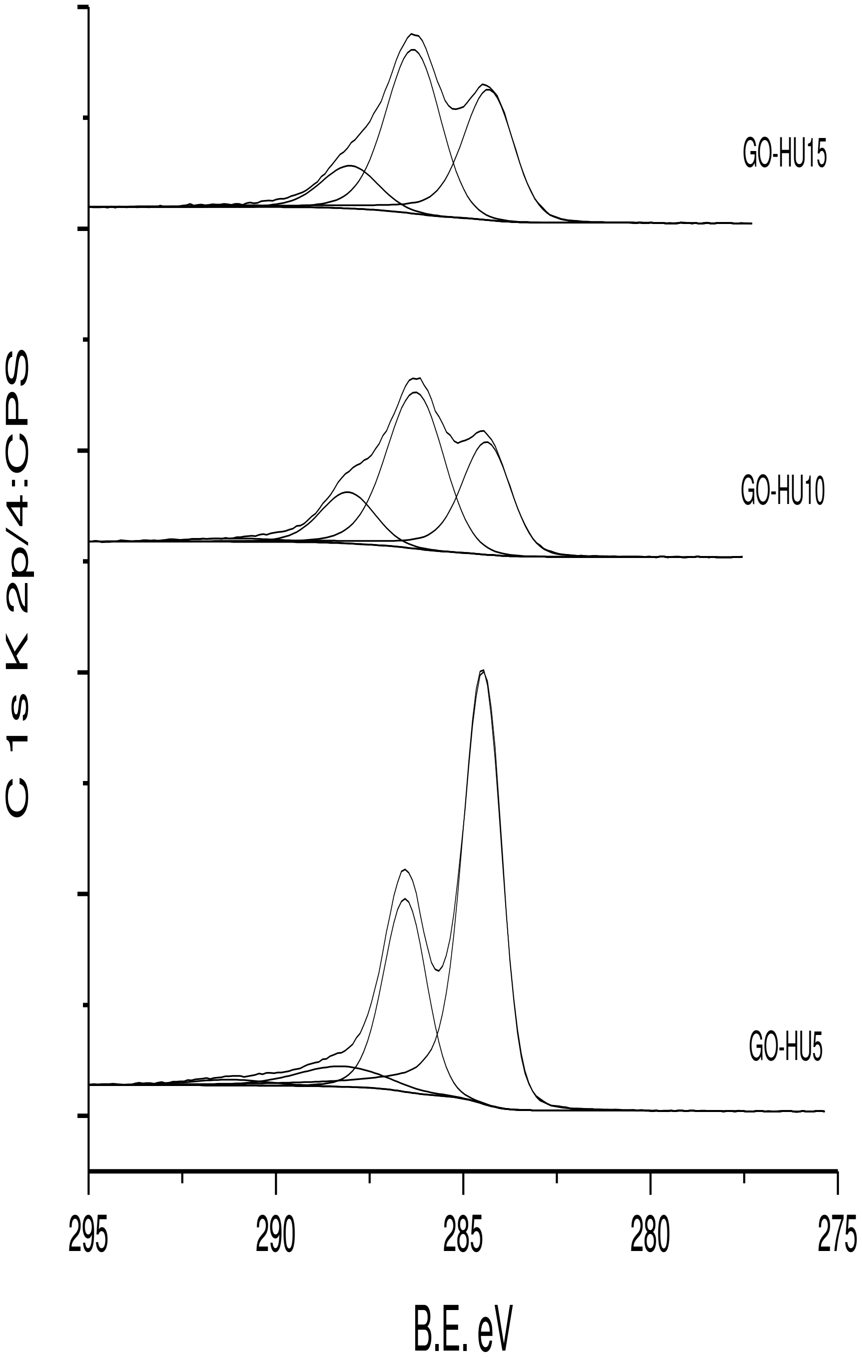

Figure 5.5.2 XPS C1s region of Hummers graphitic oxide samples GO-HU5 to GO-HU15

XPS was also used to quantify the amount of oxygen and sulphur on each of the Hofmann and Hummers materials. The implications of these quantities have already been described in chapter 4 (section 4.8) with respect to their effect on activity of epoxidation of dec-1-ene. In summary, all samples were found to be abundant to some degree in oxygen and sulphur. As expected, higher amounts of oxidant led to higher oxygen coverage on the obtained materials, although this was not a linear trend. It was found that for a catalyst to be active in the epoxidation of dec-1-ene, a minimum of 20 wt% of oxygen was required. As shown below (table 5.5.1) this was achieved using amounts of potassium chlorate of 20g and above. However it was found that by extensively washing these catalysts, the amount of sulphur present on the surface is dramatically reduced and results in lower oxidised GO materials becoming active. Highly oxidised Hummers samples such as GO-HU10 and GO-HU15 were found to be much higher in sulphur contamination (2.4 and 2.9 %) respectively. A high amount of sulphur also remained on these catalysts after washing compared to Hofmann catalysts suggesting the presence of covalently bound organosulphates as previously described. These Hummers catalysts were also the most highly oxidised species owing to the powerful oxidation procedure.

**Table 5.5.1 XPS comparison of various Hofmann and Hummers graphitic oxides produced using increasing amount of oxidants. The table shows the relative abundances of oxygen and sulphur present on each of the catalyst before and after washing.**

| | | **Unwashed** | **Unwashed** | **Washed** | **Washed** |
|---|---|---|---|---|---|
| | Oxidant (g) | O (wt %) | S (wt %) | O (wt %) | S (wt %) |
| **Hofmann** | 1 | 9.0 | 0.9 | 7.7 | 0.3 |
| | 2 | 8.9 | 0.8 | 10.4 | 0.3 |
| | 4 | 14.6 | 1.3 | 13.4 | 0.4 |
| | 5 | 15.2 | 1.5 | 17.0 | 0.4 |
| | 10 | 15.1 | 1.9 | 13.9 | 0.5 |
| | 15 | 18.6 | 1.4 | 17.8 | 0.4 |
| | 20 | 21.1 | 1.4 | 19.2 | 0.3 |
| | 25 | 21.7 | 1.4 | 20.5 | 0.4 |
| | 30 | 25.0 | 1.3 | 24.6 | 0.6 |
| | 45 | 28.3 | 1.3 | 28.3 | 0.7 |
| | 55 | 27.9 | 1.2 | 29.0 | 0.6 |
| **Hummers** | 5 | 24.8 | 1.3 | 22.1 | 0.5 |
| | 10 | 31.2 | 2.4 | 30.3 | 1.0 |
| | 15 | 33.2 | 2.9 | 34.2 | 1.1 |

## 5.6 Conclusion

Graphitic oxide has been extensively characterised by a number of techniques. The effect of amount of oxidant in both Hummers and Hofmann catalysts has been explored. This has allowed the previously unseen stepwise transformation from highly crystalline graphite to graphitic oxide to be observed through XRD, XPS and raman spectroscopy. The full characterisation of these materials regarding their functionality and level of oxidation has allowed for the further understanding of their relative activities for the epoxidation of dec-1-ene. GO materials were found to have high levels of lattice disorder and various functional groups such as hydroxyl, epoxy, carboxylic acids and ketones. The inactivity of low oxidised (<20 wt% oxygen) samples can be understood by the need for a certain level of oxidation partnered with the deleterious covering of sulphur. Washing these samples leads to activation after removal of this poison as previously described in chapter 4.

The low activity of Hummers samples may be explained by the presence of covalently bound organosulphates, as suggested by TGA, which remain to a high level (1 wt%) even after washing of the catalysts. These highly oxidised species also contain a higher amount of carboxylic groups compared to Hofmann catalysts shown by FT-IR and XPS which agrees with reports by other research groups. It was not possible to associate activity with any one functional group due to all materials being abundant in all functional groups to some degree. The search for an active species was also complicated by the detrimental effects of sulphur. However with more efficient cleaning of catalysts it may be possible to obtain real unhindered activity values for the epoxidation of dec-1-ene allowing us to possibly associate the relative abundance of certain species with activity thus allowing us to design a more efficient carbocatalyst.

Future studies within this field should utilise online analysis and in situ studies for the monitoring of functional groups in various environments. TGA-MS or TGA-FTIR can provide valuable information on evolved species from thermal decomposition. $^{13}C$ NMR could also be employed to supplement the data obtained from XPS to more accurately identify functional groups. This is due to the close association of groups in XPS and overlapping of spectra. A more in depth re-use study is also required to assess the stability of these materials under epoxidation conditions and how functionality might change after multiple uses.

## 5.7 References

---

1 S.Eigler, C.Dotzer, A.Hirsch, M.Enzelberger, P.Muller, *Chem.Mater*. 2012, **24**, 1276-1282.

2 S.Eigler, C.Dotzer, F.Hof, W.Bauer, A.Hirsch, *Chem.Eur.J*. 2013,**19**,9490-9496

3 A.Dhakshinamoorthy, A.Primo, P.Concepcion, M.Alvaro, H.Garcia. *Chem-Eur.J*. 2013, **19**, 7547.

4 N.R.Wilson, P.A.Pandey, R.Beanland, R.Y.Young, I.A.Kinloch, L.Gong, Z.Liu, K.Suenaga, J.P.Rourke, S.J.York, J.Sloan, *ACS Nano*, 2009, **3**, 2547-2556.

5 V.Schwartz, W.Fu, Y.T.Tsai, H.M.Meyer, A.J.Rondinone, J.Chen, Z.Wu, S.H.Overbury, C.Liang, *Chem.Sus.Chem*, 2013, **6**, 840-846.

6 M.Naebe, J.Wang, A.Amini, H.Khayyam, N.Hameed, L.H.Li, Y.Chen, B.Fox, *Scientific reports*, 2014, **4**, 4375.

7 S. Navalon, A. Dhakshinamoorthy, M. Alvaro, H. Garcia, *Chemical reviews*, 2014, **114**, 6179-6212.

8 C.K.Chua, Z.Sofer.M.Pumera, *Chem.Eur.J*. 2012, **18**, 13453-13459.

# 6

# Discussion: The future of graphitic oxide. Preparation methods and use in catalysis.

### 6.0 Current methods for the production of graphene related materials

The current large scale production of graphene requires the use of powerful oxidants and also highly acidic mixtures to oxidise graphite to graphitic oxide. This can then be exfoliated to graphene oxide and subsequently chemically or thermally reduced to form graphene like reduced graphene oxide. The Hummers oxidation method[1] or a modified Hummers method is most commonly employed to carry out the initial oxidation step. This employs potassium permanganate as the oxidant which is added to a mixture of sulphuric acid and sodium nitrate. The sulphuric acid is crucial due to its high oxidising power and also for its ability to probe between the layers of graphite. This is essential for increasing the interlayer distance of the graphite, allowing access between the layers to the oxidant, thus facilitating basal plane oxidation. Sodium nitrate is employed to form nitric acid *in situ* which increases the oxidising power of the mixture and has also been shown to further increase the interlayer distance, complimenting the effect of the sulphuric acid. The result of this efficient and aggressive oxidation is the almost complete loss of graphitic character from the parent graphite. Oxidation of the basal plane leads to the introduction of oxygen functional groups and as a result, a higher $sp^3$ to $sp^2$ ratio. Further oxidation of the surface leads to enough functional groups to create sufficient ring strain in order to break up the graphitic lattice. This yields smaller particles of graphitic oxide which are abundant in basal plane hydroxyl and epoxy groups and edges which are abundant in carboxylic moieties. Repeating of this process leads to the almost complete loss of crystallinity and a doubling in d-spacing from approximately 3.5 Å to 6.9 Å. Even though this is the most commonly used method for the production of bulk graphene, the material produced is of a lower quality than can be achieved using other methods. This is due to the large amount of surface defects introduced into the lattice during oxidation. Damage to surface can also occur during the exfoliation step, commonly achieved *via* sonication. This has been shown to result in much smaller particles which are abundant in surface defects. Finally, chemical and thermal reduction methods can also introduce defects and, in the case of hydrazine, heteroatoms into the structure. The combination of these factors result in a final graphene or reduced graphene oxide film which is far from pristine and of medium quality compared to other methods. These methods, as described in earlier chapters involve either the direct exfoliation of graphite using ionic solvents and high stirring speeds[2,3] or mechanical exfoliation first studied by Andre Geim[4]. These methods produce high quality graphenes with minimal defects and are therefore ideal for study in applications which utilise graphene's electrical capabilities. However, the low scale on which graphene is produced by these methods has hampered its utilisation on an industrial scale, despite its observed thermal, electrical, optical and mechanical properties on the lab scale. The study of graphene on any appreciable scale in the lab must be achieved by the Hummers oxidation, and therefore the results are not fully representative of the theoretical potential of graphene. It should also be noted that even this method of oxidation is not fully applicable on the industrial scale and until recently was only made in batches as large as 5 grams. This is due to the use of high amounts of acid and also the production of unstable active species such as dimanganese heptoxide. The high explosive nature of these species limits production due to the need to keep the entire system at a low enough temperature to avoid explosions (<95 °C). This is difficult due to the highly exothermic nature of this method. The addition of hydrogen peroxide to quench residual dimanganese heptoxide also limits the overall economy of this process due to its high cost. Further problems arise when scaling up the essential washing of the obtained graphitic oxide. Due to the clay like material obtained by the Hummers method and the high swelling capacity of the graphitic oxide, thorough washing becomes tedious. For these reasons, on the laboratory scale, simple filtration methods cannot be employed as the initially acid mediated graphitic oxide is practically impermeable to water and filtration times become unreasonable. Therefore repeated centrifugation must be employed to separate the solid from the acidic waste. The material must be continually re-dispersed in fresh deionised water and centrifuged until a neutral pH is obtained or the removal of sulphur ions is confirmed by testing with barium nitrate. Centrifugation is not without its drawbacks too as high amounts of this acid waste are produced, roughly 2 litres of highly acidic waste per 5 grams of starting graphite is generated by continuous use of water in order to reach neutrality and a graphitic oxide which is low in contaminants. Complete removal of residual species from the oxidation such as manganese, sulphur, nitrogen and sodium is rarely achieved and in some cases impossible through washing with water due to the incorporation of these elements into the covalent structure of the lattice.

In summary, the highest throughput method available for production of graphitic oxide and in essence graphene is not entirely scalable itself to that of industrial needs. It also produces lower quality graphene than other methods and cannot hope to match them in that sense due to the oxidative nature of the procedure and the destructive methods which must follow. Garcia *et al.*[5] provided a concise summary of the available methods for the production of graphene or reduced graphene oxide in a review concerning the carbocatalysis of these materials. The conclusions of the authors are summarised below (table 6.0.1).

**Table 6.0.1 Advantages and disadvantages of available methods for the production of graphene.**

| Method | Advantages | Disadvantages |
|---|---|---|
| **Chemical oxidation (Hummers, Tour, Hofmann Staudenmaier)** | Large scale production | Medium to low quality graphene<br>High level of impurities and defects.<br>Low electrical conductivity.<br>Major production of contaminated waste during washing<br>Explosive chemical intermediates. |
| **Pyrolysis of precursors i.e. sugars** | Low cost due to abundance of sugar feedstock.<br>Green synthesis. | Medium quality graphene |
| **Chemical vapour deposition (CVD)** | High quality graphene<br>Low level of impurities | Small scale production |
| **Mechanical exfoliation** | High quality graphene | Tedious and time consuming |

| | | |
|---|---|---|
| **(scotch tape method)** | | Very low production |
| **Direct exfoliation** | High quality graphene | Extremely low quantities<br>Need for removal of ionic liquids |

The use of graphitic oxide or its exfoliated analogue graphene oxide as carbocatalysts has increased rapidly in recent years. For use in catalysis, less importance is placed on the retention of surface structure and the prevention of these defects as the electrical properties of the material are not as important. In fact, defects and higher number of edges lead to an increased free energy of the surface which can be a more desirable quality for catalysis.

Bielawski and co-workers showed that graphene oxide was an efficient catalyst in oxidation and hydration reactions[6]. Here, the authors described that highly oxidised material produced by Staudenmaier or Hummers methods showed no difference in activity for the oxidation of benzyl alcohol. Reports by Pumera *et al*[7] found clear differences between graphene based materials produced using either potassium chlorate or potassium permanganate as oxidants. These differences included the level of oxidation, oxygen functionality and position of the oxygen atoms on the surface, the number of surface defects, the presence of heteroatoms on the surface and also electrical capabilities of the reduced graphenes[8]. These are some of the few cases in which preparation method has been studied for its effect on catalysis or electronic applications.

As previously mentioned, the most commonly employed method for most applications is the Hummers method due to the production of highly oxidised species. However recent studies have found that certain residues remain on the surface from the preparation methods and could be contributing to the observed qualities of the final material. One of these residues is in the form or organosulphate which, instead of being a removable impurity, has been shown to hydrolyse to form sulphonic acid groups[9] (figure 6.0.2). The authors described a process in which treatment of the surface in a solution of sodium hydroxide facilitated the removal of this organosulphate. Thermal decomposition of the sulphate was also observed to occur at temperatures above 200 °C, using TGA-MS.

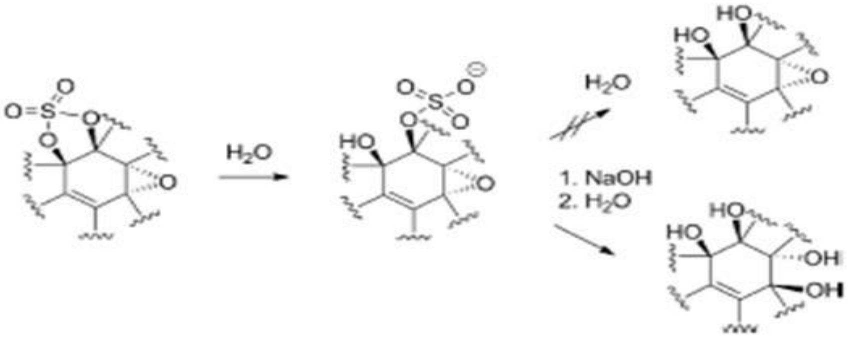

**Figure 6.0.2 Hydrolysis of organosulphates and subsequent removal by sodium hydroxide**

As previously described in earlier sections, the presence of these sulphate groups has enabled the use of GO in the acid catalysed ring opening of epoxides[10] and other reactions such as Freidel-crafts[11] additions and acetalisation of aldehydes[12]. However, as we have shown in this study, the presence of sulphur on our GO materials appears to be extremely detrimental to the activity of the materials for the epoxidation of dec-1-ene. Amounts as low as 1 wt% of sulphur were shown to completely inhibit the reaction from occurring, especially when supported on lowly oxidised catalysts. Removal of this sulphur was shown to be facilitated by a vigorous washing step using high purity water. This led to materials produced with amounts of potassium chlorate as low as 4 g being active for dec-1-ene epoxidation. Highly oxidised graphitic oxide catalysts produced by the Hummers method did not increase in activity even though low amounts of sulphur were being removed. This may be rationalised by the previously explained study by Eigler *et al* suggesting organosulphates may be strongly bound to the GO surface and removal by simple water washing is not possible, instead requiring treatment by sodium hydroxide. Our study confirms the difference in sulphate groups found on low or high oxidised materials.

It also becomes clear that the commonly employed technique of centrifugation for separation and washing of GO materials is not sufficient for the removal of problematic impurities such as sulphur despite these being present at relatively low concentrations (ca~ 1 wt%). The commonly observed discrepancies between the level of impurities in reported catalysts can possibly be explained by the various scales on which GO materials are produced. A comparison of work conducted by leaders in this field is given below (table 6.0.2). Attention is paid to the type of chemical oxidation, source of carbon, purification step and drying method. These are compared to our modified Hofmann method in the first entry of the table.

**Table 6.0.2 Comparison of methods for the production of graphitic oxide regarding oxidation method, separation and washing technique and drying method. (DE Dead end filtration, HF Hot filtration, CF Cross flow filtration)**

| **Authors** | **Method of prepation** | **Starting material** | **Scale** | **Purification method** | **Drying method** |
|---|---|---|---|---|---|
| **Pattisson *et al.*** | Modified HO, HU, Modified HU | <20um | 5 g | 1.Centrifuged until neutral pH. Inactive<br>2. 0.3 g washed 300 ml DI water | HO -110 °C<br>HU- 30 °C vac oven 96h (removing from vac every 12 h to separate agglomerated catalyst) |
| **Hummers and Offeman[1].** | HU | Flake graphite | 100 g | HF after $H_2O_2$ addition. Filter cake washed with 14 L of warm water. Redispersed in 32 L of water. Remaining salt impurities removed by resinous anion and cation exchangers. Centrifuged. | 40 °C over phosphorous pentoxide *in vacuo* |
| **Tolle, Gamp, Mulhaupt[13].** | HU | - | 60-120 g | Dialysis or DE and/or CF. | DE- 5 d 40 °C vacuum, Dialysis-40 °C 200mbar, air flow, 14d, Cross flow- air 40 °C 5 d |
| **Chowdury, Singh, Paul[14].** | HU | 20, 45, 150 um | 2 g | DE- Sintered glass funnel. Washed with 10 % HCl | 45 °C 24 h |
| **Chua, Sofer, Pumera[7,8]** | HU, HO, ST, TO | <20um | 0.5 g | Filtered, 1 L ultrapure water, 5 % HCl solutions. | 50 °C 5 d |
| **Bielawski[6]** | HU, ST | Flake graphite | - | - | - |
| **Pumera.** | St, HO, HU | <50um | 5 g | 3 L water, Decanted, 5 %HCl. Centrifuged | 60 °C vac oven 48 h |
| **Garcia[10].** | HU | - | - | Centrifuged, collection of supernatant at 15000 rpm | Freeze drying |

In our work, it was found that oxidation of graphite using varying amounts of oxidant in both Hummers and Hofmann preparation methods yielded vastly different materials, characterised by x-ray diffraction (XRD), fourier transform infrared spectroscopy (FTIR), x-ray photoelectron spectroscopy (XPS), Raman spectroscopy, microwave plasma atomic emission spectroscopy (MP-AES) and ion chromatography (IC). It was found that further to their differences in catalytic behaviour, they also exhibited different physical properties which were observed during washing and drying steps. Lowly oxidised samples such as GO-HO1, GO-HO2, GO-HO5 and GO-HO10 exhibited handling qualities similar to graphite. Separation *via* centrifuge was facile due to the low amounts of lattice break up and high graphitic character. It was also possible to dry these catalysts in a conventional oven at 110 °C in static air. The materials obtained were easily ground for preparation for use in reaction with dec-1-ene. Intermediately oxidised samples such as GO-HO15, GO-HO20, GO-HO30, GO-HO45, GO-HO55 and GO-HU5 required slightly more intensive work up with regard to re-dispersing in deionised water. These catalysts were found to be slightly coarser and darker in colour compared to the graphitic-like low oxidised samples. However they were still able to be dried at 110 °C in static air without problems. Highly oxidised samples such as GO-HU10 and GO-HU15 displayed far different physical properties. As previously mentioned, these catalysts formed clay like materials when dispersed in acidic or aqueous media. Washing of these catalysts *via* centrifuge was not an amicable task due to the difficulty in re-dispersing the materials in deionised water after centrifugation. Obtaining a neutral pH during washing was also a lengthy process presumably due to the inefficiency of the centrifuge to quickly remove intercalated sulphur. Drying of these highly oxidised samples presented further problems. The employment of drying methods commonly quoted in the literature, such as 60 °C in a vacuum for 48 hours resulted in rapid drying of the GO and the production of an extremely dense and ungrindable material. After multiple attempts, it was found that obtaining a useable catalyst required drying at no more than 30 °C in a vacuum oven over a 96 hour period during which the catalyst was regularly dispersed to prevent agglomeration and burning of the material. It was found that if the dense material was produced, re-dispersion in water was not possible and therefore the batch was a failure. As well as these hard masses of GO, it was found that excessive heat treatment would result in paper thin graphene-like films adhering to the side of the drying vessel. These were also not able to be re-dispersed or ground to a powder. It is unclear as to why this occurred when other research groups had successfully reported the use of these conditions. For example Pumera *et al*. produced similar GO materials using Hofmann and Hummers methods which were dried at 60 °C in a vacuum oven. The authors prepared catalysts on the same scale to this study with the only variation in preparation method being the starting graphitic material (<50µm). In any case, it became apparent that this catalyst was inefficient for the epoxidation of dec-1-ene. This reinforces the point that the commonly used highly oxidised Hummers type materials are perhaps not optimal for all applications. Certainly, their preparation offers many problems, from hazardous intermediates to inefficient drying and washing techniques. We have shown that lowly oxidised materials are much more manageable in their preparation and may in fact be the better choice for certain catalytic applications.

Tolle *et al*[13] studied the possibility of scaling up of the Hummers method for the production of graphitic oxide and subsequently graphene. A major problem in the chemical oxidation of graphite arises from the use of powerful oxidants and the formation of explosive active species. In the case of the Hummers method, potassium permanganate reacts with sulphuric acid to form dimanganese heptoxide *in situ*. The decomposition of dimanganese heptoxide (scheme 6.0.1) occurs at temperatures above -10 °C. This acts as a source of oxygen for the oxidation of the graphite and is therefore essential to this process. Ozone is also produced which can also help to oxidise graphite[15]. However dimanganese heptoxide is explosive at high temperatures and must be kept below 95 °C. This provides challenges to the scale up of this reaction due to the potential of hot spots within the reactor to occur.

$$2Mn_2O_7 \xrightarrow{T > -10^{\circ}C} 8MnO_2 + 2nO_3 + (6-3n)O_2 \quad (0 < n < 2)$$

**Scheme 6.0.1 Decomposition of dimanganese heptoxide at low temperatures**

In the study by Tolle *et al.*[13] GO was produced on a 60 and 100g scale. The authors initially described the importance of quenching manganese intermediates by deionised water (scheme 6.0.2) and further by hydrogen peroxide (6.0.3). The addition of water at this step can lead to temperatures above 90 °C and therefore ice water was used in this case to control the exothermic hydration of sulphuric acid.

$$Mn_2O_7 + H_2O \longrightarrow 2HMnO_4$$

**Scheme 6.0.2 Quenching of dimanganese heptoxide with deionised water**

The addition of hydrogen peroxide facilitates the consumption of insoluble managanese compounds produced from both the decomposition and hydration reactions of the dimanaganese heptoxide species. Due to the manganate being present in large excess, the addition of hydrogen peroxide was conducted slowly in order to reduce the amount of foaming which occurred due to the production of oxygen.

$$MnO_2 + H_2O_2 + 2H^+ \longrightarrow Mn_2^+ + O_2 + 2H_2O$$

$$2MnO_4^- + 5H_2O_2 + 6H^+ \longrightarrow 2Mn_2^+ + 5O_2 + 8H_2O$$

**Scheme 6.0.3 Quenching of insoluble manganese compounds by addition of hydrogen peroxide**

The main finding of this study was the ability to achieve low levels of impurities by employing sequential filtering techniques partnered with various pH switching with base or acid. An initial acid washing using 5% HCl facilitated the initial dead end filtration by preventing swelling of the GO material, thus allowing removal of large amounts of manganese impurities. The subsequent treatment with NaOH and cross flow filtration allowed for the removal of sulphur impurities. The use of pH switching, dead end and cross flow filtration also dramatically reduces purification time and amount of water needed compared to dialysis techniques or dead end filtration by itself. This combined method provides GOs with sulphur levels as low as 1 wt%. The use of nitric acid resulted in lower levels of contaminants and avoids the addition of chlorine as a result of HCl washing. This method could therefore be used to produce catalysts for the epoxidation of dec-1-ene which as we have shown has a high dependence on the presence of sulphur. Another important technique used in the study was the online measurement of conductivity during cross-flow filtration to assess the amount of ions present in the waste water. This allowed for the accurate determination of an end-point production of multiple batches with a similar impurity level. This is in stark contrast to the use of a barium nitrate as an end point test for sulphur, the sensitivity of which is questionable for production of highly pure and reproducible catalysts.

## 6.1. New methods for the greener production of graphitic oxide materials

As previously described, the problems associated with graphitic oxide and reduced graphene synthesis result from the production of explosive intermediates and materials which are high in various impurities such as sulphur, manganese and potassium. Sulphuric acid has few possible replacements due to its excellent intercalating effects and high oxidising capabilities. Possible alternatives with equal or higher oxidising power, such as hydrogen peroxide or ozone do not possess the ability to efficiently intercalate the graphitic layers for oxidation of the internal basal planes.

Attempts have been made to utilise the intercalating properties of sulphuric acid for the production of graphene in the absence of an additional oxidant such as potassium permanganate. Savaram and co-workers[16] studied the use of hydrogen peroxide with sulphuric acid to form piranha solution. When graphite was immersed with intercalation compounds such as ammonium persulphate and sulphuric acid and exposure to microwave energy, it was found that "paper-thin" graphenes could be formed. These were found to be highly conductive due to the low amounts of oxygen functionality, low levels of impurities and the relatively defect-free structure. This method is promising for the production of graphenes in the absence of powerful oxidants and avoids the production of large volumes of waste water. However this method is not suitable for the production of graphitic oxide due to the low amounts of oxygen added to the surface.

The pyrolysis of sugars has huge potential for the large-scale production of graphene oxide nanosheets (GON). Tang *et al*[17] studied this bottom up synthesis which includes no acid, oxidant or toxic waste products. Exposing sugar solutions to hydrothermal conditions (160-200 °C) GONs can be formed one layer at a time on the solution interface (figure 6.1.1).

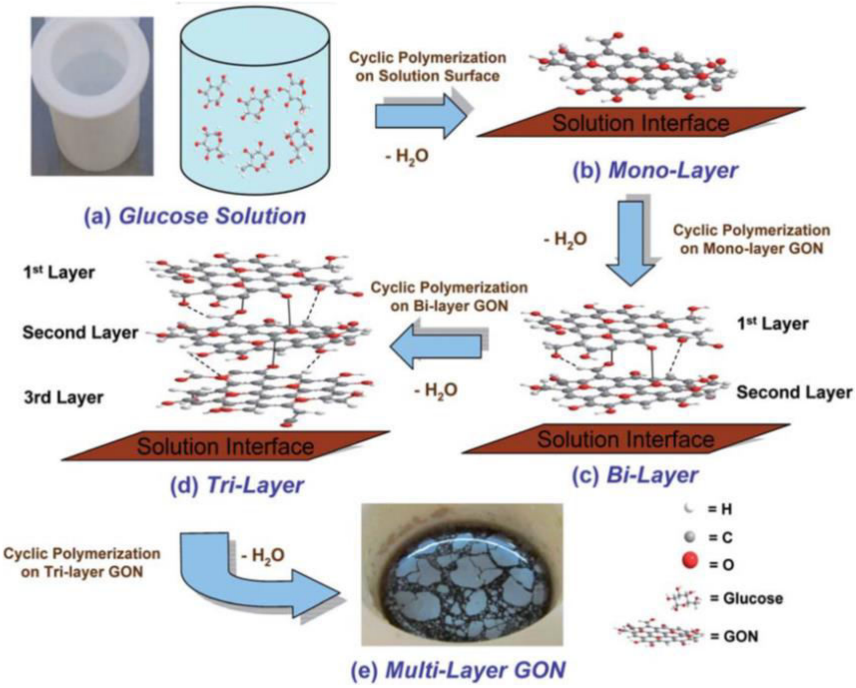

**Figure 6.1.1 Bottom up synthesis of GONs by hydrothermal synthesis from glucose solutions[17]**

The obtained GONs were said to exhibit electrical and optical properties analogous to those produced from conventional methods. The materials were also shown to be highly tunable according to the annealing conditions. Most importantly, the GONs were made in the absence of sulphur and therefore could provide a large scale synthesis method for the production of GOs and GONs for use in sulphur sensitive catalytic applications such as our own. The pyrolysis of other biomass sources such as chitosan[18] and alginate[19,20] has been shown to be effective in production of GO.

### 6.2 Conclusion

The current chemical oxidation pathways from graphite to graphitic oxide raise many problems including explosive intermediates, high levels of impurities and also large volumes of waste on the 5 g lab scale. As we have shown in the epoxidation of dec-1-ene, the nature of the graphitic oxide is crucial to the activity of the catalyst regarding level of oxidation and sulphur. Highly oxidised GOs are difficult to wash and require close control over the drying conditions in order to achieve a useable final material. It was shown by Tolle *et al* that it is possible to scale up the Hummers method to 100 g and achieve low levels of impurities, although this requires the combination of multiple filtration methods and also multiple washing steps during which the pH was switched. Cross-flow filtration provides an alternative to the seemingly inadequate washing technique of centrifugation and when partnered with online conductivity measurements, can achieve highly pure and reproducible catalysts. It is well known that the oxidants used in the chemical oxidations, such as potassium chlorate and potassium permanganate are in high excess. However we have shown that the use of lower amounts of oxidant can be employed to achieve GOs with an optimum level of oxidation. These were shown to be more manageable in purification and also more active in the epoxidation of dec-1-ene than highly oxidised GOs. Therefore, the scale up of these epoxidation catalysts would be safer and less toxic than their highly oxidised counterparts. We suggest that other applications could also benefit from the specific tuning of the GO preparation method rather than the employment of the current full oxidation methods. This is due to the detrimental effects that can arise from such methods including high levels of sulphur, manganese and potassium, heteroatom functionality and also the incorporation of surface defects. Finally, the green synthesis of GONs *via* the pyrolysis of sugars, proposed by *Tang et al* is extremely promising, especially for sulphur sensitive applications such as the epoxidation of dec-1-ene. It is our intention to continue the study of graphitic oxide as an oxidation catalyst and also explore the alternatives for the production of highly pure and highly active materials. The pyrolysis of sugars could yield a completely sulphur free catalyst and therefore help to optimise GO for this given reaction. It is clear that different applications require alternative preparation methods. Those that require high conductivities or pristine layers may require more sophisticated methods than those that can tolerate such characteristics. Indeed, some applications relish the unintentional sulphur or heteroatom functionalities. However it should stand that the main goal is the safe and reproducible production of GO materials that are scalable and tunable to specification.

### 6.3 References

---

1 W.S. Hummers Jr, R.E. Offeman, *J. Am. Chem. Soc*, 1958, **80**, 1339.

2 S.Zhang, M.S.Miran, A.Ikoma, K.Dokko, M.Watanabe, *J.Am.Chem.Soc*.2014, **136**, 1690

3 P.Bhunia, E.Hwang, Y.Yoon, E.Lee, S.Seo, H.Lee, *Chem.Eur.J*.2012, **18**, 12207.

4 K.S. Novoselov, A.K.Geim, , S.V. Morozov, D.Jiang, Y.Zhang, S.V.Dubonos, I.V.Grigorieva, A.A.Firsov, *Science*, 2004**, 306**, 666-669

5 S.Navalon, A.Dhakshinamoorthy, M.Alvaro, H.garcia. *Chem rev*. DOI 10.1021/cr40073347

6 D.R.Dreyer, H.-P. Jia, C.W.Bielawski, *Angew.Chem.,Int.Ed*.,2012, **49**, 6813-6816.

7 C.K.Chua, Z.Sofer.M.Pumera, *Chem.Eur.J*.2012, **18**, 13453-13459

8 H.L.Poh, F.Sanek,A.Ambrosi, G.Zhao,Z.Sofer, M.Pumera, *Nanoscale*, 2012, **4**, 3515-3522.

9 S.Eigler, C.Dotzer, F.Hof, W.Bauer, A.Hirsch, *Chem, Eur. J*, 2013, **19**, 9490-9496.

10 A.Dhakshinamoorthy, M.Alvaro, P.Concepcion, V.Fornes, H.Garcia, *Chem.Commun*., 2012, **48**, 5443-5445.

11 A.V.Kumar, K.R.Rao, *Tetrahedron Lett*., 2011, **52**, 5188-5191

12 A.Dhakshinamoorthy, M.Alvaro, M.Puche, V.Formes, H.Garcia, *ChemCatChem*, 2012**, 4**, 2026.

13 F.J.Tolle, K.Gamp, R.Mulhaupt, *Carbon,* 2014, 432-442.

14 D.R.Chowdhury, C.Singh, A.Paul, *RSC Adv*,2014, **4**, 5138.

15 P.Krwczyk, *Chem Eng J*., 2011, **172**, 1096-1102.

16 K.Savaram, M.Kalyanikar, M.Patel, R.Brukh, C.Flach, R.Huang, M.R.Khoshi, R.Mendelsohn, A.Wang, E.Garfunkel, H.He, *Green Chemistry*, DOI: 10.1039/c4gc01752h.

17 L.Tang, X.Li, R.Ji, K.S.Teng, G.Tai, J.Ye, C.Wei, S.P.Lau, *J.Mater.Chem*., 2012, **22**, 5676.

18 A.Primo, P. Atienzar, E.Sanchez, J.MDelgado, H.Garcia, *Chemical communications*, 2012, **48**, 9254-9256.

19 P.Atienzar, A.Primo, C.Lavorato, R.Molinari, H.Garcia, *Langmuir*, 2013, **29**, 6141-6146.

20 A.Primo, A.Forneli, A.Corma, H.Garcia, *ChemSusChem*, 2012, **5**, 2207-2214.

# 7

## Conclusions and future work

The epoxidation of alkenes is an extremely important and valuable chemical process which until now, for terminal linear alkenes above ethene, has required the use of expensive sacrificial oxidants or catalytic amounts of radical initiators for the activation of atmospheric oxygen. Here, the aerobic epoxidation of dec-1-ene has been achieved in the absence of radical initiators and without the need for stoichiometric reagents such as hydrogen peroxide. This has been achieved using graphitic oxide as a carbocatalyst and upon which no active metal centres are present. This is to the best of our knowledge the first example of this for the epoxidation of alkenes.

The catalytic epoxidation of alkenes is most commonly achieved using supported coinage metals such as silver and gold. However the activity of these catalysts relies heavily on the aforementioned oxidants or initiators. The initial attempts to improve the carbon supported gold catalyst for the epoxidation of dec-1-ene proved unsuccessful. These attempts included variation of the preparation method, replacement of the gold with other coinage metals and also formation of bimetallics. Most of these resulted in a drop in the activity and/or selectivity to the epoxide. In some cases, such as the use of Au-Cu bimetallics, a slight increase in activity was observed although this was suspected to be due to leaching of the copper from the carbon support. This could be assessed by re-use studies and elemental analysis of the product solution in future work.

Derivitisation of the carbon support has led to a number of interesting results. One of these is the potential of iron catalysts for the aerobic epoxidation of dec-1-ene in the absence of radical initiators. This could lead to future low cost epoxidation catalysts. The most important finding however is the catalytic ability of graphitic oxide for the epoxidation of dec-1-ene. Graphitic oxide has shown remarkable versatility as a catalyst over the past few years, however its use as an oxidation catalyst has been limited to simple reactions. In the few instances where graphitic oxide has been used for epoxidation, it has been present as a support rather than as a carbocatalyst.

The investigation of this activity for this difficult reaction posed some major challenges with regards to reproducibility and identification of active species. The preparation method of graphitic oxide plays an important role in the activity of the final material. The highly oxidised Hummers materials commonly used for the bulk preparation of graphene from graphitic oxide exhibit low or no activity compared to low oxidised Hofmann catalysts. Further investigation and the production of a range of both Hofmann and Hummers catalysts suggests that a certain level of oxidation of the surface is required. For the epoxidation of dec-1-ene to occur, at least 20 wt% of oxygen is required on the graphitic oxide surface. However activity does not continue to increase with oxidation and highly oxidised species exhibit a drop in activity, with an optimum level of oxygen being at around 25 wt%. All catalysts show a degree of sulphur contamination observed *via* X-ray photoelectron spectroscopy and ion chromatography. On removal of this sulphur via an extensive washing step it is possible to activate samples with oxygen loadings down to approximately 15 wt%, however the optimum level of oxidation remains unchanged at 25 wt%. The drop in activity in highly oxidised species may be attributed to inefficient washing techniques, strongly intercalated sulphur species and even the presence of covalently bound organosulphates incorporated during the powerful oxidation procedures.

Characterisation of these progressively oxidised materials has for the first time demonstrated the transformation from highly crystalline graphite to highly oxidised graphitic oxide materials in great detail. The use of XPS, TGA, FT-IR, Raman and XRD has demonstrated the inherent differences between these materials and has highlighted the difficulty in assigning one particular structural model. However, low oxidised materials are seen to retain a high degree of their graphitic character with the incorporation of low amounts of hydroxyl and epoxy oxygen functionality and surface defects. Highly oxidised species exhibit a degraphitisation of the surface as shown by XRD and XPS in which the surface is highly abundant in various oxygen functionalities including a higher number of carboxylic acid groups. The interlayer distances of these materials are also shown to be approximately twice that of the parent graphite.

Future work should aim to investigate the possible complete removal of sulphur *via* the use of sodium hydroxide washings for the development of a highly active catalyst. The intentional doping of active catalysts with sulphur species could also confirm this contaminant as a poison for the epoxidation of dec-1-ene. Should this be confirmed, methods for the preparation of graphitic oxide in which no sulphur is present such as the pyrolysis of sugars should lead to highly pure and efficient graphitic oxide catalysts. Obtaining a method which provides highly pure and reproducible catalysts will eventually allow the tuning of surface species, the investigation of an active species and reaction mechanism

In this study, dec-1-ene was used as a model reactant for the epoxidation of an α-alkene. However future work should also extend the use of graphitic oxide as an oxidation catalyst to a wide range of alkenes and many other substrates. The investigation of both linear and cyclic alkenes such as hex-1-ene and cyclooctene will give a clue as to the versatility of this catalyst and its potential for the production of lower chain epoxides.

Graphitic oxide could also be used as a support for metal nanoparticles for use in the epoxidation of dec-1-ene utilising the ability of graphitic oxide to activate atmospheric oxygen partnered with a potentially highly active metal. This has been briefly investigated during this study however a much fuller investigation is needed.

The use of multiple characterisation techniques is essential for the understanding of the graphitic oxide materials. Future work will expand the range of techniques used in this study to compliment and improve their findings. Online analysis such as TGA-IR and TGA-MS will give vital information into the species evolved during thermal decomposition and could possibly confirm the suspected presence of covalently bound organosulphates. Other techniques such as *in-situ* XRD could further explain the stabilities of these materials under various conditions. A complete re-use study is also required to identify the stability of these materials under reaction conditions and the extent to which they can be re-used or re-generated. This will be partnered with the previously mentioned characterisation studies to track changes to the active surface.

This study has laid the foundations for a highly efficient epoxidation catalyst to be developed but has also raised the issue of the possible need to customise graphitic oxide materials to each specific application. Conventional Hummers catalysts are not necessarily the best option for all applications and as previously reported by other groups may need various work ups and purifications. Moving away from highly oxidised species may also eradicate the need for powerful oxidants which produce highly explosive intermediate species such as chlorine dioxide and dimanganese heptoxide. This would facilitate the production of these catalysts on a large scale.